COMPRESSIBILITY CHARACTERISTICS OF SUBMARINE SEDIMENTS AND SETTLEMENT ESTIMATION FOR OCEAN STRUCTURES

A THESIS

Presented to

The Faculty of the Division of Graduate

Studies and Research

By

Gordon Warren Callender, Jr.

In Partial Fulfillment

of the Requirements for the Degree

Doctor of Philosophy

in the School of Civil Engineering

Georgia Institute of Technology

June, 1973

COMPRESSIBILITY CHARACTERISTICS OF SUBMARINE SEDIMENTS

AND SETTLEMENT ESTIMATION FOR OCEAN STRUCTURES

Approved:

William F. Brumund, Chairman

George F. Sowers

Charles E. Weaver

Date approved by Chairman: June 20, 1973

DEDICATION

This dissertation is dedicated to three people who strongly influenced my early education:

Gordon Warren Callender, Sr.
Mary Frances Schultz Callender
Harriett Ogden

ACKNOWLEDGMENTS

A large number of people have helped make this study of the consolidation of submarine sediments possible. I owe a particular debt of gratitude to Dr. William F. Brumund, my major professor, for his enthusiasm, willing ear, and many helpful ideas; to Professor George F. Sowers for making it possible for me to work on a doctorate, and for his interest and help not only in getting ship time aboard the *Kit Jones*, but for taking time from his busy schedule to be on my committee; to Dr. Charles E. Weaver for having all X-ray diffractions run and for his helpful thoughts concerning clay mineralogy and sedimentary processes in general; and to Dr. George Keller, Director, Marine Geology and Geophysics Laboratory, National Oceanic and Atmospheric Administration, for not only providing the cores from the Gulf of Maine and the Hudson Submarine Canyon, but for initially providing the idea of studying the apparent preconsolidation of submarine sediments. Although he had no direct interest in my work, Dr. Billy Mazanti provided several helpful suggestions.

Several people from the Marine Institute (University System of Georgia), went out of their way in providing information or in allowing rescheduling of ship time. I appreciate the efforts of Dr. David Menzel, Director, Dr. Albert Green, Jr., former Assistant Director, Mr. Charles Durant, Resident Manager, Dr. James Howard, and Bob Woolsey. Captain Jimmy Rouse, James Gault and Richard Stubbs of the *Kit Jones* did

more than their normally required duties during coring work off the Georgia Coast.

Special appreciation is extended to Dr. Maurice Ewing, Director, Lamont-Doherty Geological Observatory, and to Dr. John Milliman, Woods Hole Oceanographic Institution for their time and stimulating discussion.

Thanks are due to Captain F. C. Auman, Captain R. I. McFarland, Commander W. B. Wright, Commander F. H. Lewis, Jr., Commander W. J. Eager, and Lieutenant Commander D. E. Bottorff, all of the United States Navy, for their help in various aspects of my doctoral program. Also I would like to particularly acknowledge the help that I received from Commander Noel Grady, Jr., Mr. H. Herrmann and Mr. K. Rocker of the Naval Civil Engineering Laboratory, Port Hueneme, California.

Rolland Brown fabricated the hydro plastic-corer used off the Georgia Coast, machined the Constant Rate of Strain test chamber and provided more technical help than I can ever thank him for. Ray Joyner provided the electronics expertise that allowed the recording equipment to function. It would be hard to say enough about his efforts.

Mr. Peter Thompson of the Chrysler Space Division went out of his way to provide information on the Atlantis program.

The National Oceanographic Data Center kindly provided computer printouts concerning previous bottom sampling and coring off the Georgia Coast.

Nine other students took time from their studies to take part in the research program either in the laboratory or on the coring cruises.

I sincerely appreciate the efforts of Sam Clemence, Joe Skelton, Gary Bigham, Clarence Matthews, Eddie Hughes, Mike Merrill, Jim Sailors, John Lohr and John Woolery.

Thanks are expressed to Mrs. P. P. Murawski for proofreading the rough draft of the dissertation.

Finally I have to express my thanks to Winter and Catherine for doing without their Father for many nights and to my sometime operations officer, supply officer, intelligence officer, data processor, lab technician, and clerk-typist, who is also known as wife--Ann Callender.

TABLE OF CONTENTS

APPENDIX Page

LIST OF TABLES

LIST OF ILLUSTRATIONS

SUMMARY

Effects of high hydrostatic pressure on the compressibility of submarine sediments have in the past been assumed to be negligible. Previous compression tests have indicated that these sediments are overconsolidated, but by all other indications they are normally consolidated. For this reason the sediments are generally termed "apparently preconsolidated." Aging (slow deposition resulting in consolidation under accumulating overburden at essentially hydrostatic pressure) and diagenetic changes have been postulated as the causes of "apparent preconsolidation." Only a few estimates of settlement caused by the primary consolidation of submarine sediments that can be compared to the actual settlement of structures are extant. All estimates found in the literature have been made using standard one dimensional terrestrial soil mechanics procedures.

In the testing program constant rate of strain consolidation tests were employed using *in situ* pore water pressures to determine the effects of high hydrostatic pressure on compressibility and to develop an improved method of predicting settlement caused by primary consolidation.

Samples of submarine sediments were obtained by using an open barrel hydro plastic-corer. All core sites were on the continental margin off the eastern United States and varied from an area where the less-than-two-micron fraction was mainly kaolinite and montmorillonite

(off the Georgia Coast) to the upper Hudson Submarine Canyon and the Gulf of Maine where the less-than-two-micron fraction was mainly illite and chlorite.

The effects of high hydrostatic pressure on the compressibility of submarine sediments were found to be significant. Samples tested at *in situ* pressures displayed greater compression indices and higher values of "apparent preconsolidation" pressure than comparable samples tested at atmospheric conditions. A relationship relating the existing overburden pressure, the hydrostatic pressure, and the "apparent preconsolidation" pressure was developed. The major cause of "apparent preconsolidation" was found to be hydrostatic pressure effects. A new method of computing settlement caused by primary consolidation was employed to estimate the settlement of three test foundations. The agreement between actual and predicted settlement was very good.

NOMENCLATURE

Throughout this dissertation the following distinctions apply:

Symbol/ Letter	Means	Example
Bar	Average	$\bar{C}_f$ - Average compressibility of a floc.
Prime	Effective	p'_o - Effective stress developed by existing overburden.
Delta	Change	$\Delta\sigma'$ - Change in effective stress.

A	Area, or the A-pore pressure parameter.
A_f	Value of the A-pore pressure parameter at failure.
A_s	Area of contact between solid particles.
A_T	Total area of a plane cutting through the point of contact between solid particles, or activity.
A_w	Area of water in a horizontal plane cutting through the point of contact between solid particles.
a	Area ratio.
A_v	Coefficient of Compressibility.
α	Ratio of the average excess pore pressure change to the excess pore pressure change at the base of the sample.
B	Standard consolidation test.
BP	Back pressure.
b/r	Dimensionless void ratio change ratio.
C	Constant rate of strain consolidation test where sediment was not subjected to high pore water pressure, or compressibility of porous material.

$\bar{C}$	Average compressibility of porous material over many small increments of pressure.
C_a	Area ratio.
C_c	Compression index.
C_F	Correction factor for lateral volume change caused by vertical load.
C_f	Compressibility of a floc.
$\bar{C}_f$	Average compressibility of a floc over a given interval of hydrostatic pressure (u_h).
$\bar{C}_f/\bar{C}$	Ratio of prestress.
C_i	Inside clearance ratio.
C_o	Outside clearance ratio.
C_s	Compressibility of the solid particles in a soil.
C_s/C	Compressibility ratio.
C_w	Compressibility of water.
C_ϵ	Strain index.
c	Cohesion.
c/p'	Ratio of cohesion to either effective overburden or apparent preconsolidation pressure (c/p'_o or c/p'_c, respectively).
c_v	Coefficient of consolidation.
D	Dielectric constant.
D_e	Minimum inside diameter of the core barrel.
D_s	Minimum inside diameter of the core head, nose or cutting shoe.
D_t	Maximum outside diameter of the core barrel.
D_w	Maximum outside diameter of the core head, nose or cutting shoe.
E	Young's modulus (subscripts x, y, z denote direction).

E_i	Electric field intensity at a specific point.
E_o	Electric field intensity at a known reference point.
e	Void ratio.
$\bar{e}$	Average void ratio of the sediment mass.
Δe	Change in void ratio.
e-log $\Delta\sigma'$	Relationship between void ratio and effective stress on a logarithmic scale (as developed from consolidation test data).
e_b	Void ratio at the base of a sample as measured during a constant rate of strain consolidation test.
e_f	Final void ratio.
e_o	Initial void ratio.
ϵ	Unit axial strain (subscripts x, y, z denote direction), or ionic charge.
ϵ-log $\Delta\sigma'$	Relationship between unit axial strain and effective stress on a logarithmic scale (as developed from consolidation test data).
η	A function that depends on a, the angle of shearing resistance and the shear strength.
G	Georgia coast.
γ'	Submerged unit weight.
γ_m	Mass unit weight.
γ_s	Saturated unit weight.
γ_{sw}	Unit weight of sea water.
γ_w	Unit weight of fresh water.
H	Hudson Submarine Canyon, or corer penetration, or thickness of stratum of sediment, or height of sample.
ΔH	Change in stratum thickness (settlement), or change in sample height (consolidation).
$\partial H/\partial L$	Hydraulic gradient.

ΔH_c	Change in stratum thickness (settlement) corrected for lateral strain.
H_o	Initial sample height.
I_l	Liquidity index.
I_p	Plasticity index.
k	Coefficient of permeability, or Boltzmann constant.
L_g	Core gross length.
LIR	Load increment ratio. Ratio of applied load to the previous total load in a standard consolidation test.
M	Gulf of Maine.
m	Proportionality constant.
m_v	Coefficient of volume change.
n_i	Concentration of particles at a specific point.
n_o	Concentration of particles at a known reference point.
ν	Poisson's ratio.
P	Constant rate of strain consolidation test where sediment was subjected to high pore water pressure.
p	Pressure.
p_c'	Apparent preconsolidation pressure--the stress existing in the sediment. For terrestrial material this is the preconsolidation pressure.
p_c'/p_o'	Overconsolidation ratio.
p_o'	Effective stress developed by the existing overburden.
R	Remolded, or rate of strain.
R_f	Final dial reading.
R_i	Initial dial reading.
R_o	Dial reading at which primary consolidation begins.

R_{90}	Dial reading at which primary consolidation is 90% completed.
R_{100}	Dial reading at which primary consolidation is for practical purposes 100% completed.
r	Rate of change of average void ratio.
ρ	Charge density.
S	Degree of saturation.
S_o	Initial degree of saturation.
S_T	Sensitivity.
σ	Unit axial stress (subscripts x, y, z denote direction).
$\Delta\sigma$	Change in total stress (subscripts x, y, z denote direction).
σ'	Unit axial effective stress (subscripts x, y, z denote direction).
$\Delta\sigma'$	Change in effective stress.
$\Delta\sigma'/\sigma'$	Load increment ratio: Ratio of the applied change in effective stress to the previous effective stress in a standard consolidation test.
σ_s	Stress in the solid phase.
σ_w	Stress in the liquid phase.
ψ	Electric potential at a point, or angle of intrinsic friction.
T	Temperature (either C or K).
t	Time.
u	Neutral stress, or pore water pressure.
$\Delta\bar{u}$	Average excess pore pressure.
Δu_b	Excess pore pressure as measured at the bottom of a sample during a consolidation test.
$\Delta u_b/\Delta\sigma$	Ratio of the excess pore pressure at the base of the sample to the total vertical stress.

u_h	Neutral stress caused by hydrostatic pressure.
V	Volume.
ΔV	Volume change.
V_s	Volume of solid particles.
V_T	Total volume.
V_v	Volume of voids.
V_w	Volume of water.
v	Discharge velocity.
w	Natural water content.
w_l	Liquid limit.
w_p	Plastic limit.
x	Distance between two charges particles, or horizontal direction.
Δx	Change in the x-direction.
y	Horizontal direction.
Δy	Change in the y-direction.
z	Vertical distance, or depth below sediment-water interface.
Δz	Change in the z-direction.
z_i	Ionic valance.

CHAPTER I

INTRODUCTION

> *The use of the sea and air is common to all; neither can a title to the oceans belong to any people or private persons. . .*
>
> -Elizabeth, Queen of England (1580)*

It is appropriate in this age that a woman should have spoken so wisely of the sea so many years ago.

Originally stimulated by the loss of the Nuclear Submarine *Thresher*, our national interest in the sea and sea floor has increased because the sea appears to offer possible long-term solutions to growing energy, food and space problems. In large part because of the impetus of demand, exploitation of the resources of the sea in general, and of the continental margins in particular has increased tremendously in the last decade. Adjacent to the eastern coast of the United States, the continental shelf generally forms an exploitable submerged extension of the coastal plain. Seaward of the shelf and extending to abyssal depths is the continental slope which varies from about 300 to 700 km in width. Together these features comprise the major part of the eastern continental margin of the United States.

Coincident with developing interest in the sea, has been man's effort to place structures in the ocean.

---

*Statement to the Spanish Ambassador, Bartlett (9).

The continental margin of the Gulf of Mexico has become dotted with offshore platforms constructed by the oil industry. These structures and their associated pipelines and offshore production and storage facilities, are generally supported by deep foundations. As a consequence, settlement problems are generally of less concern than for another class of structures which are supported on shallow foundations. This latter class is made up of various installations ranging from manned habitats to remote acoustic arrays. A third class of structures utilizes anchors and positive bouyancy for foundation support. Like structures on deep foundations, these positively bouyant structures are not affected by settlement.

While the depth of use of anchored structures is apparently limited only by the capability of placing the anchor, in practice because of their positive buoyancy they are subject to the whims of water movement. Cost and the ability to drive piles* currently places a depth limit on the use of deep foundations.

By the end of 1970 offshore platforms had been constructed in water depths of about 125 m and designs were being prepared to install a platform at a water depth of about 330 m (Raecke and Migliore (145)). Since the limit of the continental margins might generally be at 3000 or more meters, it can be seen that pile-supported structures cannot at present fulfill the needs for structures founded in the deeper regions of the continental margins.

---

*Because of the nature of the environment piles used in offshore structures are fewer in number, but many times larger than piles used in terrestrial work.

As a result, when necessity requires structures in these areas, and negative buoyancy is required for stability, the only current answer is to use a shallow foundation. Unfortunately, significant portions of the outer continental margin are covered with fine-grained sediments of high plasticity (silts and clays). Structures placed on these materials may undergo significant detrimental settlement. The consequence is that on these sediments shallow foundations can be used only for relatively small, light structures (*unless* buoyancy can be increased to reduce the load the structures put on the foundation and thus the sediment).* Plans have been prepared to utilize relatively large structures on shallow foundations (Stiles and Kessler (193); "Atlantis Program Proposal" (5); Hironaka and Hoffman (70); Herrmann, Raecke, and Altertsen (67); and others). A number of large manned and unmanned structures have actually been deployed on shallow foundations (Anderson and Herrmann (3); Raecke (142)). However, all of these deployments appear to have been on firm sandy sediments or rocky bottoms. To date only a few large *unmanned* structures have actually been deployed on relatively soft sediments. Of the installations which have been reported in the literature, only one was designed with the idea of limiting settlement. Recovered after almost a year on the ocean floor in water depths of 200 m, the Naval Civil Engineering Laboratory's Seafloor Construction Experiment

---

*A unique exception to this statement is a very heavy, negatively buoyant pipeline repair facility used by J. Ray McDermott Co., in the Gulf of Mexico. The facility is mobile and after being located at the desired site it is allowed to sink into the soft sediments. A leveling system is used to compensate for differential settlement during the repair operation (Raecke (142)).

Structure was essentially a concrete cylinder. Weighing about 8600 kg (submerged) the cylinder and its 4.6 m square concrete mat foundation were emplaced separately. Together they applied a pressure of 50 gm/cm^2 to the sediment. The placement of the structure on a separate foundation marked the first time a sizable concrete structure had been placed separately from its foundation at such depths ("Retrieval of Deep Sea Structures" (145); Raecke (144)).

Thus as larger, heavier, more complex structures are deployed in the deeper areas of the continental margins, increasingly more reliable settlement estimates will be required to prevent unsatisfactory performance, failure and loss of equipment, and uneconomical overdesign. Hironaka and Smith (71), Anderson and Herrmann (3), and Herrmann, Raecke, and Albertsen (67), noted that foundation design for most structures located on cohesive seafloor sediments is mainly governed by settlement considerations.

Submarine Geotechnique

Oceanography is the study of that part of the earth covered with sea water. It is concerned with employing the sciences to understand the fluid system that covers over 70 per cent of the earth's surface. *Ocean Engineering* is that body of technology necessary for the effective use of the sea to meet the needs of mankind. Within ocean engineering the study of submarine sediments(employing techniques used by civil engineers) for the purpose of determining their engineering properties is commonly known as *marine geotechnique*. In reality this appears to be somewhat of a misnomer since geotechnical engineers who work with

terrestrial soils tend to regard sediment deposits which have been removed from the marine environment (by uplift for example) as marine, while those which are submerged are considered to be submarine. The distinction between marine and submarine is employed throughout this dissertation.

Before the increased interest in the ocean, studies concerned with ocean sediments were mainly conducted by submarine geologists (Geological Oceanographers), who were attempting to understand sedimentation and circulation patterns and measure the depths of accumulated sediment. Now, with practical considerations becoming increasingly important, submarine geotechnique has become a new discipline. Its aim is to develop methods of providing estimates of *in situ* sediment parameters accurate enough to insure adequate design of seafloor structures so that their operation will not be impaired by adverse *sediment consolidation* or *failure*.

Determination and Use of Engineering Parameters

The application of terrestrial soil mechanics techniques to submarine sediments has in general proved extremely useful, but offshore exploration is somewhat more complicated. Because complications tend to compound inaccuracies inherent in terrestrial soil mechanics methods, terrestrial methods should not be blindly applied to submarine work (McClelland (112)).

Ideally, tests conducted *in situ* would provide the best estimate of desired engineering parameters. For practical purposes in terms of settlement this would entail a full-scale test of the prototype;

consequently, the next best alternative is to perform laboratory tests that simulate as closely as possible the *in situ* conditions. Samples for laboratory testing can be obtained essentially by two means:*

1. Cores taken by a bottom sitting apparatus.
2. Cores taken from the surface by some type of gravity corer.

Although both typesof cores usually experience the same changes in hydrostatic pressure and temperature as they are brought to the surface, the more controlled conditions of the bottom sitting apparatus probably result in a better core. This method is considerably more expensive than *efficient* surface gravity coring.

Problems associated with obtaining relatively undisturbed gravity cores are discussed in detail in Appendix A. Very generally these problems result from the method of sampling, which can to some degree be offset by design of the corer, and the abrupt changes in temperature and hydrostatic pressure.

Once a core is obtained, consideration of the effect of the change in its environment and the sampling operation must be considered in relating properties obtained from it in laboratory tests to those same properties *in situ*. Every core that is obtained undergoes some change; however, if the relative magnitude of change is not sufficient to alter significantly the sediment properties, then the core material can be used in the laboratory to obtain design parameters. In general, the

---

*Depth considerations are assumed to preclude the use of divers to take cores (their current routine work limit is about 100 m). Special submarines can take relatively small cores, but they are very, very expensive.

effects of sampling *disturbance* cause the core material to be weaker than the *in situ* deposit and to seem to be less preconsolidated (Schmertmann (168); Nacci and Huston (123)). According to Scott (169), a sample raised from a water depth of 700 m would experience a volume expansion caused by the water in its pores of about 0.3 per cent. In addition to this volume expansion, as the pressure is reduced gases may come out of solution causing further volume changes. Warmer temperatures can also cause expansion and increased detrimental organic activity.

Between the time the core is collected and the time it is tested, further disturbance is likely--it can only be minimized, not eliminated. The environmental changes can be reduced by keeping the core refrigerated as much as possible; however, Sverdrup, Johnson and Fleming (194), indicated bacterial activity, once initiated during sampling, will continue. It will cause changes in the oxidation-reduction conditions and pH of the pore fluid. Thus the biophysico-chemical conditions, which are related to compressibility characteristics, are also changed. If the cores are allowed to lose moisture by evaporation, further physico-chemical changes will occur from increased ion concentrations in the remaining pore fluid as well as from changes in the pore water stress. Finally, only very careful handling and testing procedures can keep down physical disturbance from shock.

In addition to disturbance problems, consideration must be given to the relative location of the core site and the actual structure emplacement site. Complications result from wind, tides, currents and even navigation. For example, when working beyond the sight of land

it would be only by chance that a core could be obtained from the exact site where a two-meter diameter foundation was actually to be located. Some very elaborate equipment could provide accuracy of the nature necessary to accomplish such a task, but it would probably not be economically justifiable. At a distance of about 400 km from land general accuracy between 5 and 75 m is possible.

Not only is the relationship between the core site and the *planned* foundation location uncertain, the *actual* foundation location can, because of adverse weather or equipment inaccuracy, be different from the planned location. As a result, the foundation must be designed so that it can withstand the worst possible situation, not at a given site, but over a given area (Herrmann, Raecke, and Albertsen (67)).

Area of Immediate Practical Interest

As previously indicated, settlement of structures founded on shallow foundations on fine-grained sediments appears to be a critical design problem. For practical reasons the continental margins appear to be the area of immediate interest. Although a good deal of the sediment found on the margin is land derived (terrigenous), on the outer portions of the slope, and in certain areas of the shelf the sediment consists of the remains of microorganisms and other matter that has settled very slowly through the water column (pelagic). This latter material is much more common to the deep ocean, consequently a distinction is made here between deep sea sediments (mainly pelagic) and sediments from the continental margins which may be mixtures of terrigenous and pelagic material. Although Nafe and Drake (124) indicated that the 200 m contour

seems to be the dividing line between relatively pure terrigenous and relatively pure pelagic sediment, local conditions will cause considerable variations, if in fact any distinct boundary is discernible.

Uniqueness of Submarine Sediments

Chapter VII and Appendix C describe in some detail a phenomenon of submarine sediments called "apparent preconsolidation" or "apparent overconsolidation." As conceived in the study of terretrial soils if, at any depth in a deposit the soil has been fully consolidated only by the existing weight of soil which is above it, then the deposit is defined as being normally consolidated. If some previous process, glaciation or desiccation for example, has caused the deposit to consolidate under stresses greater than those which presently exist, then the deposit is said to be overconsolidated. Certain laboratory tests allow the soil to be classified into these categories.*

In these same laboratory tests many submarine sediments appear as an anomalous material, having some characteristics of overconsolidated deposits and some of normally consolidated deposits. In general no known natural phenomena appear to have caused true overconsolidation;** consequently, these submarine sediments are termed "apparently preconsolidated." This statement is strictly true concerning deep sea sediments; however, the fine-grained sediments on the continental margins appear to be divided in the nature of consolidation characteristics.

---

*A deposit is said to be underconsolidated if it has not fully consolidated under the weight of the existing overburden.

**A possible exception might be cementation.

Natural processes currently active on the margins include tides, waves, bottom currents, erosion and widespread horizontal and vertical organic acticity. Thus some sediments on the continental margins may appear to be overconsolidated because of the dynamic activity of the ocean, while others may be "apparently preconsolidated" for reasons similar to deep-sea sediments.

In addition, sea level during the Pleistocene is estimated to have been from 130 to 170 m lower (Shepard (173)). Consequently, much of the upper continental margin was exposed and the sediment desiccated, and thus truly overconsolidated. In many areas the Pleistocene boundary can be established by a relatively abrupt transition in the character of the sediment with depth.

Purpose of Research

The purpose of this research is to examine the effects of *in situ* hydrostatic pressure (i.e. of the sea itself) on the consolidation characteristics of submarine sediments. In the past, hydrostatic pressure has been *assumed* to have a negligible effect on the consolidation characteristics of submarine sediments.

In conjunction with this work an explanation of the phenomenon of the "apparent preconsolidation" of submarine sediments will be proposed.

Based on the results of the study of hydrostatic pressure and "apparent preconsolidation," a method will be proposed to improve the estimation of settlement of structures founded on the cohesive sediments of the continental margin of the Eastern United States.

Methods of Accomplishing Research Goals

A high-pressure test chamber capable of allowing submarine sediments to be tested as constant rates of strain under either atmospheric pressure or elevated pore water pressure equivalent to the *in situ* was constructed. A hydro plastic-corer (see Appendix A) was used to obtain material from both north and south of Cape Hatteras for use in the testing program (see Appendix B). Figure 1 roughly shows the general relationship of Cape Hatteras, the continental margin, the coastal plain, the major abyssal features and the core sites from which the test material was obtained.

By utilizing the unique pressure chamber for tests on sediment with two distinctly different clay mineralogies and by conducting the tests with and without high pore water pressure, the effects of *in situ* pressure were determined, and a method proposed to improve settlement prediction for structures founded on these particular sediments.

As a check on the proposed method, it was applied to data from actual foundation tests. The data were furnished by the Naval Civil Engineering Laboratory. It came from two sites off the coast of Southern California where the clay mineralogy was estimated to be within the extremes represented by the material from the sites shown on Figure 1.

A Note on Format, Units and Hydrographic Boundaries

A great deal of information which only indirectly applied to the testing program has been grouped into seven appendices. Where it is pertinent to the testing program reference has been made to it in the text.

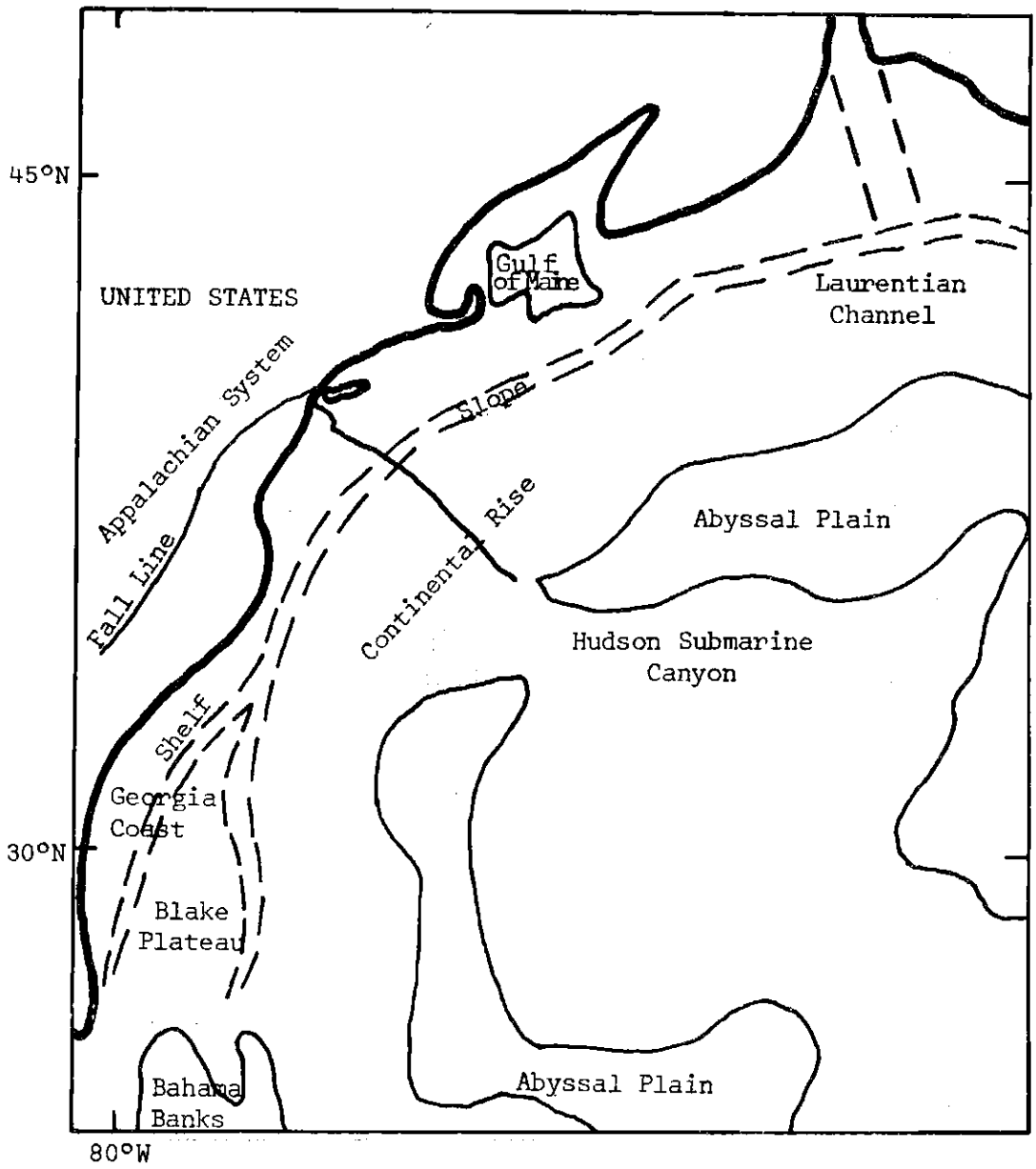

Figure 1. Relationship of Major Submarine Features off the Eastern Coast of the United States (after Heezen, *et al.* (64))

Units

In keeping with the current trend of gradual conversion to the metric system with one exception all units have been converted to their metric equivalents using the following conversions:

$$1 \text{ in} = 2.54 \text{ cm}$$

$$1 \text{ lb/ft}^2 = 0.5 \text{ gm/cm}^2$$

The one exception is the use of inches on certain figures and in certain equipment descriptions where duplication of the equipment would be hindered by converting units to the metric system.

Hydrographic Boundaries

The following *arbitrary limits* have been applied in describing the samples and sampling locations:

Deep sea--water depths greater than 3000 m.

Continental margins--shoreline to 3000 m including the continental shelf, slope and rise.

Deep water cores--cores obtained from water depths between 100 and 1000 m.

Shallow water cores--cores obtained from water depths less than 100 m where dynamic surface phenomena (waves, tides, etc.) are known to be active.

CHAPTER II

HISTORICAL BACKGROUND

Because of the uniqueness of the testing program no exact historical precedent could be found in the literature. A brief historical review is presented below covering the various areas combined into the overall study.

Coring

Because coring was only a means and not an end in itself, detailed historical information has been placed in Appendix A.

Laboratory Consolidation Testing

The following review pertains to one-dimensional consolidation testing (see Appendix D).

Testing with High Pore Water Pressure

In terrestrial soils work consolidation tests are used to determine parameters which can be employed to estimate the settlement of structures placed on the *in situ* soil. Consolidation testing and settlement estimates are more fully described in Chapters IV, V, and VI, and Appendices E, F, and G. Back pressure is a term applied to artificially elevated pore water pressure. In terrestrial soil testing, back pressure is generally used to insure a high degree of saturation. Because of the nature of terrestrial deposits and the available commercial testing apparatus, back pressures greater than about 4 kg/cm^2 are

rarely used. As an indication of back pressures required in submarine investigations simulating *in situ* conditions, a back pressure of 20 kg/cm^2 would be required for a sample from a water depth of 200 m.

Lowe, Zaccheo and Feldman (109) reported results of consolidation tests on materials described only as organic silts. They used back pressures up to about 4.6 kg/cm^2. The results of tests on these soils run at atmospheric pressure, compared to those at high pore water pressure would not be expected to show striking differences because of high initial degrees of saturation. Unfortunately only four tests were conducted on two different materials. In one set of tests compression was greater when no back pressure was used, in the other set compression appeared about the same in both tests. Lowe, Zaccheo and Feldman explained the former case by indicating that factors other than back pressure controlled the compressional behavior of the samples. They concluded that the use of back pressure in consolidation testing would permit more accurate prediction of *time-rates* of settlement of structures on saturated soils. Unfortunately, as Seed (171) has indicated, their results were conflicting and cannot be used to clarify the effect of elevated pore water pressure on the compressional behavior of terrestrial soils.

The general trend in considering the effect of very high hydrostatic pressure in dealing with the consolidation of submarine sediments was set by Hamilton (59):

> The only pressure which causes consolidation is that transmitted through the mineral structure. In the deep-sea floor this pressure for the upper portion of the sediments will consist of the weight of the mineral grains in water (hydrostatic uplift) with no relation to water depth.

This statement, while correct, does not fully describe the consolidation problem in that it seems to indicate only the weight of the mineral grains influences consolidation of submarine sediments.

As a corollary to Hamilton's statement the Terzaghi concept of effective stress was *assumed* to be directly applicable to these deposits (see Appendix C).

In a series of experiments Vey and Nelson ((206) and (207)) attempted to determine the effect of very high hydrostatic pressure (up to 720 kg/cm^2) on the engineering properties of submarine sediments. They used a pressure chamber and loaded the deposits in the same manner as conventional or standard consolidation tests (see Chapter V). The tests were conducted with remolded material from the Pacific Ocean. Since the material was remolded,* much or all of its uniqueness of a submarine deposit was destroyed. The first series of tests employed a range of applied pressures that were normal for terrestrial work, but which were far too high for even relatively undisturbed submarine sediments.** No conclusive results were possible. The second series of tests employed a rangeof applied pressure that was more in keeping with the extremely soft nature of the material. The tests were conducted at temperatures approaching the *in situ*. Unfortunately, the variation among the samples

---

*Remolding means the material was thoroughly mixed so that any effects of previous stresses were completely destroyed. Material of this nature would be unacceptable for use in determining design parameters.

**This mistake was not uncommon in early work with submarine sediments--see the curves presented by Nielsen (127) and the discussion in Anderson and Herrmann (3).

prior to the test was significant. For example, the general differences in initial void ratios was about 0.5. Figure 2 presents the *best* results from Vey and Nelson's work. It shows the effect of a load range that was excessive in relationship to the material used, and indicates the *least* amount of sample variation in their test program. Vey and Nelson concluded from their work that high hydrostatic pressure increased the time to reach 100 per cent of primary consolidation (see Appendix D), had little or no effect on the magnitude of primary consolidation, and had no effect on the magnitude of secondary consolidation.

Despite their conclusions, several workers (Monney (119); Hironaka and Smith (74); Noorany and Gizienski (132)) have been critical of their work, pointing out that because of sample variability their results were really inconclusive.

Application of One-Dimensional Consolidation Procedures to Submarine Sediments

Although Keller (87) felt that standard techniques and relationships for terrestrial deposits might need modification for use with submarine sediments, Noorany and Gizienski (132) indicated that sediments from the continental margins did not appear to have any unique characteristics that would invalidate the use of terrestrial soil mechanics procedures. Herrmann, Raecke, and Albertsen (67) noted that the range of properties of submarine sediments were beyond that normally encountered in terrestrial work.

In the case of consolidation, standard terrestrial one-dimensional procedures have generally been assumed applicable for submarine sediments. Only two proposed modifications have been found in the

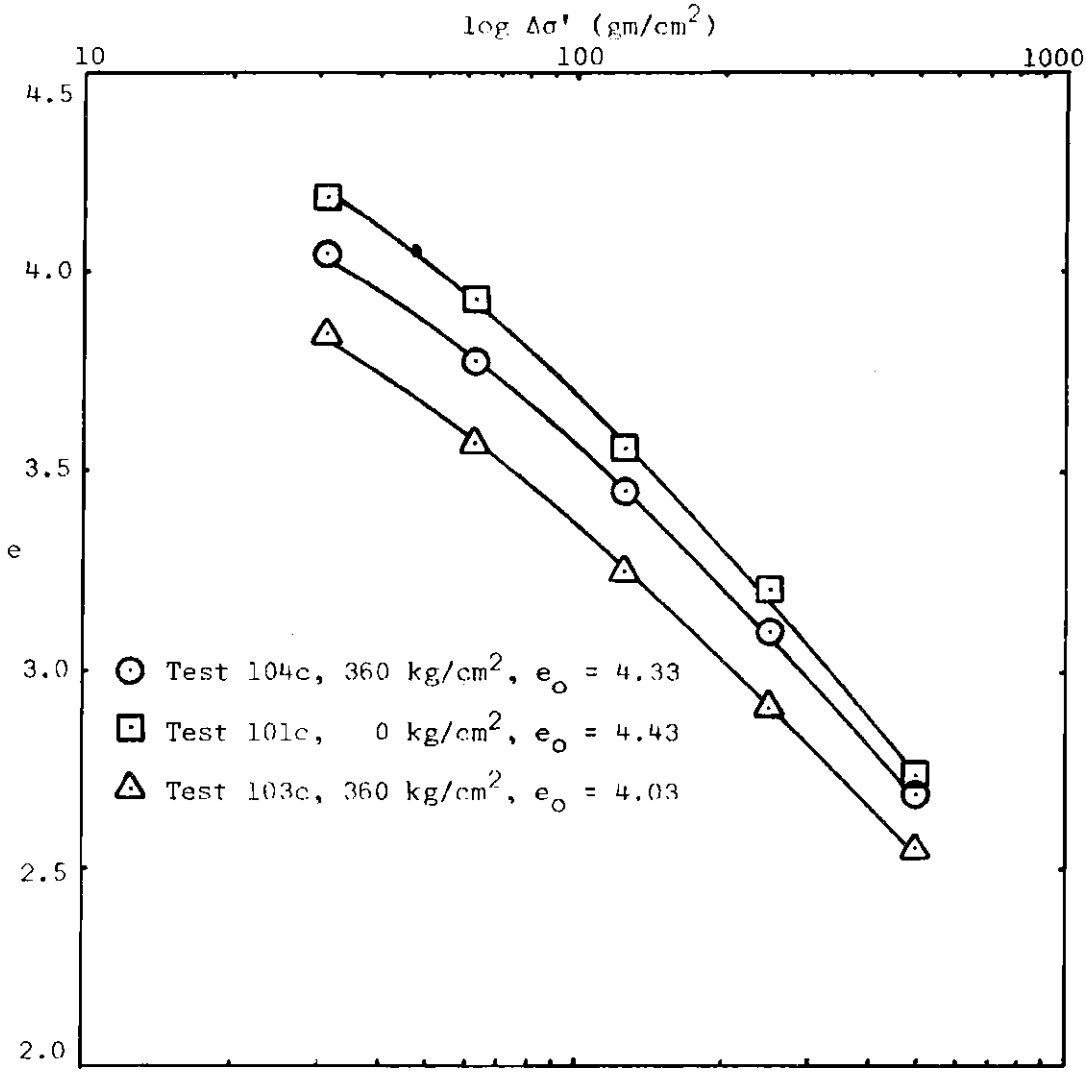

Figure 2. Test Results from Vey and Nelson (207)

literature. Herrmann, Raecke, and Albertsen (67) indicated that when making settlement estimates for structures founded on submarine sediments, computations should be made by dividing the deposit into layers eight centimeters thick and computing the settlement separately for each layer. This may give the best results for computations of total settlement and time-rate of settlement, but as indicated in Appendix G, for settlement caused by primary consolidation use of thicker layers can produce adequate estimates.

In a series of papers (Delflache, Bryant, and Cernock (34); Bouma, *et al.* (17); Carpenter, Thompson, and Bryant (27)) curves were presented from a few tests that were said to be typical of a large number of consolidation tests performed on submarine sediments from the Gulf of Mexico. Despite the difference in the papers, the *published* curves were the same in each paper. Samples were taken with a 7.6 cm diameter *piston* corer. The material came from three locations in the Gulf which were in general at depths greater than the maximum depth of the continental margin. Some amount of back pressure was utilized during the tests. For two of the curves presented, sample disturbance appears from the shape of the curves to have been significant. Based on somewhat conflicting and incomplete data which showed e-log $\Delta\sigma'$ curves with marked upward concavity in the virgin regions (after initially straight sections) the authors proposed using a value of C_c that was less than the value taken from the initial straight line portion of the virgin curve. Because of the omission of some data points and the fact that at relatively high pressures the e-log $\Delta\sigma'$ curve for any soil will display concavity in the

virgin region, the authors' method of selecting C_c is not recommended.

In summary, it would appear that the practical use of the virgin part of the e-log $\Delta\sigma'$ curve has been overlooked by Delflache, *et al.* In the first place, stresses resulting from structural loads for which primary consolidation would be expected to be of interest are hardly likely to be more than about 100 to 200 gm/cm^2. If they were greater, bearing capacity considerations would govern the problem. In this range the curves presented by them were straight. Curves of e-log $\Delta\sigma'$ even for terrestrial work are considered unique only as long as the *structure* of the material does not change.* Ural (204), working with loads to 1,000,000 gm/cm^2 on terrestrial soils, reported a virgin curve that was in several respects similar to those presented by Delflache, *et al.* Esrig, Davison, and Peck (42) reported that in the neighborhood of 100,000 gm/cm^2 the compression index of the terrestrial material with which they worked was considerably reduced. Pressures of this magnitude in relation to terrestrial material are analogous to the higher stresses employed by Delflache, *et al.* during their consolidation tests on submarine sediments. Consequently, statements indicating that the main difference between terrestrial soils and submarine sediments can be seen in consolidation tests where submarine sediments yield *two* values for C_c, while terrestrial soils yield only one, are felt to be very misleading.

---

*Using rapid loading *in a consolidometer*, and material from the Gulf of Mexico, Chmelik, 1970, observed shear failures to occur at 16 kg/cm^2.

Constant Rate of Strain Consolidation Testing

Appendix D describes standard consolidation and constant rate of strain consolidation testing. The rather arbitrary divisions which have been made in describing the consolidation of terrestrial soil deposits is also discussed in this appendix. These divisions have been recognized as being somewhat artificial, but necessary in order to interpret the results of standard consolidation tests. Crawford (31) described the separation of consolidation into primary and secondary effects as being an empirical division of a continuous compression process. He felt that the relative contribution of each effect was largely a function of the laboratory test procedure, particularly the rate of loading. He further indicated that large discrepancies between settlement predicted from laboratory tests, and that actually observed in the field, were due to the rate of compression in the laboratory compared to what actually took place in the field. Crawford conducted a series of standard tests where each test was performed so that the incremental loads were left on the sample for varying times ranging from one day to one week (within a test, each load was left on the sample for the same length of time). Two additional types of tests were conducted. In the first type the sample was loaded as soon as it reached the end of primary consolidation under the previous load increment. In the second type a sample was loaded at a constant rate of strain (CRS) in a standard loading frame. Crawford found that for the standard tests, the longer each load increment remained on the sample, the farther the curve on an e-log $\Delta\sigma'$ plot was shifted down and to the left (see also Chapter VII). Results obtained

from the test run at a constant rate of strain were approximately identical with those obtained in the standard test when the sample was loaded immediately at the end of primary consolidation. Crawford's work showed that as long as each load increment was maintained on the sample for the same length of time, the compression index was relatively unaffected. However, the value of the preconsolidation pressure decreased the longer each load increment remained on the sample (see Chapter VII). Thus the value of preconsolidation pressure was greatly influenced by the rate at which the sample was loaded. These findings agree with those of Leonards and Ramiah (105), and Newland and Alley (126), but contradict the early work of Langer (99), who indicated as the loading rate decreased, the curves shifted to the right for relatively stiff, less permeable soil. For soft material, Langer found little difference in curves obtained by using varying loading rates. His tests *were* significantly affected by side friction (see Appendix E).

Since field loading rates in terrestrial work are several orders of magnitude less than those used in the laboratory, the effects of laboratory loading rate are even more important when field settlement estimates are considered. Crawford also noted that the coincidence of e-log $\Delta\sigma'$ curves obtained by loading a sample in a standard test at the end of primary and by loading a sample at a constant rate of strain (slowly enough so that excess pore water pressures were negligible) was an apparent paradox. In the former test the rate of consolidation was due to primary effects (hydrodynamic expulsion of pore water). In the latter test practically only secondary effects (consolidation at zero

excess pore water pressure) was involved. These observations led Crawford to conclude that further development of consolidation theory was being inhibited by preoccupation with an unrealistic division of a continuous consolidation process. He proposed conducting laboratory tests at small constant strain rates so that the effects of abrupt loading and relatively rapid rates of strain developed in standard laboratory consolidation tests would be avoided.

Using remolded material (Crawford had used relatively undisturbed samples), Wahls and DeGodoy (209) found that tests conducted at constant rates of strain gave values of compression index that were from 10 to 15 percent greater than values obtained from standard tests, and that values of preconsolidation pressure were also generally less. Significant errors in their tests probably occurred from the fact that remolded material caused excess pore pressures to be considerably higher than those Crawford recorded. In itself this might not have been significant, but their pore pressure measuring system was relatively flexible and appreciable lags in pore pressure measurement were more important than in Crawford's work (see Chapter IV).

In a second paper, Crawford (32) reported a number of tests on a very sensitive clay at constant rates of strain. From test to test the strain rate was varied, but within any one test it remained the same. In general, the faster rates of strain tended to give higher values of preconsolidation pressure than the slower rates. Crawford attributed this to the probability that plastic resistance to compression is larger at higher rates of strain (Taylor (197)--see also Appendix C). Crawford

does not emphasize that at higher rates of strain the amount of excess pore pressure developed in the sample is also larger than at lower rates of strain, and as a consequence the consolidation process may be somewhat different. Crawford also appears to have shown that the *amount* of consolidation that will occur in laboratory test samples is dependent on the *average* rate of compression under a particular load and is not greatly affected by variation in loading rate as long as average values are similar. He extends this concept to indicate that the main question to answer in relation to using laboratory tests to predict actual field settlement is: What is the maximum average rate of strain that can be used in the laboratory to allow accurate prediction of actual settlement?

Smith and Wahls (186) presented the results of an extensive CRS testing program involving both artificially sedimented and relatively undisturbed samples. In their work they developed methods of estimating all the parameters that can be obtained from standard consolidation tests except for those parameters related to recompression and secondary effects. Because of equipment limitations in CRS work up to this point, sample unloading after a test had begun was not possible. Wissa, *et al.* (215), developed an elaborate CRS apparatus that allowed unloading, and could maintain a constant load on the sample when stopped (thus apparently allowing parameters to be developed for the estimation of secondary effects). In addition, they developed in more detail the theoretical considerations of CRS testing. The work of Smith and Wahls, and Wissa, *et al.*, as it relates to this research, is described in more detail in Appendix D. As previously mentioned, consolidation tests on soft

submarine sediments require a much lower range of loads than would normally be used for terrestrial material. In general, the range of loads in this testing program were two orders of magnitude less than those of Smith and Wahls.

Summary

The compressibility characteristics of submarine sediments have been studied for about one and one-half decades. During that period of time only Vey and Nelson (206,207), have published information concerning the effect of high hydrostatic pressure. Their work has been criticized for several reasons.

Within the past decade, a new type of one-dimensional consolidation test called the Constant Rate of Strain test has been developed. It is well suited to testing soft material at high pore water pressure; however, to date there has been no published information on the use of this type of test with submarine sediments.

All published estimates of the settlement of structures founded on submarine sediments have utilized one-dimensional consolidation procedures based on the assumption that the sediment was normally consolidated.

CHAPTER III

HYPOTHESES

Objectives

As indicated in Chapter I, the objectives of this research program were:

1. To determine the effects of reapplying the *in situ* hydrostatic pressure in the laboratory on the consolidation characteristics of submarine sediments;

2. To explain the phenomenon of apparent preconsolidation of submarine sediments; and

3. To propose a method of estimating the settlement of structures founded on submarine sediments.

Approach

Skempton (180) has indicated the Terzaghi equation for effective stress

$$\sigma' = \sigma - u \qquad (1)$$

should be modified for certain soil-water conditions. Using Skempton's concept, the following equation has been developed to show the effect of hydrostatic pressure on submarine sediments:

$$p_c' = p_o' + \bar{C}_f/\bar{C}\ u_h \tag{2}$$

where p_c' is the apparent preconsolidation pressure;

p_o' is the effective overburden pressure;

$\bar{C}_f$ is the average compressibility of a floc over a given interval of hydrostatic pressure (u_h); and

$\bar{C}$ is the average compressibility of the sediment over many small pressure increments.

A detailed development of Equation (2) is given in Appendix C.

In effect the proposed equation indicates that if either the hydrostatic pressure or the ratio of prestress ($\bar{C}_f/\bar{C}$) is large, then the value of the effective stress in the soil will be larger than that estimated by assuming Equation (1) to be valid. It is hypothesized that the more complete equation for effective stress is required if accurate estimates for effective stress are to be made for submarine sediments. Direct use of Equation (1), without considering the effect of hydrostatic pressure on the effective stress, is hypothesized to be the major cause of the "apparent preconsolidation" found to exist in these sediments.

Equation (2) has a definite practical value in that it indicates that *in situ* stress conditions, on which settlement estimates must be based, are directly related to the hydrostatic pressure. In turn, this relationship means the use of Equation (3) would not be appropriate:

$$H = \sum_{i=1}^{n} H_i \left(\frac{C_c}{1 + e_o} \log \frac{p_o' + \Delta\sigma'}{p_o'} \right)_i \tag{3}$$

Because of the highly compressible nature of submarine sediments,

it is hypothesized that reasonably accurate estimates of ΔH can be made, assuming only virgin compression with consolidation starting from the effective stress corresponding to the apparent preconsolidation pressure indicated in Equation (2). Use of such an effective stress would result in an expression for settlement with the following form:

$$\Delta H = \sum_{i=1}^{n} H_i \left[C_\epsilon \log \frac{p_c' + \Delta\sigma'}{p_c'} \right]_i \qquad (4)$$

The various terms in Equation (4) are explained in Appendix G. To determine whether or not Equation (4) provides better estimates of the settlement of structures founded on submarine sediments than Equation (3), both equations were used to estimate the settlement of three instrumented test foundations deployed in the Pacific Ocean (see Appendix G). The results of the settlement estimates were then compared to the actual recorded settlements.

In order to examine the hydrostatic pressure effects in relationship to Equation (2), four series of consolidation tests were conducted on submarine sediments. The procedures and equipment used are described in the following chapters.

Series B tests were performed in a lever-type consolidometer. These tests are identified by a "B" and are referred to as "standard" tests.

Series C and Series P tests were performed in the constant rate of strain test chamber described in Chapter IV. The "C" tests were conducted with pore water pressures equal to atmospheric pressure, while

the "P" tests were conducted with pore water pressures equal to the *in situ* hydrostatic pressure for the particular sediment being tested. All "C" and "P" tests are referred to as "constant rate of strain" or "CRS" tests.

The fourth series of tests were the only tests conducted on remolded material. These tests were designated either "RC" or "RP" depending on whether or not the pore water had been pressurized.*

Any differences in the compressibility characteristics found in the comparison of test results between tests on *relatively undisturbed* material conducted with and without elevated pore water pressure (i.e. C and P tests) could be attributed to either high hydrostatic pressure or aging/diagenesis, or a combination of these factors.

Since remolding destroys any effects of aging or diagenesis tests on remolded samples should be devoid of any such influences. Thus any differences found in tests on remolded material conducted with and without elevated pore water pressure would have to be caused by the elevated pressure. This in turn would reinforce the hypothesis that hydrostatic pressure is the *major* cause of the apparent preconsolidation observed in submarine sediments.

All sediments used in the testing program are fully described in Appendix B. Cores obtained from off the Georgia Coast and test samples obtained from these cores are designated by the letter "G." Similarly, those from the Gulf of Maine are designated "M" and those from the Hudson Submarine Canyon are designated "H."

---

*RP indicates remolded material and pressurized pore water.

CHAPTER IV

INSTRUMENTATION AND EQUIPMENT

Field

Gravity coring was accomplished from three different ships. In each instance a wire line and winch was used to lower and raise the coring apparatus. Coring equipment is described in Appendix A.

Laboratory

Core Storage

A soft wax of the type described by Keller, Richards and Recknagel (91) was used with heavy-duty aluminum foil to reduce moisture loss while the core sections were stored in the laboratory (see Chapter V). A chest-type household freezer, modified to maintain storage temperature between 4°C and 8°C, was employed to store the cores. It was a closed system and, over a period of 19 months, water loss from a 1000 ml beaker of sea water also placed in the freezer was negligible. The capacity of the freezer was 20 individual 305 cm cores cut into sections up to 70 cm long; however, it was never filled to capacity.

Care was taken whenever melting the soft wax not to exceed about 100°C, since indications are that excess heating causes loss of hydrocarbons and changes the properties of the wax, reducing its imperviousness (Keller, Richards and Recknagel (91)).

Sample Trimming

An electro-osmotic saw, similar to the electro-osmotic knife described by Chmelik (30), and used by several laboratories involved in working with submarine sediments (Keller (89)), was employed to reduce sample disturbance during trimming. The power supply provided 13 volts (DC) and currents were from 120 to 220 milliamps. These values are considerably lower than those used by Chmelik.

CRS Test Chamber

Dimensions and component parts of the CRS Chamber are shown on Figures 3 and 4; Figure 5 is a photograph of the chamber disassembled.

General Description. Design of the chamber was based on the requirements that consolidation testing could be conducted by a constant rate of strain technique at applied back pressures from 0 to 72 kg/cm^2. In addition, the chamber had to be able to withstand the corrosive activity of sea water for varying lengths of time up to several weeks. Finally, the system had to be easily flushed, ideally allowing complete de-airing, and it had to be capable of measuring, with relatively rapid response, the excess pore pressures developed in the sample during testing. The chamber excess pore pressure sensing system is discussed in more detail later.

An aluminum alloy in the medium-to-high strength category (6061-T6) was selected because of best meeting the requirements (Myers, Holm, and McAllister (122)) and being available and relatively easily machined.*

*After 18 months and over 70 tests with salt water, no corrosive action, other than reduced luster, was apparent.

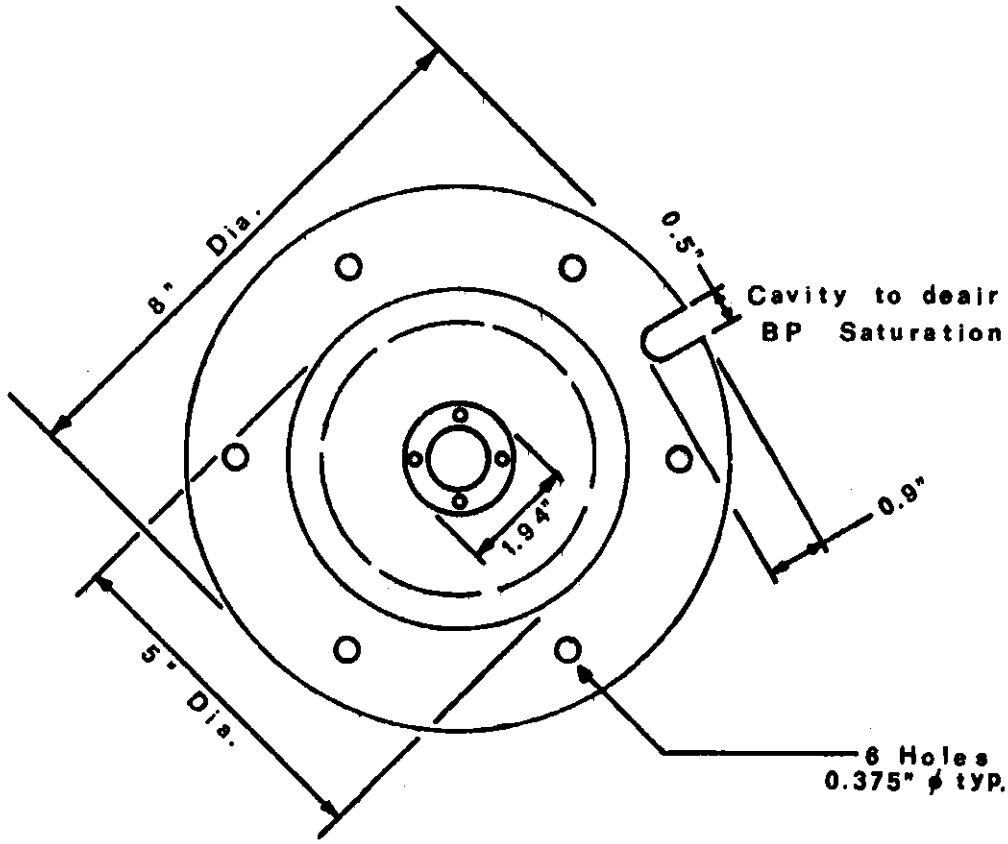

PLAN VIEW

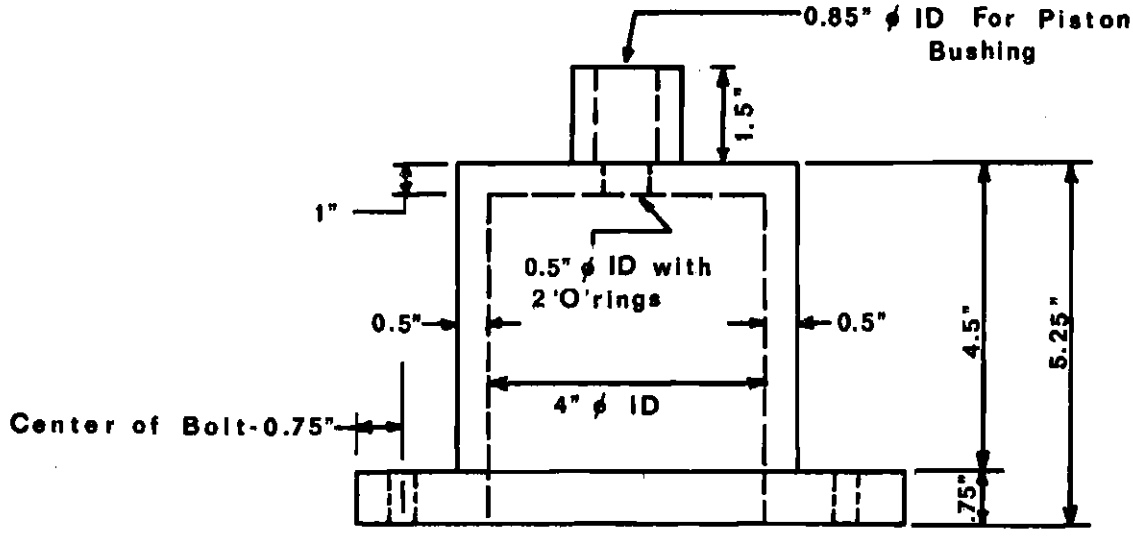

ELEVATION VIEW

Figure 3. Chamber Dome (After Matthews (111))

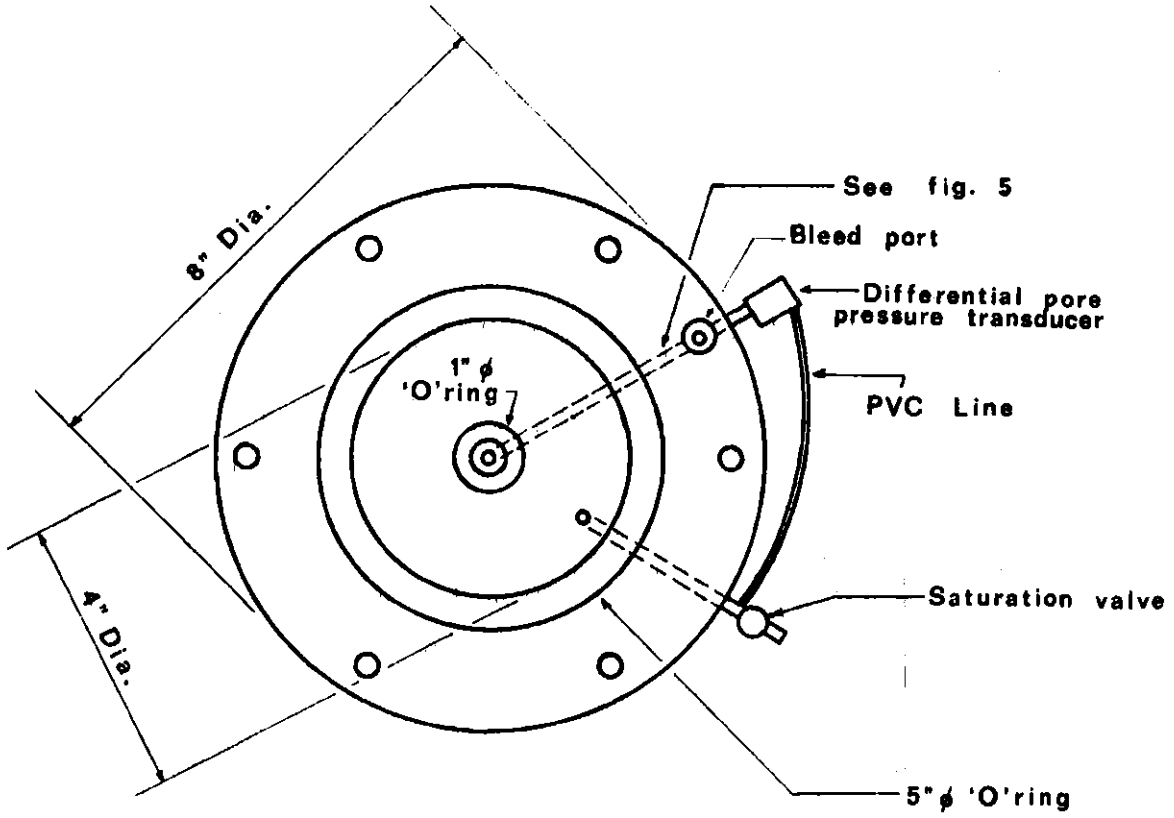

PLAN VIEW

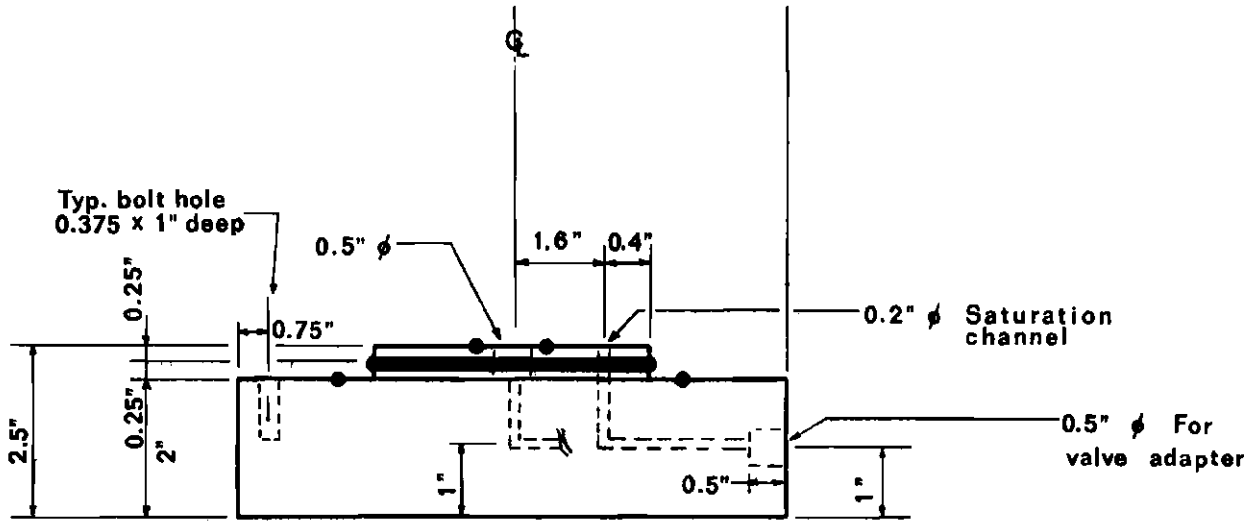

ELEVATION VIEW

Figure 4. Chamber Base (After Matthews (111))

Figure 5. Constant Rate of Strain Test Chamber (Disassembled) (After Matthews, 1972)

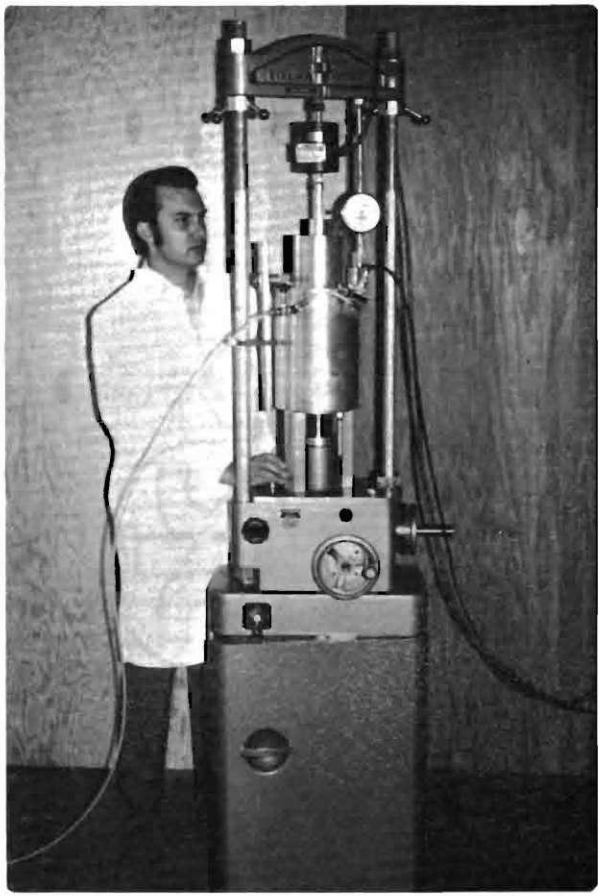

Figure 6. Constant Rate of Strain Test with Back Pressure

The chamber had two main parts--the dome and the base. Structural design was predicated on the maximum desired back pressure and a factor of safety of two was used at the most critical section--the top of the chamber dome.

The Chamber Dome. The purpose of the dome was to provide a containment vessel for the salt water surrounding the sample, and to act as a guide for the loading piston. A bushing housing protruded above the top of the dome. The sample was loaded by inserting a piston through this housing. Lateral support for the 1.27 cm diameter shaft (piston) was provided by a 1.27 cm stainless steel ball bushing. The shaft was solid case hardened and ground 1060 steel, plated with stainless steel. It was 1.27 cm in diameter and 15.2 cm long with a bulb on one end and the other end spherically ground. Two O-rings served to seal the piston as it passed through the top of the dome. These O-rings could be easily installed or removed with a dental explorer, depending on whether or not the test was to be run with or without back pressure. The notch in the dome aligned with the bleed port in the base, which functioned as a backup means of flushing the system or relieving the back pressure.

Six high-strength steel bolts served to connect the dome and base. Figure 6 is a photograph of the assembled chamber during a CRS test with back pressure.

The Chamber Base. The base functioned as a holder for the sample, consolidation test ring and porous stones (all described later in this chapter), and a frame for the pore water pressure sensing system (also described later). The proced re for flushing the chamber base is

described in Chapter V. The base contained three O-rings--two sealed the system as a whole and one insured no drainage of pore water from the *base* of the sample during testing.

The Chamber Excess Pore Pressure Sensing System. As described in Chapter V, the chamber base is flushed by running water through the 0.51 cm diameter saturation channel and the 0.318 cm diameter channel between the opening for the bottom porous stone and the differential pore pressure transducer. Wissa (21) indicated that use of channels around this size will reduce system measuring errors. Too much flexibility in the excess pore pressure measuring system can result in a lag in the response of the system to changes in pore pressure, and thus erroneous records of excess pore pressure in relation to applied stress. According to Whitman, Richardson, and Healy (212), the least flexibility is provided by a system where the sensing element is rigidly connected directly to the drain line from the base of the sample, and the sensing element is an electrical transducer. This was the system utilized for measuring excess pore pressures during the CRS tests. A Pace Wiancko Pore Pressure Transducer (Model KP15) not affected by corrosive media was selected. This model differential transducer is capable of several ranges of operation. For the testing program a sensing plate covering the range 0 to 72 gm/cm^2 was employed. Because the transducer measured the excess pore water pressure above a reference pressure (atmospheric or the level of applied back pressure), 0.645 cm diameter Imperial Eastman polyvinyl tubing (capable of withstanding pressures of 144 kg/cm^2) was used to connect the reference side of the transducer to the saturation channel.

Since this tubing was not directly involved in the excess pore pressure sensing system, its flexibility was not important. Excess pore pressures at the base of the sample were sensed by the side of the transducer connected to the opening for the bottom porous stone (see Figure 4).

Two modes of operation were involved. Back pressure was applied with pumps (described later in this chapter); tests without back pressure were run with a 1.11 cm diameter, 100 ml burette connected to the transducer reference side with flexible tubing (through the saturation valve). The burette was adjusted so that the height of water in it was equal to the height of water above the sample in the chamber dome.

Equipment in Contact with the CRS Test Sample

A standard 6.35 cm diameter by 1.91 cm high Anteus truncated top porous stone and cap were used, in conjunction with the piston previously mentioned, to load the sample. The testing ring was also a standard teflon-lined Anteus consolidation ring; its use is described in some detail in Chapter V.

The bottom porous stone was 5.2 cm in diameter by 0.635 cm thick. It was inlaid in, and so that its top was flush with, an aluminum housing. Double the thickness of the stone, the circular housing had an outer diameter equal to the inner diameter of the Anteus testing ring. A threaded male connecting member was an integral part of the housing allowing the stone-housing assembly to be screwed into the chamber base. When in place a 0.318 cm channel vertically through the bottom of the housing and the male connector allowed excess pore pressure at the base of the sample to be sensed by the transducer. An O-ring around the

circumference of the housing below its midpoint served, in conjunction with one of the O-rings in the chamber base, to prevent drainage from the base of the sample during testing.

The Back Pressure Generation System

This system is shown schematically in Figure 7.

Pressures from 0 to about 0.72 kg/cm^2 of the desired back pressure were applied with a large volume displacement pump manufactured from Roper Corporation parts (capacity 0 to 720 kg/cm^2). The remaining back pressure was applied with a low displacement Enerpac model P28 pump (capacity 0 to 2880 kg/cm^2). Valves were Marsh Instrument Company Model 1924 FFG (capacity 1 to 720 kg/cm^2). Gages were Ashcroft 0 to 72 kg/cm^2 capacity. Since back pressure tests were relatively infrequently run, the gages were calibrated only prior to being put into the system. A separate cylindrical aluminum, hydraulic storage tank 6.6 cm in diameter by 30.5 cm high was employed with the Enerpac Pump. During the test the back pressure was held at the desired level by a Greer 216 kg/cm^2 series, one pint accumulator (see Chapter VI). Polyvinyl flexible tubing used in the system was 0.635 cm in diameter. It was manufactured by Imperial-Eastman Corporation (rated capacity 144 kg/cm^2).

Recording Equipment for CRS Test

Figure 8 shows schematically the method used to record loads and excess pore water pressures during the CRS tests. A photograph of the equipment is included as Figure 9.

Load. A 136 kg capacity BLH Type U3G1 load cell was mounted against the top of the load frame (see following description). The load

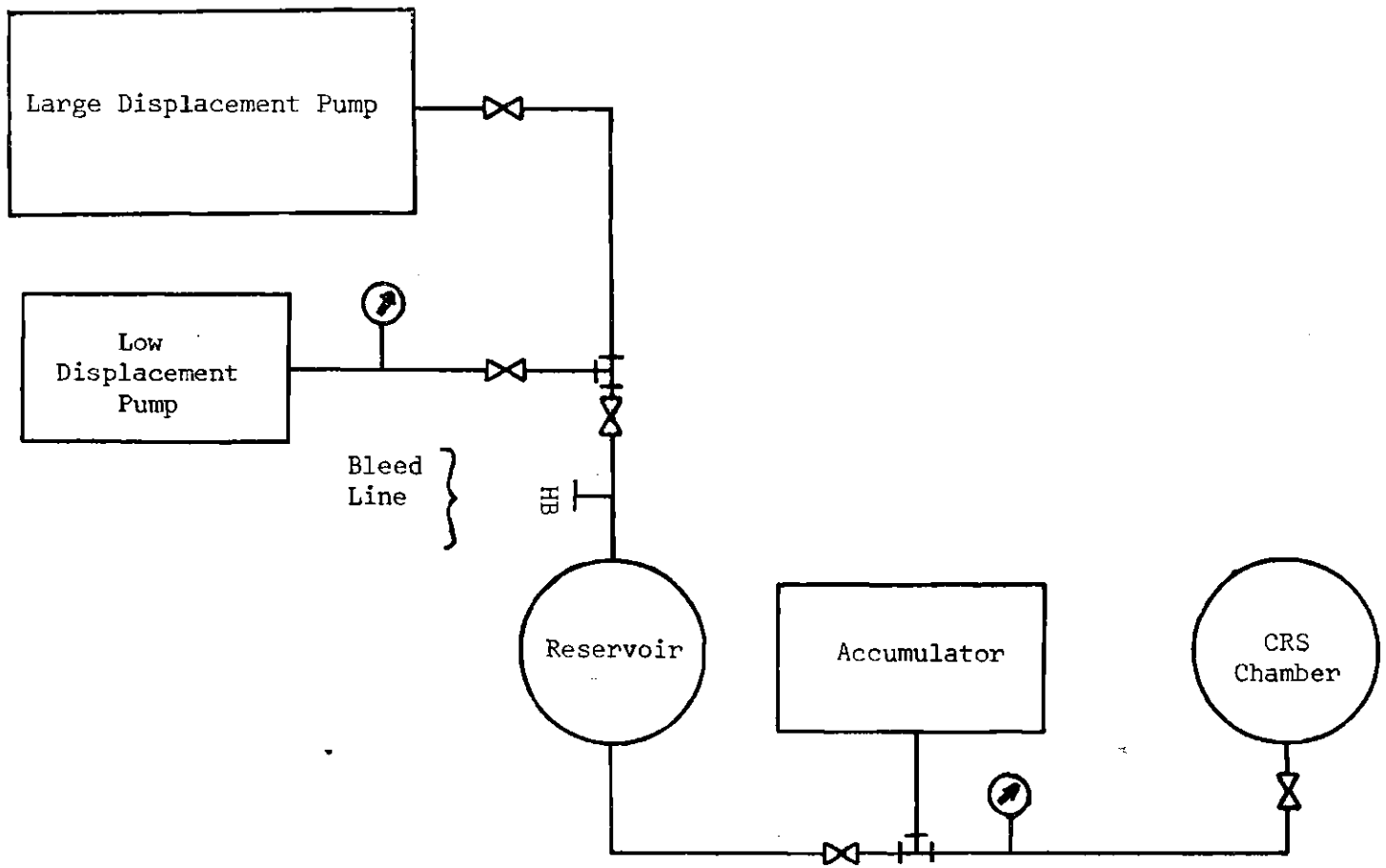

Figure 7. Back Pressure Saturation System

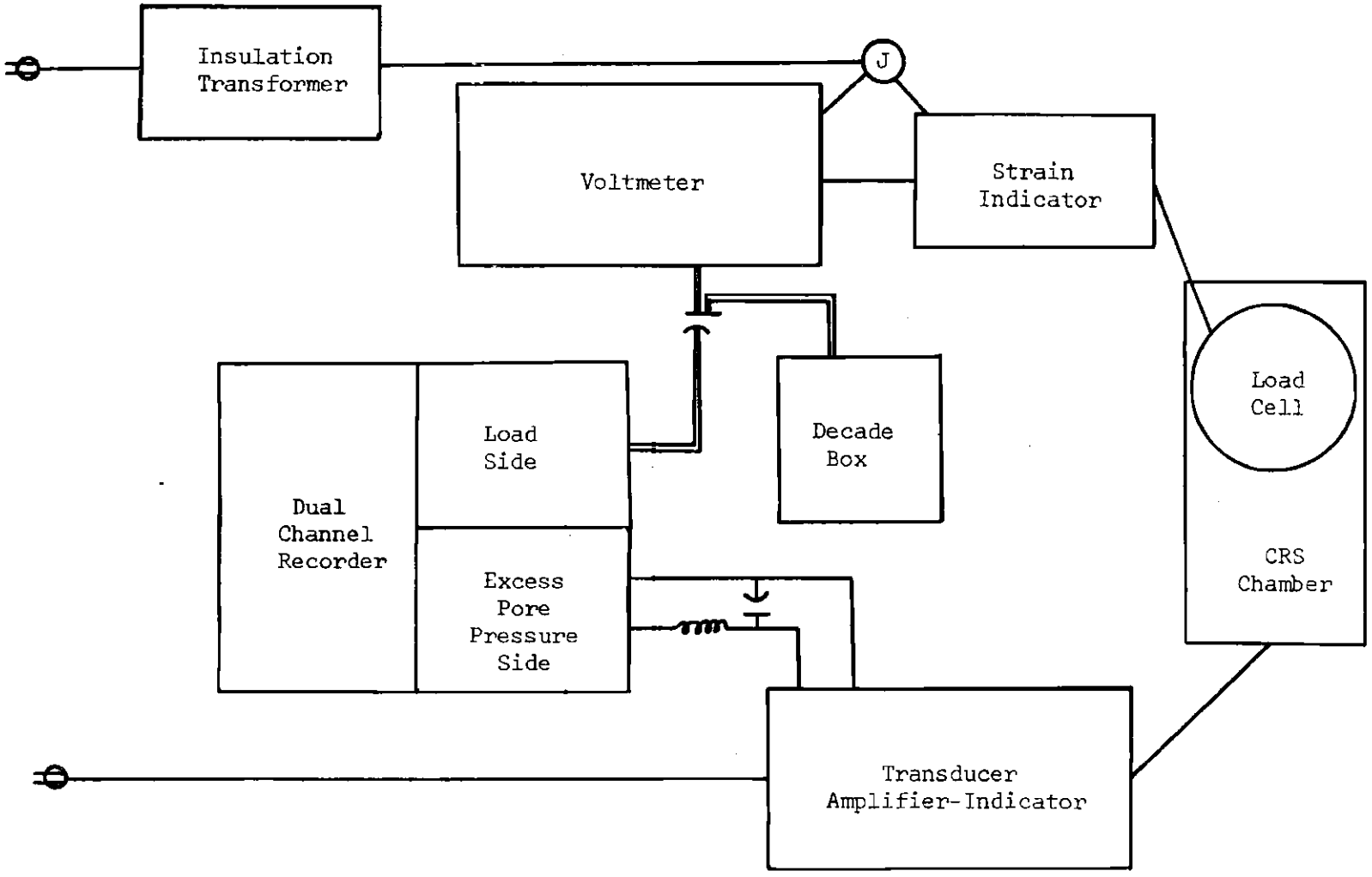

Figure 8. Load and Excess Pore Pressure Sensing System

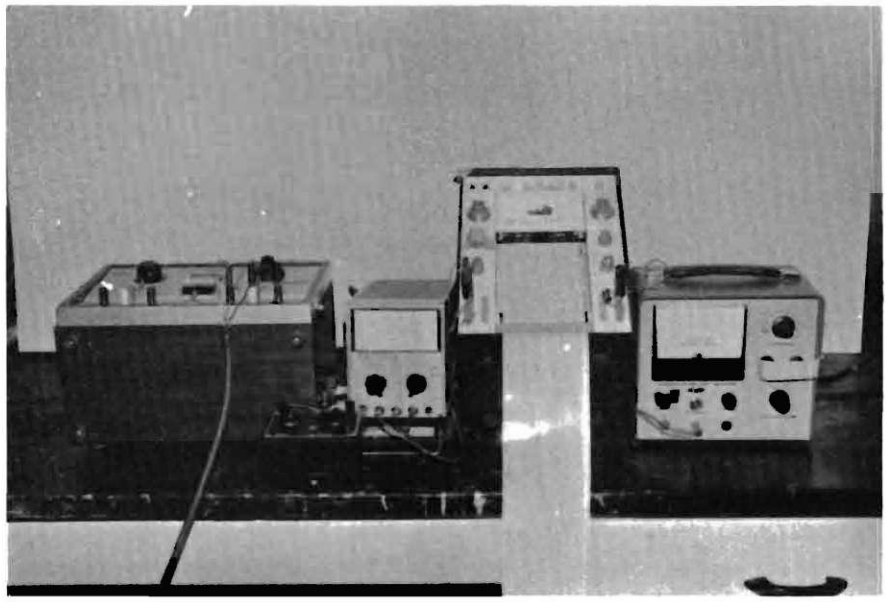

Figure 9. Constant Rate of Strain Test Recording Equipment

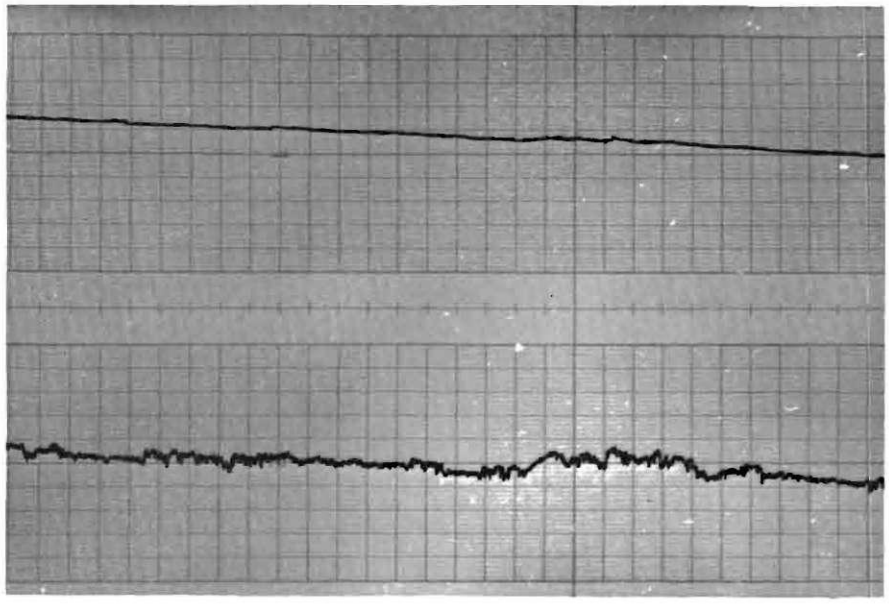

Figure 10. Strip Chart from Constant Rate of Strain Test (Upper--Load, Lower--Excess Pore Pressure)

cell was connected through a model 120C BLH Strain Indicator and a Hewlett-Packard Model 410C Voltmeter to the left channel of a Brush 220 Model 15 6327 57 dual channel recorder. The recorder was operated at a speed of one mm/min for all tests. The speed was checked about every fifth test; no variation was recorded. Several times during the testing program the load system was calibrated. Weights of known amount were suspended from the load cell and the change in reading on the strain indicator (gage factor of two) recorded. The plot of strain indicator reading vs. load was linear in all cases. Between calibrations changes in strain indicator readings over the range 0 to 136 kg equivalent to a maximum of 0.0906 kg were recorded. Since each calibration occurred after the load cell had been temporarily removed for other testing programs, these changes were attributed to the force with which the BLH load cell was secured to the load frame. The appropriate calibration curve was used to adjust the sensitivity of the Brush recorder prior to each test. One complete travel of the pen across the recorder's left channel was set equal to 13.6 kg of load. A maximum load of 20.4 kg was based on the limitation of the Hewlett-Packard Voltmeter. Loads in the range 13.6 to 20.4 kg were recorded by manually repositioning the pen on the left channel of the recorder during the test. For the majority of tests, the desired sample strain was reached before the load exceeded 13.6 kg.

Excess Pore Water Pressure. The Pace Wiancko differential pore pressure transducer in the chamber base was connected thorugh a Sanborn Model 311A Transducer Amplifier-Indicator to the right channel of the

Brush recorder. Several times during the testing program the excess pore pressure measuring system was calibrated. A burette (the *right* burette) was connected by flexible tubing into a special aluminum adapter which screwed into the opening in the chamber base threaded to receive the bottom porous stone. A second burette (the *left* burette) was connected by flexible tubing to a saturation valve. Essentially the two burettes were standpipes. When placed in a two-arm burette holder so that the level of water in them was the same and equal to the level of water in the chamber base saturation channel, the Sanborn Transducer-Amplifier Indicator recorded zero excess pore pressure. When the right burette was raised a distance calculated to be equal to an excess pore water pressure of 0.072 kg/cm^2, the Sanborn Indicator sensitivity was adjusted to equal its maximum capacity. The value of 0.072 kg/cm^2 was also the maximum capacity of the Pace transducer. Finally, the sensitivity of the right channel of the Brush recorder was adjusted so that one complete travel of the pen across it was equal to 0.072 kg/cm^2.

System Response. Noise from a variety of other equipment in the laboratory was a problem. Figure 8 shows the manner in which an isolation transformer was used to reduce this noise enough to allow satisfactory recording of load and excess pore pressure. A photograph of a typical section of a strip chart for one test is shown in Figure 10. During calibrations the response of the Sanborn Indicator, Hewlett-Packard Voltmeter, and both pens of the Brush Recorder were visually observed to be relatively rapid (on the order of one second or less), consequently system damping is not considered to affect the test results.

Sample Strain. Strain was measured by a Federal Gage (capable of measuring deflections to 0.0001 in) mounted as shown in Figure 6. Prior to the start of the test, the gage was zeroed. Gage reading procedure is indicated in Chapter V. All readings are based on the assumption that movement of the loading machine and chamber is equal to the change in height of the sample, and furthermore that change in sample height divided by original sample height is equal to sample strain at any time during the test.

Load Generation System

A Wykeham Farrance Model T57 Load Frame with rates of feed adjustable between 0.000061 and 0.76 cm/min was employed to load CRS test samples. As indicated by Monney (119), normal consolidation equipment and techniques require modification to test adequately soft submarine sediments. The CRS method, at low rates of strain possible with the Wykeham Farrance Load Frame, allows controlled testing to begin at extremely low loads (limited only by the submerged weight of the top porous stone). The load frame is shown in Figure 6.

Various rates of feed were used during the testing program. Each time a new rate was set the machine was timed during the test to insure the rate set was the actual rate of feed as measured by the Federal Gage. As accurately as the gage could be read the set rate and the recorded rate were the same. An exception occurred during the initial portion of each test (see Chapter V).

A cylindrical adapter block of aluminum was machined so that it sat on the load frame piston. It was the same diameter as the chamber

base and allowed the base to be perfectly stable when placed in the load frame. Once positioned and leveled in the load frame the adapter remained there during whole testing program.

Standard Consolidation Test

The apparatus used for the standard tests was a typical lever-type consolidometer. Minor variations from standard commercial models are covered in Chapter V. Calibration was accomplished with the BLH load cell used in the CRS tests. Incremental weights were normally based on a load increment ratio of one (LIR equal to 1.0), and consisted of small plastic bags of lead shot weighed to the nearest 0.01 gm. The loading lever arm/plate was counterbalanced so that no load except the top porous stone, cap, and stainless steel ball was on the sample until the next increment of load was placed on the plate (even though the consolidometer loading head was in contact with the ball).

CHAPTER V

PROCEDURE

Field Work

Coring

Except as noted below, the shipboard procedure for obtaining cores was that described in *Instruction Manual for Obtaining Oceanographic Data* (80) for hydro plastic-corers without pistons.

National Oceanic and Atmospheric Administration (NOAA) hydro plastic-coring devices were used to obtain the cores from the Gulf of Maine and the Hudson Submarine Canyon.

The vessel employed for all coring done off the Georgia Coast was not ideally adapted to working with the hydro plastic-corers used by NOAA; therefore, the following modificatins were made:

The weights were cast so that they could remain on the weight stand throughout the coring operation (i.e. a doughnut shape).

A system of three long bolts which completely passed through the poly vinyl chloride pipe (PVC) and weight stand were used to attach the PVC to the stand.

O-rings secured in the weight stand were used to improve the water-tight seal between the PVC and weight stand.

In addition, the core cutter used when coring off the Georgia Coast had a stepped 5°/30° cutting edge in lieu of the 5° taper employed on NOAA core cutters.

The reason for strengthening the core cutter was the abundance of silt and fine sand size material it would have to penetrate off the Georgia Coast.

When coring the relatively fine sediments in the Hudson Submarine Canyon and in the Gulf of Maine, the finger-type core catcher was wrapped with a piece of polyethylene to improve its core retention ability.

Electrician's tape was wrapped around the plastic caps to reduce moisture loss.

Core Transportation

Cores from the Gulf of Maine were transported upright in a panel truck from Norfolk, Virginia, to Atlanta, Georgia. They were iced down and secured with line. A heavy blanket was used to cushion them.

Cores from the Georgia Coast and the Hudson Submarine Canyon were cut into 50 cm lengths and placed in large styrofoam containers. The Georgia cores were transported upright in a panel truck and the Hudson cores in a U-Haul trailer.

After transportation, core shortening was found only in the top sections of cores from the Gulf of Maine and the Hudson Submarine Canyon.* Consequently, core shortening was not a factor in the testing program.

---

*Cores from the Hudson Submarine Canyon were transported in 50 cm lengths; those from the Gulf of Maine were transported in lengths that varied from about 50 to 70 cm.

Laboratory Work

Core Storage

In the laboratory a 50%-50% mixture of beeswax and mineral oil (Lambe (97)) was used to coat the area where the cap overlapped the PVC (i.e. the area sealed with electrician's tape). Next the core section was entirely wrapped in heavy-duty aluminum foil (secured with rubber bands), measured, weighed and placed upright in a household freezer.* The maximum length of the stored core sections was 70 cm; most were 50 cm or less.

Storage at temperatures approaching or less than *in situ* retards organic activity; however, ZoBell (218) presented data indicating that even though stored at *in situ* temperature, once the material has been subjected to temperatures above the *in situ*, bacterial changes will continue at rates greater than before sampling.

Bozozuk (19) mentions storing samples of terrestrial material in 10 cm lengths. Using shorter lengths undoubtedly reduces moisture migration, but it increases the possibility of moisture loss while cutting and between the PVC and cap. The 50 cm lengths proved practical, and only two sections had to be discarded because of moisture migration and subsequent desiccation.**

---

*The freezer was modified to allow the cores to be stored at 4°C to 8°C.

**Core Section M7-4 was placed in storage on 1 August 1971 at a weight of 5578 gms. Over a period of 19 months and 20 days, 12 weight determinations were made and the core section was cut eight times. The total weight loss was 27 gm. For the samples from core M7 reported here, the general length of storage was about 16 months. Samples from core M3 were in storage the next longest time--about 13 months.

Core X-Raying

Prior to cutting, X-ray work can be used to locate undesirable discontinuities in the sampled material (Stanley and Blanchard (191)). Although all core sections were not X-rayed prior to cutting, those that were thought to be of questionable value were. As a result one complete core from the Gulf of Maine was discarded because of numerous small rocks (up to 2.5 cm × 1.2 cm × 0.6 cm) along its length. Two other core sections were discarded because of large voids.

Cutting Cores

After removal from the freezer, the core section was weighed. Then the aluminum foil was removed and the desired section cut utilizing a metal band saw.* The remaining core section was recapped, taped, waxed, wrapped, measured, weighed and stored in the freezer.

Sample Trimming

Samples were extruded by holding the sample (still in the PVC) horizontal and placing a glass plate covered with clear plastic freezer wrap against one end. While holding the plate tightly against the PVC, the PVC was turned 90° so that it rested on the plate. The PVC was then tenderly moved upward leaving the sample exposed on the plate. It was found that for the softest material no slumping occurred as long as the sample was not longer than about seven centimeters.

CRS Samples. Extrusion of the sample onto the plate covered

---

*The core section is horizontal for the duration of the cut (15 to 30 seconds). Vibrations from the saw are minimal and the blade travels in one direction which is preferable to a back-and-forth sawing operation. Cutting with a soldering gun was tried (Smith and Nunes (184)) without much success.

with freezer wrap was accomplished so that relative movement between the PVC and sediment was in the same direction as when the coring device initially penetrated the ocean floor. The top of the untrimmed sample rested on the plate.* Approximately 0.6 cm of sediment was gently cut from the sample (i.e. that material adjacent to where the band saw cut the core section).

A stainless steel Anteus cutting shoe greased with molybdenum disulfide was attached to a trimming frame head with masking tape to ensure the weight of the ring was not applied to the sample.

The glass plate (with sample) was placed on the trimming frame base and the head (with cutting shoe taped to it) was gently lowered until it contacted the sediment. Then the trimming frame lock screw was tightened preventing the head from moving.

Trimming was accomplished with the electro-osmotic saw. The least disturbance was made by making small cuts from the edge of the sample inward toward the cutting shoe and at the same time making a forward and slightly upward motion with the saw. After trimming 0.3 to 0.6 cm below the cutting shoe (around the circumference of the sample) the trimming frame lock screw was loosened and the frame head and cutting shoe lowered about 0.3 to 0.6 cm. The process was repeated until between 0.6 and 1.2 cm of sediment protruded above the cutting shoe (the trimming frame head had a slot which allowed the sample to be seen).

---

*Prior to extrusion this plate and a special plexiglass sample transfer plate covered with freezer wrap were weighed with the Anteus teflon-lined consolidation test ring greased with molybdenum disulfide.

The tape was removed from the cutting shoe/trimming frame head and the head raised allowing the sample, cutting shoe and plate to be removed from the trimming frame. Using the osmotic saw, the sample was trimmed so that its face was flush with the cutting shoe. The ring and sample were inverted onto a second plate covered with freezewrap and the sample trimmed flush again. A circular piece of polyethylene cut to the diameter of the cutting ring was slightly moistened and laid on the sample. Then an Anteus shaving block was placed on the polyethylene.* The block, cutting shoe and sample were inverted using the original plate. The shoe slipped down over the block forcing part of the sample above the cutting shoe. The sample was trimmed flush with the shoe for a third time. As finally trimmed the sample was 6.35 cm in diameter and 2.54 cm high.

The Anteus consolidation test ring was placed on the cutting shoe and the plexiglass sample transfer plate positioned on top of the test ring. Next, the assembly was inverted so that the order became (bottom to top): transfer plate, test ring, cutting shoe, shaving block. Slowly the shaving block was removed and the Anteus Porous Stone (top stone) taken from the deairing chamber** and gently placed on the sample. The use of the top porous stone during the transfer of the sample is recommended because it was found that parts of some samples tended to

---

*The polyethylene prevents the sample from adhering to the shaving block.

**Top and bottom porous stones were kept underwater when not in use, and were deaired for at least 20 minutes prior to each test.

adhere to the cutting shoe even though it was greased with molybdenum disulfide.

Once the sample came to rest on the transfer plate the cutting shoe, porous stone and polyethylene were removed (in that order). The test ring was covered with the glass plate originally used in weighing and the two plates, ring, and sample weighed to obtain the wet weight of the soil.

Van Zelst (205) found that most disturbance during trimming occurred when top and bottom sample faces were cut level with the trimming ring. For this reason extra care was taken when trimming the sample faces; however, some samples of softer material proved to be quite disturbed and test results could not be used. The cause was probably a relatively impervious layer of remolded material at the faces.

Standard Samples. The procedure for samples used in the standard tests is similar except that no special transfer plate, shaving block or separate cutting shoe were used (the sample was trimmed directly into a stainless steel ring greased with molybdenum disulfide).

Trimmings. During trimming three moisture content determinations were made from the trimmings and some material retained in polyethylene plastic freezer-refrigerator food bags for classification tests.

Consolidation Tests

Standard consolidation tests were performed in general as outlined in Lambe (97). The device was a fixed ring type fabricated at the shop of the School of Civil Engineering. It was similar to

commercial lever-type consolidometers.

Standard Tests. A 6.03 cm diameter by 2.79 cm high stainless steel test ring, machined so that the cutting edge was less than 5°, was used for these tests. The total stresses employed never exceeded 1280 gm/cm^2 * and were usually less than 640 gm/cm^2; therefore, deflection of the machined ring under the lateral pressure of the saturated sediments was not a factor in the tests.

Testing began at 5 gm/cm^2 (effect of partially submerged top porous stone and steel ball) and for most tests proceeded at LIR equal 1.0. Because of the low loads used, a BLH load cell was employed to calibrate the consolidometer. Most tests were run so that loading occurred as soon as primary consolidation for the previous increment was 100 per cent completed (based on Taylor's square root of time method of determining R_{90} **). Certain tests were conducted so that the sample was allowed to consolidate 24 hours under each load increment, and some tests were run with LIR not equal to 1.0 for the whole test.

CRS Tests. Flushing the CRS system was accomplished by connecting the CRS chamber base saturation valve to a fresh water spigot and opening the valve and the bleed ports in the Pace-Wiancko differential pore pressure transducer. Water was allowed to flow until air bubbles ceased to come out of the saturation channel. With the water running, a finger was placed over the channel exit port in the chamber base causing water and air to be expelled from the pressure side bleed port

---

* Tests on core G6 are an exception.

** Several workers have indicated a preference for this method for determining R_{100} for soft materials (see Appendix D).

of the transducer. With the water shooting out of this port in a strong stream an allen head wrench (provided with the transducer) was used to close the port. Next the saturation valve to the chamber base was closed, the water turned off and the chamber base disconnected from the spigot. Flexible tubing from the spigot was placed so that the drain line from the chamber base to the transducer was flushed. A strong stream of air and water was ejected from the chamber base drain line side bleed port of the transducer. As with the reference side bleed port, an allen head wrench was used to close the drain line side bleed port. Once the system was flushed excess water was removed from the chamber base using paper towels and a syringe. Particular care was taken to remove water in O-ring grooves and from the bottom of the bolt holes.

After removing the bottom porous stone from the deairing chamber it was screwed into the chamber base. Excess water was carefully removed from the top of the stone. Then the transfer plate (with sample and test ring on it) was butted up against the bottom porous stone (utilizing the semi-circle cut from the transfer plate for that purpose). The test ring (with sample) was moved across the transfer plate so that the sample was positioned over the bottom porous stone. The transfer plate was removed and test ring pushed down over the bottom porous stone, thereby seating the sample. Next, the top porous stone was put onto the sample. Finally, the chamber dome was put on and secured with six high-strength steel bolts. The bolts were tightened alternately to develop the best seal. Together the chamber base and dome form the CRS test chamber.

After the chamber was filled with salt water* it was placed on the aluminum adapter block already seated in the Wykeham Farrance load Frame. A cable from the Sanborn transducer amplifier-indicator was connected to the Pace pore pressure transducer.

To flush the back pressure generating system the accumulator was connected to a spigot. After ensuring the valves to the pumps were closed, the spigot was turned on and the hose bibb just upstream of the hydraulic reservoir opened. A plastic container was used to collect the strong stream of fluid which was ejected. When air ceased to appear (i.e. only water came from the hose bibb), the valve was shut and the spigot turned off. Then the connection to the spigot was broken and the line carefully reconnected to the chamber base saturation valve. Once the connection was made the valve to the base was opened. Before inserting the piston into the chamber, the valve to the low displacement pump was barely cracked. The piston was inserted and the valve closed. The chamber was positioned under the BLH load cell and the jamb nut carefully screwed down until it was seated against the piston. Finally, the Federal gage was zeroed, the valves to the pumps opened and the first increment of back pressure applied.

Initial saturations between 90 and 100 per cent were found for practically all samples tested. The back pressure saturation procedure used was adapted from the work of Lowe and Johnson (108). Back pressure was applied in increments of 1.08 kg/cm^2 up to 5.4 kg/cm^2. Then two

*To inhibit corrosion of the ball bushings, the chamber was filled with salt water up to the bottom of the ball bushings and a squeeze bottle with distilled water used to complete filling.

increments of 2.16 kg/cm^2 were applied bringing the pressure to 9.7 kg/cm^2. Finally one increment was utilized to raise the system to the test back pressure. The system pressure was allowed to equalize for 20 minutes under each increment before the following increment was applied.

After the system had stabilized under the desired back pressure, the valves to the pumps and between the pumps and the accumulator were all closed (the low displacement pump was used only during the final stages of back pressure application for small adjustments). Using the BLH Strain Indicator, the Hewlett Packard Voltmeter was adjusted so that it was on scale. The Sanborn transducer amplifier-indicator was also adjusted to be on scale and both channels on the Brush dual channel recorder zeroed with the appropriate position adjustments.* After re-zeroing the Federal gage, the Wykeham Farrance load frame (previously set to the desired rate of feed) was switched on, thus beginning the test.

All procedures for the test with back pressure apply to the test without back pressure except that the O-rings sealing the piston were not used and instead of connecting the chamber to the back pressure generating system, a burette partly filled with water and a piece of flexible tubing were employed to provide a reference head of water equal to that above the sample in the chamber. Obviously, the back pressure saturation procedure does not apply to this type of test.

---

*All recording equipment was allowed to warm up at least 20 minutes before each test, and the Brush recorder allowed to be in the paper moving mode 20 minutes before each test.

Consolidation of CRS test samples under the effects of the top porous stone and from the back pressure saturation procedure appear to have been negligible; however, a correction for the top porous stone was made (see Chapter VII).

Because of the O-ring seal around the piston during tests with back pressure, a separate test without a sample, but in all other respects the same as the actual back pressure test was run. This "back pressure calibration test"* was utilized to determine the effects of the O-rings sealing the piston. These effects were then subtracted out of the results obtained from the actual test.

Except for the initial and final readings, no further readings were necessary during the normal CRS tests (since the recorder and load frame run at known constant rates). For the back pressure tests, firmly seating the load frame base plate caused the particular load frame employed to run at a speed which did not equal the desired speed for about the first 0.005 to 0.01 in of travel. For this reason, and because small temperature changes in the lab were found to cause minor back pressure variations, random readings of water temperature,** back pressure and load frame travel were made during the tests with back pressure.

After a back pressure test was completed, the Federal gage was read and the strip chart marked at the time of the reading. The load

---

*One was run for each back pressure test.

**These readings were made in a container of water adjacent to the CRS test chamber.

frame, the recorder and the other equipment was switched off. Next, the valves to the pumps and accumulator along with the bleed valves on the pumps were opened. After the back pressure had bled off, the valve to the CRS chamber base was closed and the lines to the pumps and to the transducer amplifier-indicator disconnected. Then the jamb nut was raised until it was completely back into the load cell. Using the fine adjustment, the load frame was run back down until its base plate was firmly seated (the Federal gage reading was again zero).* Running the load frame back down was important, since it meant each test was started from about the same position.

After removing the chamber from the load frame, the salt water was allowed to drain from it. The dome was unbolted and the sample removed for a void ratio determination. Finally the whole system was *rinsed with fresh water* to reduce corrosion.

To preclude air drying of the porous stones between tests, they were stored under water.**

CRS Tests on Remolded Material. A special series of tests were run on remolded samples. The series consisted of four groups of two tests each. These special tests were run as standard CRS tests with the following exceptions.

---

*Care was taken to insure that the load frame base plate was firmly seated since play in the gear system caused the back pressure to bleed off during the back pressure saturation procedure.

**Before storing, the stones were rinsed with a strong jet of water. This reduced problems with the stones becoming less permeable by the accumulation of soil fines.

Remolded material was placed in an Anteus cutting shoe with a spatula. The sheaving block was used to obtain a CRS sample with the same dimensions as previously indicated. Unused remolded material was replaced in storage until the first test was run.

The first remolded sample was placed in the chamber and back pressurized. After the desired back pressure had been applied for a certain period of time, the back pressure was removed, the piston taken off the sample and the O-rings sealing the piston removed. Next, the chamber was replaced in the load frame and the burette connected to allow a test without back pressure to be run. Finally the piston was replaced and a test without back pressure run. This whole process varied from one to two days, depending on the testing rate and time the back pressure was allowed to remain on the sample.

After completion of the first test, the remaining material was removed from storage, remolded again and exactly the same procedure employed, *except that the sample was not subjected to any back pressure.* This sample was allowed to sit under the top porous stone in the chamber filled with salt water for the same length of time prior to the beginning of the test as the first sample. Thus the only difference between the two samples in a group was that the first sample had been subjected to very high hydrostatic pressure prior to testing and the second had not. During the test neither sample was subjected to back pressure.

CHAPTER VI

RESULTS

Rate of Sediment Deposition

Richards (150) has shown that a plot of natural water content vs. the logarithm of laboratory vane shear strength for a particular material generally is a straight line for deep-sea sediments. He further noted that a similar type of plot using porosity instead of water content (for a saturated material the substitution of water content for porosity would not affect the curve) could be used to compare relative rates of deposition: The faster the rate of deposition, the steeper the slope. Based on the slopes shown in Figure 11, the relative rates of deposition would be (fastest to slowest): G8 and G 11/6, H6, H4, M3 and M7, G6, H20.*

Consolidation Tests

Tables 1, 2 and 3 summarize data from the consolidation testing program. With the exception of samples from cores G6 and G8, the strain at the end of practically every test was greater than 20 per cent. Table 4 indicates the relative importance of initial compression, primary consolidation and secondary compression for a random sample of standard tests.

---

*G8 and G 11/6 are shallow water cores from off the Georgia Coast (Ogeechee River area) and Doboy Sound, Ga., respectively. All the other cores are deep water cores from the Hudson Submarine Canyon (H4, H6 and H20), from the Gulf of Maine (M3 and M7), and from the Florida-Hatteras Slope (G6).

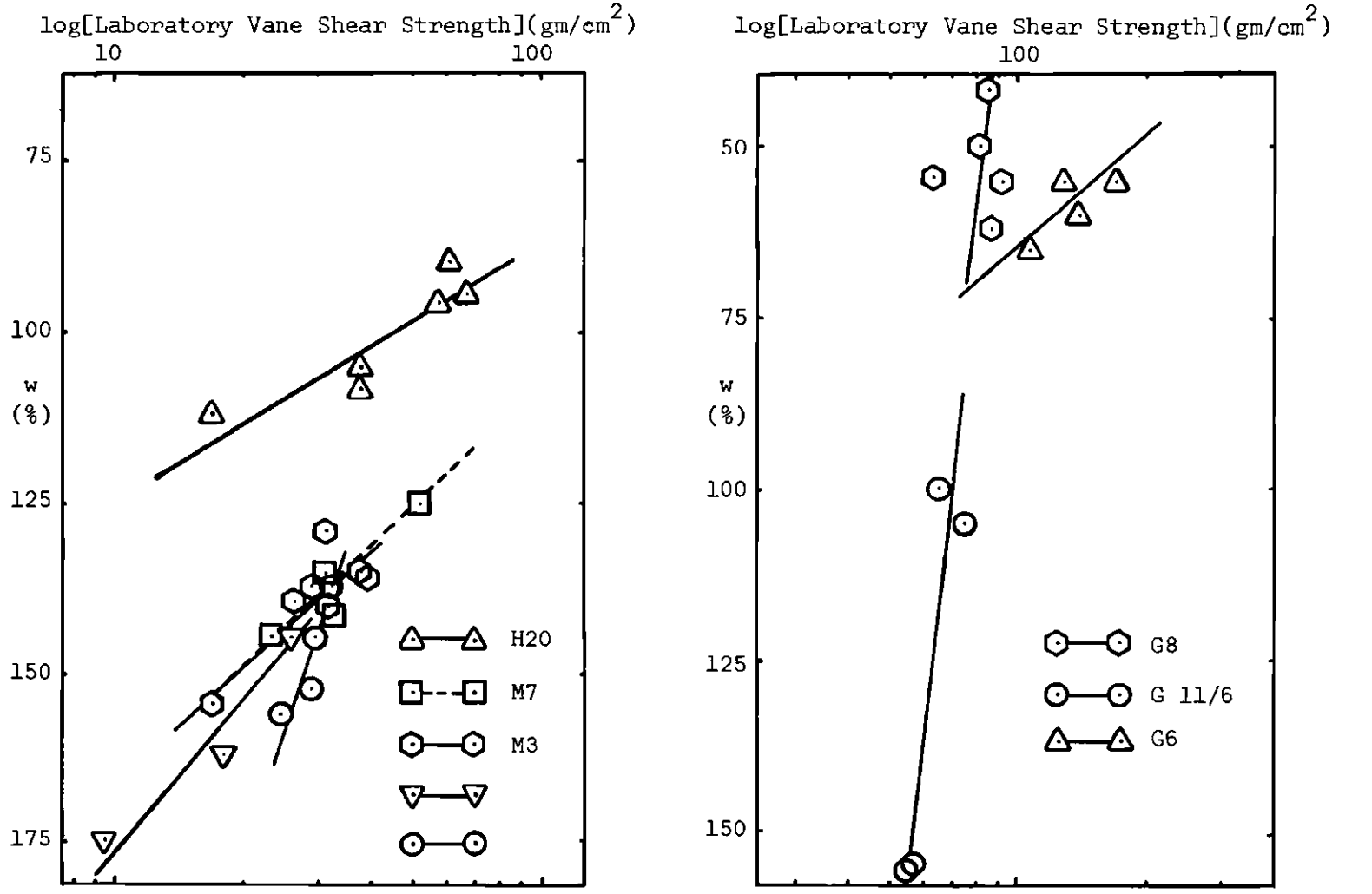

a. Sediments rich in illite and chlorite

b. Sediments rich in kaolinite and montmorillonite

Figure 11. Laboratory Vane Shear Strength vs. Natural Water Content

Table 1. Data from Standard Tests

Test	Type of Test	$\Delta\sigma'/\sigma'$	Test Duration (Hours)
B-H4-2	2	0.5	6.0
B-H4-5	2	1.0	3.8
B-H4-4	2	1.0	3.3
B-H4-7	2	1.0	3.1
B-H4-1	2	1.0	3.0
B-H6-1	2	1.0	3.4
B-H20-1	1	1.0	194.0
B-H20-4	2	1.0	4.3
B-H20-3	2	1.0	4.0
B-M3-4	2	1.0	5.8
B-M7-2	1	1.0	216.0
B-M7-1	2	1.0	6.5
B-G 11/6-4	1	1.0	212.0
B-G 11/7-4	2	1.0,0.5,1.0	6.3
B-G6-1	2	1.0	1.0
B-G8-1	2	1.0	1.0

Type 1 Test--load increments added every 24 hours.

Type 2 Test--load increments added as soon as R_{100} reached for previous increment.

Table 2. Data from CRS Tests

Test	R %/min.	Test Duration Hrs.	Maximum Values					Time of $(\Delta u_b)_{max}$ Hrs.	Time of $(\Delta u_b)_{max}$ as % of Test. %	$\Delta u_b/\Delta\sigma$ at $(\Delta u_b)_{max}$ %
			$(\Delta u_b/\Delta\sigma)$ %	Time of $(\Delta u_b/\Delta\sigma)$ Hrs.	Time of $(\Delta u_b/\Delta\sigma)$ as % of Test. %	Δu_b at $(\Delta u_b/\Delta\sigma)$ gm/cm^2	(Δu_b) gm/cm^2			
C-H4-8	0.06	6.0	35	1.4	23	64	84	6.0	100	30
C-H4-4	0.048	8.5	23	7.5 - 8.5	88-100	5-74	74	8.5	100	23
P-H4-1	0.024	19.2	32	0.8	4	3	56	19.2	100	32
C-H4-5	0.024	16.0	28	9.7	61	36	56	16.0	100	18
C-H4-3	0.024	21.0	20	1.8	9	4	50	21.0	100	8
P-H4-2	0.024	20.0	11	20.0	100	52	52	20.0	100	11
C-H4-7	0.012	30.0	9	10.2 - 30.0	34-100	16-40	40	30.0	100	9
C-H4-2	0.0072	70.0	7	51.8	74	10	27	70.0	100	4
C-H4-1	0.0072	65.5	6	16.5	25	4	19	63.5	97	3
C-H4-6	0.0048	92.0	0	-	-	0	0	-	-	0
P-H6-3	0.024	19.4	10	19.4	100	49	49	19.4	100	10
P-H6-1	0.0072	67.5	5	42.5	63	14	20	67.5	100	4
C-H6-1	0.0072	68.0	4	30.0	44	8	14	68.0	100	2
P-H20-2	0.024	16.3	50	2.3	14	20	98	16.3	100	16
C-H20-3	0.024	17.0	32	14.5	85	35	100	17.0	100	16
C-H20-2	0.024	17.5	16	14.2	81	65	81	17.5	100	14
C-M3-7	0.024	19.5	20	14.5	74	49	81	19.5	100	17
C-M3-5	0.0096	47.5	10	28.0	59	22	30	43.5	92	9
P-M3-4	0.0072	48.4	26	8.5	18	7	19	48.4	100	6
C-M3-6	0.0024	192.0	12	58.0	30	8	9	190.0	99	3
P-M7-1	0.024	16.1	22	16.1	100	106	106	16.1	100	22
C-M7-1	0.024	18.5	19	18.5	100	87	87	18.5	100	19
C-M7-6*	0.0048/ 0.024	74.5 - 1.8	4/19	40.4/1.8	54/100	4/88	8/88	74.5/1.8	100	3/19

Table 2. Continued

P-G 11/8-2	0.08	5.1	17	4.0	78	42	82	5.1	100	15
C-G 11/8-4	0.08	4.5	10	4.5	100	38	38	4.5	100	10
C-G 11/6-2	0.024	17.0	13	14.5	85	58	69	17.0	100	12
P-G6-1	0.08	2.0	0	1.6	80	2	2	1.6	80	0
C-G6-1	0.06	3.0	5	0.7	23	4	113	3.0	100	5
P-G 11/7-4	0.08	4.8	25	4.8	100	98	98	4.8	100	25
C-G 11/7-4	0.08	4.5	25	4.5	100	103	103	4.5	100	25

NOTE: All values of Δu_D > 72 gm/cm^2 are extrapolated.

*Dual rate test. Rate increased to 0.024%/min after 74.5 hrs.

Table 3. Results from the Consolidation Tests

Figure	Test	Sample Trimming Time Hrs.	w %	e_o	S_o %	γ_m gm/cm^3	C_c	Casagrande p'_c gm/cm^2	Casagrande p'_c/p'_o	Sowers p'_c gm/cm^2	Sowers p'_o	Max. T. Variation Per Test °C	Average Test T. °C
(Depth of Samples--cm)	B-H4-4		141	4.03	88	1.28	1.55	82	2.62	48	1.51		
	C-H4-6		146	4.08	91	1.31	1.68	68	2.02	58	1.57	2.5	18.5-25.5
	C-H4-7		146	4.02	92	1.31	1.55	60	2.18	46	1.69		
12 (91-130)	B-H4-7		142	3.96	91	1.31	1.45	82	3.17	45	1.73	0.5	19.0
	C-H4-8		144	3.92	93	1.33	1.44	78	2.87	45	1.67		
	C-H4-4		141	3.71	90	1.31	1.34	75	2.27	45	1.36	3.5	17.0-26.0
	C-H4-5		137	3.84	90	1.31	1.45	80	2.32	48	1.38		
		1.0-1.5											
17 (132-180)	B-H4-2		128	3.64	89	1.33	1.35	102	2.41	70	1.65		
	B-H4-5		134	3.74	91	1.33	1.38	82	2.23	55	1.49		
	C-H4-2		129	3.69	88	1.31	1.31	100	2.00	62	1.24	2.5	17.0-21.0
	P-H4-1		133	3.73	90	1.33	1.53	105	2.23	65	1.38		
	P-H4-2		132	3.72	90	1.33	1.57	100	2.06	65	1.34		
30 (140-164)	B-H4-1		124	3.46	90	1.34	1.23	110	2.78	68	1.71		
	C-H4-1		122	3.38	92	1.38	1.23	132	3.23	82	2.01	8.0	17.5-19.0
	C-H4-2		120	3.37	90	1.34	1.25	122	2.80	78	1.70		

Table 3. Continued

18 (96-118)	C-H6-1	1.5-1.8	134	3.70	92	1.34	1.52	120	3.87	82	2.66	1.5	19.0-23.0
	P-H6-1		131	3.72	90	1.33	1.71	128	3.70	88	2.54		
	P-H6-3		152	4.09	96	1.34	1.92	125	4.62	90	3.33		
	B-H6-1		141	3.95	91	1.31	1.79	120	3.87	82	2.08		
21 (99-127)	B-H20-1	0.8-1.5	103	2.91	93	1.46	1.00[1]	108[1]	2.29[1]	78[1]	1.65[1]	3.5	16.0-19.0
	B-H20-3		101	2.91	93	1.44	1.03	110	2.56	78	1.80		
	B-H20-4		101	2.86	94	1.46	1.02	130	2.52	80	1.55		
	C-H20-2		107	2.83	97	1.48	1.02	115	2.57	83	1.83		
	C-H20-3		99	2.62	97	1.51	0.99	120	2.24	78	1.45	1.5	20.5-22.0
	P-H20-2		98	2.61	96	1.51	1.05	120	2.48	90	1.86		
16 (132-158)	B-M3-4	1.5-1.8	142	3.97	94	1.36	1.26	75	1.69	52	1.18	1.5	20.0-21.0
	C-M3-5		149	4.01	97	1.38	1.25	80	1.93	52	1.26		
	C-M3-6		142	4.04	95	1.38	1.22	80	1.74	60	1.30		
	C-M3-7		147	4.00	95	1.36	1.20	72	1.48	52	1.07		
	P-M3-4		146	3.91	96	1.38	1.31	75	1.59	58	1.22		
16 (132-158)	B-M3-4	1.5-1.8	142	3.97	94	1.36	1.26	75	1.69	52	1.18	1.5	20.0-21.0
	C-M3-5		149	4.01	97	1.38	1.25	80	1.93	52	1.26		
	C-M3-6		142	4.04	95	1.38	1.22	80	1.74	60	1.30		
	C-M3-7		147	4.00	95	1.36	1.20	72	1.48	52	1.07		
	P-M3-4		146	3.91	96	1.38	1.31	75	1.59	58	1.22		

Table 3. Continued

20 (197-224)	B-M7-1	1.0-1.5	139	4.03	95	1.38	1.27	82	1.37	52	0.88	1.5	17.0-20.5
	C-M7-1		136	4.07	92	1.36	1.28	85	1.33	62	0.89		
	B-M7-2		143	4.20	94	1.39	1.32[1]	75[1]	1.21[1]	50[1]	0.81[1]	3.0	20.0-20.5
	C-M7-6		147	4.23	95	1.38	1.29[2]	74	1.27[2]	54[2]	0.93[2]		
	P-M7-1		132	3.80	96	1.41	1.32	110	1.69	68	1.03		
13 (48-66)	B-G6-1	0.8-1.0	57	1.68	91	1.67	0.32	295	7.39	215	5.38	1.0	17.0-19.0
	C-G6-1		56	1.61	92	1.69	0.31	280	9.33	188	6.25		
15 (56-65)	C-G 11/8-4	1.5	122	3.25	95	1.43	1.37	112	2.07	72	1.33	2.5	20.0-21.0
	P-G 11/8-2		127	3.36	97	1.43	1.42	105	1.69	70	1.13		
14 (85-109)	B-G 11/7-4	0.8-1.5	181	4.82	95	1.38	2.96	155	1.19	115	0.88	2.0	20.5-21.0
	C-G 11/7-4		197	5.06	97	1.30	3.08	160	1.69	130	1.38		
	P-G 11/7-4		209	5.32	97	1.30	2.80	140	1.44	112	1.15		
19 (83-102)	B-G 11/6-4	0.8-1.3	197	3.97	94	1.31	2.06[1]	182[1]	1.96[1]	140[1]	1.50[1]	3.0	20.0-20.5
	C-G 11/6-2		156	4.19	96	1.34	2.30	198	1.68	160	1.36		

Table 3. Continued

	P-G6-1[3]	0.8	63	1.86	91	1.62	0.31	225	10.45	110	5.11	1.0	18.5
	B-G8-1[3]	0.8	61	1.71	94	1.66	0.78	485	12.5	350	8.98	0.5	19.0
	Remolded Material												
28	RC-H4-1		120	3.42	92	1.33							
	RP-H4-1		120	3.36	93	1.34							
29	RC-H20-1		92	2.64	92	1.43							
	RP-H20-1		93	2.68	92	1.43							
26	RC-G6-1		51	1.57	88	1.64							
	RP-G6-1		54	1.61	90	1.64							
27	RC-M3-1		129	3.56	95	1.36							
	RP-M3-1		130	3.70	94	1.34							

[1] R_f values are:

Test	C_c	p_c'	p_c'/p_o'	p_c'	p_c'/p_o'
B-H20-1	1.00	90	1.91	65	1.38
B-M7-2	1.36	62	1.01	45	0.73
B-G 11/6-4	2.06	130	1.40	110	1.18

[2] If the change in rate of strain is ignored, these values are (respectively): 1.56, 1.32, and 1.02.

[3] Data not shown on ϵ-log $\Delta\sigma'$ plots.

Table 4. Comparison of Selected Standard Consolidation Tests

Test	LIR	S_o %	e_o	$\frac{(1)}{(1)+(2)}$ %	$\frac{(3)}{(1)+(2)+(3)}$ %
B-H20-1	1.0	93	2.91	1	29
B-M7-2	1.0	94	4.20	1	36
B-G 11/6-4	1.0	94	3.97	3	39
B-H4-2	0.5	89	3.64	5	
B-M3-4	1.0	94	3.97	2	
B-G6-1	1.0	91	1.68	7	

(1) = Settlement caused by initial compression.

(2) = Settlement caused by primary consolidation

(3) = Settlement caused by secondary compression (24-hour load increment duration)

Figures 12 through 21 present sets of curves that resulted from tests on samples that were similar enough to compare in relation to curve shape. In Table 3 these sets are further subdivided into groups so that values of C_c and p_c' can be compared for samples that are considered to be *almost exactly similar*.

Figure 12 compares five CRS tests, each conducted at differing rates of strain to two standard tests where the sample was loaded as soon as primary consolidation was completed. The cores presented in Figures 13 through 18 in most cases compare CRS tests with and without back pressure to standard tests where sample loading occurred at R_{100}. In the case of the cores from Doboy Sound (Figures 14 and 15) back pressures of 36 kg/cm^2 were used, even though the material was obtained from water depths of only about 10 m. Figure 13 has no test with back pressure plotted because the back pressure test from this core had a significantly different initial void ratio.

Figures 19 through 21 compare CRS tests and standard tests where each load increment was allowed to remain on the sample for 24 hours. For these latter tests the data have been plotted twice--once using the strain occurring at the end of primary and once for the final strain.

All standard tests were conducted using a load increment ratio (LIR) of one except for test B-H4-2 (LIR equals 0.5) and test B-G 11/7-4 (LIR equals 1.0, 0.5, 1.0). Testing time for most standard tests ranged between 1.0 and 6.5 hours. For tests where loads were allowed to remain on the samples for 24 hours, times ranged between 188 and 216 hours. Duration of CRS tests ranged from 2 to 192 hours (see Tables 1 and 2.

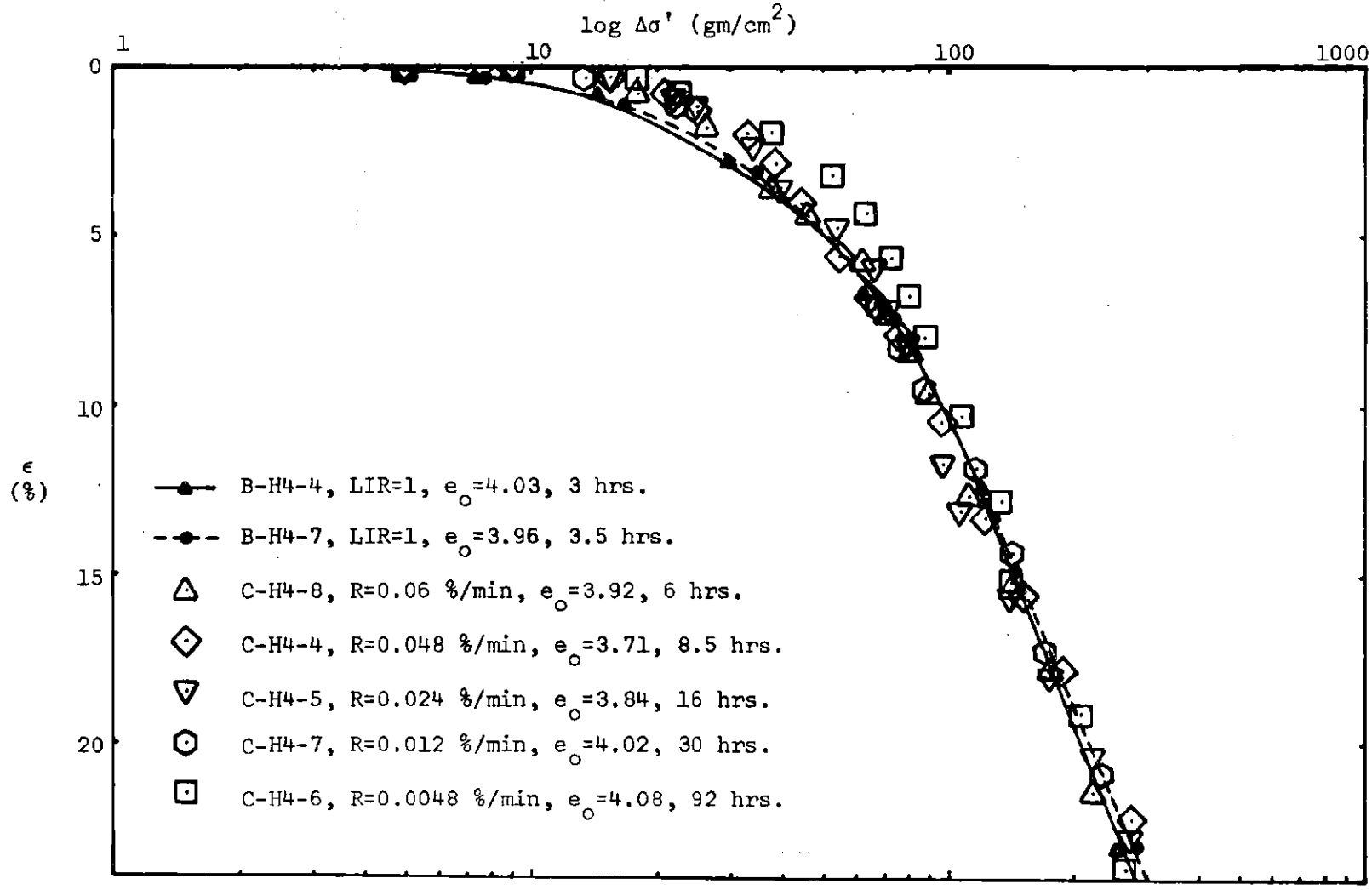

Figure 12. Effect of Rate of Strain on CRS Tests

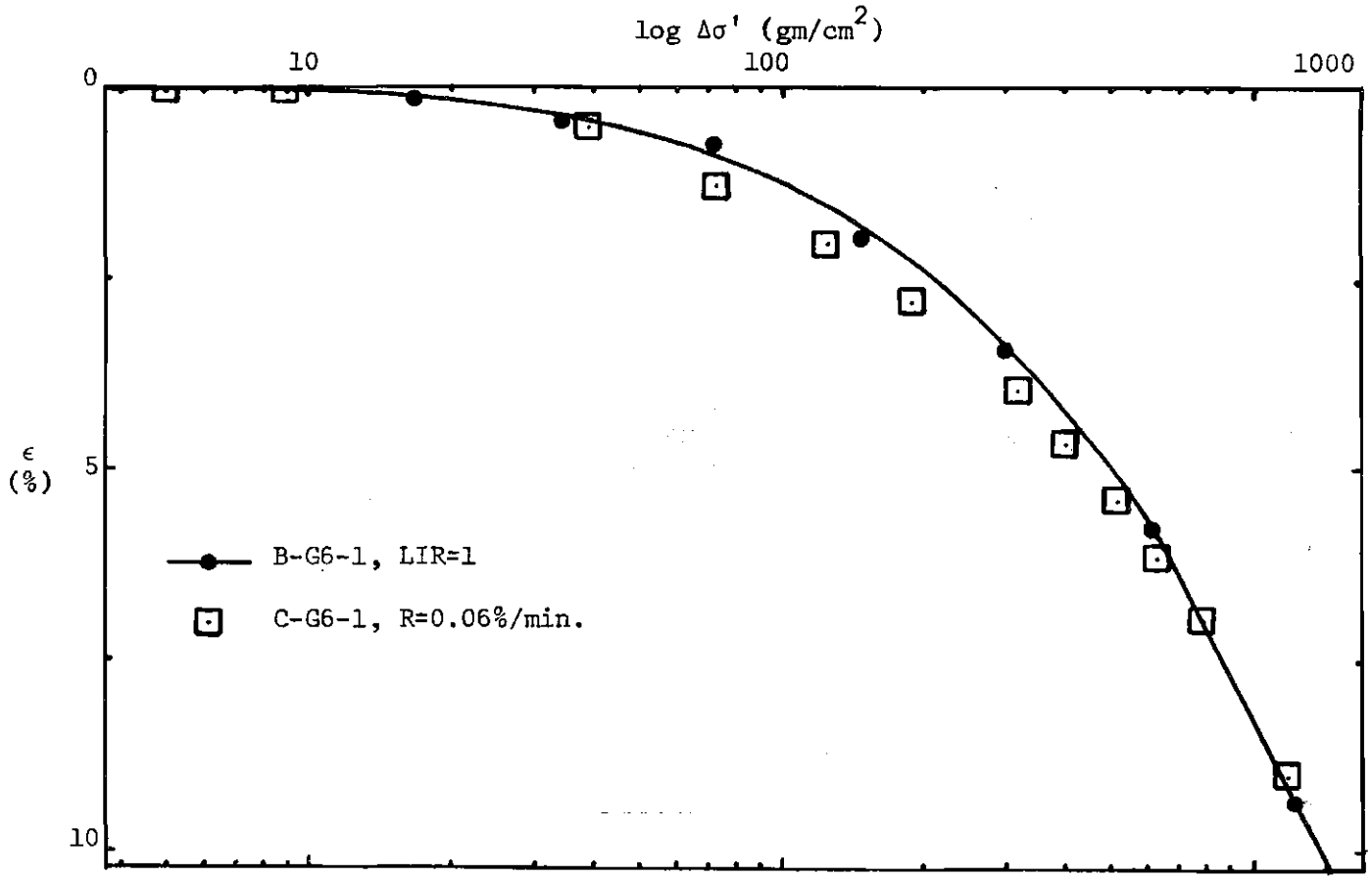

Figure 13. Comparison of CRS and Standard Tests (Florida-Hatteras Slope)

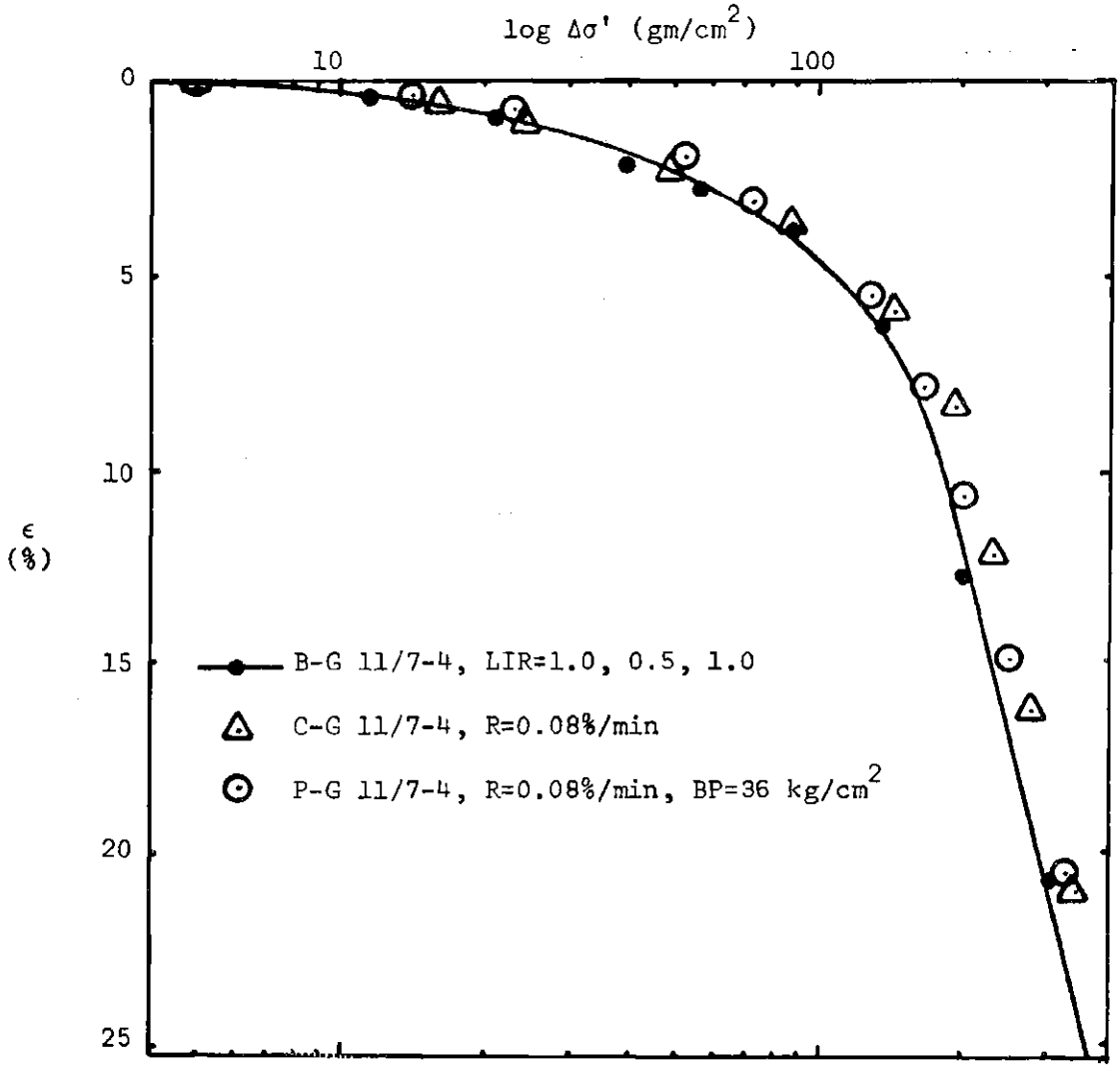

Figure 14. Comparison of CRS and Standard Tests (Doboy Sound, Georgia)

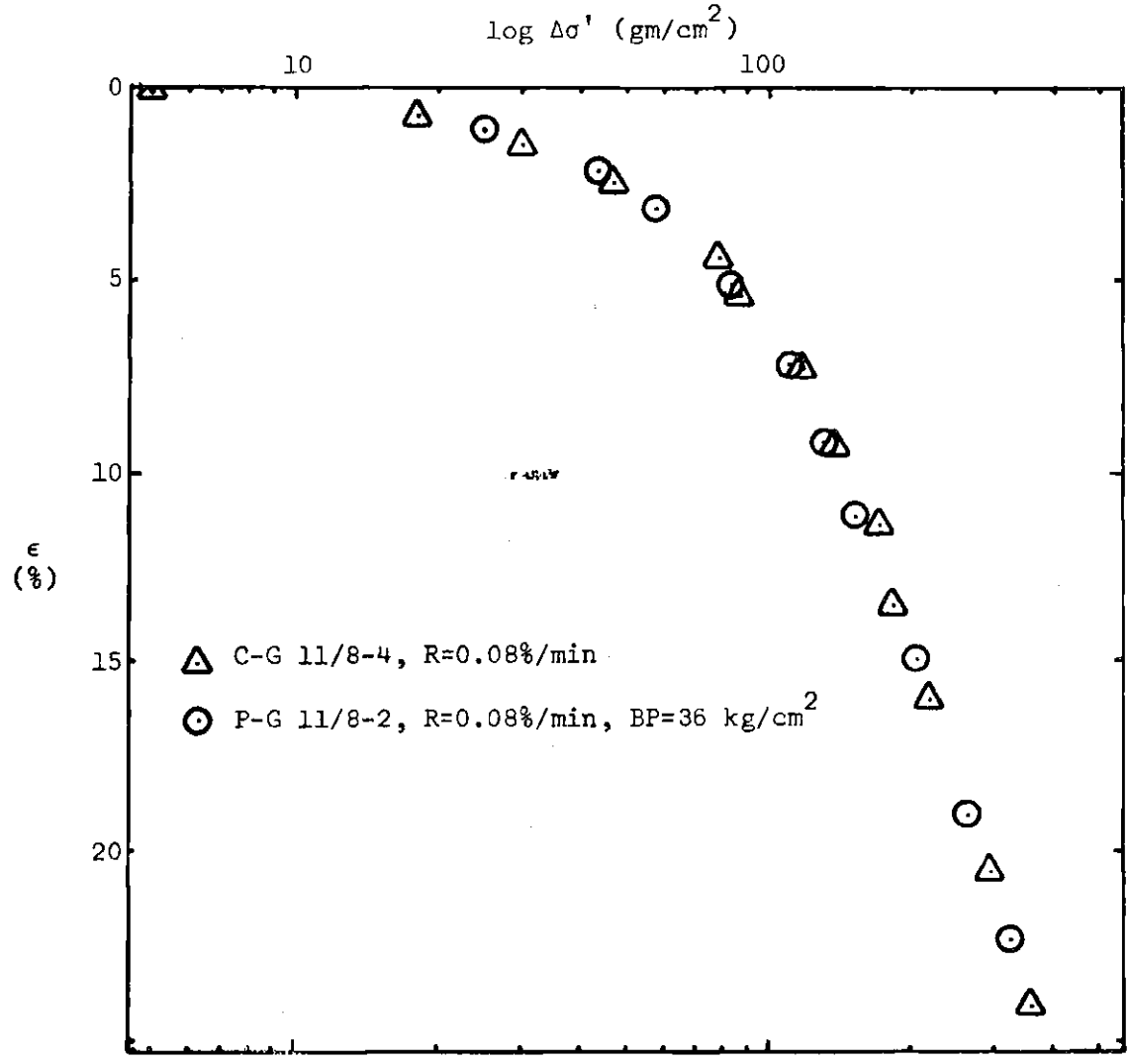

Figure 15. Comparison of CRS Tests with and without Back Pressure (Doboy Sound, Georgia)

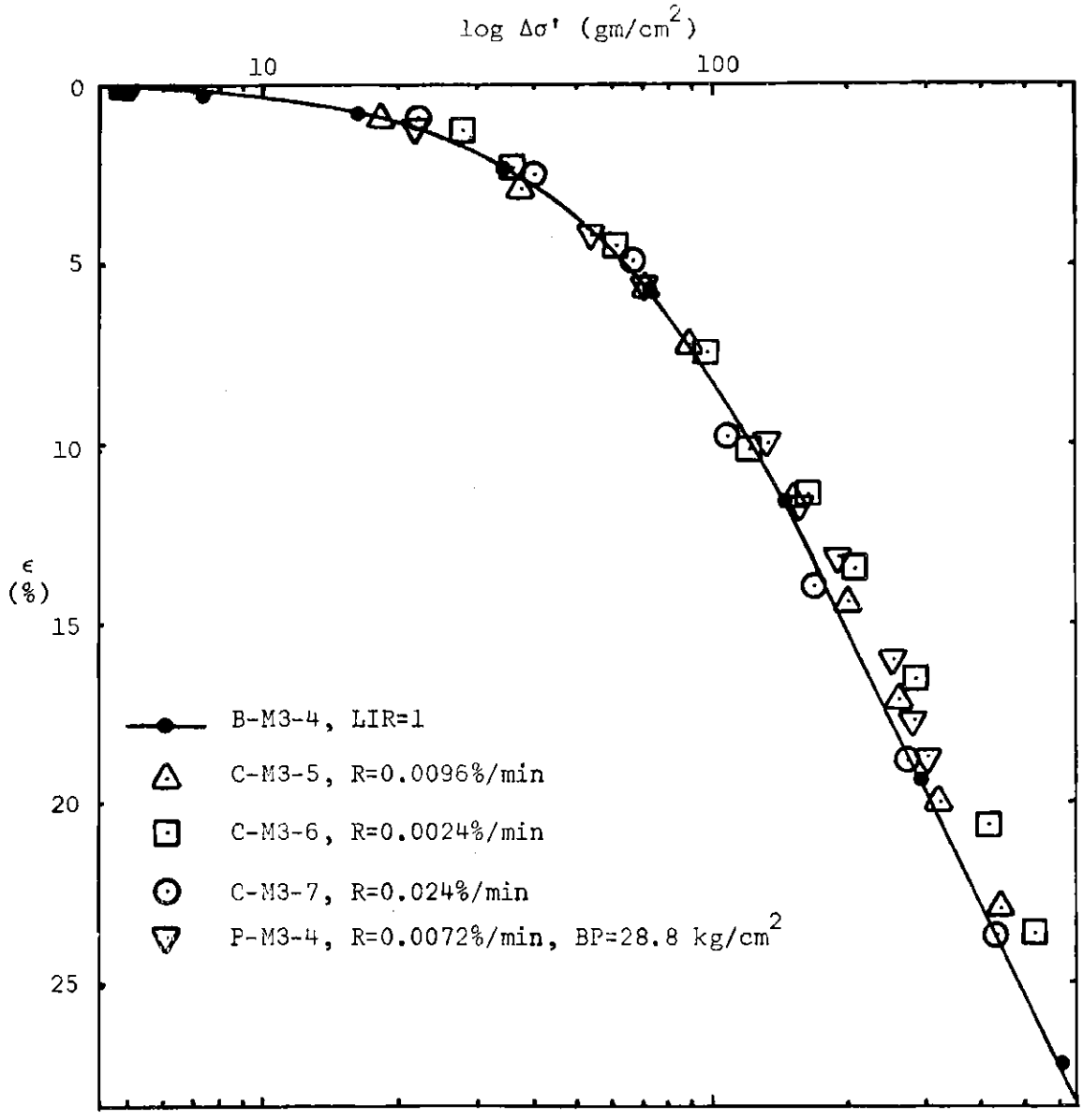

Figure 16. Comparison of CRS and Standard Tests (Gulf of Maine)

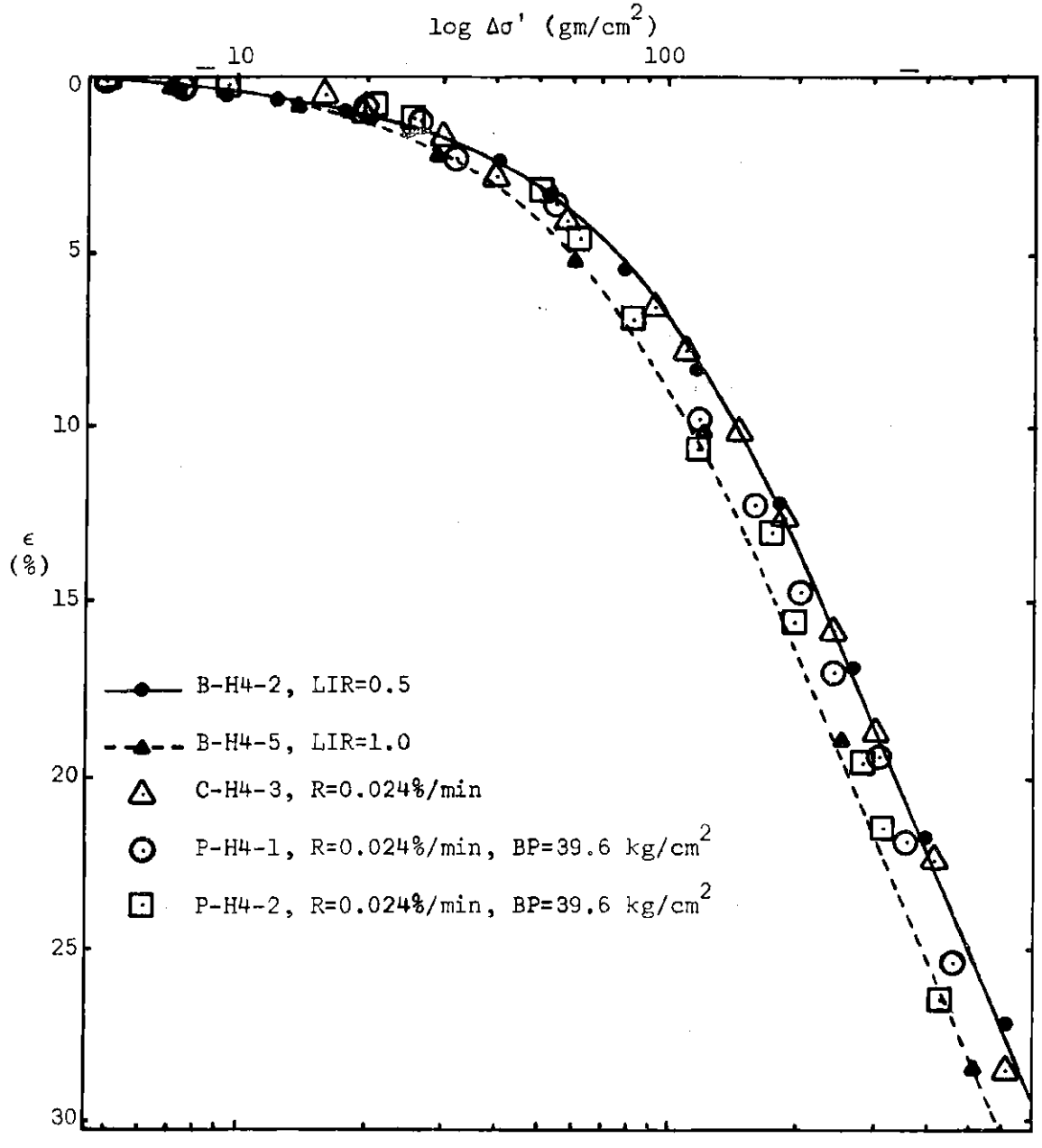

Figure 17. Comparison of CRS and Standard Tests (Hudson Submarine Canyon--H4)

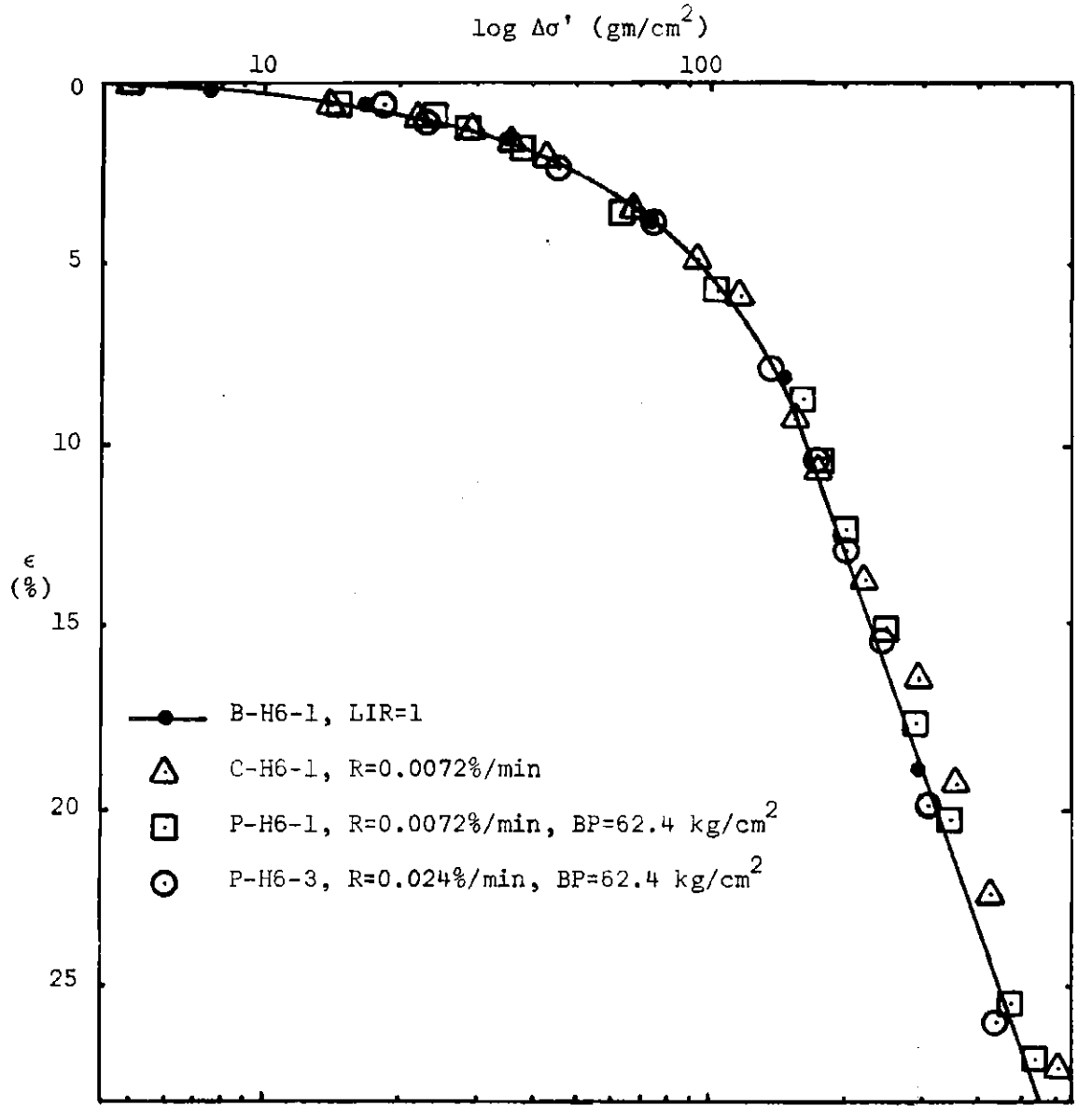

Figure 18. Comparison of CRS and Standard Tests (Hudson Submarine Canyon--H6)

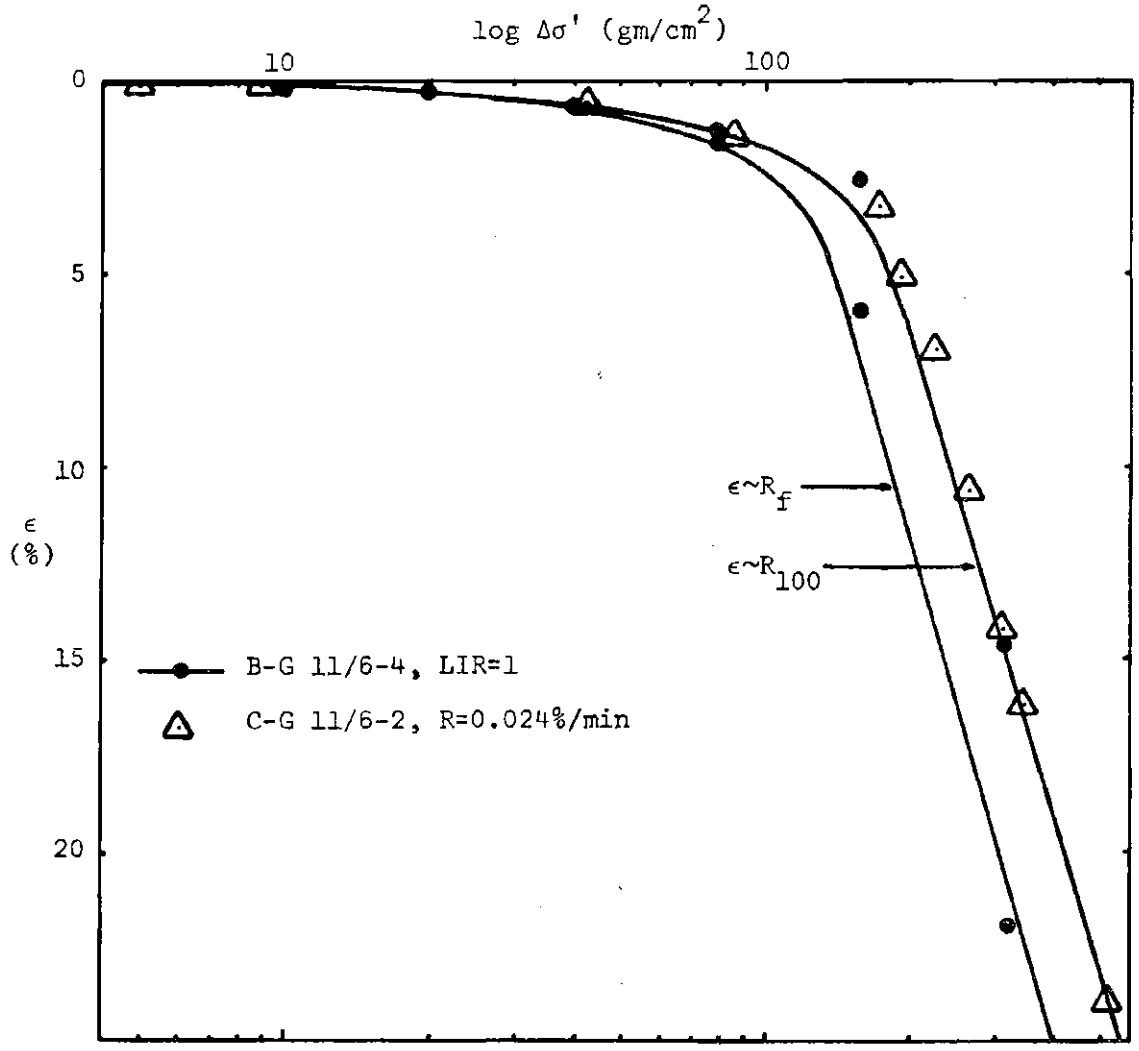

Figure 19. Comparison of CRS and Standard Tests with Load Increment Durations of 24 Hours (Doboy Sound, Georgia)

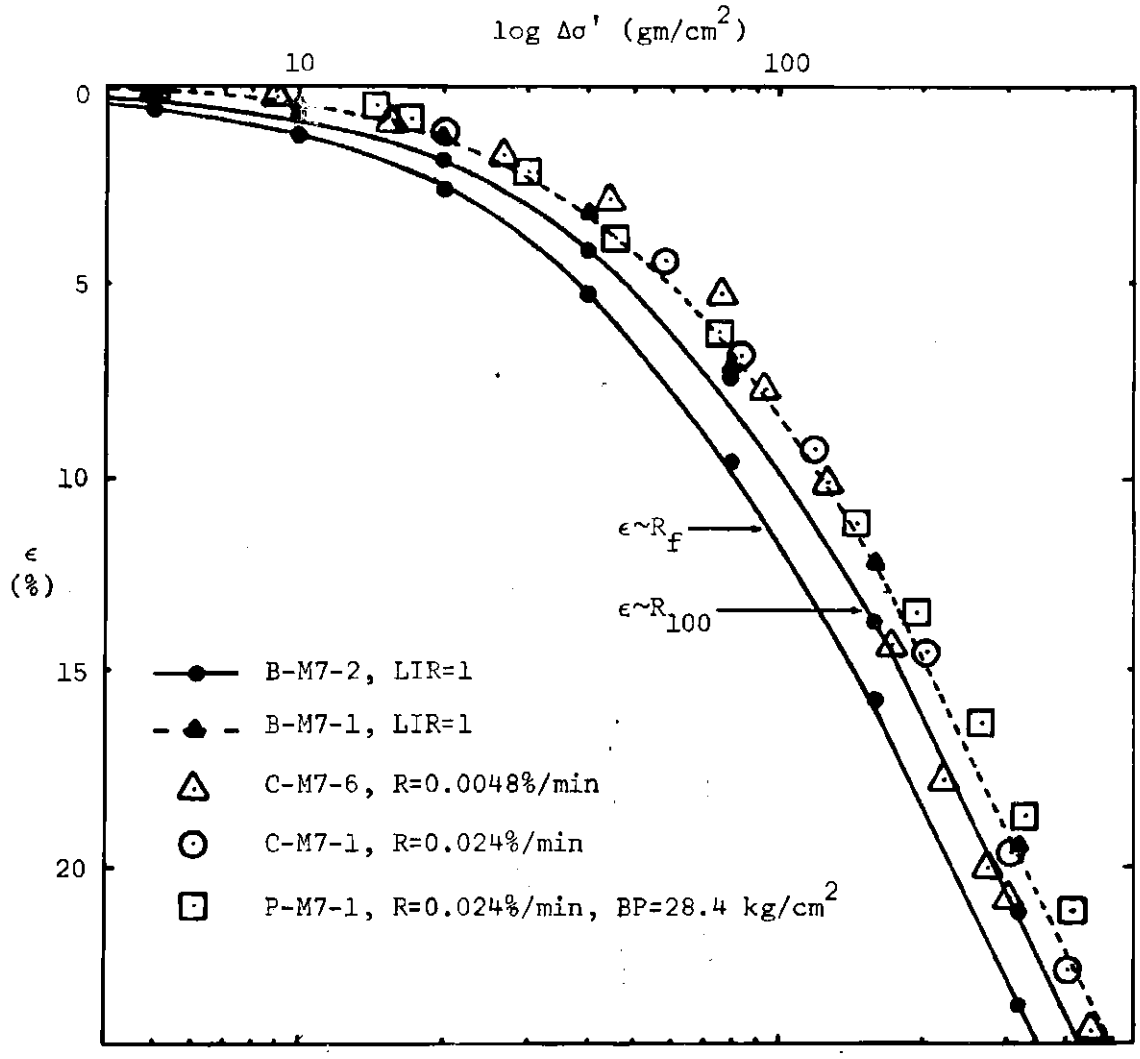

Figure 20. Comparison of CRS and Standard Tests with Load Increment Durations of 24 Hours (Gulf of Maine)

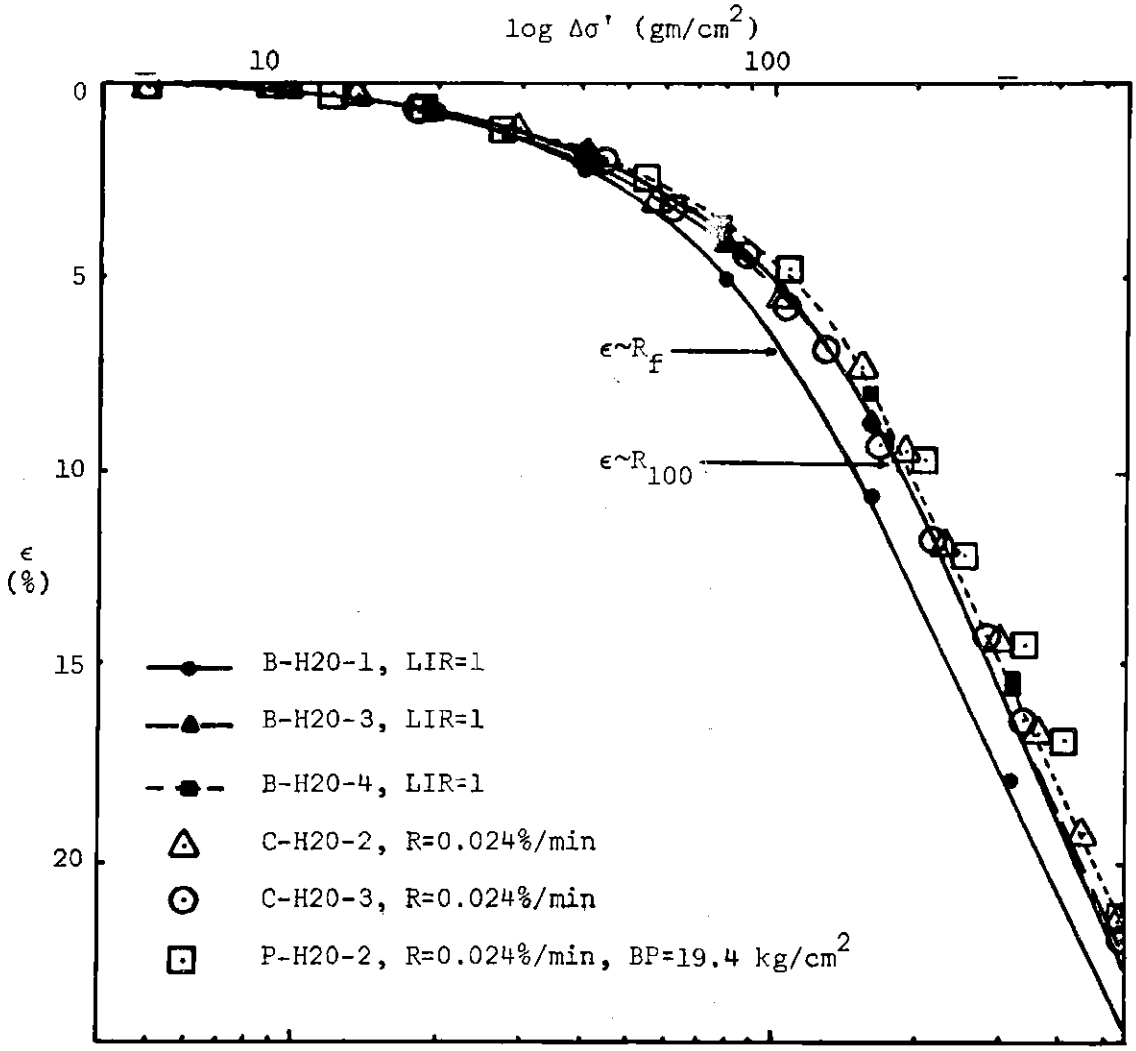

Figure 21. Comparison of CRS and Standard Tests with Load Increment Durations of 24 Hours (Hudson Submarine Canyon)

Excess Pore Pressure Measurement in the CRS Tests

Base pore pressures during the CRS tests varied considerably from test to test, and within a given test. Table 2 summarizes pore pressures measurements in relation to total applied stress. The range of $(\Delta u_b/\Delta\sigma)_{max}$ was 0 to 50%, with maximum values obtained in the Hudson Submarine Canyon material and minimum values obtained in the Georgia Coast samples (for comparable rates of strain). For rates of strain less than 0.024%/min. $(\Delta u_b/\Delta\sigma)_{max}$ was generally less than 10% for all material. There was no pattern as to time of occurrence of $(\Delta u_b/\Delta\sigma)_{max}$.

It was generally found that $(\Delta u_b)_{max}$ did not coincide with $(\Delta u_b/\Delta\sigma)_{max}$, but was associated with the end of the test when the applied total stress was a maximum. As the rate of strain increased, $\Delta u_{b_{max}}$ also increased. Values of $(\Delta u_{b_{max}}/\Delta\sigma)$ ranged from 0 to 30% and were generally less than 10% for rates of strain less than 0.024%/min.

The previous information on base pore pressure relates only to tests on relatively undisturbed sediments. Eight tests (data presented later in this Chapter) were conducted on remolded material. For these tests $(\Delta u_b/\Delta\sigma)_{max}$ ranged from 25 to 96% where the samples were subjected to elevated back pressure, and from 61 to 100% for non-pressurized samples. In all cases $\Delta u_{b_{max}}$ occurred at the end of the test. In most cases $(\Delta u_{b_{max}}/\Delta\sigma)$ was much less than $(\Delta u_b/\Delta\sigma)_{max}$.

Rates of Strain

The range of rates of strain used in the testing program varied from 0.0024%/min to 0.06%/min. Most tests were run at a rate of 0.024%/min (see Table 2). In general, if the material was relatively coarse,

or was rich in kaolinite, rates greater than 0.024%/min insured that $(\Delta u_b/\Delta\sigma)_{max}$ remained less than 50% during the test. All tests except two were conducted at a single rate of strain that was continuously applied from the beginning to the end of the test (i.e. the loading machine was not stopped during the test). Test C-H4-2 (data presented later in this Chapter) was halted for 24 hours when the test was in the region of the apparent preconsolidation pressure.

Two rates of strain were used in test C-M7-6. On Figure 20 all data points for this test except the last two represent a rate of strain of 0.0048%/min. The last two points resulted from an increased rate (0.024%/min). The effect of an immediate jump in the ratio $(\Delta u_b/\Delta\sigma)$ caused the curve to begin to become less steep.

Separation of Primary and Secondary in Standard Tests

Because the Taylor square-root of time method of separating primary and secondary effects allows prediction of the end of primary before secondary effects become significant, it is considered to be better suited for use with submarine sediments (see also Appendix D).

Compression Index

Values of strain were plotted directly on an ϵ-log $\Delta\sigma'$ diagram which was found to be much easier to use and better adapted to comparing several consolidation tests than the conventional e-log $\Delta\sigma'$ diagram.

It was also shown in Appendix D that values of C_ϵ from ϵ-log $\Delta\sigma'$ plots could be easily converted to C_c values for use in settlement analyses. Table 3 lists values of C_c determined from the various curves in Figures 16 through 21. For any particular figure where initial void

ratios are comparable, there was no *significant* variation in C_c between the B and C series tests shown on the figure. Where initial void ratios were similar, a *slightly* greater value of C_c was found for tests conducted with *in situ* hydrostatic pressure (P series tests) compared to comparable tests conducted at atmospheric pressure (C series tests). Table 5 lists these comparisons.

Table 5. Variation in C_c Among Various Tests

Test	Back Pressure kg/cm^2	e_o	C_c	P_c'* gm/cm^2
B-H4-2	A	3.64	1.35	70
B-H4-5	A	3.74	1.38	55
C-H4-3	A	3.69	1.37	62
P-H4-1	39.6	3.73	1.53	65
P-H4-2	39.6	3.72	1.57	65
C-H6-1	A	3.70	1.52	82
P-H6-1	62.4	3.72	1.71	88
C-H20-3	A	2.62	0.99	78
P-H20-2	19.4	2.61	1.05	90
B-M3-4	A	3.97	1.26	52
C-M3-5	A	4.01	1.25	52
C-M3-6	A	4.04	1.22	60
C-M3-7	A	4.00	1.20	52
P-M3-4	28.8	3.91	1.31	58
C-G 11/8-4	A	3.25	1.37	72
P-G 11/8-2	36.0	3.26	1.42	70

A = atmospheric pressure
B = standard test
C = CRS test without back pressure
P = CRS test with back pressure
H4,H6 clayey-silt
H20 sandy clayey-silt
M3 silty-clay
G 11/8 clayey-silt

*By Sowers' method.

One exception to this statement does occur. For tests run at rates of strain of 0.0048%/min or less, and as long as $(\Delta u_b/\Delta\sigma)_{max}$ was less than 4%, a different curve shape was found. The ϵ-log $\Delta\sigma'$ from C-H4-6 (Figure 16) and C-M7-6 (Figure 20) plot above the other curves in the region of preconsolidation pressure and then display more steepness in the virgin compression region. The values of C_c determined for these curves are larger than those for comparable tests at faster rates of strain. Where the strain rate is less than 0.0048%/min and $(\Delta u_b/\Delta\sigma)_{max}$ is greater than 4%, this characteristic curve shape is not apparent (test C-M3-6, Figure 20).

In terms of general trends, the great variation in C_c for the Doboy Sound cores (see Table 3) is striking (range--1.37 to 3.08). Values of the compression index from the Gulf of Maine and Florida-Hatteras slope cores were very uniform. Within each of the Hudson Canyon cores the values of C_c varied relatively little, but two trends can be noted as water depth increased:

1. The variation of C_c within the core increased.

2. The values of C_c increased. The averages were 1.02, 1.42, and 1.74, respectively, for H20, H4 and H6.

Comparison of Compression Index with Natural Water Content. A plot of compression index vs. natural water content had no apparent pattern. There was no correlation between the data and the relationship proposed by Nishida (128).

Comparison of Compression Index with Liquid Limit. Figure 22 presents relationships for compression index and liquid limit for some

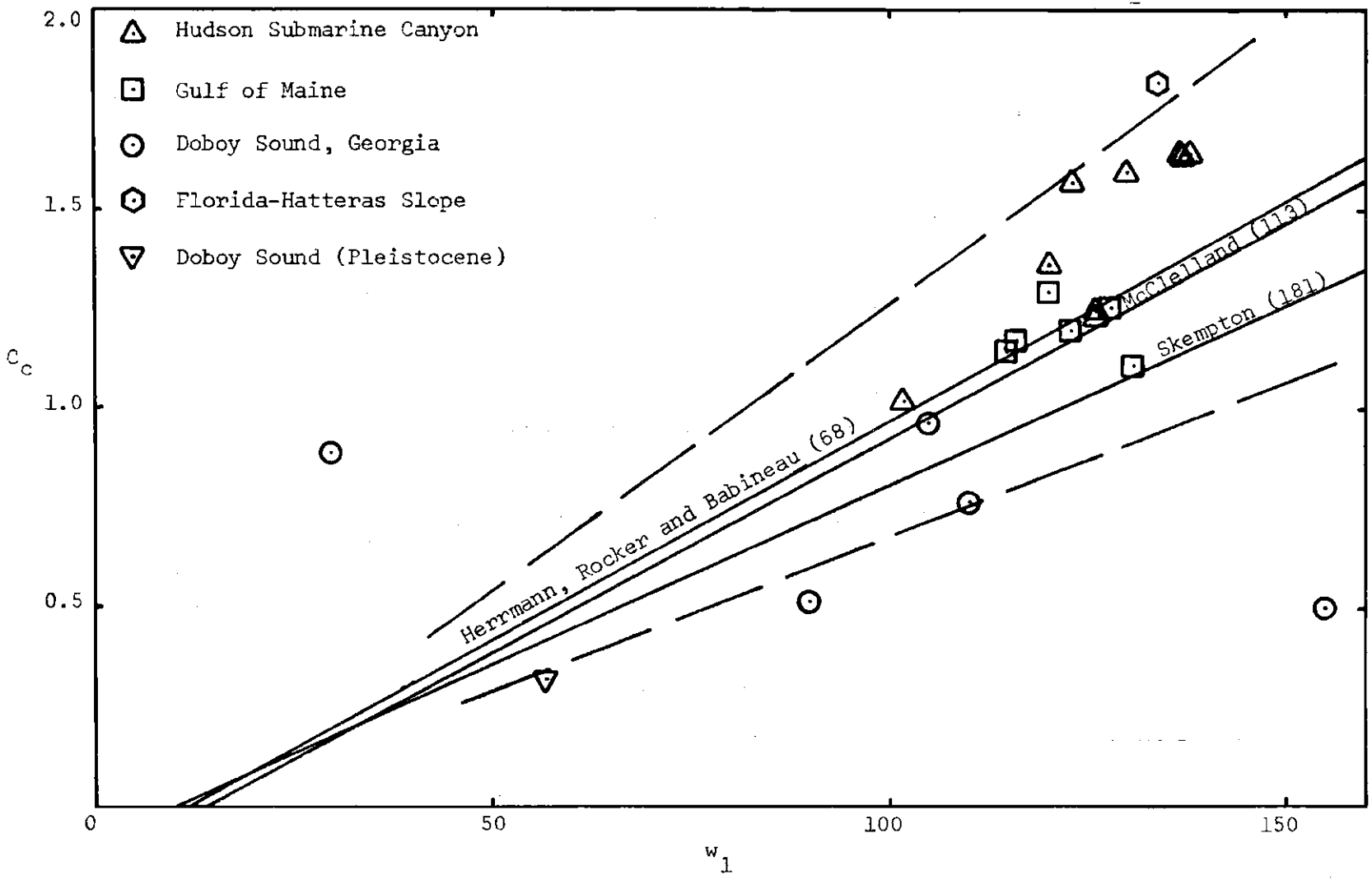

Figure 22. Compression Index vs. Liquid Limit

of the consolidation tests. The relationships proposed by Herrmann, Rocker and Babineau (68), McClelland (113), and Skempton (181), are also indicated on this plot. That of Herrmann, Rocher and Babineau gives the best agreement with the data. For material where the less-than-two-micron fraction was mainly illite and chlorite, the data plots within the ± 30% range that the investigators gave as the range of validity based on work at the Naval Civil Engineering Laboratory, Port Hueneme, California.

Comparison of Compression and Strain Indices with Initial Void Ratio. Variation in initial void ratio gave the most consistent agreement with variation in material compressibility for all cores. Figure 23 shows strain index plotted against initial void ratio. Variation in initial void ratio gave the most consistent agreement with variation in material compressibility for all cores. Figure 23 shows strain index plotted against initial void ratio.

The best correlation between any parameter and C_c was found to be e_o. Figure 24 shows that for material rich in kaolinite and montmorillonite the best relationship between C_c and e_o is described by a line whose equation is:

$$C_c = 0.75\ (e_o - 1.25) \qquad (5)$$

By far the best relationship for the material rich in illite and chlorite was found to be a line represented by the equation (see Figure 24):

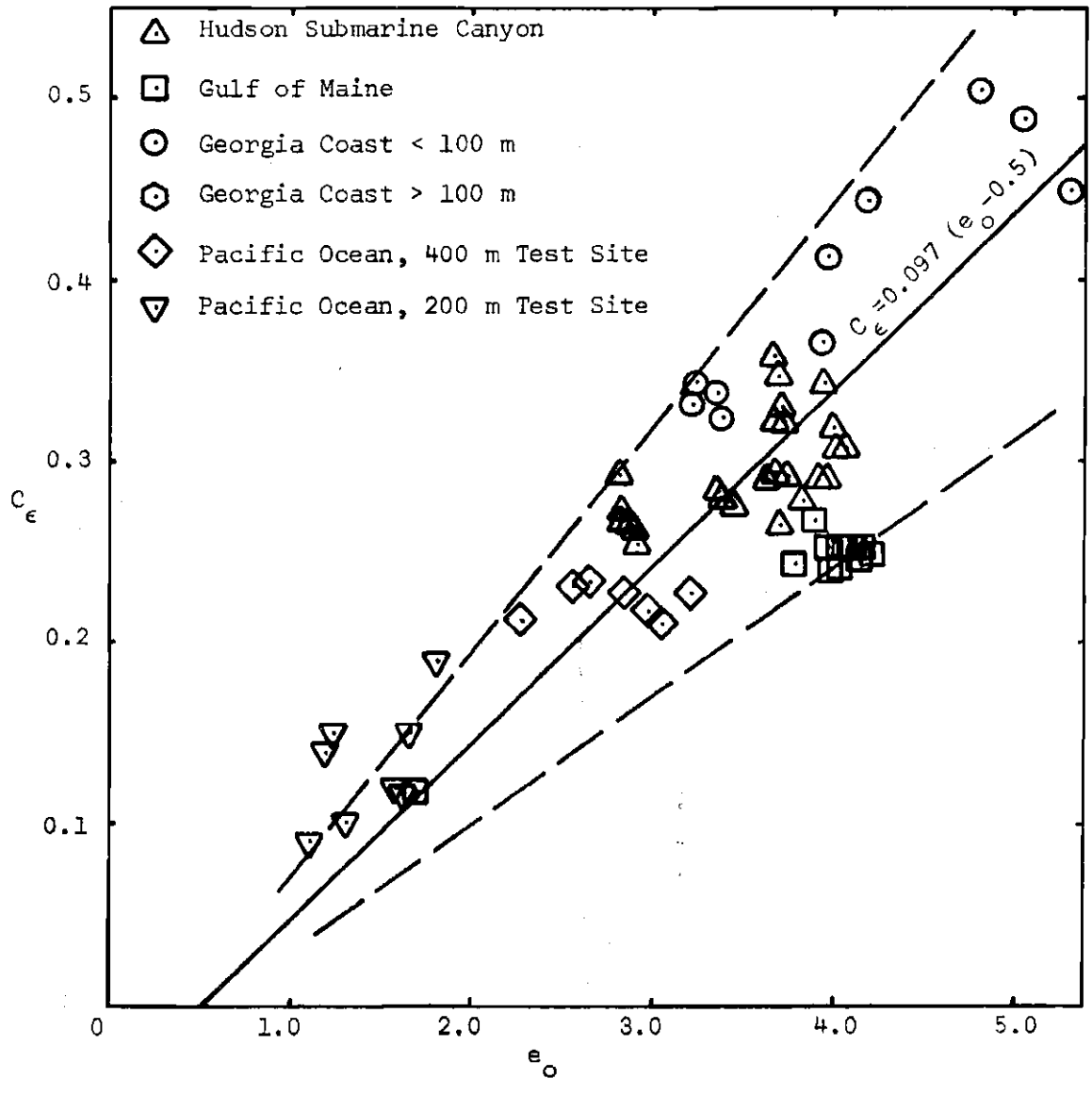

Figure 23. Strain Index vs. Initial Void Ratio

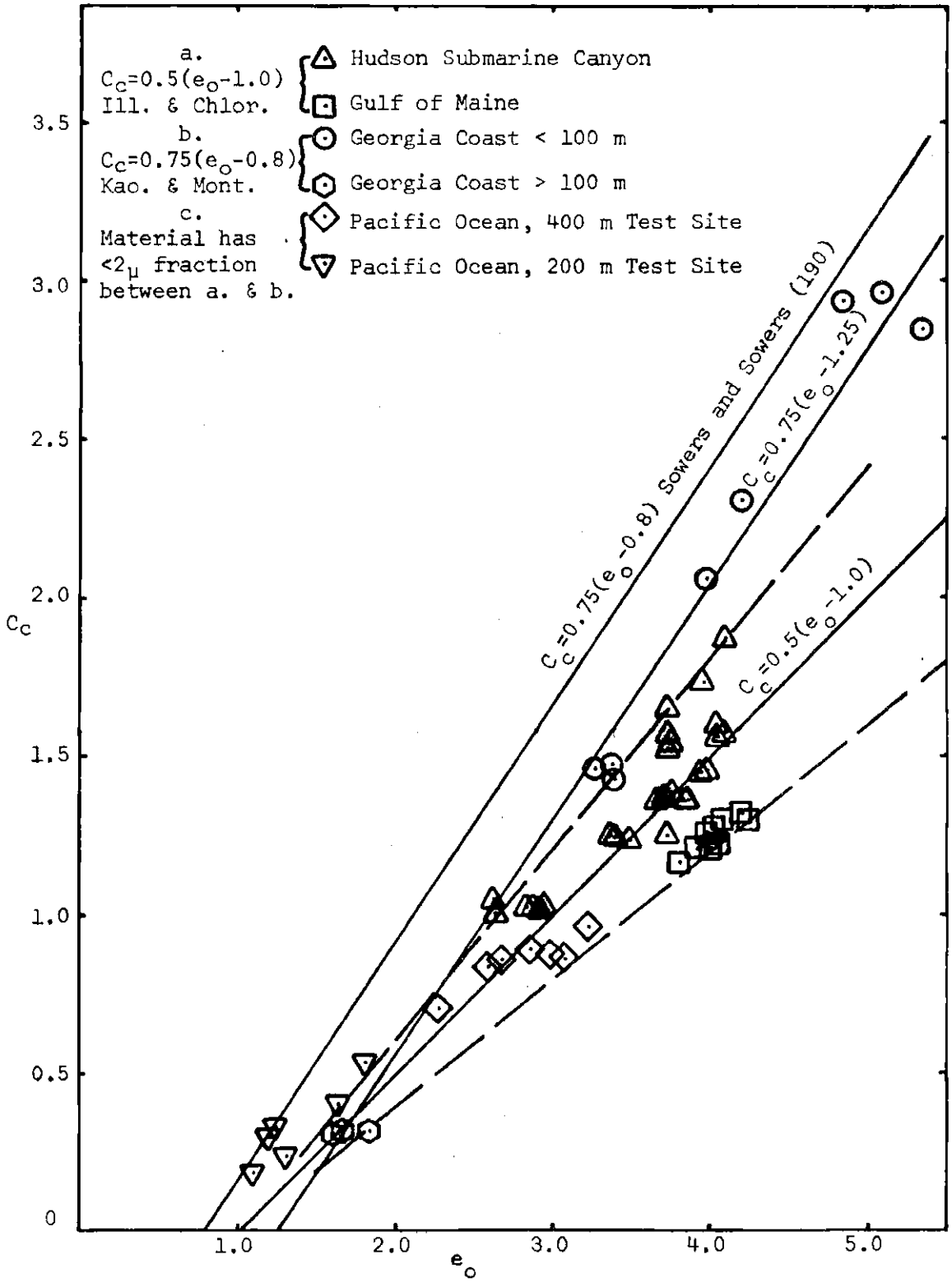

Figure 24. Compression Index vs. Initial Void Ratio

$$C_c = 0.5(e_o - 1.0) \qquad (6)$$

These relationships are patterned after similar ones given by Sowers and Sowers (190). The lower limit of their range of equations, based mainly on work with saprolitic soils, is also shown on the figure. All data from the Gulf of Maine and the Hudson Submarine Canyon plot within ± 20% of the line represented by Equation (6). Data from the Doboy Sound cores generally plot nearer the lower bound proposed by Sowers and Sowers.

On both Figures 23 and 24, data from consolidation tests conducted by the Naval Civil Engineering Laboratory on cores from two foundation test sites are also shown.

c/p' vs. I_p. Figure 25 shows data from five cores where the laboratory vane shear strength is assumed equal to the undrained shear strength. Only five data points are presented because vane shear strength and plastic limit tests were only conducted *together* at *five* locations. In the (a) portion of the figure, the data are plotted with the c/p' ratio being equal to c/p'_o. For terrestrial material this is the standard representation. Bjerrum (13) has shown that for several terrestrial materials c/p'_o vs. I_p data plot as the straight line shown on the figure.

The data points shown plotted in the (b) portion of the figure are for the c/p' ratio equal to c/p'_c, where p'_c was estimated by using Equation (2) with appropriate values from Table 6 (explained on the next page). Very clearly this latter representation more closely

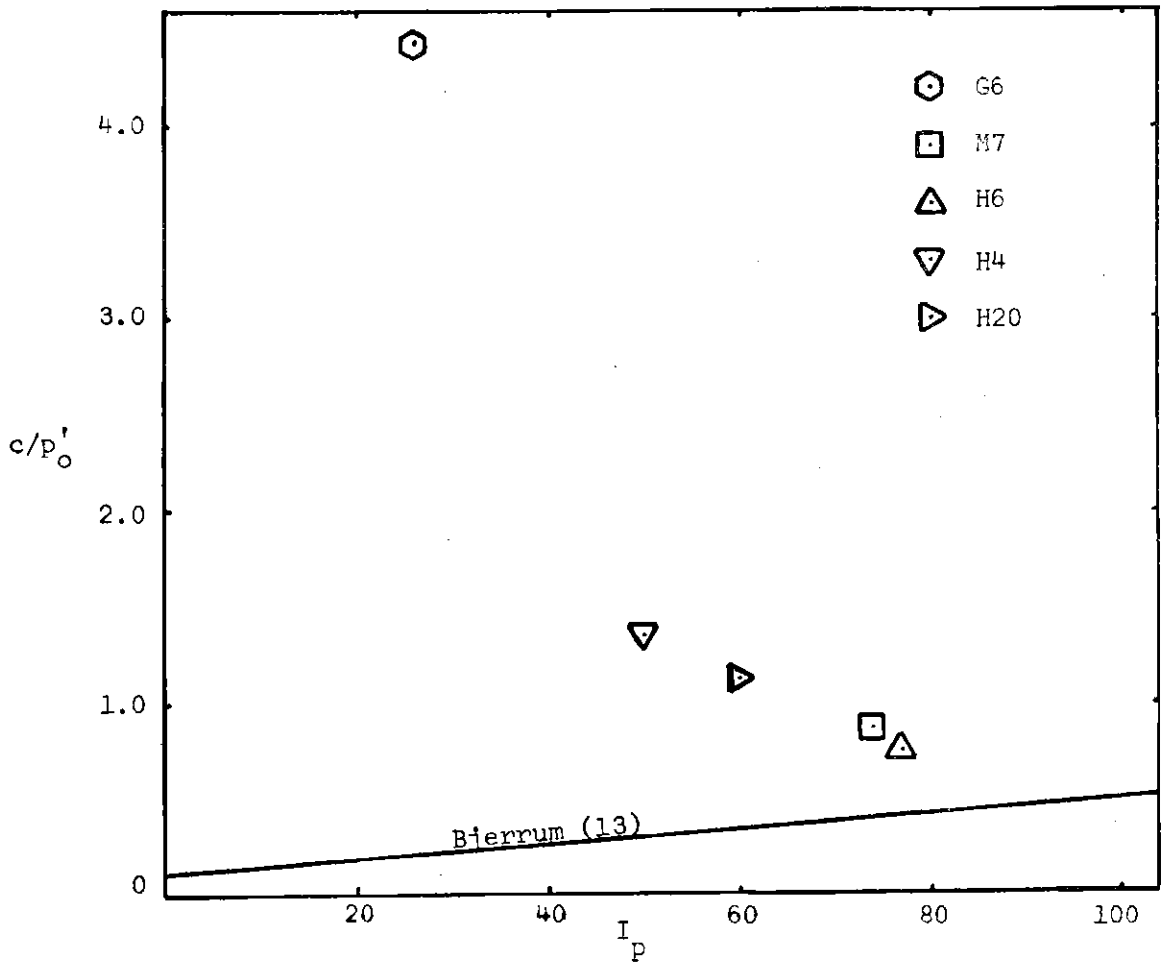

a. Effective Pressure Equals Effective Overburden Pressure

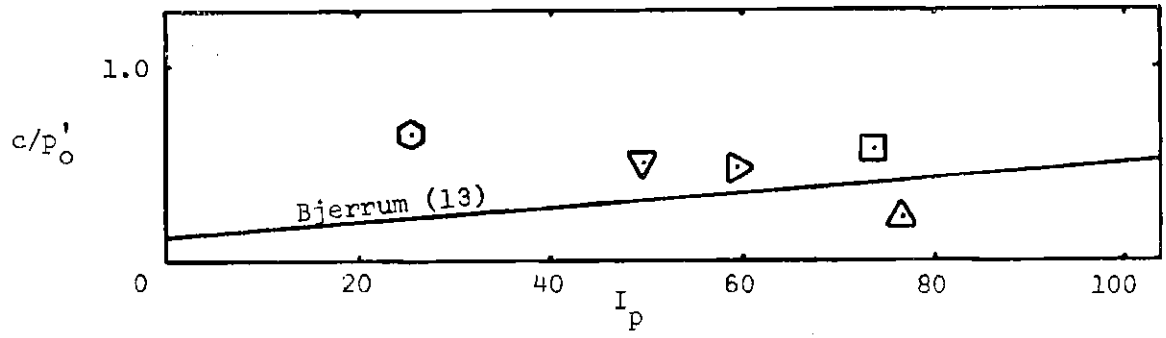

b. Effective Pressure Equals Apparent Preconsolidation Pressure

Figure 25. Ratio of Laboratory Vane Shear Strength to Effective Pressure vs. Plasticity Index

approaches the straight line proposed by Bjerrum.

Preconsolidation Pressure

There was no distinguishable trend in values of p_c' between standard and CRS tests for any given figure. For standard tests where each load increment was allowed to remain on the sample for 24 hours, p_c' for the curves plotted using ϵ values determined from R_{100} was always larger than for curves plotted using ϵ values determined using R_f. Where standard tests were conducted at load increment ratios of one, and CRS tests without back pressure were run so that the ratio $(\Delta u_b/\Delta\sigma)_{max}$ was greater than 4% but less than 50%, the comparable CRS tests with back pressure show a greater value of "apparent preconsolidation pressure" (where p_c' is computed by the Sowers' method). This does not apply to the Doboy Sound cores.

The highest ratios of p_c'/p_o' were found in cores G8 and G6 from off the mouth of the Ogeechee River and from the Florida-Hatteras slope (see Appendix B). The Gulf of Maine cores showed some variation in this ratio. Using the Sowers' method, core M7 seems to have little or no apparent preconsolidation. As with C_c the Hudson Submarine Canyon cores seemed to show a tendency for the ratio (p_c'/p_o') to increase with water depth.

Effect of Water Depth on Apparent Preconsolidation Pressure.

Equation (2) was developed in Appendix C:

$$p_c' = p_o' + \bar{C}_f/\bar{C}\ u_h \qquad (2)$$

An examination of the literature failed to produce any other *quantitative* relationship relating the various factors felt to influence the apparent preconsolidation of submarine sediments. To attempt to verify Equation (2) values of $\bar{C}_f/\bar{C}$ were backfigured from the CRS tests performed at *in situ* hydrostatic pressures. These values are shown in Table 6 along with analogous values for some terrestrial materials given by Skempton (180).*

Table 6. Ratio of Prestress

	Material	Skempton C_s/C*	$\bar{C}_f/\bar{C}$
1.	Vermont Marble	0.08	
2.	Clay (high effective stress)	0.02	
3.	Calcareous Ooze (high effective stress)	0.01	
4.	Core G6 (calcareous sandy-silt)		0.0038
5.	Core H20 (sandy clayey-silt)		0.0022
6.	Dense Sand	0.0015	
7.	Core H6 (clayey-silt)		0.00093
8.	Core H4 (clayey-silt)		0.00045
9.	Core M3 (highly plastic silty-clay)		0.00036
10.	Loose Sand	0.0003	
11.	Overconsolidated Clay	0.00025	
12.	Core M7 (highly plastic silty-clay)		0.000074
13.	Normally Consolidated Clay	0.00003	

*Data from Skempton (180). All values of C_s/C except two and three represent computations for water at atmospheric conditions.

C_s is the compressibility of the solid particles.

C is the compressibility of the material.

*The ratios of $\bar{C}_f/\bar{C}$ and C_s/C are not the same; however, as shown in Appendix C they are analogous.

If Equation (2) is valid, it indicates that *hydrostatic pressure can have a significant effect on the amount of settlement computed for structures founded on soft submarine sediments.* Therefore, additional testing was conducted to try to determine whether or not high hydrostatic pressure could affect compressibility. Figures 26 through 29 were developed from CRS consolidation tests on remolded material. Each figure shows two curves. One curve represents a test where the material was temporarily subjected to high hydrostatic pressure (the pressure was removed before the test was conducted).* The other curve represents a test on an almost identical sample, under identical loading conditions except that the sample was never subjected to high hydrostatic pressure. In every case the sample that had been pressurized proved to be less compressible.

Comparison of Time Required to Conduct Consolidation Tests

Table 7 compares total test time and man-hours required to conduct various standard and CRS tests. For the standard tests, *test duration is increased at least 3000%* by allowing each load increment to remain on the sample 24 hours. In general the standard tests loaded as soon as R_{100} was reached were of the same duration as the faster CRS test; however, in terms of man-hours expended, the CRS tests required about one-third of the effort of the standard tests.

*No measurable change in sample height caused by the application and removal of high hydrostatic pressure was recorded. Possible change in sample height was checked by visually observing the position of a scribe mark on the piston which rests on the top porous stone.

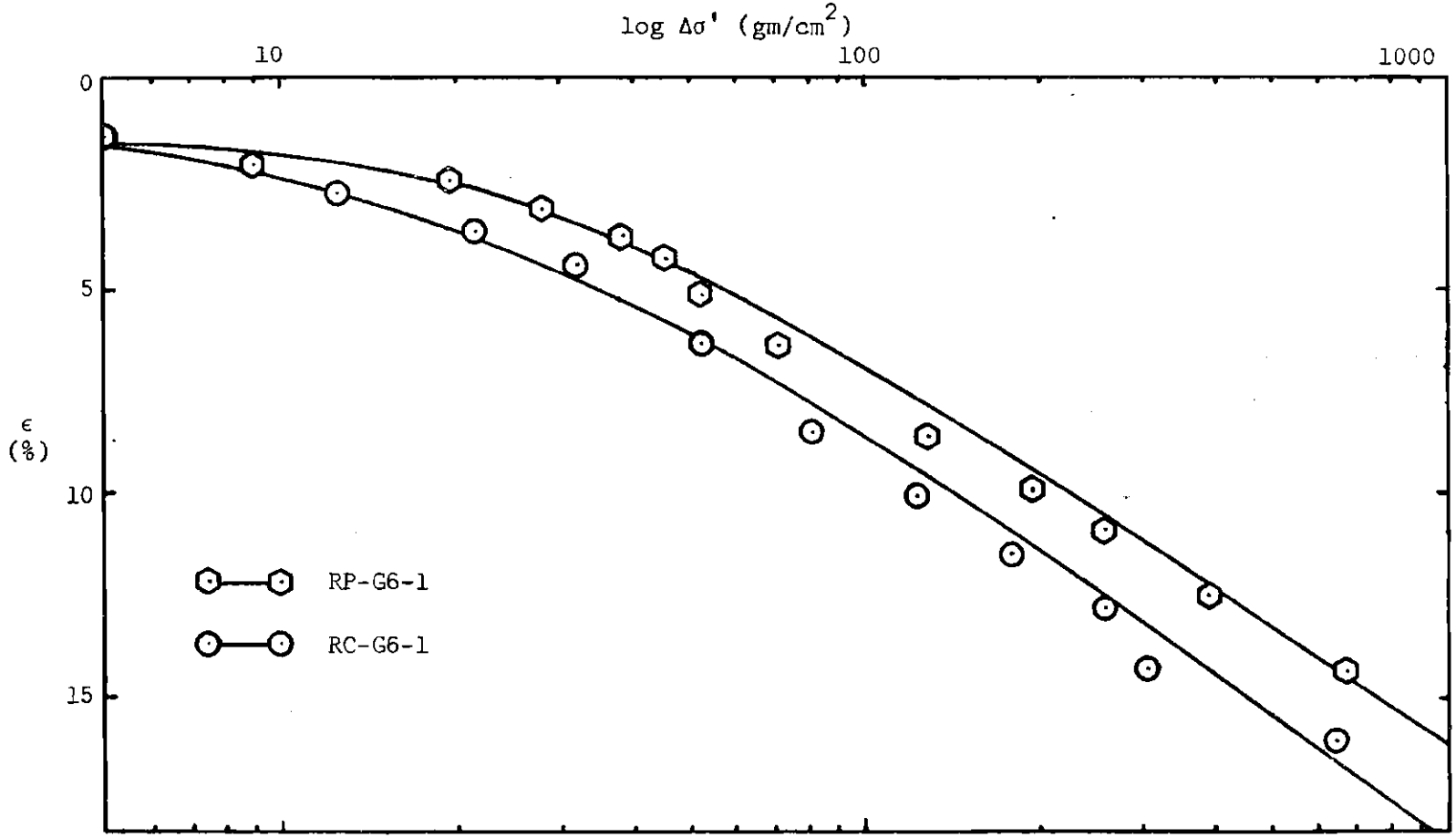

Figure 26. Comparison of Pressurized and Non-pressurized Tests on Remolded Material (Florida-Hatteras Slope)

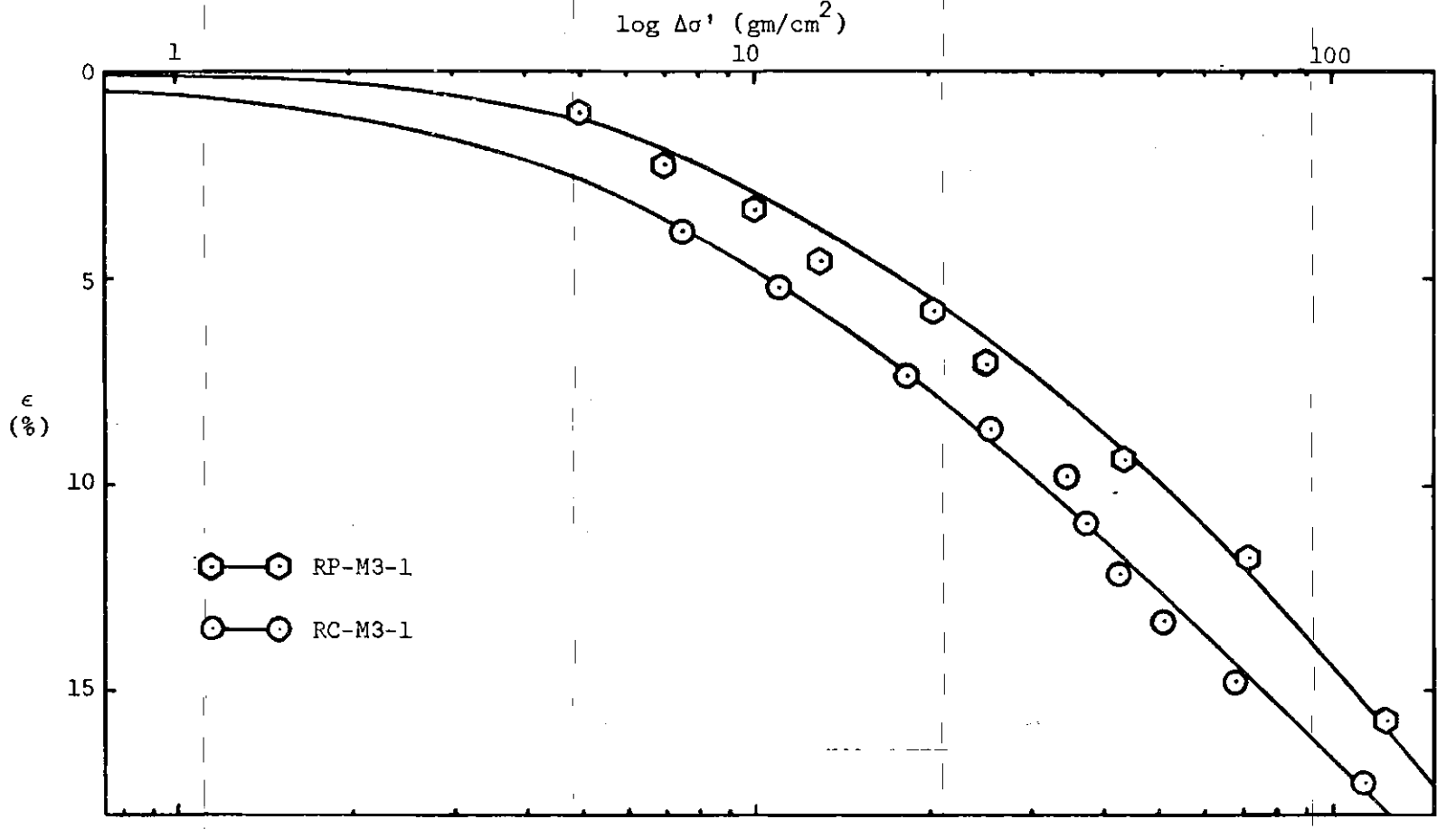

Figure 27. Comparison of Pressurized and Non-pressurized Tests on Remolded Material (Gulf of Maine)

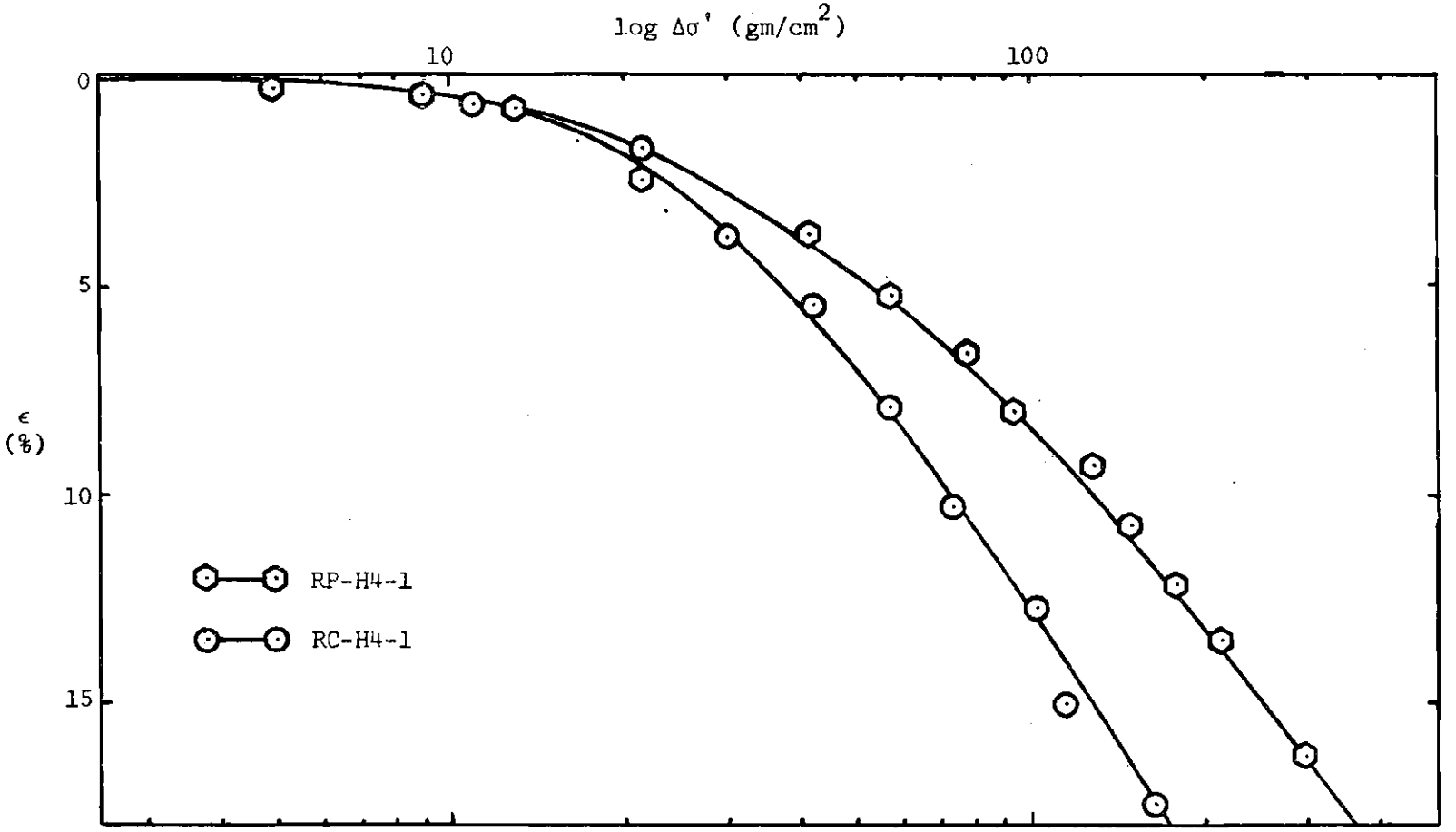

Figure 28. Comparison of Pressurized and Non-pressurized Tests on Remolded Material (Hudson Submarine Canyon--H4)

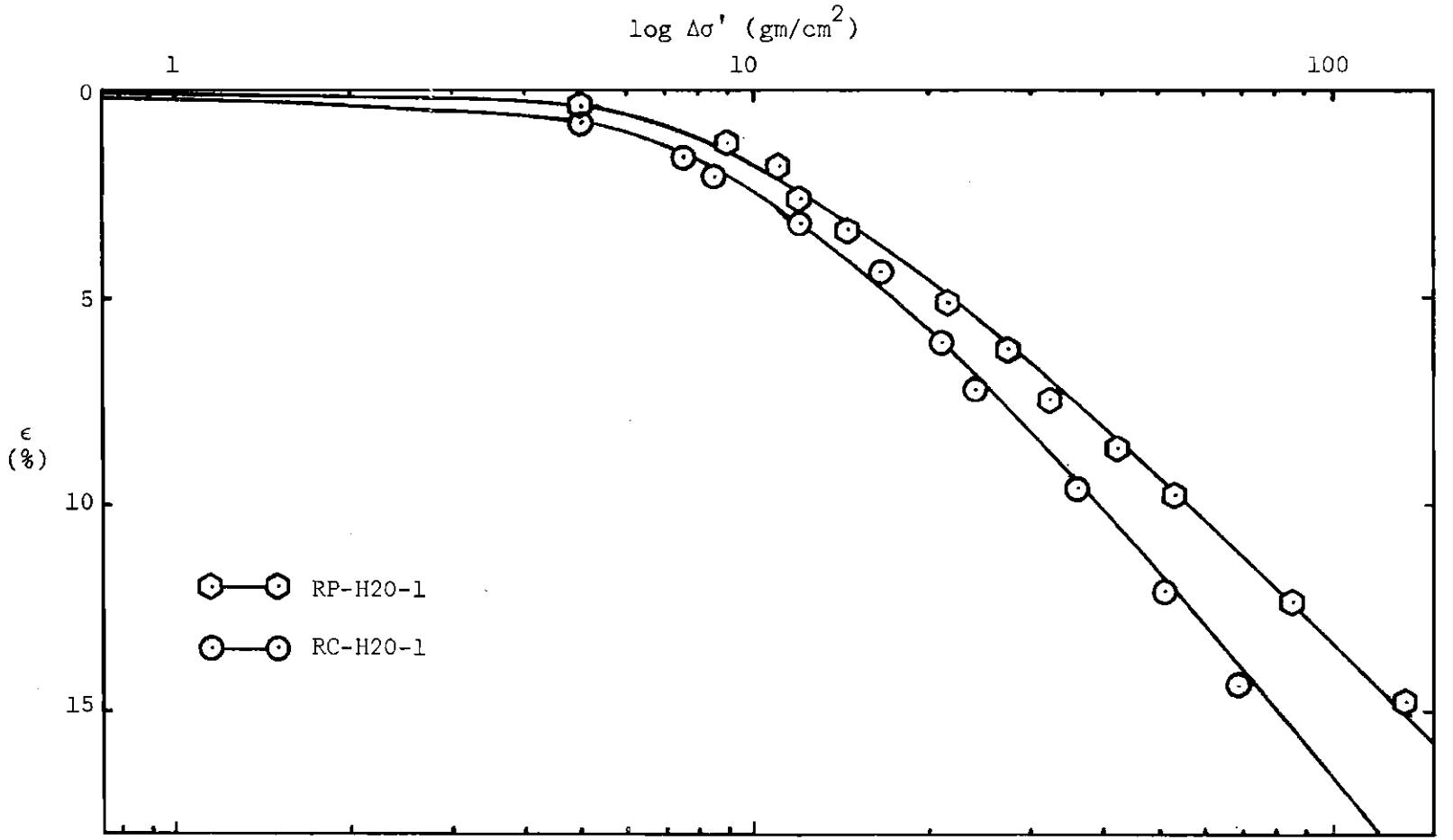

Figure 29. Comparison of Pressurized and Non-pressurized Tests on Remolded Material (Hudson Submarine Canyon--H20)

Table 7. Comparison of Test Duration and Man-Hour Effort

Test	Test Type or Rate of Strain (%/min)	Test Duration* (hrs)	Effort** (MH)
Standard			
B-H20-1	(1)	194.0	9.8
B-M7-2	(1)	216.0	10.8
B-G 11/6-4	(1)	212.0	9.8
B-H20-3	(2)	4.0	5.8
B-M7-1	(2)	6.5	8.3
B-G 11/7-4	(2)	6.3	8.1
CRS			
C-H20-2	0.024	17.5	2.1
C-M7-6	0.0048/0.024	76.3	2.5
C-M7-1	0.024	18.5	2.1
C-G 11/6-2	0.024	17.0	2.1
C-G 11/7-4	0.08	4.5	2.1

(1) Loads put on at 24-hour intervals.
(2) Loads put on as soon as R_{100} reached.

*Time test actually in progress.

**Includes time for cutting PVC, trimming, preparation of equipment, removal of specimen after test, and readings made during test.

Indications of Secondary Effects from a CRS Test

Figure 30 displays data from a CRS test which was halted for 24 hours. Because the equipment was not designed with the idea of measuring secondary effects, the load decreased very slightly during the period the equipment was off. Despite this small variation, the initial

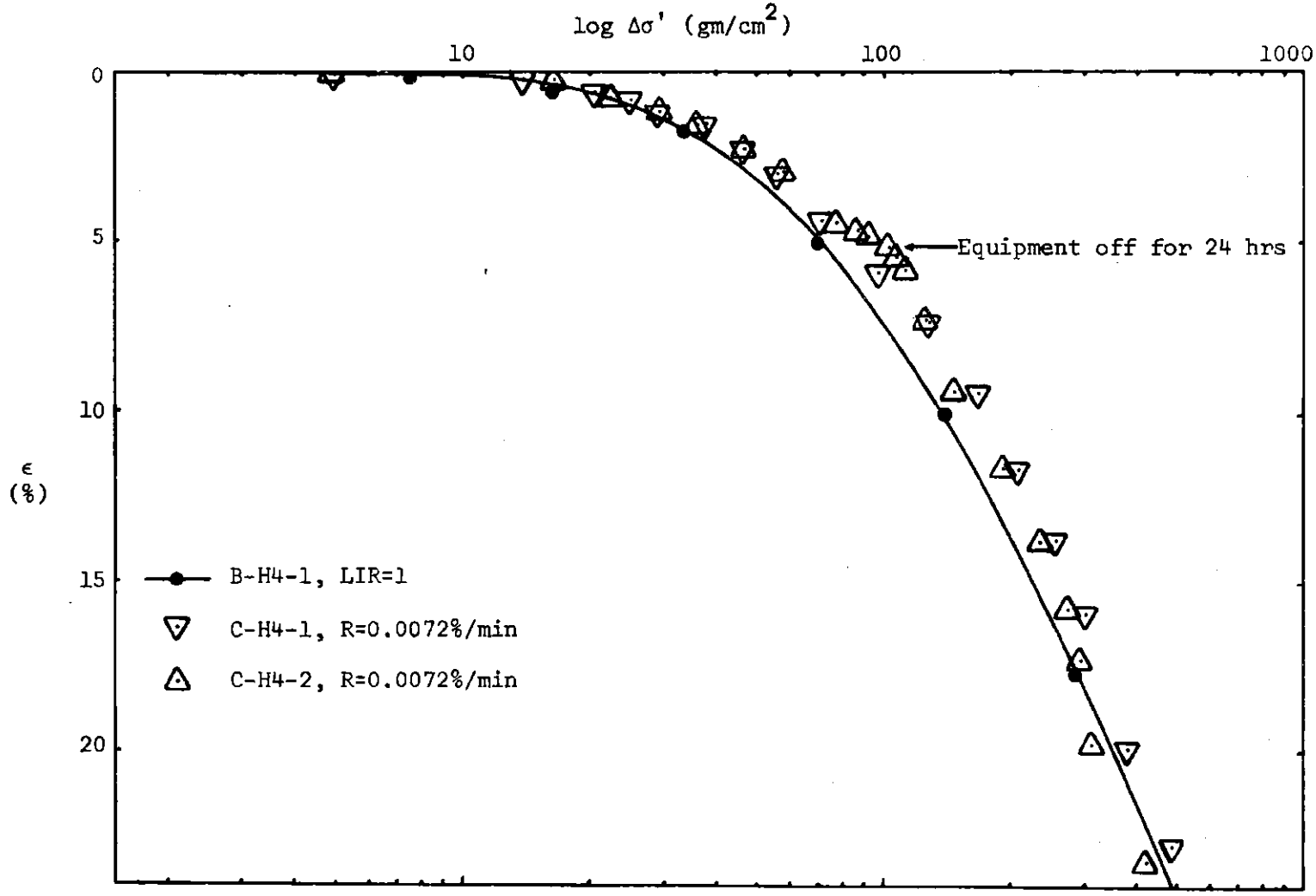

Figure 30. Comparison of CRS Tests with and without Secondary Effects to a Standard Test

increased resistance to compression and later tendency for greater compressibility are clearly shown. The two other curves on the figure are for comparison.

Settlement Analysis

As indicated in Appendix G, Equation (4) was proposed for computing settlement caused by *primary* consolidation of submarine sediments:

$$\Delta H = \sum_{i=1}^{n} H_i \left(C_\epsilon \log \frac{p_c' + \Delta\sigma'}{p_c'} \right)_i \qquad (4)$$

Table 8 lists the values of settlement computed using this equation and Equation (3)* for three actual foundation tests (see Appendix G). Information on foundation settlement at two times after the settlement caused by primary consolidation had ended is also shown. These values indicate that secondary effects appear to be at least as important as primary consolidation at both test sites.

*Equation (3) is presented in Chapter III.

Table 8. Summary of Settlement Analyses

Test	Water Depth m	Stress Increase gm/cm^2	Computed Values of Settlement Based on Primary Consolidation: Max Eqn (4) cm	Avg Eqn (3) cm	Avg Eqn (4) cm	Observed Settlement Caused by Primary Consolidation: Amount cm	Time hrs	Amount After 100 Hrs cm	Amount After 1000 Hrs cm
Fm2	200	75	4.2/2.9-4.2	8.2/ 7.0	3.6/3.1	2.9	25	3.3**	8.4**
L3	400	50	5.3/3.7-5.3	12.6/12.6	4.7/4.7	4.8	4	8.1**	-
FM3*	400	75	9.2/6.4-9.2	19.6/19.6	8.0/8.0	10.7	25	13.5	18.6

NOTE: All computed values of settlement are given as "uncorrected/corrected for lateral effects" (see Appendix H).

*Observed values do not include effects of a bearing capacity failure that occurred when the foundation was being put in place; however, large values of settlement are probably related to this failure.

**Values include most of primary consolidation and some secondary compression.

CHAPTER VII

DISCUSSION OF RESULTS

Test Samples

Disturbance

Sampling. Factors that could cause coring disturbance have been outlined in Chapters V and VI, and in Appendix E. Undoubtedly, these factors affected the cores used in the testing program; however, those associated with the coring device were probably minimized by the design of the corer. Ross and Riedel (164) indicated open barrel hydro plastic-corers are capable of taking relatively undisturbed cores up to three meters in length. Richards (149) indicated that only the upper 40 to 75 cm of sediment would be recovered *completely*. Although the remainder of the core would be disturbed, it would still be useable for engineering purposes.

Since no material from the top of the cores was used, brief periods when the cores were horizontal probably did not significantly affect the compressibility of the core section tested.

Because of the organic content and H_2S odor, biophysico-chemical changes resulting from stress relief and increased temperature were probably most significant in the Hudson Submarine Canyon cores. The effects of these factors probably did not affect the test results significantly.

Transportation. All cores were transported in essentially the

same manner (see Chapter V). All possible precautions were taken to reduce disturbance from shock. Core shortening occurred only in the top sections of the cores and was thus not a factor in the testing program.

Storage. Sections of core M7 were in storage for the longest time of any core. As indicated in Chapter VI water loss was negligible, and the relative homogeneity of the core material throughout each section indicated moisture migration was probably minimal. Although it was in storage for the longest period of time, the length of the core section M7-4 (see Chapter VI) was 30 cm or less during most of the storage period. This probably helped to minimize moisture migration over such a long period of time.

Trimming. Problems during trimming were discussed in Chapter V. Except as previously noted, there is no reason to believe the trimming process affected one sample any more than another. Although trimming times varied, water loss during trimming was probably not significant (see following discussion of saturation).

Analysis of Disturbance. In general as disturbance increases, the core material will be more compressible than the *in situ* sediment, and will indicate a lower value of apparent preconsolidation pressure. The relative degree of disturbance can be roughly estimated by comparing curves on an ϵ-log $\Delta\sigma'$ diagram. Based on the curves presented in Figures 12 through 21 the most disturbed material is felt to be that from cores M7 and G6,* and the least disturbed is felt to be that from

*Although M7 and G6 were the most disturbed cores used in the

the Doboy Sound cores.

Hironaka (69) indicated that a decrease in vane shear strength with depth near the base of a core could be attributed to disturbance (as long as water content did not increase). The bottom portion of core G6 appears to show this trend and may be relatively disturbed. This agrees with what is known from the recovery of this core (Brumund (20)). However, material for the testing program came from above this region.

Based on the foregoing discussions it is felt those parts of the cores utilized in the testing program are relatively undisturbed and can be used to evaluate the sediment compressibility.

Terzaghi Assumptions

Taylor (197) fully describes the Terzaghi theory. The assumptions listed here are the only ones considered to require additional treatment.

Homogeneous Material

Groups of samples are represented on Figures 12 through 21. For each figure the samples represented have similar natural water contents, initial void ratios, degrees of saturation, and unit weights. Certain samples which are represented on the figures have void ratios which are felt to vary enough from the other samples that they should not be considered in comparing C_c and p_c' values. For this reason, only samples which have almost exactly the same void ratio are grouped together in

---

testing program, the data from tests on these cores are considered to be valid enough for test comparison.

Table 3. For example, Figure 12 shows seven curves, but on Table 3 the data appear in one group of three, and two groups of two.

Organic carbon contents (see Table 10, Appendix B) are not felt to significantly influence the compressibility characteristics, particularly since submarine sediments tend to exhibit relatively large amounts of secondary compression anyway. The values of organic carbon content in the table are only estimates based for the most part on similar material from the same general regions.

Anomalous features such as small intact shells, worm holes, worms, etc., can cause significant inhomogeneity. Samples known to have these features were discarded. In a few cases, where a shell was on the sample surface, it was carefully removed and the small cavity filled with trimmed material.

Darcy's Law

Because of the void ratios of the material used in the testing program and the fact that primary consolidation was completed relatively rapidly, Darcy's Law is felt to be valid.

Saturation

Saturation was not 100 per cent, but was probably not a significant factor in the testing program. If air in the sample voids had been a *major* contributor to sample compressibility, its effect would be observed in the data presented in Table 4. Thus the assumption that saturations were sufficiently high to allow the use of the Terzaghi theory is reinforced by the data presented in this table. Additional indications that the air in the samples was not a significant factor in

the consolidation process can be obtained by comparing similar tests with and without back pressure. If air had been a significant factor, the samples tested without back pressure would have probably been much more compressible.

Pressure-Void Ratio Relationship

Equation (40) (see Appendix D) ignores secondary effects. Since the sediments used in the testing program displayed significant amounts of secondary compression (see Table 4) this assumed relationship does not *strictly* hold. As will be discussed later, to a large degree secondary effects have been removed from the tests and for this reason it is felt the assumption is met as well as for most soils that do not exhibit significant secondary effects.

Effects of Certain Factors

Side Friction and Temperature

Based on the information provided in Appendix E, side friction and temperature variation are not felt to affect significantly the computation of the *amount* of primary consolidation in the tests reported here. If side friction were significant enough to alter any test results based on Appendix E, it would probably slightly depress the first part of the recompression portion of the ϵ-log $\Delta\sigma'$ curves obtained from the standard tests. Even if this was the case, the effect on C_c and p_c' would be relatively insignificant.

The only test where a significant temperature variation (8°C) occurred during the test was C-H4-1 (Figure 30). Since this test compares fairly well with a standard test where there was an insignificant

temperature variation, it is felt that the temperature effect was negligible. As can be seen from Table 3, the average temperature variation among the three tests shown on the figure was only 1.5°C. For test C-H4-2 which indicates how secondary effects might be considered using CRS equipment, the temperature variation was 3°C.

Tests B-H4-4, C-H4-6, and C-H4-7 are compared in Table 3. This group of tests had the largest variation in average test temperatures (7°) of any of the tests compared. Because the curves for test C-H4-7 (average temperature--18.5°C) and test B-H4-4 (average temperature 25.5°C) show very good agreement, the effects of temperature variation were probably negligible. Test C-H4-6 which was used to demonstrate the shape of the ϵ-log $\Delta\sigma'$ curve when hydrodynamic effects were practically zero, had an average temperature of 20.0°C.

In relation to *in situ* temperatures, tests on material whose clay size fraction was primarily illite and chlorite were performed at temperatures within about 20°C of the *in situ*. For material rich in kaolinite and montmorillonite, test temperatures were within 10°C of the *in situ*. In relation to the clay mineralogies neither of these variations is considered significant (see Appendix E).

Air Bubbles in the System

According to Lee and Black (101), flushing techniques for drain lines between the base of a sample and a pore pressure transducer may not be completely effective, and trapped air bubbles must be dissolved to insure accurate and timely pore pressure measurements.

For soft soils that were normally consolidated, Lee and Black

found that the effect of air bubbles in a drain line similar to that of the chamber base was not significant, particularly at low pressures. Based on this work the *possible* presence of any air bubbles in the drain line is not considered to have had a significant effect on the testing program.

Back Pressure

As indicated in Chapter V, small reductions in back pressure were found to correlate with *minor* temperature variations. Although this might be the cause of the pressure drops, Wahls (208) cites data indicating that a very small amount of leakage occurs around O-ring seals. In either case, by making periodic readings during tests with back pressure, and knowing the amount of load changed for a given change in back pressure, appropriate corrections could be made. Consequently, drops in back pressure had no effect on the results presented.

As previously indicated, saturations were sufficient to assume the validity of Terzaghi's assumption of 100 per cent saturation. Despite the degree of saturation, the back pressure applications were made in small increments over time intervals that allowed pressure stabilization throughout the system. Because of this *slow* method of application, as indicated by Lowe and Johnson (108), water will flow into the pore space occupied by air both forcing it out and dissolving it, while the sediment skeleton is maintained at its original volume. The excellent initial agreement between CRS tests with and without back pressure and standard tests shown on Figures 14 through 18, 20 and 21, indicates that the back pressure saturation procedure caused negligible volume change.

For the tests with remolded material, similar back pressure saturation techniques were employed. Lowe and Johnson indicated that, for the procedure used, the only requirement was that the initial sample saturation be of the order of 90 per cent or more. Consequently there is no reason to believe there was any significant volume change during the saturation of remolded samples.

Secondary Effects

Secondary effects are important in most submarine settlement problems. Table 4 indicates that secondary compression is important in the sediments used in this testing program.

Because the main interest in these sediments was to develop (1) an improved method of predicting settlements caused by *primary* effects and (2) a means of explaining the apparent preconsolidation of submarine sediments, secondary effects were "filtered out" of the majority of standard and CRS tests. In the latter case, this was done by conducting most tests at rates of strain sufficiently high to insure hydrodynamic action (as indicated by $\Delta u_b/\Delta\sigma$ values). In the former case, secondary was not allowed to become significant. This was accomplished by loading most samples as soon as they reached R_{100} as determined by the Taylor square root of time method (see Appendix D). Although all the material demonstrated significant secondary compression, Figure 44 (Appendix D) indicates that at LIR equal to 1.0 type I curves (Wahls (208)) are obtained from a plot of change in sample height vs. the logarithm of time. It is noted that after 24 hours the determination of R_{100} from this type of plot is still not possible. Indications are that when R_{100}

is determined, it will be larger than values determined by Taylor's method. Because the Taylor plot allows R_{100} to be determined *before* significant secondary effects occur, it is felt to be the more valid relationship for these high void ratio sediments. It is also felt that, because the sample is allowed to experience significant secondary effects before R_{100} can be predicted, for these sediments the Casagrande logarithm method provides R_{100} values significantly affected by secondary. It is noted this concept is in contrast to Leonards (102), who indicated values of R_{100} determined by the Taylor method were generally less reliable than those determined by the Casagrande method. On the other hand, Burmister (22) found good correlation between the Taylor method and field tests on very soft soils.

Thus, because of the manner in which the tests were conducted, secondary influences were negligible in relationship to values of p_c' and C_c determined for the samples. Six samples are exceptions to this statement:

1. Tests C-H4-2, C-H4-6, and C-M7-6 were used to demonstrate how secondary effects *might be* evaluated with CRS equipment.

2. Tests B-G 11/6-4, B-H20-1, and B-M7-2 were used to relate standard tests where each load increment was allowed to remain on the sample 24 hours to standard tests loaded immediately after consolidation had reached the R_{100} value under the previous load increment.

Secondary Effects with CRS Equipment. Although the testing program was not concerned with secondary effects, three tests were conducted that indicate that secondary effects may be observed by the use

of CRS test equipment. Two tests were conducted at such a low rate of strain that the ratio $(\Delta u_b/\Delta\sigma)_{max}$ was less than 4 per cent. For these tests the ϵ-log $\Delta\sigma'$ curves were quite different from curves for other tests. Because of the nature of the tests (i.e. no excess pore water pressure--hydrostatic conditions), the compressibility resulted from secondary compression.

The third test was conducted so that for a period of 24 hours the sample was loaded at an almost constant load (by halting the test). When loading was begun again the sediment had an initial increased resistance to compression and then displayed a steeper virgin curve compared to comparable standard and CRS tests.

Testing Rate. The rate at which a consolidation test is conducted appears to be very important in relationship to secondary effects. Use of the CRS test has added further support to earlier work with low load increment ratios (Leonards and Altschaeffl (103) for example). Constant rate of strain tests have shown sediment structure to have important time dependent resistance to compression.

All recent work found in the literature indicates that as the loading rate (standard tests) or rate of strain (CRS tests) decreases, secondary effects tend to shift the e-log $\Delta\sigma'$ curve down and to the left. Although C_c values are negligibly affected, p_c' values are reduced. Crawford (31) indicated that this effect caused settlement computations to be high. For the few test groups listed in Table 3 where two comparable CRS tests were run at different rates of strain, C_c values were similar, but the values of p_c' found for the slower tests

were higher than the faster tests. At least two reasons are possible for this: (1) Usually the rates of strain were not greatly different. (2) The rates of strain for these particular tests were high enough so that hydrodynamic effects governed the consolidation process. For standard tests the results were in complete agreement with Crawford's work.

As previously indicated, at rates of strain of 0.0048%/min or less, and where $(\Delta u_b/\Delta\sigma)_{max}$ is less than 4%, a different ϵ-log $\Delta\sigma'$ curve shape was found (see Figures 12 and 20, tests C-H4-6 and C-M7-6). Apparently no CRS researchers have noted such a curve. Curves of this type display higher values of p_c' and C_c than comparable curves governed by hydrodynamic effects as determined in both standard and CRS tests. Their shapes are in a general way similar to the shape of curve C-H4-2 (Figure 30) after the sample had been allowed to undergo dissipation of excess pore pressure at relatively constant load. A similar curve is also presented by Wissa, *et al.* (their Figure 8). Leonards and Altschaeffl (103) have shown that where compressibility of certain soils is determined by using reduced load increments the e-log $\Delta\sigma'$ curve tends to bell out in the area of the preconsolidation pressure and then demonstrates a somewhat steeper virgin compression curve--not unlike those of the test curves just discussed. In a standard test Wahls (208) indicated the cause of this was that the time to reach R_{100} decreased with decreasing load increment ratio allowing physico-chemical phenomena to develop more resistance to compression before the next load increment was placed on the sample.

In summary, two situations appear to exist:

1. If Crawford is correct--lowering the strain rate to values just sufficient to insure dominant hydrodynamic action will cause the ϵ-log $\Delta\sigma'$ curve to shift to the left and down (analogous to allowing long load durations in a standard test).

2. If the strain rate is so slow that hydrostatic conditions predominate, the curve will tend to bell out in the region of the preconsolidation pressure and will then have a somewhat steeper virgin compression curve (in a general way comparable to a quasi-preconsolidation effect obtained from using low load increment ratios in a standard test). Although Wissa, *et al.* (215) indicated tests where $\Delta\sigma$ equals $\Delta\sigma'$ simply allowed direct use of the data, for the sediments tested in this program it would seem such a test could be developed into a method of predicting either secondary or primary and secondary (perhaps by using visco-elastic methods--see also Byrne (24) and Smith and Wahls (185)).

Finally, it appears from this testing program that satisfactory results can be obtained using rates of strain that induce values of $(\Delta u_b/\Delta\sigma)_{max}$ up to 50 per cent. Smith and Wahls (185) also found that 50 per cent appeared to be the upper limit for reliable results.

Initial Conditions

As indicated in Chapters V and VI, initial test conditions are very important when tests at low loads are being compared. For each test the top porous stone and cap (and ball in the case of the standard tests) constituted the first load on the sample. For the standard tests

the apparatus was rapidly placed under the loading head and the change in height noted. For all the tests on undisturbed materials, the change was less than 0.005 cm (the applied pressure was five gm/cm^2). Some special standard test samples (not listed here) were allowed to remain under the loading head for periods of time corresponding to the period required for back pressure saturation in the CRS tests. For the small imposed pressure the additional change in sample height over these extended periods was negligible.

Based on these data, values of sample displacement under the CRS porous stone and cap (which also developed a pressure of five gm/cm^2 when submerged) were estimated and incorporated into the test results along with the applied pressure of five gm/cm^2.

For back pressure tests the friction between the loading piston and the O-rings effectively kept the piston weight from being applied to the sample. For CRS tests without back pressure, the pressure caused by the weight of the partially submerged piston did affect the sample since no O-rings were used in these tests. For this condition the additional pressure and change in sample height (estimated from a similar pressure in the standard test) were added to the CRS test results.

In this way initial test conditions were equalized.

For remolded materials (Figures 26 through 29) similar procedures were used. Because the time the back pressure remained on each sample (RP-H4-1, RP-H20-1, RP-G6-1, RP-M3-1) varied, a separate standard test was conducted over an equal time period in order to determine the appropriate changes in sample height under the submerged weight of

(1) the porous stone and cap and (2) the porous stone, cap and piston.

Significance of Water Depth

The Doboy Sound cores (G 11/6, G 11/7, G 11/8) and core G8 are from relatively shallow water (maximum depth was 40 m). Some important characteristics of these cores are:

1. They seem to show a trend of *increasing* void ratio with depth in the first 100 cm.

2. They appear to be composed of rapidly deposited terrigenous material.

3. The Doboy Sound cores display considerable scatter in the relationship of void ratio vs. depth.

4. The Doboy Sound cores are relatively heterogeneous.

Cores G6, M3, M5, M7, H4, H6 and H20 are from relatively deep water. Compared to the four shallow water cores, these cores consisted of relatively uniform, slowly deposited mixtures of terrigenous and pelagic materials. Thus, they are significantly different from the shallow water cores.

Compression Index

As with most submarine sediments, values of C_c were larger than values determined for similar terrestrial deposits. The cause of the large values is probably the very large void ratio of the submarine sediments. For this reason it would be expected that correlations between void ratio and C_c would be possible. Figure 24 presents the best correlations between C_c and any parameter examined in this testing

program. Sowers (188) indicated that the data from the Georgia Coast cores might represent a separate range of values. As indicated in Chapter VI and Appendix B, the clay mineral fraction of the cores can be used to relate these sediments to the saprolitic soils on which Sowers and Sowers (190) based the equation plotted in Figure 30. For this reason a line parallel to their line, but shifted so that the zero intercept is 1.25, is proposed for correlating e_o and C_c for the Georgia Coast cores used in this testing program. Equation (5) (Chapter VI) is the equation for this line. The fact that values of e_o and C_c for core G6 plot well with respect to this line may indicate that disturbance from coring was not too important in the case of this core. Equation (6) is a similar equation for the Hudson Submarine Canyon and Gulf of Maine cores which have a different mineralogy from the Georgia Coast cores.

Between shallow water cores from Doboy Sound and cores from depths of water greater than 100 m, significant differences in the variation of C_c are noted. In the former case C_c reflects both the heterogeneous nature of the material and a rapid rate of deposition, in the latter case it reflects the homogeneity of the sediment with depth, and relatively slow deposition.

Among the Hudson Submarine Canyon cores there was a trend for C_c values to be greater as water depth increased. Between axis and flank there is a significant change in amount of sand size particles and also in rate of deposition. Both these factors, more sand and slower deposition could be the cause of the flank core having smaller values of C_c

than the axis cores.

No significant variation between C_c determined from standard tests and values determined from CRS tests without back pressure was noted. However, as indicated in Table 5 the sediments displayed larger values of C_c when tested with back pressure than when tested without back pressure (for the effect of back pressure on p_c', see the following section). Where standard tests at LIR equal 1.0 are available for comparison, C_c values from the CRS back pressure tests are also larger. The probable reason for this is that the application of back pressure simulates the original environment of the sample. Thus, some of the disturbance which resulted from stress relief is compensated for, and the specimen compresses as though it were less disturbed.

Based on the results of this testing program, little support can be found for the method of estimating C_c for submarine sediments proposed by Delflache, Bryant and Cernock (34) (see Chapter II). It seems possible that the dual values of C_c they reported, based on the *two* curves they are known to have published, resulted from the manner in which they conducted their tests. Their method is not recommended for practical use in computing settlements of ocean structures with shallow foundations currently being deployed on soft submarine sediments.

Apparent Preconsolidation

Both the Sowers and Casagrande methods were used to compute the preconsolidation pressure. Because the Sowers method is "more reproducible" and because it gave more consistent results, it is considered the better method for estimating p_c' for these sediments (see Table 3).

The fact that the Sowers method is more consistent in determining p_c' for submarine sediments is very important. Because the Casagrande method requires interpretation of the curve inflection point, more human error is introduced. In all cases the value of p_c' determined by the Sowers method was less than that found by the Casagrande method.

Except for most samples from core M7, all samples displayed an apparent preconsolidation effect. As previously indicated, core M7 was in storage for a lengthy period of time. Bozozuk (19) showed that values of p_c' for block samples of a sensitive clay were reduced about 5 per cent after 17 months of storage in a humidity room. It seems likely, despite the fact water loss was negligible, and C_c probably not significantly affected, that a reduction in p_c' occurred for core M7, thus tending to mask a preconsolidated condition similar to that noted for core M3.

Secondary Effects

Figures 19, 20 and 21 indicate that if a sample is allowed to undergo significant secondary compression, the value of p_c' determined from the ϵ-log $\Delta\sigma'$ curve will be less than for a sample for which secondary compression is less.*

Bjerrum (14) indicated that conventional procedures for determining p_c' for certain *marine* clays indicated apparent preconsolidation.

---

*Table 3 indicates that even if each load increment is left on the sample 24 hours, values of p_c' developed from an ϵ-log $\Delta\sigma'$ curve based on using R_{100} values for strain (instead of R_f values), are not greatly different from p_c' values determined from an ϵ-log $\Delta\sigma'$ plot for a comparable sample where each load increment is allowed to act as the sample reaches R_{100}.

By correlating postulated geologic history and long-term settlement studies of several buildings in Norway he concluded that the compression characteristics of a clay that displayed delayed compression could not be conveniently explained by a single curve in an e-log $\Delta\sigma'$ diagram. Several curves, each representing the e-log $\Delta\sigma'$ relationship at a specific time of sustained loading, were required. This is in contrast to a single instantaneous compression curve which indicates void ratios at the end of excess pore pressure dissipation. Bjerrum's procedures probably have considerable practical value if geologic history can be determined as well as it apparently can for the Norwegian clays he used. For the case of the sediments employed in this testing program the geologic history is not so clear. Consequently, even though these sediments display significant delayed compressions, Bjerrum's method is not easily applied. To determine p_c', as in the case of C_c, secondary effects have been filtered out and the value of p_c' computed is based only on primary consolidation.

Because of the differences in strain rates between the laboratory and the field, it is diffcult to determine p_c' reliably from standard laboratory tests. CRS tests can be conducted at strain rates *closer to* values actually existing in the field and consequently should produce more reliable results. Where secondary effects are prevented from influencing the standard tests, the strain rate problem is less important and laboratory values of p_c' for use in computing settlement of actual structures are considered to be more reliable.

p_c'/p_o'

The ratio p_c'/p_o' is generally known as the overconsolidation ratio. Values for the sediments used in this program are tabulated in Table 3. As indicated in Chapter VI, by all indicators, these cores consist of normally consolidated material (except for core G8); however, the cores can be grouped into two classes according to depositional environment: (1) material rapidly deposited in relatively shallow nearshore waters where waves, tides and currents are continuously active, and (2) material deposited more slowly in deeper waters where natural physical oceanographic forces are generally much less active.

Because of different environments cores G 11/6, G 11/7, G 11/8 and G8 have been subjected to a much different stress history than the other cores used in the testing program.

The highest value of p_c' and p_c'/p_o' was found in core G8 for which no value of plasticity could be obtained. It also has a very high sand content consisting of quartz and heavy minerals. Consequently, it is felt that the high value of p_c' can be attributed to the sand content and probably to a type of physical overconsolidation caused by rapid deposition and the natural forces which are active on the continental shelf.

Other shallow water cores, although apparently normally consolidated, based on values of liquidity index, are known to have been stressed by the dynamic activity of tidal variation. At certain depths in these cores physical overconsolidation has been observed. Because of the generally heterogeneous nature of these cores and their different stress history, they are felt to display apparent preconsolidations for

different reasons (discussed later in this chapter) than the deeper water cores. Values of p_c' for tests on these cores conducted at high back pressures are less than values for comparable tests with no back pressure.

All the deeper water cores demonstrated apparent preconsolidation. It is felt that even core M7 would have appeared preconsolidated if it had not been in storage for such a relatively long time. A comparison of CRS tests with back pressure, without back pressure (where hydrodynamic effects were significant) and standard tests (with LIR equal to 1.0) indicates that in all cases the tests with back pressure displayed higher values of p_c'.

The core from the Florida-Hatteras Slope has a relatively high sand content mainly consisting of carbonate debris. Next to core G8, G6 displayed the highest apparent preconsolidation. Because of the high carbonate content, the cause of apparent preconsolidation in this core may be different from that in other deep water cores (discussed later in this chapter).

Values of apparent preconsolidation were higher in core H6 than in Core H20. Although core H4 occupies an intermediate depth between H6 and H20, it displays apparent preconsolidation that is closer to H20 than H6. The reason for this is not readily apparent, but may be in part due to the fact that H4 has a slightly larger clay size fraction than either core H6 or H20.

Possible Causes of Apparent Preconsolidation

Physical processes such as glaciation, permanent change in sea level, and desiccation during lower sea level, probably did not significantly influence any of the sediment used in the testing program. The shallow water sediments are influenced by transient changes in sea level and by a stress history involving repeated fluctuations in pore water pressure caused by dynamic loading rapid enough to preclude drainage. These forces are postulated to be the cause of apparent preconsolidation in cores G8, G 11/6, G 11/7 and G 11/8.

For all deep water cores the sedimentation process described in Appendix C is felt to be generally applicable. There appears to be little disagreement that where deposition is slow, a unique type of sediment structure can develop. Hamilton (60) indicated that slow deposition resulted in all compression being secondary in nature. Thus, in addition to possible diagenetic changes, the structural resistance of soft sediment to compressibility would result from the action of whatever mechanism produces secondary compression.

Richards and Hamilton (152) postulated that slow deposition allowed intergranular bonds to form that had the effect of cementation, although *no* cementation was visible. This agrees in general with the discussion in Appendix C. For the deep water cores examined here, where carbonate content was relatively low, the resistance to compression causing apparent preconsolidation is felt to be the result of slow rates of sedimentation of flocs through a gradually increasing stress field. This process produces ". . . sediment structures which are

capable of supporting more sediment without consolidation, and in which there has been little consoliation. . ."* as evidenced by small changes in void ratio within the upper few meters of the material. The bonds of this structure are thus the result of a physico-chemical stress system unique to the ocean. Monney (119) appears to be one of the few who have considered that the relative "strength" of these bonds may be related to the huge hydrostatic pressures under which the structure is formed.

Before discussing the question of the part played by hydrostatic pressure, another unique characteristic of submarine sediments must be examined. Where pelagic processes are involved in the sediment formation, the tests of microorganisms (usually silaceous or calcareous) and carbonate debris from other forms of organic activity will be found in varying quantity. Relative to the cores tested, only the carbonate debris appears important, but it is noted that the effect of microorganisms *can be* very important.

Core G6 is the only core used that had a relatively high calcium carbonate content. Although actual cementation is unlikely, it seems probable that the interparticle bonds are strengthened by the presence of calcium carbonate. Unlike core G8, the large sand size fraction in G6 was mainly carbonate debris, and even though the grain size curves were similar, G6 displayed significant plasticity. For this reason it is felt that the high value of p_c'/p_o' determined for core G6 is not

---

*Richards and Hamilton (152).

completely attributable to its relatively coarse nature, but reflects the influence of calcium carbonate content.

Equation (2) was developed in Appendix C as a means of relating the factors involved in causing apparent preconsolidation. In this equation the term ($\bar{C}_f/\bar{C}\ u_h$) represents the effects of both the hydrostatic pressure and the interparticle bonding forces (indirectly through structural compressibility). The term thus provides a measure of the effect of the environment on the sediment. If, as most workers indicate, all the apparent preconsolidation effect can be attributed to interparticle bonds regardless of water depth, then Equation (2) is not valid. Comparisons of p_c'/p_o' determined for submarine sediments with p_c'/p_o' postulated as being capable of being developed by secondary consolidation, indicate that the whole preconsolidation effect cannot be attributed simply to interparticle bonds irrespective of water depth: Richards reported values of p_c'/p_o' of 1.1 to 11 for submarine sediments; Noorany (129,130) reported values from 10 to 55 for silts and clays and values up to 88 for sediment that was mainly calcareous microorganisms;* values determined in this research varied from 0.8 to 6.2 by the Sowers method and from 1.2 to 10.4 by the Casagrande method.

In a summary of published work on settlement, Seed (171) noted values of p_c'/p_o' resulting from secondary effects could be as much as two. It is realized that laboratory strain rates and "aging" times are

*Noorany's maximum values are from samples from within the top 60 cm of the sediment; therefore, even small errors in p_o' could make a large difference in the ratio p_c'/p_o'. Richards' samples are from varying depths within about the top 300 cm of the sediment.

very much different from those in the field, but it appears difficult to see how values of p_c'/p_o' of the orders of magnitude reported could completely be caused by interparticle bonds, regardless of water depth.

Thus to *paraphrase* Burmister (22), soft submarine sediments *in situ* in natural deposits are inherently *prestressed,* laterally confined and preconsolidated materials.

Ratio of Prestress ($\bar{C}_f/\bar{C}$)

Table 6 indicates values of $\bar{C}_f/\bar{C}$ (the ratio of prestress) backfigured from CRS tests (conducted at *in situ* pore water pressures) using Equation (2). Inserted at appropriate locations are values of C_s/C determined by Skempton (180) (see also Laughton (100)). Only values from back pressure tests were used in computing values of $\bar{C}_f/\bar{C}$ because these tests most closely reproduce the actual *in situ* conditions.

It appears the $\bar{C}_f/\bar{C}$ ratio is large in relation to C_s/C values for similar type material. Skempton indicated his values were determined for water at essentially atmospheric conditions. For high hydrostatic conditions it would be expected that the compressibility of the skeleton would decrease more from that at atmospheric conditions than would the compressibility of the solid particles and their bound water. In addition, the compressibility of a floc would probably be slightly greater than the compressibility of a solid particle. Thus, the ratio of $\bar{C}_f/\bar{C}$ would be expected to be higher at high hydrostatic pressures than the C_s/C ratio would be at atmospheric pressure.

Rate of Deposition

If the contribution of secondary and diagenetic effects are

significant in relation to hydrostatic prestressing effects, then apparent preconsolidation pressures should be greatest where deposition is slowest, irrespective of water depth (assuming it can be shown that deeper water does not mean *a priori* slower rates of sedimentation). In other words, if time effects are the major contributing factor to large values of p_c'/p_o' for submarine sediments, then for similar deposits, the largest p_c'/p_o' values should come from areas where deposition is slowest. Examination of Figure 11 and Tables 10 and 12 shows that core H20 comes from shallower water than core H6, and because of the environment the deposition rate is relatively slower than for H6. Both cores have relatively the same mineralogical background and the same clay size fractions (although H6 has slightly more silt size particles). In contrast to the preceding suppositions, the highest values of the p_c'/p_o' ratio are found in core H6--faster deposition and *deeper water*. A similar relationship exists between H4 and H6. Core H4 is from shallower water, and appears to be more slowly deposited, but core H6 displays higher values of p_c'/p_o'.

Effect of Hydrostatic Pressure on Shallow vs. Deep Water Cores

Assume high hydrostatic pressures have little direct effect on the development of structural resistance to compression. If this is the case, then where submarine sediments have an established structure, slow application of high back pressures that do not alter the structure should make no difference in compression characteristics. Thus, the relationship of values of p_c'/p_o' in tests with and without back pressure should be the same, regardless of the level of back pressure applied.

Based on a limited number of tests (Table 3) for the Doboy Sound cores, application of back pressures well above the *in situ* produced lower values of p_c'/p_o' than for tests without back pressure. For materials from deeper water, elevation to *in situ* back pressures produced higher values of p_c'/p_o' in relation to tests without back pressure. Although these differences may be caused by different clay mineralogies, it seems probable that the effect of subjecting the Doboy Sound cores to hydrostatic pressures far above any past pore water pressure altered their compressibility by some physico-chemical mechanism. According to Wang (210), as the external pressure is increased the viscosity of water decreases because of the disruption of the orderliness of the water structure (see Appendix C). Hydrated ions become more mobile, which may result in a loss of resistance to compression. In the case of the sediments already subjected to high hydrostatic pressure, repressurizing would simply reestablish to a large extent their normal environment, and partially equalize changes introduced by coring and stress relief. The result would be increased resistance to compression. This is exactly what is observed.

Tests on Material Where Aging and Digenetic Effects Have Been Destroyed

As final support for the concept of a prestressing effect caused by high hydrostatic pressure, eight tests were conducted on remolded material (these are the RC and RP series tests shown in Table 3). Figures 26 through 29 clearly show that application of back pressure caused increased resistance to compression. Because of the manner in which the tests were conducted, previous stress history and aging

effects were negligible.

Remolding, as would be expected (Lambe (98) and Schmertmann (158)), produced decreased permeability and large values of ($\Delta u_b/\Delta\sigma$). In general this ratio was larger for tests that had not been pressurized--an indication of lower permeability. Since the time between remolding and the beginning of the tests was the same for each pair of tests normal thixotropic effects should have been equal. Because remolded materials have only the structure that can develop through thixotropy, their compressibility to a large degree depends on the phases present. Since these tests were run relatively soon after remolding, based on the work of Skempton and Northey (183), thixotropic effects were probably not significant relative to the effect of the solid and fluid phases in resisting compression. Thus the difference between the curves in each set of tests can only be attributed to the prestressing effect of the back pressure causing an increased resistance to compression--a hydrostatic prestressing effect.

Summary

All experimental evidence from this testing program indicates that hydrostatic prestressing effects are at least as important as secondary and diagenetic effects in the apparent preconsolidation noted to exist in the upper few meters of submarine sediments. Equation (2) appears to represent an accurate relationship among the factors influencing the resistance to compression of these materials.

Settlement Analysis

> . . . Settlement analyses usually give results which at best are crude estimates. However, as long as the accuracy is not misrepresented, there can be little question that the crude estimate is much more valuable than the pure guess which often is the only alternative. (Taylor (197).)

The process utilized to estimate the settlement of foundations caused by primary consolidation at two test sites in the Pacific Ocean is fully described in Appendix G.

As long as secondary effects are not excessive, values of C_c have been shown to vary relatively little, no matter by what method they are determined (an exception may result at high back pressure--this is discussed later). Apparent preconsolidation pressure is more sensitive to testing procedure; therefore, values of p_c' used in estimating the settlement of the test foundations were obtained by replotting standard test data from the foundation sites using values of R_{100} to determine the strain for each load increment. In effect this removed at least part of the secondary effects. To determine values of p_c' at the mid-layer heights into which the top few meters of the sediment profile was divided (see Appendix G) known values of p_c' from the standard tests were plotted vs. depth. A linear relationship resulted. McClelland (113) found a similar relationship for shallow water submarine clays from the Gulf of Mexico.

Mid-layer values of p_c' thus determined were used to compute settlement from the equation:

$$\Delta H = \sum_{i=1}^{n} H_i \left(C_\epsilon \log \frac{p_c' + \Delta\sigma'}{p_c'} \right)_i \qquad (4)$$

Use of this equation is fully explained in Appendix G. It is assumed that for the very small loads used in the initial part of the consolidation test, e_o for the laboratory and *in situ* curves are for practical purposes equal. Support for the use of p_c' in this manner can be obtained from Bjerrum (14) who pointed out that for normally consolidated clays where p_c' is greater than p_o', and at depths where the ratio of c/p' was constant, p_c' should be used for p' instead of p_o'. If this substitution is made then c/p_c' vs. I_p values should plot along the straight line proposed by Bjerrum (13). Referring to Figure 25, the effect of replotting values of vane shear strength divided by p_c' instead of p_o' can be clearly seen.

Stress Distribution

Employment of the Boussinesq method of stress distribution was explained in Appendix G. It is felt that this method is no less valid for submarine sediments than for terrestrial deposits.

Lateral Effects

Correction for lateral effects is discussed in Appendix G. The range of values employed is felt to be representative of the prestressed character of the deposits postulated earlier in this chapter.

Estimation of Actual Settlement Caused by Primary Consolidation

Adapting the Taylor square-root of time method to distinguish the actual foundation settlement caused by primary effects has as its

main redeeming grace the fact that it seems to be the most appropriate approach in view of the shape of the curves of settlement vs. the square root of time. Use of the method in this manner is consistant with its employment in standard laboratory tests to determine the end of primary consolidation. Since the foundation test apparatus was put in place, in either one or two increments the relationship between laboratory and field loading rates is not nearly as different as is the case in normal terrestrial work. For these reasons the values determined for settlement caused by primary consolidation for each of the foundation tests are felt to be representative of the actual settlement attributable to primary consolidation of the *in situ* sediment.

Predicted vs. Observed Settlements

As indicated in Table 8, the agreement between the observed settlement and that predicted by using Equation (4) was quite good. In terrestrial work, because of disturbance, predicted settlement is usually significantly greater than actual settlement. That this is not the case here may be in large part caused by the fact that back pressure CRS tests indicate that at *in situ* hydrostatic pressure not only is p_c' greater than when no back pressure is used, but C_ϵ is also greater. Because of the location of the ϵ-log $\Delta\sigma'$ curves on the logarithmic scale, *in situ* values of C_ϵ and p_c' substituted into Equation (4) are somewhat compensating. In fact it appears possible that the larger C_ϵ values may dominate the situation and cause *in situ* settlement attributable to primary consolidation to be as large or larger than that predicted by Equation (4). As Leonards (102) and Schiffman, Chen and

Jordan (167) have indicated, when so many unknowns and assumptions are involved in settlement estimates results such as these must be considered "fortuitous." However, it is felt that *the proposed method is a definite improvement over the use of Equation (3)* to predict settlement caused by the primary consolidation of submarine sediments (see Table 9).

CHAPTER VIII

CONCLUSIONS

Based on the results of consolidation tests performed on relatively undisturbed gravity cores of submarine sediments, the following conclusions are proposed.

1. Where only information concerning the amount of settlement caused by primary consolidation is required, constant rate of strain consolidation tests on submarine sediments require fewer man hours than standard consolidation tests and produce settlements estimates as good or better than any other method.

2. If only the amount of settlement caused by primary consolidation is of interest, and only standard consolidation test apparatus is available, the best and quickest estimate of settlement can be obtained by conducting the consolidation tests so that the load increment duration is adjusted to insure the sample is loaded as soon as R_{100} is reached. The load increment ratio should be equal to one.

3. Values of apparent preconsolidation pressure determined from constant rate of strain tests without back pressure, and from standard tests conducted as described in conclusion two should be increased by about 10 per cent to compensate for test conditions which vary from the *in situ* (i.e. pore water not at elevated pressure).

4. Different relationships exist between the initial void ratios of submarine sediments and their compression indices depending on

whether the composition of the less-than-two-micron fraction of the sediment is mainly illite-chlorite or kaolinite-montmorillonite; these relationships are:

Kaolinite-montmorillonite $C_c = 0.75\ (e_o - 1.25)$

Illite-chlorite $C_c = 0.5\ (e_o - 1.0)$

5. The major cause of the apparent preconsolidation of submarine seciments from water deep enough so that dynamic surface effects are negligible is the effective stress increase at the microscopic points of closest approach of the mineral grains caused by the high hydrostatic pressure. The apparent preconsolidation pressure, the effective overburden pressure and the hydrostatic pressure are related by the expression:

$$p_c' = p_o' + \bar{C}_f/\bar{C}\ u_h$$

6. The best method of taking into account the effects of hydrostatic pressure on the compressibility characteristics of submarine sediments is to consider the apparent preconsolidation effect in the settlement estimate. This can be done by computing settlement caused by primary consolidation from the relationship:

$$\Delta H = \sum_{i=1}^{n} H_i \left[C_\epsilon \log \frac{p_c' + \Delta\sigma'}{p_c'} \right]_i$$

7. Pending further research, the following guidelines are

recommended for estimating settlement caused by the primary consolidation of sediments (water depths 100 to 1000 m) which exhibit an apparent preconsolidation effect that cannot be attributed to the dynamic action of surface phenomenon.

C_c and p_c' should be determined (in order of priority) from:

a. CRS tests with *in situ* hydrostatic pressure, and where $\Delta u_b/\Delta\sigma$ ranges between 4 and 50 per cent.

b. CRS tests where the sample pore water is at atmospheric conditions, and where $\Delta u_b/\Delta\sigma$ ranges between 4 and 50 per cent.

c. Standard incremental loading consolidation tests (LIR equal to 1.0) which have been started at very low loads and where the loading range covers the stress that the foundation will develop in the sediment. Each load increment should be applied as soon as the consolidation under the previous increment has reached the R_{100} value as determined by the Taylor square root of time method.

If either method b or c is used, the values of p_c' determined should be increased about 10 per cent to compensate for the lack of *in situ* hydrostatic pressure.

The value of p_c' should be determined by the intersection of tangents drawn to the initial and virgin portions of the laboratory consolidation curve.

Settlement should be computed from the expression:

$$\Delta H = \sum_{i=1}^{n} H_i \left(C_\epsilon \log \frac{p_c' + \Delta\sigma'}{p_c'} \right)_i .$$

CHAPTER IX

RECOMMENDATIONS FOR FURTHER RESEARCH

1. For the sediments used in the testing program core shortening was found only in the top 50 cm. It is recommended a study be undertaken to develop a method of predicting the depth in a core over which core shortening should be expected during transportation to the laboratory.

2. It appears from the tests reported here that good correlation can be established between e_o and C_c for submarine sediments. The effects of water depth (rate of deposition?), calcium carbonate content and mineralogy of the less-than-two-micron fraction may all affect the e_o vs. C_c relationship. It is recommended a study be conducted to isolate the effects of these variables.

3. During the testing program the effect of stopping the CRS equipment was found to be related to secondary compression. It is recommended that CRS equipment and procedure be developed to allow prediction of settlement caused by secondary effects. This requirement is also important to terrestrial work since the use of more and more marginal land means increasing compressibility problems. The labor-saving advantage of CRS equipment is somewhat offset by current inability to determine secondary effects with it.

4. It appears from the tests reported here that very slow rates of strain produce consolidation at negligible excess pore water

pressure. It is recommended a study be conducted to determine if CRS equipment can be utilized to develop a simple testing procedure that will allow settlement to be predicted as a continuous process.

5. The ratio of prestress as a cause of the apparent preconsolidation of submarine sediments is a new concept. Tests with submarine sediment reported here from water depths roughly between 100 and 1000 m appear to establish its role in causing apparent preconsolidation. It is recommended that a CRS chamber be constructed that is capable of hydrostatic pressures comparable to *in situ* pressures found on the lower continental slope and continental rise to establish its effect at greater depths.

APPENDIX A

CORING EQUIPMENT

As indicated in Chapter IV, three different vessels were used to obtain cores. Coring was accomplished even from the relatively small *Kit Jones* (length 20 m).

There is a growing body of literature (Richards (149); Richards and Keller (154); Richards and Parker (155); Rosfelder and Marshall (162); Inderbitzen (77); McCoy, *et al.* (114); Ling (105)) indicating that open barrel gravity coring devices provide less disturbed samples of fine grained submarine sediments than piston corers with similar specifications. Emery and Hülsemann (39) indicated that open barrel gravity corers designed without considering parameters set forth by Hvorslev (75), provide relatively disturbed samples. Richards and Keller (154) indicated that prior to 1958 corers used by marine geologists did not provide samples suitable for determination of engineering properties. The development of the hydro plastic-corer by the U. S. Hydrographic Office (Richards and Keller (154)) based on Hvorslev's recommendations, and its detailed testing (Burns (23)) allows surficial samples of submarine sediments sufficiently undisturbed for engineering purposes to be obtained. Table 9 lists the values of Hvorslev's recommendations for various hydro plastic-corers and, for comparison, for a spade corer (which provides a sample similar in shape to block samples sometimes used in terrestrial work).

Table 9. Hvorslev Recommendations for Hydro Plastic-Corers

Corer	Core (cm)	Maximum Useable Length (cm)	C_i	C_o	C_a	Reference
Ideal Maximums		2 to 3D[4]	0.75 to 1.5	2 to 3[5]	10[4]	(75)
USHO[1]	8.12[3]	203	1.6	13.4	56.8	(154)
Richards	10.07[3]	229	0	0	13.0	(106)
This research	8.12[3]	248	1.3	1.4	22.4	(76)
Spade	20.3×30.4[2]	61	0	0	2.7	(106)

[1]Hydrographic Office.

[2]Rectangular box.

[3]Diameter.

[4]Larger values are acceptable with high-speed penetration.

[5]Can be more with small angle for cutting edge.

D = Diameter.

C_i = Inside clearance ratio.

C_o = Outside clearance ratio.

C_a = Area ratio.

Based on the above considerations, the coring device listed in Table 9 as "This research" was employed to obtain material for the consolidation testing program. The corer was constructed from U. S. Coast and Geodetic Survey plans titled "Hydro Plastic-corer, class 84."

Minor modifications made for the particular corer used off the Georgia Coast are described in Chapter V. Figures 31 and 32 are photographs of the corer assembled and disassembled.

Calculations for operation of the triggering mechanism and subsequent penetration of the corer into the ocean floor are described by Richards and Parker (155).

To avoid excess hydrostatic pressure being developed on the sample during penetration, the check valve in the top of the weight stand was fabricated so that it was as large as the inner diameter of the core barrel.

Core barrels were 305 cm lengths of 7.6 cm nominal diameter (8.9 cm OD, 0.316 cm wall thickness) "Type A Light Wall Rigid PV-Duit," a polyvinyl chloride conduit (PVC). This material was employed because it has physical properties that compare well with those of steel (Richards and Keller (155)), but is still light enough to handle in relatively long sections. In addition, it is practically impervious to sea water (Richards and Keller (154,155); and Keller, Richards and Recknagel (91)); does not react chemically with the sediment (Keller (86,88)); is available commercially; and can be easily cut.

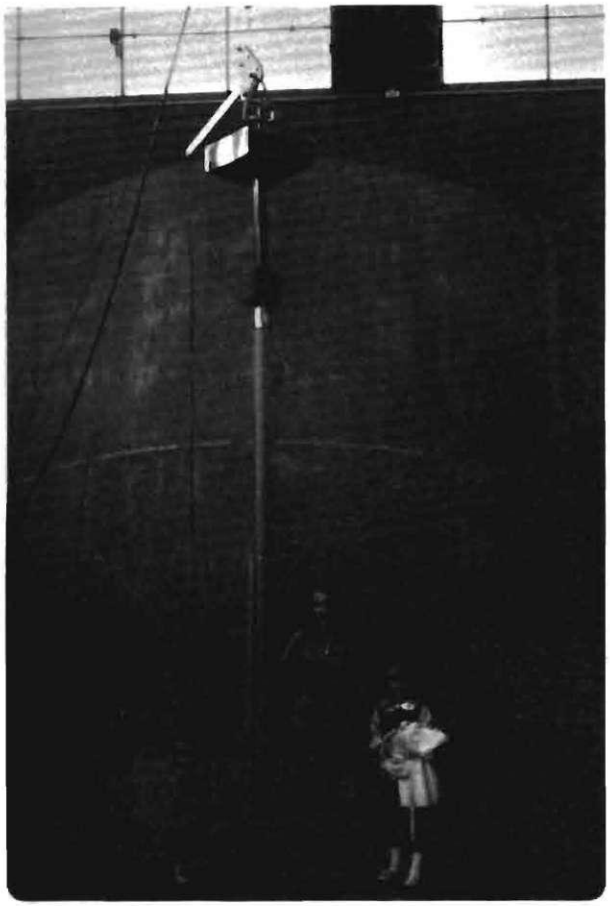

Figure 31. Hydro Plastic-Corer (Assembled)

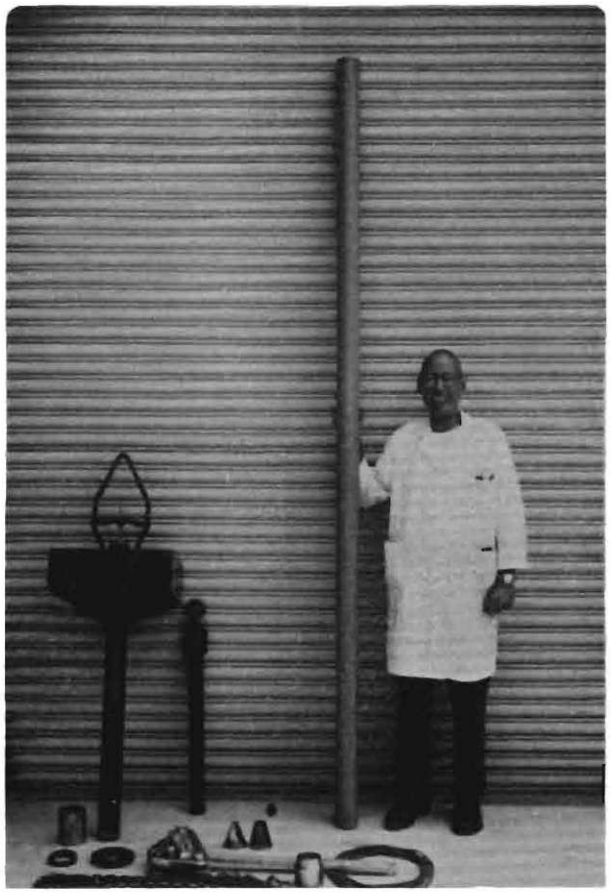

Figure 32. Hydro Plastic-Corer (Disassembled)

APPENDIX B

DESCRIPTIVE INFORMATION CONCERNING THE CORES AND CORE SITES

None of the sediments used in the testing program can be classified as deep sea sediment; however, despite their origin, all of them, with the exception of the cores from water depths less than 100 m, displayed many of the characteristics of deep sea sediments.

All the cores came from the continental margin of the eastern United States.

General Description of the Eastern Continental Margin of the United States

Just over a decade ago it was more or less common practice to distinguish the continental slope from the continental shelf by considering the shelf to be that zone inside the 200 m contour. Shepard (173) proposed defining the shelf as the area inside the shelf break (a marked change in slope) or, for extensive deep plateaus, a maximum depth of 600 m.

Using the shelf break as the dividing line, the shelf of the eastern United States reaches maximum widths off Georgia (130 km) and off the northeastern coast of the United States (beginning off New Jersey and continuing north). The general trend in width variation is indicated on Figure 1. Seldom is the shelf break found at a depth greater than 60 m. One exception occurs just north of Cape Hatteras

where the break is 120 to 160 m deep. This anomaly is significant to sediment distribution on the continental shelf and upper slope (Milliman, Pilkey and Ross (117)).

In general, while the continental shelf-slope juncture is reasonably limited, the end of the slope and beginning of abyssal depths is usually hard to define. A vast area known as the continental rise generally effectively obliterates any distinct change from slope to abyssal depths. This characteristic pattern can be seen on Figure 1 for that part of the eastern continental margin of the United States north of Cape Hatteras. South of Cape Hatteras a relatively more unique topography exists. There is no continental rise. Instead, several more or less distinct features exist. The Florida-Hatteras slope transitions into the Blake Plateau, a wide, relatively sediment-barren plain from 800 to 1200 m below the ocean surface. While the inner plateau slope is about 1.5°, the outer slope is as much as 50° or more (Shepard (173)).

Cape Hatteras appears to provide a very distinct dividing line, not only topographically, but from a sedimentation standpoint. At Cape Hatteras the shelf reaches its narrowest between southern Florida and the Laurentian Channel. Just to the north of the Cape, the sediments of the Maryland-New Jersey continental margins appear as a possible third distinct category (not considered here). Once north of New Jersey and south of Cape Hatteras, the influence of different sediment sources and relict Pleistocene features can be discerned. According to Neiheisel and Weaver (125), the prominence of the clay mineral

kaolinite in the less-than-two-micron fraction of sediments to the south of Cape Hatteras is diagnostic of the influence of rivers draining the saprolitic soils of the southeastern piedmont. Abundant chlorite and illite in sediments found on the continental shelf off northern areas subjected to Pleistocene glaciation reflect the fact that these clay minerals are the main ones available for steam transportation from New Jersey northward. These findings are in accord with those of Griffin, Windom, and Goldberg (55), who showed that clay minerals found in ocean sediments from relatively high latitudes are mainly illites and chlorites (mechanical weathering products) and those from relatively low latitudes are mainly kaolinite with some montmorillonite (chemical weathering relatively more important).

Cores for this research were obtained from three distinct areas. Two areas are probably topographical features of Pleistocene glaciation. Both are on the continental shelf. According to Swift (195), the Gulf of Maine (samples labeled "M") contains a series of relatively deep basins probably excavated by glaciers from soft coastal plain strata, while the Hudson Submarine Canyon (samples labeled "H") may be a relict river channel incised into the shelf during lower sea level. The third area from which cores were obtained ranges from an inshore estuarine environment to the upper Florida-Hatteras slope off the Georgia coast (samples labeled "G").

Georgia Continental Margin

Figure 33 shows the stations from which cores were obtained. This series of cores (G6, G8, G10, G11) provided a range of material

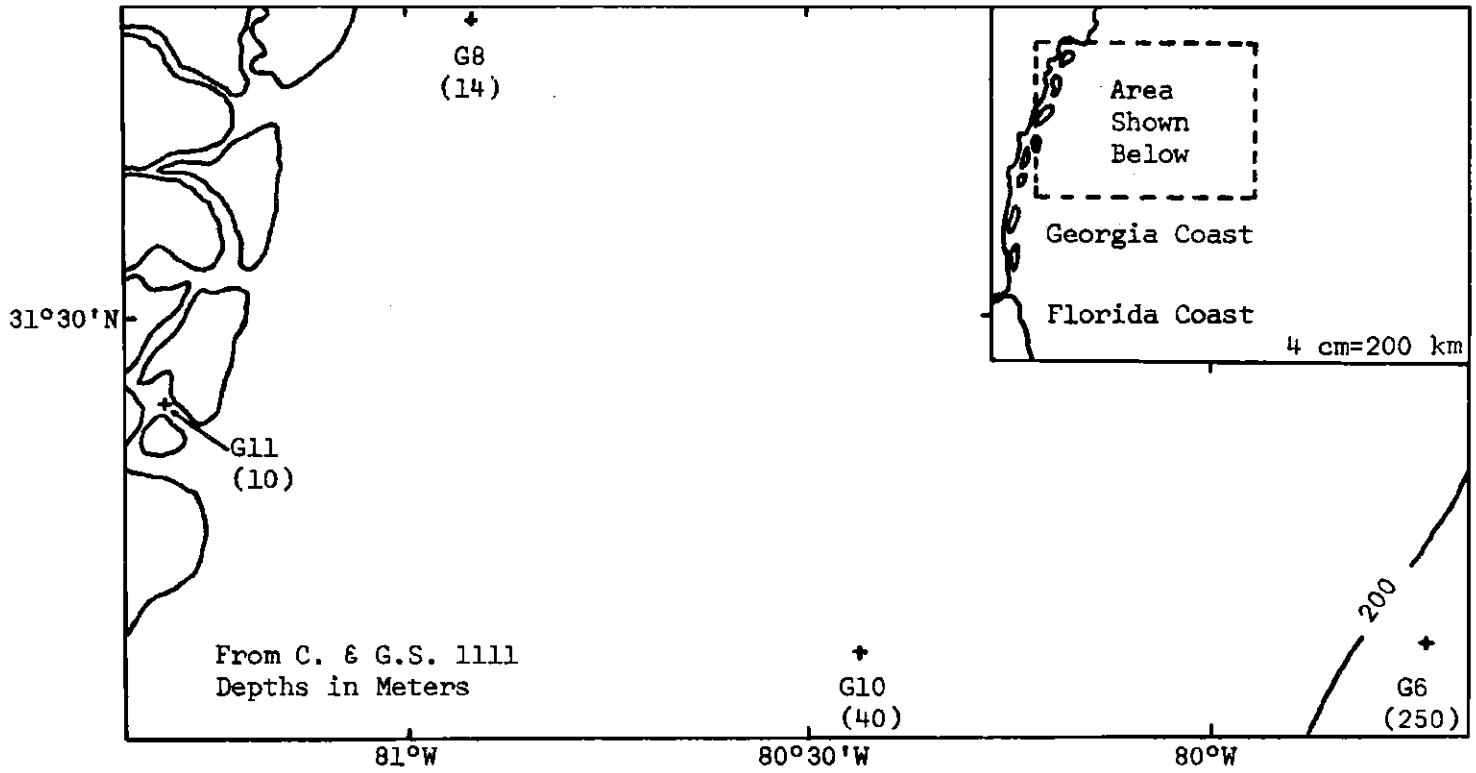

Figure 33. Stations off the Georgia Coast

representing most of the environments of the Georgia continental margin.

In general, piedmont rivers drain erodable land and carry sizeable suspended loads. Neihersel and Weaver (125) have shown that although the Altamaha and Ogeechee Rivers (which reach the Atlantic near stations G11 and G8, respectively) have drainage area characteristics which are different, both rivers discharge large concentrations of kaolinite into the ocean. Once in the ocean, early chemical alteration of kaolinite is minimal. Its concentration in surficial coastal sediments in areas such as Doboy Sound (G11) and off the Ogeechee River (G8) is controlled by physical factors. Neiheisel and Weaver further noted that dilution of kaolinite by montmorillonite reflects the effect of river drainage of the coastal plain (as compared to the kaolinite of the piedmont). In relation to the much larger Altamaha, the Ogeechee provides less kaolinite, but more montmorillonite (as a percentage of kaolinite).

Away from the nearshore areas, kaolinite concentration diminishes and the illite concentration (generally 10 to 15 per cent of the less-than-two-micron fraction in rivers) increases. Bigham (11) indicated montmorillonite showed a marked tendency to be deposited immediately seaward of tidal inlets.

Dipping gently seaward the Georgia continental shelf is an extension of the Atlantic Coastal Plain. Kaplan (82) postulated that nearshore sediments were moved down by longshore drift from the north, while the coarser sands offshore were identified as relict Pleistocene

sediments and were considered to be contributed by Georgia's rivers. Thus southern longshore drift may be the major source of recent lagoonal sediments. Pilkey (141) noted that glauconite and phosphate found in sediments from the central and outer shelf indicated they were relict. Similar conclusions were reached by Gorsline (53). In addition, he noted that troughs and basins found on the shelf and generally filled with fine-grained material (station G10) are evidence of structural deformation. Swift (195) indicated that a subdued channel (possibly G10) on the shelf correlated with the Altamaha River.

Past the shelf break the upper Florida-Hatteras slope, according to Gorsline (53), is covered with fine sands rich in carbonate. Swept by the extreme western edge of the Gulf Stream, sediments from this area, which includes station G6, are poor in clay minerals (less-than-two-micron fraction) and probably largely pelagic in nature.

Bottom temperatures over the study area off the Georgia Coast range from 15 to 20°C.

Gulf of Maine

General Topography

Seaward of the New England Coast, the Gulf of Maine forms a highly glaciated irregular floored depression containing at least 21 basins, separated by low swells and banks. Two channels, east and west of Georges Bank provide deep water entrances to the gulf (Ross (162)). Georges Bank and the Scotian Shelf provide a barrier above the Continental Slope. According to Shepard (173), tidal currents sweep across Georges Bank into the Gulf of Maine. Stetson (192) indicated

that during Pleistocene times considerable portions of the Gulf of Maine were dry.

Wilkinson Basin

Measured between the 260 m isobath, Wilkinson Basin is roughly 65 km long and 10 km wide. It tends in a NW-SE direction, and is the largest basin in the Gulf of Maine. Murray (121) listed its threshold depth at 280 m and its maximum depth at 320 m, while Faas (45) indicated water depths vary between 254 and 285 m. The basin appears to have relatively smooth slopes and a flat bottom. Figure 34 shows the stations from which cores were obtained. Surficial sediments in the basin are soft silty-clays that are probably a composite of older reworked Pleistocene glacial materials and varying concentrations of foraminifera tests (Milliman, Pilkey and Ross (117), Ross (163), and Torphy and Zeigler (201)). Fass (45) indicated the dominant clay minerals in the less-than-two-micron fraction of the sediments were illite and chlorite. Bottom temperatures in the basin are relatively constant at about 5° C.

Hudson Submarine Canyon

General Topography

One of the most prominent seafloor features on the U. S. continental margin, the canyon cuts 850 m into the shelf and slope, for all practical purposes linking the modern Hudson River to the deep ocean. Heading in 90 m of water, the canyon consists of two or three branches out to a depth of 180 m. Traced seaward from the junction of the branches, the canyon's axis winds gently downslope, intersected by numerous small tributaries. According to Heezen, Tharp and Ewing (64),

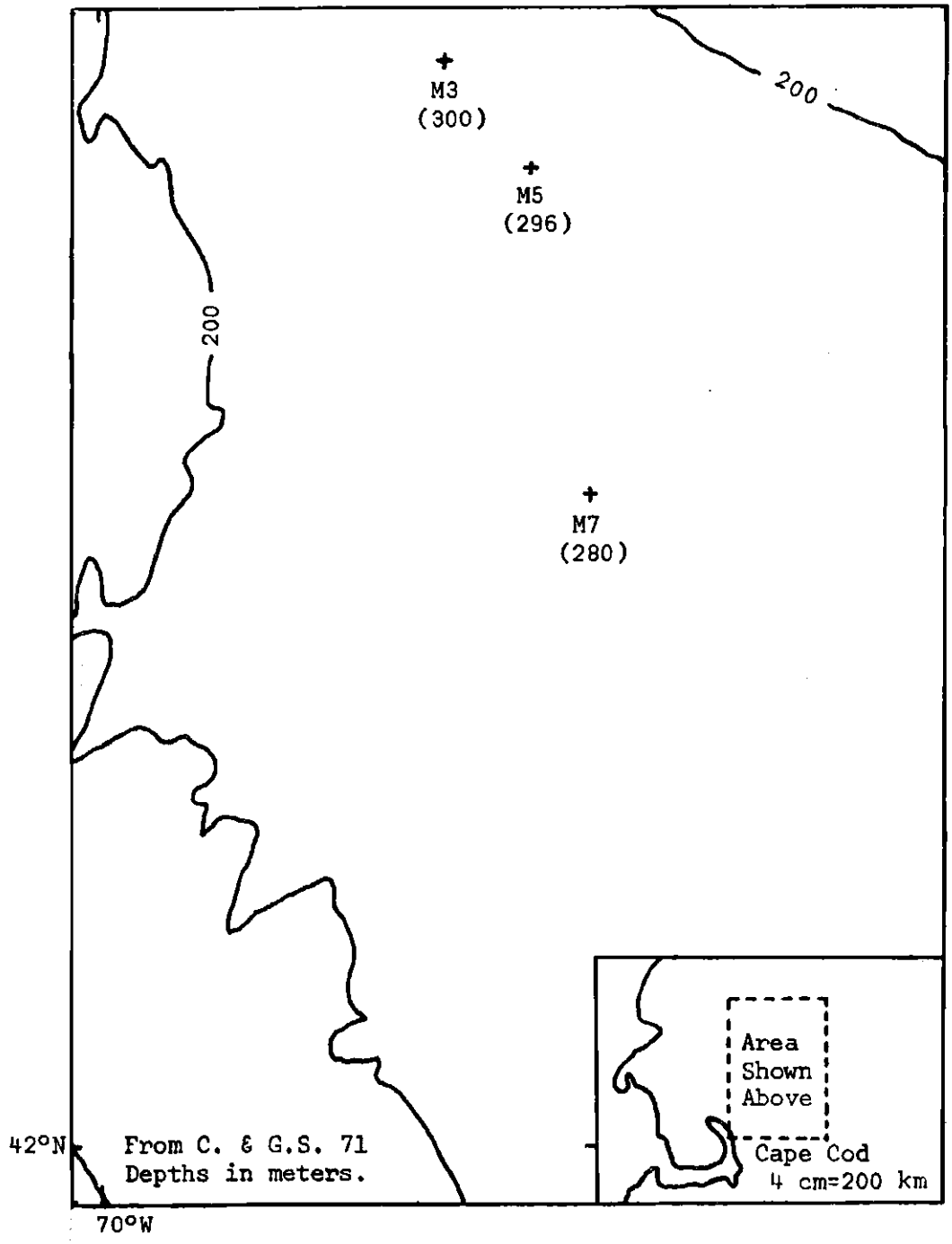

Figure 34. Stations in the Gulf of Maine

the canyon changes from a gorge (1900 m deep) in its upper reaches, to a channel (90 m deep) at the base of the continental slope, to a "lower gorge" (550 m deep) before it finally reaches the ocean floor. This lower gorge seems to be what Shepard and Dill (174) call a fan valley.

Upper Reaches of the Canyon

The upper reaches of the Hudson Submarine Canyon are defined here to be that portion of the canyon axis and flanks between the 100 and 1000 m isobaths.

Working with the research submarine ALVIN, Keller (85) reported bottom currents from 0.04 to 0.53 knots in the general area of the cayon from where cores H4 and H6 were taken. At one location turbidity was noted as being concentrated in a zone 3 to 5 m above the canyon bottom. Based on this work, Keller tentatively concluded that currents appeared to be under tidal control and that sediment seemed to be transported down canyon in suspension.

Figure 35 shows the general area of the upper reaches of the canyon and the location of the three stations from which cores were obtained.

Sediments from the upper reaches of the canyon have been found to be relatively thick deposits of fine silts, sometimes stratified with fine sand (Shepard and Dill (174)).

Bottom water temperatures in the upper reaches of the canyon are estimated to vary between 5 and 15°C.

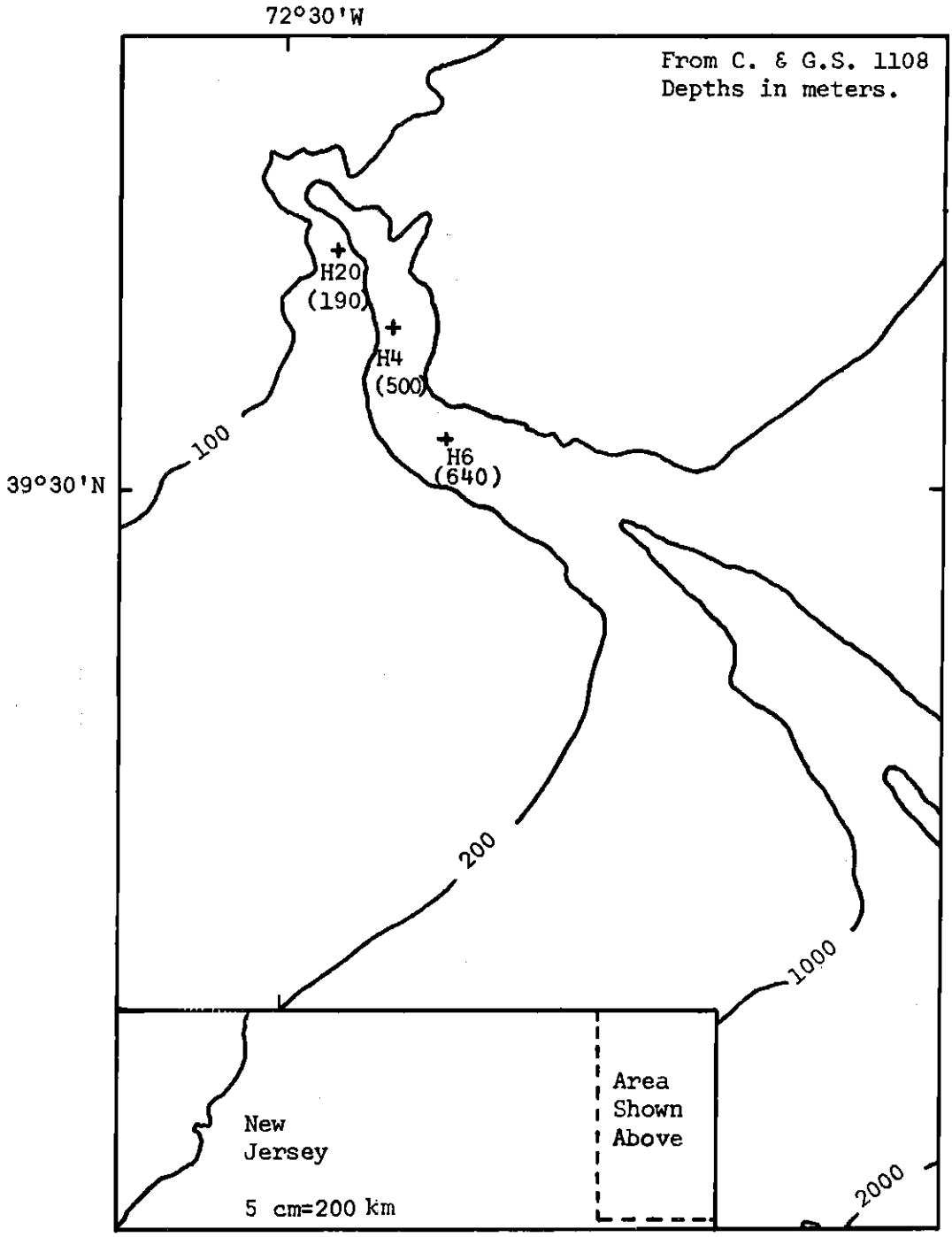

Figure 35. Stations in the Hudson Submarine Canyon

General Description of the Cores

Various classification and mineralogical tests performed on the cores are listed below. Differences in test procedure from that used on similar terrestrial material are described. Unless otherwise indicated, all tests were conducted based on information in Lambe (97). Tables 10, 11 and 12 indicate the results of the various tests and form the basis for the following description of the test sediments.

1. *Natural Water Content (w).* Oven temperature was 105°C ± 5°. Only the values of w in Table 3 were corrected for salt content.

2. *Atterberg Limits* (w_l,w_p). Samples were air-dried down to the test water contents.

3. *Plasticity Index* (I_p). Sediment will be highly plastic for I_p greater than about 40. Sediments composed mainly of microorganisms are an exception. For these sediments the plasticity index cannot be determined.

4. *Liquidity Index* (I_l). Values for submarine sediments are generally greater than 1.0, indicating that the sediments are normally consolidated.

5. *Activity* (A_T). Similar activities indicate similar geologic origins. High values can be caused by swelling clay minerals and calcareous microorganisms (Einsele (38)).

6. *Laboratory Vane Shear Strength.* Authority: Richards (149). The rate of vane rotation used was 70°/min. This rate was selected based on the work of Halwachs and Monney (58). Vane strengths are assumed to approximate undrained strengths. For other views see

Table 10. Core Site and Mineralogy Data for Materials Used in the Testing Program

Core	Date Taken	Latitude N.	Longitude W.	Water Depth M.	Regime	Unified Class.	$CaCO_3$ %	Estimated Organic Carbon %	<2μ %	Ill. %	Chlor. %	Mont. & Vermic. %	Kao. %	Total Length Cm.
H4	9/72	39°35.5'	72°25.2'	500	C.Axis	MH	1-5	2.8-3.0	34	68	32	-	-	190
H6	9/72	39°32.0'	72°23.0'	640	C.Axis	MH	2-6	2.1-3.5	27	71	29	-	-	152
H20	9/72	39°38.0'	72°27.5'	190	C.Flank	MH	3-7	1.8-3.3	23	65	35	-	-	149
M3	7/71	42°44.0'	69°41.2'	300	Basin	CH	0-2	1.6-1.8	57	67	33	-	-	178
M5	7/71	42°39.7'	69°36.4'	296	Basin	CH	-	2.0-2.2	60	73	27	-	-	186
M7	7/71	42°26.6'	69°33.8'	280	Basin	CH	0-4	1.7-1.8	55	74	26	-	-	236
G 11/6	6/72	31°24.1'	81°18.4'	10										203
G 11/7	6/72	31°24.1'	81°18.4'	10	Sound	MH,ML	2-5	2-4**	6	2	-	39	59	198
G 11/8	6/72	31°24.1'	81°18.4'	10										229
G6	5/72	30°45.6'	79°57.0'	250	Slope	ML	24-28	2-3**	18	16	-	53	31	158
G8	6/72	31°48.7'	80°55.2'	14	Shelf	ML	13-14	<1.0	12	8	-	47	45	109
G10*	2/71	31°08.4'	80°26.3'	40	Shelf	CH	-	-	48	7	-	50	43	41

*Box core. All others taken with hydro plastic-corers. Material from this core was not used in the testing program. Data are included for information only. All sieves included significant quartz particles with angularity increasing between the No. 50 and No. 120 sieves. There were few heavy mineral grains. Calcite was present in small quantity on most sieves.

**High. Arman method.

Table 11. Atterberg Limits

Core	Depth Cm.	w %	w_l	w_p	I_p	I_l	A_T
G 11/7	10-20	142	110	40	70	1.5	11.7
	48-51	130	90	30	60	1.7	-
	58-64	135	105	30	75	1.4	
G 11/8	2-25	150	155	120	35	0.9	-
	132-135	146	135	45	90	1.1	2.0
G8	36-38	52	41	-	-	-	-
G10	28-33	84	90	30	60	0.9	1.2
G6	64-67	55	55	30	25	1.0	-
M3	51-53	167	115	40	75	1.7	-
	95-104	140	130	50	80	1.1	1.4
	104-112	146	130	55	75	1.3	-
	135-140	138	130	50	80	1.1	1.4
	155-159	142	125	50	75	1.2	-
M7	38-48	152	120	50	70	1.5	-
	180-183	126	115	50	65	1.2	1.0
	229-231	132	120	45	75	1.2	-
H4	104-109	130	130	60	70	1.0	2.1
	135-142	133	125	45	80	1.1	-
	155-157	132	125	60	65	1.1	-
	170-175	126	125	60	65	1.0	2.2
	178-180	124	120	60	60	1.1	-
H6	119-122	136	135	60	75	1.1	-
	132-135	152	135	60	75	1.2	-
	137-145	139	140	60	80	1.0	2.4
H20	119-122	98	100	40	60	1.0	2.2

Table 12. Core Classification Data for Material Used in the Testing Program

Core	Range of e_o	Range of S_o %	Sensitivity	VSCS % Sand/ % Silt/ % Clay	Shepard[2] % Sand/ % Silt/ % Clay	Specific Gravity of Solids[3]	Depth of c/p'[4] cm	c/p'_o	c/p'_c	I_p
G6	1.61-1.68	91-92	-	50/32/18	51/26/23	2.71	61-69	4.41	0.66	25
G8	1.71	94	-	47/41/12	50/32/18	2.67	-	-	-	-
G10	-	-	-	19/33/48	21/23/56	2.70	-	-	-	-
G 11/6	3.97-4.19	94-96	7	52/16/32	57/ 6/37	2.61	-	-	-	-
G 11/7	4.82-5.32	95-97	-	18/76/ 6	18/70/12	2.61	-	-	-	-
G 11/8	3.25-3.38	95-97	-	-	- -	2.63	-	-	-	-
M3	3.91-4.04	94-97	-	2/41/57	2/18/80	2.69	-	-	-	-
M5	-	-	2-6[1]	1/44/55	1/24/75	2.71	-	-	-	-
M7	3.80-4.20	92-96	5-6	1/35/64	1/13/86	2.74	188-196	0.88	0.58	75
H4	3.71-4.08	88-93	4	3/65/32	3/65/32	2.61	103-111	1.35	0.50	70
H6	3.70-4.09	88-96	6-8	3/70/27	5/56/39	2.62	117-125	0.78	0.22	75
H20	2.61-2.91	93-97	6	13/60/27	17/53/30	2.64	117-125	1.13	0.49	60

[1]Over the whole core.
[2]In Shepard's trilineal system, clay is that material less than 0.039 mm, and silt sizes are between 0.039 and 0.65 mm.
[3]Average for several tests.
[4]Vane shear strength assumed equal to c.

Inderbitzen and Simpson (78), and Shibata (176).

7. *Sensitivity* (S_T). Most cohesive submarine sediments are sensitive (based on values of sensitivity greater than four being considered sensitive).

8. *A Pore Pressure Parameter* (A). Skempton and Bjerrum (182) indicate that A can be useful in improving settlement estimates where lateral conditions vary from those assumed. Only Moore (120) has reported A values for submarine sediments. His material was probably disturbed enough to make the values reported questionable. For clayey silt with about 10% sand he found A_f varied from 0.41 to 0.98.

9. *Specific Gravity.* Trapped air was removed by vacuum.

10. *Unit Weight* (γ_m). All values are based on $\gamma_{sw} = 32$ gm/cm^2. Values of γ_m used to determine p_o' were based on an average value of γ_m between the surface and depth at which p_o' was determined.

11. *Void Ratio* (e). For the small loads used in the testing program, the initial void ratio was for practical purposes equal to the *in situ* void ratio. For deep sea sediments, e varies relatively little in the top few meters of the sediment.

12. *Saturation* (S). Sampling and relief of hydrostatic pressure allows dissolved gas to come out of solution, reducing the degree of saturation. Disintegration of organic matter also reduces the degree of saturation as H_2S forms.

13. *Grain Size.* Lambe's combined analysis (Alternate B) was used to determine sediment grain size. The dispersing agent used was powdered hexametaphosphate in distilled water prepared as indicated by

Keller (89). The Unified Soil Classification System was used in conjunction with the subdivisions for sand sizes given in Sowers and Sowers (190).

14. *Clay Mineralogy.* X-ray diffraction procedures and quantitative methods used were essentially those given by Neiheisel and Weaver (125). Percentages are considered accurate ± 10%.

15. *Carbonate.* The acid neutralization technique described by Black, *et al.* (16) was used.

16. *Organic Content.* The method described by Arman (4) was used. The results obtained did not compare well with data provided by Reuter (148), Faas (46) and Keller (90) based on work in adjoining areas. Arman's method appears to give values which are probably high because some adsorbed water is driven off during the test.

17. *Microscopic Examination.* Random examinations were made of various grain size fractions taken from the mechanical analysis.

Doboy Sound, Georgia:
Cores G 11/6, G 11/7, G 11/8
(Water Less Than 100 m in Depth)

Three cores from the same station were obtained (G 11/6, G 11/7, G 11/8). In general, each core consisted of rather heterogeneously mixed sand, silt and clay for the first 100 cm. Within this depth range a few relatively homogeneous layers high in soft clayey, silty material were used in the testing program. From 100 cm to about 135 cm a layer of silty sand was found. Slightly below the sand a stiff clay thought to be Pleistocene in age extended for the remainder of the core. Using Keller's (88) descriptive classification, these cores were Fluvial-Marine (sand-silt) layered with Fluvial-Marine (silt-clay).

Without exception all grain size analysis showed this material to be gap graded. The material on all sieves was practically 100 per cent quartz. In the less-than-two-micron fraction the amounts of kaolinite, montmorillonite and illite varied only slightly in the top 100 cm. Because of the test method, the percentages of organic carbon shown in Table 10 are probably slightly high. Based on the *Rock Color Chart* (158), the materials used in the testing program were dark grey (N3).

Georgia Coast--Nearshore:
Core G8
(Water Less Than 100 m in Depth)

Off the mouth of the Ogeechee River the carbonate content increased and the organic carbon content decreased in relation to Doboy Sound. Montmorillonite and illite concentrations increased at the expense of keolinite. The core was more uniform, and in general more sandy (a fine sandy-silt). Compared to Core G6, G8 had an almost identical gap graded grain size curve. Quartz was the predominant mineral on all sieves. The particles were much more angular for the larger grain sizes than for similar sizes from the Doboy Sound cores. A greater concentration of heavy minerals was found on sieves between No. 80 and No. 230, than for the Doboy Sound cores. By Keller's classification system, the material was Fluvial-Marine (sand-silt).

Uchupi and Tagg (203) indicated that the shelf where G8 was cored is quite smooth. This location is at a water depth that places it on the relict-recent sediment boundary (Milliman, Pilkey and Ross

(117)), but because of the sand sizes present and the carbonate content, it is felt to be mainly recent sediment.

The material used in the testing program was dark grey (N3).

Georgia Coast--Offshore:
Core G10
(Water Less Than 100 m in Depth)

Station G10 is off the Altmaha River. The bottom was cored with a spade corer. The core was about 40 cm in length and consisted of about 20 cm of sand over a plastic dark grey (N3) clay. A Fluvial-Marine classification was made for the clay. The station was approximately 100 km offshore and about 40 km shoreward of where Uchupi and Tagg (203) indicated the shelf break occurs. It is thus well shoreward of areas known to be affected by oceanic swells and tidal velocities (Macintyre and Milliman (110)).

Florida-Hatteras Slope:
Core G6
(Water Greater Than 100 m in Depth)

This core shows significant differences from Core G8. Although sand size particles constitute about the same fraction, they are mainly shell fragments and other carbonate related debris (75% carbonate, 25% angular quartz). This is reflected in an increase in $CaCO_3$ content, which is the highest for any core used in the testing program. The carbonate content determined for this core agrees with data for the area in which it was taken (see Milliman, Pilkey and Ross (117)). The core was a dusky yellow green (5 GY 5/2) sandy-silt. By Keller's system it was Fluvial-Marine (sand-silt) bordering on Calcareous Sand and Silt. Although the organic carbon content indicated in Table 10 is probably

high, an increase over G8 is apparent. Kaolinite content was down significantly and montmorillonite and illite contents up. This change probably indicates little terrigenous material reaches this area, or is prevented from being deposited by the Gulf Stream. Consequently, pelagic processes probably control the composition of the sediment.

Gulf of Maine:
Cores M3, M5, M7
(Water Greater Than 100 m in Depth)

There was no significant difference among these cores as indicated by the data presented in Tables 10, 11 and 12. All three cores were classified as silty-clay of high plasticity and were greyish olive (10 Y 4/2) in color. By Keller's system, they were Fluvial-Marine (silt-clay). Microscopic examination of the material retained on the No. 325 sieve showed it to be partly foraminifera. The less-than-two micron fraction of the sediment was mainly illite and chlorite. The relatively low activity of the sediment reflects the abundance of illite in the clay-size fraction.

Hudson Submarine Canyon:
Cores H4, H6, and H20
(Water Greater Than 100 m in Depth)

In general there seemed to be little difference among the three cores in organic carbon (all three emitted a definite H_2S odor when cut) and calcium carbonate contents. All three cores were greenish black (5 GY 2/1) in color. Only a slight difference existed in clay mineralogy between canyon flank and axis (the predominant clay minerals were illite and chlorite). The major differences were that the H_2S smell from H20 was not as strong and it had more sand (by weight) than

did H4 or H6. By Keller's system all three cores were Fluvial-Marine (silt-clay). Microscopic examination showed the sand fraction to be mainly shell fragments mixed with a small amount of quartz. A difference in values of liquid limit also existed between axis cores and the flank core. The relatively low values of specific gravity determined for all cores could be related to the presence of organic matter. Some samples from core H4 had the lowest degree of saturation found for any material used in the testing program.

Activities in all three cores were relatively high. Since the clay mineralogies and plasticities were quite similar to the Gulf of Maine cores, this probably resulted from the clay size fraction being about half of that of cores M3, M5 and M7. Why the plasticity should remain high as the grain size increased is not readily apparent, but it might relate to the organic content.

Analysis of Sediments

Based only on sensitivities and liquid limits, all the sediments used (except for core G8) would be classified as sensitive and normally consolidated (assuming that for a liquidity index less than 0.8 the material would be overconsolidated). Plasticity indices were relatively uniform for all cores rich in illite and chlorite. Figure 36 shows that the data from the three general core locations (the Georgia Coast, the Gulf of Maine, and the Hudson Submarine Canyon) tend to plot in three separate bands parallel to Casagrande's A-line.

In general all the cores showed an increase in vane shear strength with depth, although this was more pronounced in some cores

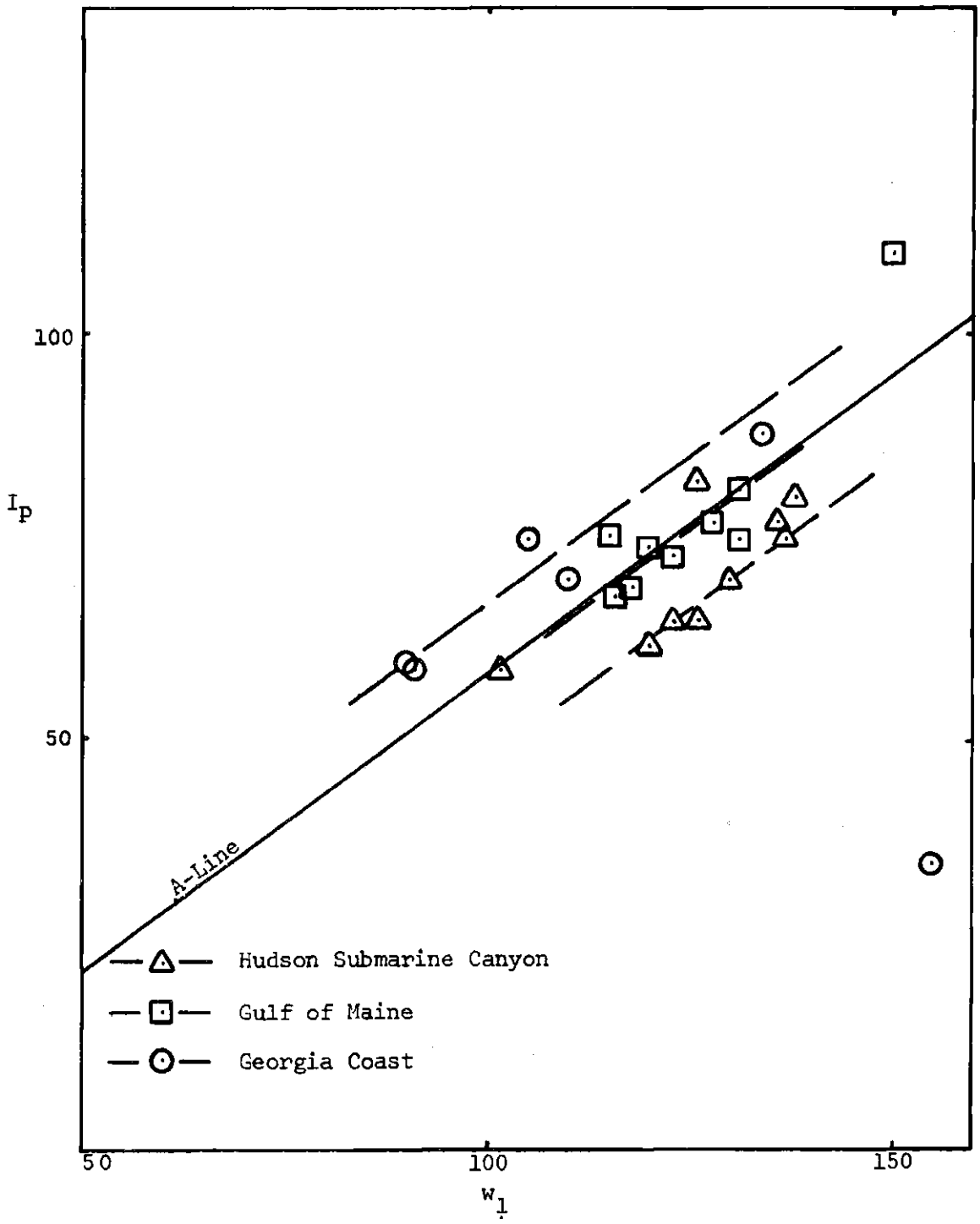

Figure 36. Relationship Between Plasticity Index and Liquid Limit

than in others. In most cases the slopes of the strength-depth profile could be correlated to similar slopes of the natural water content-depth profile on an inverse basis (see Figures 37, 38 and 39). The heterogeneous nature of the Doboy Sound Cores compared to all of the other cores can be seen in Figure 37.

Figure 40 shows the variation in void ratio with depth in most cores. For each case a line representing the average trend with depth is shown. Except for cores G 11/6, G 11/7 and G 11/8, there is little variation from the average and in general there is a *very very slight* tendency for void ratio to decrease with depth. For core G 11/7, which is like the others from Doboy Sound, there is significant scatter among the data.

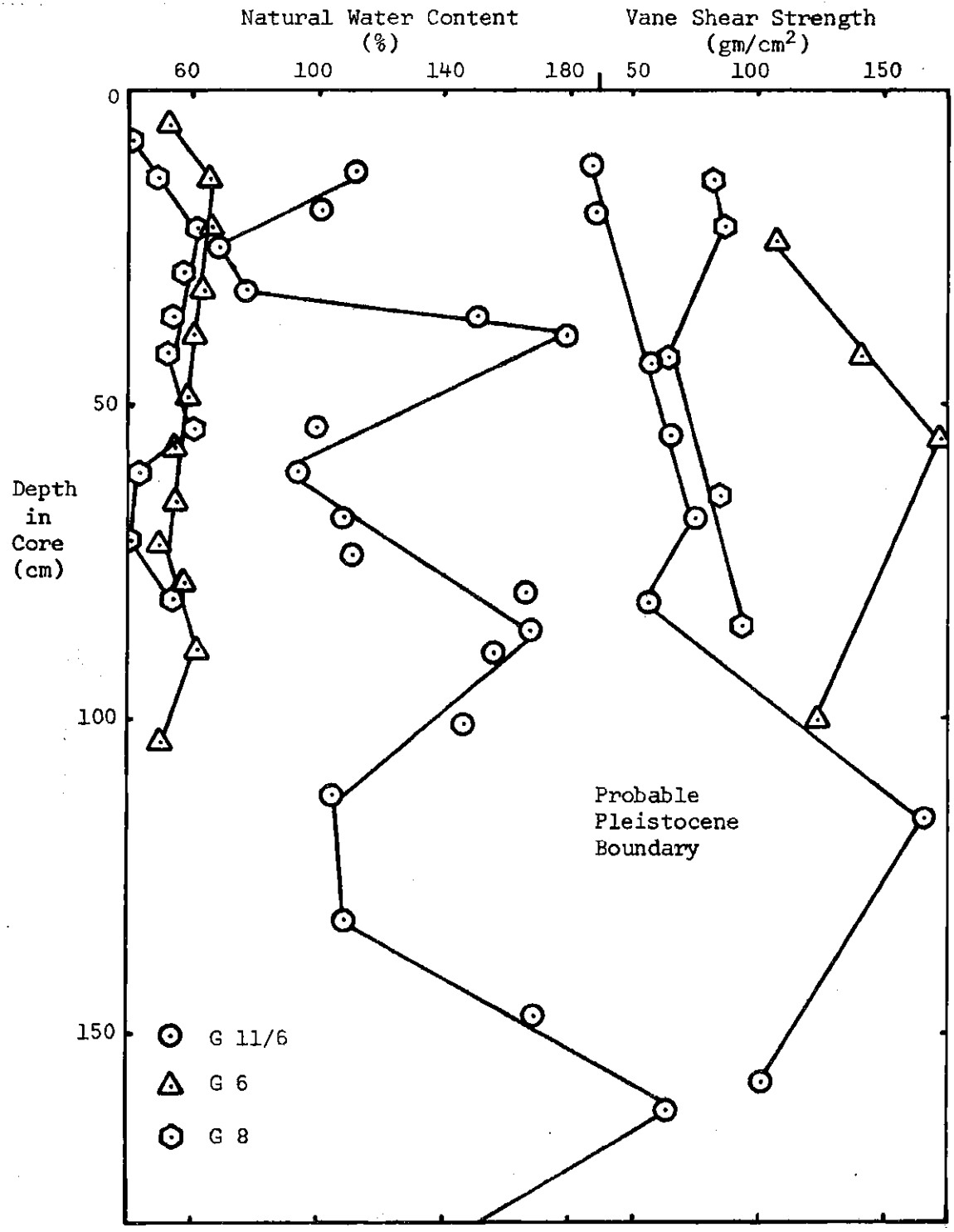

Figure 37. Natural Water Content and Laboratory Vane Shear Strength vs. Depth in Cores from the Georgia Coast

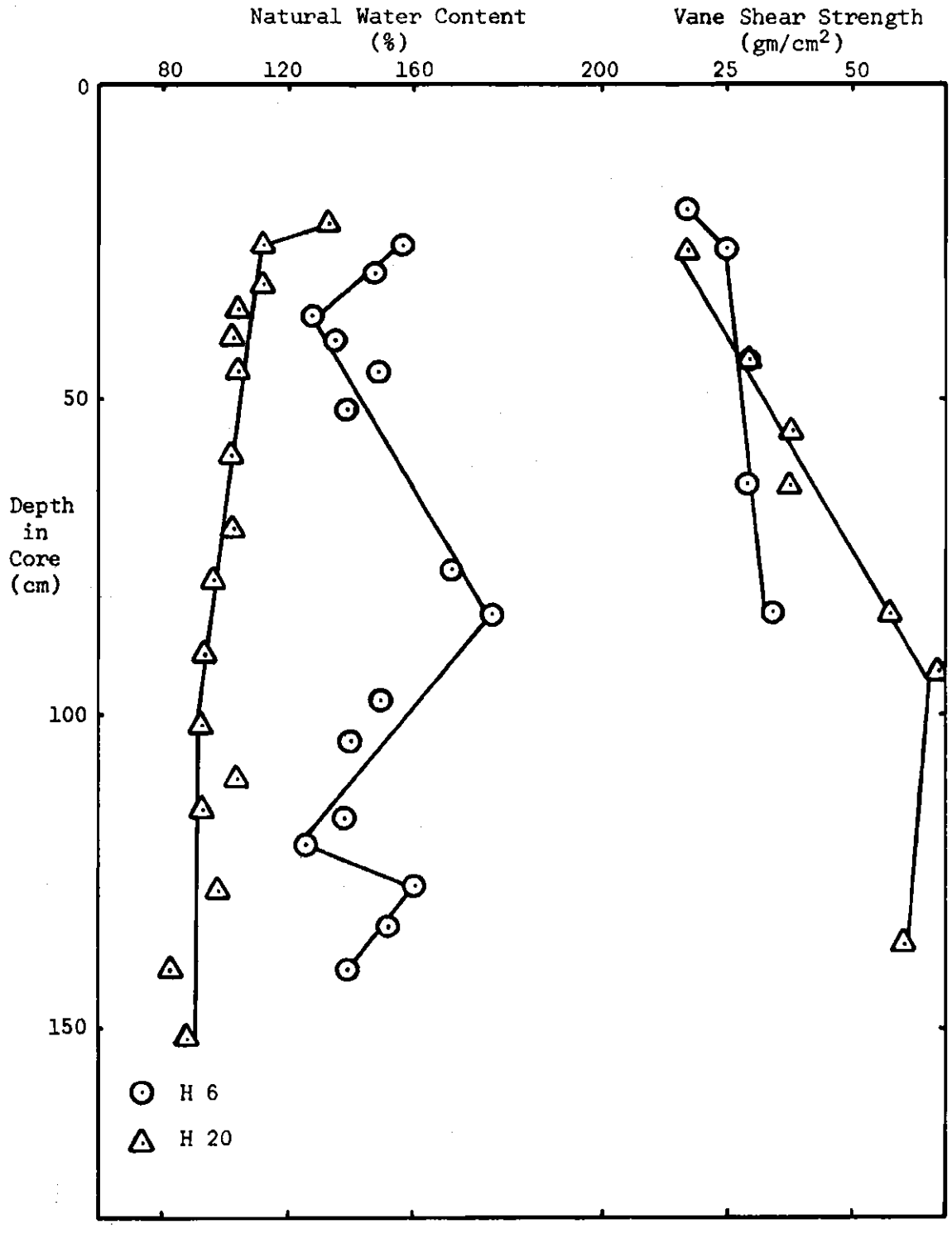

Figure 38. Natural Water Content and Laboratory Vane Shear Strength vs. Depth in Cores from the Hudson Submarine Canyon

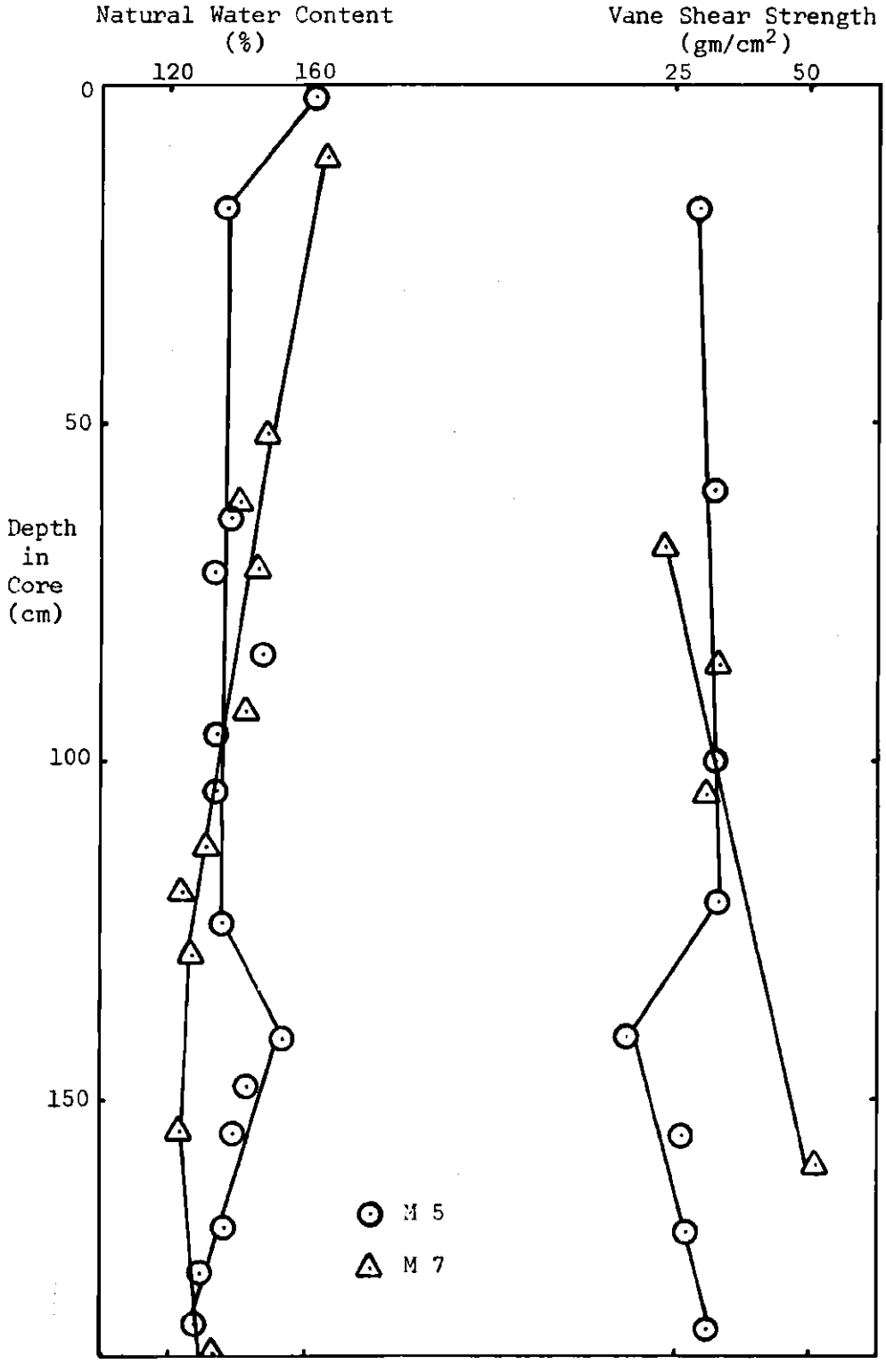

Figure 39. Natural Water Content and Laboratory Vane Shear Strength vs. Depth in Cores from the Gulf of Maine

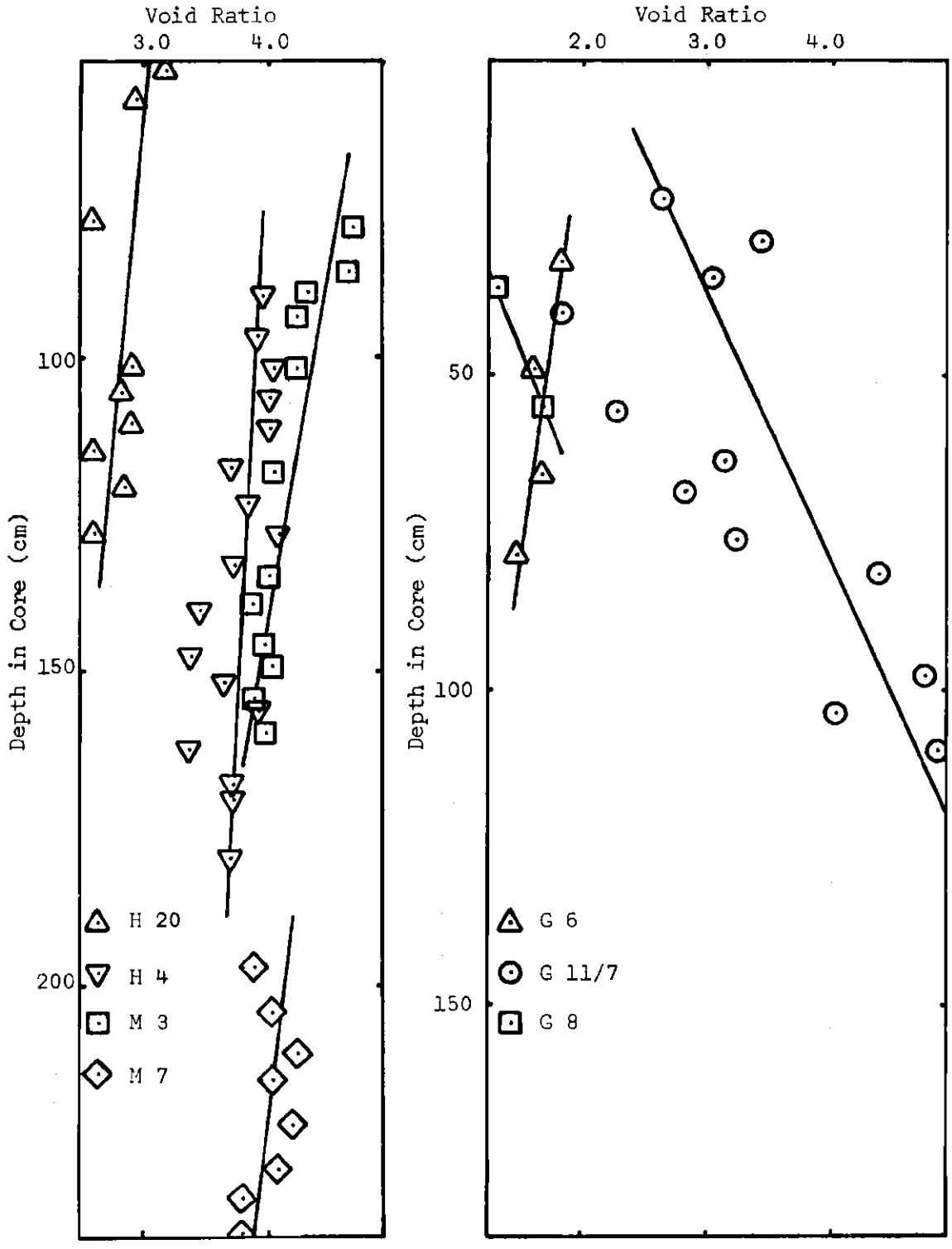

Figure 40. Void Ratio vs. Depth in Core

APPENDIX C

STRUCTURE OF SUBMARINE SEDIMENTS PRIOR TO LITHIFICATION

Sedimentation

Theoretical Considerations

The response of a sediment to the application of load or to the relief of stress depends on the structures of the sediment. In turn, the structure is a function of the number and type of bonds that exist between the individual sediment particles, ions and fluid molecules that fill the pore space in the sediment. These bonds are generally considered to be secondary valence bonds or hydrogen bonds, both of which are weaker than the primary valence bonds which are formed between atoms and molecules.

It can be shown that the distribution of particles (ions, molecules, etc.) in a force field is given by the Boltzmann Equation:

$$n_i/n_o = e^{(E_o-E_i)/kT} \qquad (7)$$

This equation can be applied to the distribution of cations in the electric field of a negatively charged clay particle. In this case E_o is assigned a value of zero at an infinite distance from the particle. Thus E_o-E_i equals $-z_i\epsilon\psi$ where z is the ionic concentration, ϵ is the charge in electrostatic units and ψ is the electric potential. The

relationship predicts that the cation concentration near the clay particle should exceed that in the solution at an infinite distance from the particle.

Poisson's equation gives the effect of a space charge on the space rate of change of the electric potential gradient:

$$d^2\psi/dx^2 = -4\pi\rho \tag{8}$$

If the space charge in an electric field is made up of ions, the space charge density from an ionic species will be ϵzn, since ϵz is the charge per ion and n is the ionic concentration. The total space charge density is the sum of space charge densities of the different ionic species:

$$\rho = \epsilon \sum_{i=1}^{n} z_i n_i \tag{9}$$

Substituting (7) into (9) and then inserting into (8) gives the Poisson-Boltzmann Equation:

$$d^2\psi/dx^2 = -4\pi\epsilon \sum_{i=1}^{n} z_i n_o e^{-z_i \epsilon \psi/kT} \tag{10}$$

If the dielectric medium is not a vacuum, the right side of (10) must be divided by the dielectric constant of the medium. The resulting equation forms the basis for the concept of a diffuse double-layer of water and ions surrounding each clay particle:

$$d^2\psi/dx^2 = -4\pi\epsilon/D \sum_{i=1}^{n} z_i n_o e^{-z_i \epsilon \psi/kT} \qquad (11)$$

A number of assumptions were used in developing this equation, and others are required to solve it. The more relevant ones are:

1. The charge is spread uniformly over the clay particle.
2. The edge to face area ratio of the clay particle is small.
3. The ions are point charges.
4. Particle sizes and shapes are uniform.
5. Particle spacing is uniform.
6. There is a minimum particle spacing below which the equation does not hold.
7. External forces are negligible.
8. The potential energy in water molecules close to the ions and clay particle does not affect the equation.

In a real sediment most of these assumptions are invalid, and the situation is complicated even more by the fact that silt and sand size particles are not considered.

The main reason for using Equation (11) is that it provides a framework within which to work and provides reasonable explanations of some observed interactions of the clay-water system. It cannot be used to provide accurate quantitative results.

Clay Minerals

Terminology used in the following description is patterned after Lambe (98). Clay minerals are crystalline materials composed of layers of sheets with definite atomic structures. The atoms in the sheets are connected by primary valence bonds. The number of layers composing the

crystalline structure is controlled by several factors including crystal lattice distortion caused by the substitution of one ion for another (isomorphous substitution), hydrogen bonding and intermolecular attractive forces.

Four clay minerals are of interest here:

Kaolinite is composed of layers of alumina and layers of silica.* A member of the Kaolin family, it is a two-layer, non-swelling clay mineral. Kaolinite's unit structure is thus two layers.

Montmorillonite is composed of layers of alumina sandwiched between silica layers. A member of the Smectite family, it is a three-layer, swelling clay mineral.

Illite is a family of non-swelling three-layer clay minerals composed of alumina layers sandwiched between silica layers. It differs from montmorillonite in that isomorphous substitution has caused some Si^{4+} to be replaced by Al^{3+} and the resulting charge deficiency is made up by potassium ions strongly bonded between adjoining unit structures.

Chlorite is a family of regular mixed layer clay minerals composed of two unit structures of talc strongly linked by a layer of magnesia.

Significance of Clay Minerals. Because of their very small size, the clay minerals have very high electric forces associated with them in relation to their surface area. These electrical forces arise from various causes and produce the plastic and cohesive character of clayey

---

*As an example, a silica layer is composed of a sheet of Si^{4+} ions and a sheet of O^{2-} ions. In the sheet of silica ions some silica has been replaced by Al^{3+} ions (isomorphous substitution).

sediments. The capacity of the various clay minerals to swell (adsorb additional water) and attract dissociated cations, is related to these electrical forces and large surface areas. Because of its small size and unsatisfied charge deficiencies, montmorillonite has the greatest affinity for cation adsorption (cation exchange capacity).

Clay-Water System

As previously indicated, the various clay minerals are crystalline materials. Depending on several factors, varying amounts of water can be adsorbed between adjoining unit structures. In simplified terms, four classes of water are involved with the clay minerals--(1) very strongly bound water in the crystalline lattice (not of interest here); (2) water strongly bound to the clay particle; (3) water influenced to varying degrees by the clay, but relatively free to move in the sediment pores ". . .; and (4) water in the . . ." pores uninfluenced by the clay. "Bound" or "oriented" water is assumed to combine category two and part of category three and is defined as that portion of the pore water which will not flow from the sediment under stresses normally applied by engineering structures. "Free water," part of category three and category four, *will* flow from the sediment under applied stress.

Several workers have conceived an ice-like crystalline structure for the water closest to the clay particle. However, the atoms of both bound and free water are in constant agitation to extents dependent on the thermal energy of the system, and this agitation in conjunction with free ions in the fluid disrupts the tendency for the water closest to the clay to form a true crystalline structure (Wang (210),

Rosenqvist (161)). The bound water does have higher viscosity and lower density (Leonards (102)) than the free water in a fresh water system (maximum density occurs at 4°C). In a salt water system maximum density occurs below the point at which ice forms; therefore, bound water with its ice-like structure would be *more* dense than the free water.

In terms of geometry, adsorbed cations extend the dimensions of the immobilized layer (Resendiz (146)).

Water has the capability to be adsorbed by the clay, mainly because it is electrically unsymmetrical.

Flocculation. Equation (11) indicates that if the concentration of ions in solution increases, the thickness of the double layer around individual clay particles will be reduced. Thus repulsive forces which tended to keep colloidal clay particles apart will be reduced. If the double layer is thin enough and colloidal clay particles come close together, interparticle attractive forces will cause them to act as one particle. Groups of particles thus become flocs (Lambe (98)).

In sea water pH increases in addition to the ionic concentration. Because of the deficiency in H^+ ions (higher pH) of the surrounding fluid, H^+ ions dissociate from the clay particle edges. In turn this causes the exchange capacity to go up (the particle has greater negative charge deficiency and cations are more readily adsorbed). Particle-to-particle attractions result in flocs. Prior to this time, the negatively charged colloidal particles appear to have adsorbed dipolar water molecules to their surfaces and evidently these molecules kept the

colloids apart (Neiheisel and Weaver (125)). Rosenqvist (150) reported work by Werner showing that flocculation occurred at greater distances when dissolved ions were present.

According to Sillen (178), once clay colloids reach the ocean, ion exchange reactions are completed with 24 hours.

As previously indicated, there are several sources of negative charge deficiencies in the clay minerals. Broken bonds leaving charges on particle edges appear to be most important in kaolinite and well crystallized chlorite and illite. For montmorillonite isomorphous substitution is probably the most important source of negative charge deficiency. Dott (36) indicated that kaolinite and illite tended to flocculate more readily at low levels of chlorinity (i.e. presumably less cations available).

Rate of flocculation is also related to the energy of the environment. Neiheisel and Weaver (125) indicated that transportation velocity is the reason why flocculation can occur in both estuaries and hundreds of kilometers out to sea. They postulated that critical velocities exist depending on particle type and other factors which, when exceeded, will halt further flocculation growth. After reaching a certain size, the floc will begin to settle through the water column.

The flocculation process described above agrees with the concept of Mitchell, Singh, and Campanella (118), that the predominant role of the double layer (in the sedimentation process) is control of the "initial soil fabric."

Development of Structure

Downward Movement in the Water Column

Sverdrup, Johnson, and Fleming (194) indicated that flocs settle with the velocity of quartz spheres between 0.005 and 0.015 mm (i.e. with velocities between 1 and 20 m/day). Floc size was dependent on the type of clay mineral, the ionic concentration of the fluid and the energy of the environment. As floc size increased, settlement velocity also increased. Because of water involved with the larger flocs, their effective density was reduced; therefore, the increase in velocity was not linearly related to size.

As the floc moves down in the water column, it becomes subjected to continuously higher hydrostatic pressures. Nielsen (127) indicated that high hydrostatic pressures should destroy the orderliness of the water structure. This would mean a reduction in double layer thickness. As the double layer thickness decreased, closer particle spacings would result in increased resistance to additional compression. Two other effects apparently not considered by Nielsen may also be significant. First as the hydrostatic pressure increases (along with a decreasing temperature), the viscosity of the water decreases. Hydrated cations tend to become more mobile. Additionally, any tendency for the floc to lose water because of closer particle spacings increases the ionic concentration of the remaining water.

Sediment Structure

Time Effects. At the ocean bottom the flocs appear to develop more distinct edge to face relationships to one another, forming an

open framework. Where the rate of deposition is very slow, flocs may remain unburied for considerable periods of time. Laboratory tests by several workers have indicated that resistance to compression under long term loading increases with time, possibly because water molecules reorient into more efficient arrangements in the vicinity of points of nearest approach of the particles (Leonards and Ramiah (105); Leonards (102); Leonards and Altschaeffl (103); Nacci and Huston (123)). Monney (119) proposed that the water surrounding clay particles is squeezed from between particles *before overlying material accumulates to consolidate the deposit.* He also proposed that particle to particle primary bonds could result. What force causes this squeezing was not indicated. At some depth in the deposit, Monney postulated that the overburden would be sufficient to overcome these primary bonds, and a classic normally consolidated profile would develop.

The mechanism of water molecule reorientation has been given as the primary reason that void ratio changes with depth are small in the upper few meters of submarine sediments. Leonards and Altschaeffl (103) showed that where the increase in effective stress is very small relative to the existing effective stress (LIR much less than 1.0), compression will be smaller than if a larger load increment ratio was used. Thus where deposition is relatively slow, the sediment will maintain relatively the same void ratio over a considerable depth.

In areas where sedimentation rates are more rapid, such as in many regions of the continental margins, the depth-void ratio relationship should be different. Because of rapid burial, water molecules do

not have as much chance to reorient at particle contacts; thus resistance to compression is less and the void ratio should show distinct changes with depth.

According to Lambe (98), the idea of bound water between contact points being forced out can only be initiated by fairly large forces. This is an explanation why in areas of relatively slow deposition the void ratio varies little with depth in the upper layers of sediment. Scott (170) further described this process, which is analogous to secondary compression in a consolidation test. He said that under appreciable applied stress the adsorbed layer yields plastically allowing clay particles to move closer.

This simplified picture may be too idealistic. Olson and Gholamreza (135) indicated that mechanisms which control compression may be different for different clay minerals. According to their concepts, compression of montmorillonite is dominated to a much greater extent by relatively long range physico-chemical interaction between the double layers surrounding clay particles than either kaolinite or illite. Kaul (83,84) found that the rate of secondary compression was increased by yielding of oriented water around adsorbed cations, and by deformation of the highly viscous adsorbed water around the clay particles. In addition, he determined that the amount that secondary compression increased with temperature was much more significant in montmorillonite than either kaolinite or illite. Different compression mechanisms may also be inferred from Chilinger and Knight's tests (29) on these same three clay minerals. They show a curve of natural water content vs.

the logarithm of effective stress. The range of test pressures was extremely high--from about 3.0 to 14,500 kg/cm^2. However, the curves for both illite and kaolinite were linear for the whole range, while that of montmorillonite had two distinct portions connected by a transition zone between about 20 and 72 kg/cm^2. They reported that the time required to remove a given amount of water during consolidation was greatest in montmorillonite and least in kaolinite. This is in agreement with Meade (115) who noted that initial water content of pure clay minerals seemed to have a greater effect on degree of particle orientation than the value of the effective stress (thus montmorillonite with higher water content than the other two would tend to approach a parallel structure more rapidly).

Contact Area. In saturated natural clays there is doubt that the individual particles ever actually physically make contact. Leonards and Altschaeffl (103) indicated they were of the opinion little (if any) actual mineral-to-mineral contact develops. According to Mitchell, Singh and Campanella (118), interparticle contacts are *effectively* solid-to-solid, and it is likely that adsorbed water and cations in the contact zone participate in the contact structure. The interparticle contact contains many bonds which may approximate primary valence bonds. These interparticle bonds may form in response to interparticle contact forces generated by applied stress, physico-chemical interaction, or both. Whatever the nature of the particle contact, Roseqvist (161) indicated that even if areas of contact were physical, for practical purposes they were zero.

Diagenesis. Krumbein and Sloss (94) listed five diagenetic processes which may alter sediment structure during and following deposition, but prior to metamorphism. They further indicated that where deposition is slow, changes may go on indefinitely after burial (even accompanying lithification). Ginsburg (52) defined *early* diagenesis as relatively brief, intensive processes which alter original sediment properties at the sediment-water interface, and to a depth of burial of a few meters. He listed organic activity (physical and chemical), physico-chemical processes (precipitation of cementing material, etc.) and purely physical processes (consolidation under accumulating overburden) as the causes of early diagenesis. The action of organisms appears to be physically important mainly in the upper few centimeters and accelerates consolidation in this region (Shepard and Moore (175)). According to Ginsburg, the precipitation of $CaCO_3$ may occur in submarine sediments at relatively shallow burial depths, *but not as a cementing agent.* He cites data from linestone formations indicating that cementation occurred only after removal from the marine environment. Furthermore, the fact that unlithified sediments have been found well below the surface on some Pacific atolls supports this view. Krumbein and Sloss (94) indicated that cementing appears to begin at fairly early stages of burial, seemingly before the sediment has been buried to a depth sufficient to produce *marked* consolidation, or even simultaneously with sedimentation. On the other hand Siever, Beck and Berner (177) found ". . . little evidence in interstitial waters for extensive dissolution, precipitation, or replacement of minerals other

than sulfides very early in the diagenetic process. . ." Rosenqvist (161) indicated cementation was unimportant in geologically young sedimented clays.

It is clear that once the flocs have come to rest on the bottom forming a matrix with water saturated voids, the freedom of circulation of the pore water is drastically reduced (Krumbein and Sloss (94)). LaFond and LaFond (95) and Murray (121) noted a slight decrease in pH with depth, probably due to decay of organic matter. ZoBell (218) showed that in general for the top 250 cm of sediment the pH of the pure fluid increased slightly with depth, and conditions became slightly more reducing. Where sediments were *rich* in organic matter, reducing conditions were more prominent. Bacterial concentrations were highest in about the top 60 cm; below about 100 cm the concentration seemed to be negligible. Other sediment-pore fluid changes have been found. Murray (121) and Friedman, *et al.* (50) indicated that interstitial waters were higher in chlorinity than the overlying waters by a few parts per thousand. Several workers (Sillen (178) and LaFond and LaFond (95)) have indicated silica contents of interstitial water greater than the overlying seawater. Fanning and Pilson (47) showed that the very small quantities of silica involved could be accounted for by the release of silica adsorbed on clay particles.

Cementation.* Cementation is one of the five processes by which diagenesis occurs. Silaceous tests and precipitates are more common in

*The information provided here is intended to relate only to sedimentary processes on the continental margins, since at great depth dissolution of calcium carbonate occurs.

the Pacific than the Atlantic Ocean. For that reason only possible carbonate cementation is important to the testing program. Although the preponderance of evidence indicates that cementation does *not* take place in the upper few meters of sediment (even if rich in carbonate) direct correlations between vane shear strength and carbonate content have been observed (Grim (56); Einsele (38); Kögler (92); Parker (137)).

Observed Structure of Submarine Sediments. Rosenqvist (161) obtained stereo micrographs made with an electron microscope showing that the structure of a relatively undisturbed *marine* clay was similar to the cardhouse arrangement proposed by Lambe (98) and almost exactly coincided with the three-dimensional sketches presented by Tan (196). Contacts appeared to exist between corners and planes. Using ultrathin sections and material from the Gulf of Mexico (depths of water: 549 and 3358 m), Bowles (18) showed that *submarine* clays had a much opener framework than Rosenqvist's micrographs indicated. Floc shapes were very irregular and it was hard to determine where a single particle began or ended. This structure appeared to be more like the honeycomb proposed by Terzaghi (198).

Summary of the Sedimentation Process

Because of the unbalanced charges associated with the clay minerals, and the pH and ionic concentration of sea water, individual particles are attracted into groups of particles called flocs. Depending on a number of variables including the size and density, and the energy of the environment, the flocs settle through the water column at varying rates. Except where the water is shallow, the flocs are

subjected to very high hydrostatic pressure before they reach the ocean floor.

Once on the bottom the flocs entrap relatively large quantities of water. The circulation of this water is thus drastically reduced. A number of biophysico-chemical changes occur which affect the clay-water relationship, and which are not clearly understood. The resulting sediment structure appears to be similar to the honeycomb structure proposed by Terzaghi.

Stresses and Volume Changes in a Two-Phase System

Volume Change

In practical work the *total deformation* can be divided into elastic distortion (immediate response of the solid particles to load) and volume change. Volume changes in two-phase materials under applied loads can result from the compression and expulsion of the water from the void spaces and from the compression of the sediment particles. For the loads involved in engineering work the compressibility of the water may be finite, but that of the solid particles will normally be negligible by comparison.

Stresses

Load is transmitted by stresses through the sediment solid phase (skeleton and layers of bound water closest to the clay particles) and the liquid phase (remainder of the bound water and the free water). In the solid phase stresses are governed by the laws of elasticity and plasticity, while in the liquid phase the laws of hydrodynamics apply. The former are referred to as effective stresses (σ') and the latter

as neutral or pore water stresses (u). For most terrestrial work, Terzaghi recognized this relationship as (Sowers and Sowers (190)):

$$\sigma = \sigma' + u \tag{1}$$

A Theory for the Development of Resistance to Compression

It was indicated in Chapter I that fine-grained submarine sediments almost invariably appear to be preconsolidated to an extent that cannot be fully attributed to the existing overburden. Although a number of possible causes for this phenomenon have been proposed, no experimental verification for any of them has been found in the literature.

Concept of Effective Stress

The following relationships are patterned after Skempton's work (180): Consider Figure 41--assuming the stresses carried by the bound and free water are not too significantly different, the following equation can be written for a horizontal plane passed through point A:

$$P = \sigma_s A_s + \sigma_w A_w \tag{12}$$

Let $a = A_s/A_T$

$$P/A_T = a\sigma_s + (1-a)\sigma_w \tag{13}$$

If σ is the total stress over the gross area (A_T) then

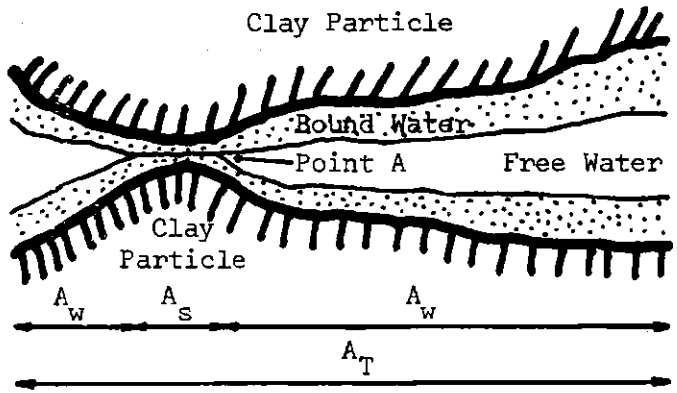

Figure 41. Concept of Contact Between Clay Particles

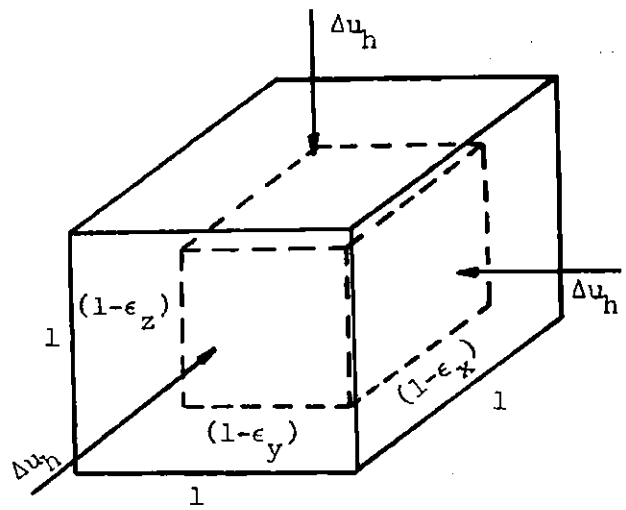

Figure 42. Unit Cube Under Hydrostatic Stress System

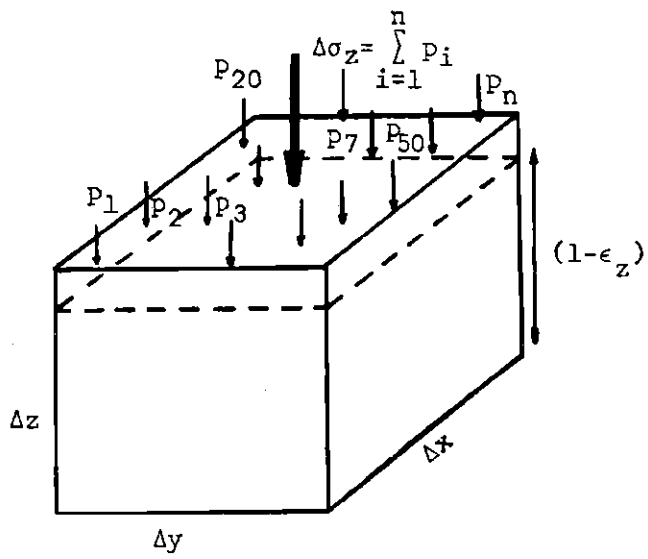

Figure 43. Laterally Confined Cube Under Uni-axial Stress System

$$\sigma = a\sigma_s + (1-a)\sigma_w \tag{14}$$

In most sediments a is very small under conditions of engineering interest; however, σ_s is very high and the term $a\sigma_s$ is called the effective stress in the soil skeleton--σ'. If σ_w is small the term $(1-a)\sigma_w \tilde{=} \sigma_w$ and Equation (14) becomes

$$\sigma = \sigma' + u \tag{1}$$

Effective Overburden Pressure (p_o')

By Archimedes' principle for hydrostatic conditions, the submerged weight of a given volume of sediment must equal the weight of that sediment in air, minus its loss of weight in water. For submarine sediments the loss of weight in sea water must be used. For sediment that is relatively uniform the submerged unit weight above a certain level may be computed on the basis of average mass unit weight (γ_m). Thus the average submerged unit weight is:

$$\gamma' = \gamma_m - \gamma_{sw} \tag{15}$$

The effective overburden pressure at a level z below the sediment-water interface is:

$$p_o' = \gamma' z \tag{16}$$

Volume Change Resulting from Hydrostatic Pressure

Consider the unit cube in Figure 42 acted on by an increased hydrostatic stress Δu_h.

$$V = 1 \tag{17}$$

$$V - \Delta V = 1 - \Delta V = (1-\epsilon_x)(1-\epsilon_y)(1-\epsilon_z) \tag{18}$$

For small strains Equation (18) becomes:

$$\Delta V = -(\epsilon_x+\epsilon_y+\epsilon_z) \tag{19}$$

For an isotropic, homogeneous, linearly elastic material $E_x = E_y = E_z = E$. For saturated material and a hydrostatic stress state

$$\Delta\sigma_x = \Delta\sigma_y = \Delta\sigma_z = \Delta u_h \tag{20}$$

It can be shown that

$$\epsilon_x = \epsilon_y = \epsilon_z = -(1-2\nu)/E\ \Delta u_h \tag{21}$$

Therefore

$$\Delta V = -3(1-2\nu)/E\ \Delta u_h \tag{22}$$

and

$$(\Delta V/V)_s = C_s \Delta u_h \tag{23}$$

where C_s is the compressibility of the solid material (assumed constant only for small changes in V and u_h) and $\Delta V/V$ is the cubical compression under hydrostatic pressure.

Compressibility of a Floc. As flocs sink in the water column, they undergo varying increases in hydrostatic pressure. By the time they reach the bottom they have experienced a hydrostatic pressure change from an atmospheric value to some depth dependent value--u_h. The solid particles and their tightly adsorbed layers are assumed to have a compressibility (C_f) which decreases with increasing pressure. In addition, the solid particles have an angle of intrinsic friction (ψ).* For the moment, ψ will be ignored.

Laughton (100) has indicated a two-phase system where the particles are not in contact will have a compressibility that can be expressed as

$$C_f = V_s/V_T \, C_s + V_w/V_T \, C_w \tag{24}$$

where C_f is the compressibility of a floc (a two-phase system);

---

*The angle of intrinsic friction expresses in a convenient way the increase in material strength with pressure. Skempton indicates it might more appropriately be defined as the angle of intrinsic *shearing* resistance.

V_w, V_s and V_T are the volumes of water, solid particles and the system, respectively; and C_s and C_w are the compressibilities of the solid particles and water, respectively.

Sverdrup, Johnson, and Fleming indicated that the compressibility of salt water decreases with depth in much the same manner as does fresh water (the variation in salinity has relatively little effect on the nearly linear compressibility of water). However, salt water *is less compressible* than fresh water (Myers, Holm, and McAllister (122)). It was indicated earlier in this appendix that in its *adsorbed state*, salt water was probably *denser* than free water. Both these observations lend validity to the assumption that the change in the compressibility of the *adsorbed* salt water with depth will be no more than the compressibility of free fresh water, which is at least an order of magnitude greater than the compressibility of the sediment particles (Wissa (214)). Thus the denser adsorbed salt water will probably have a compressibility closer to that of the solid particles than would the free fresh water. In summary, the compressibility of the floc C_f is affected by a number of variables, and changes with depth. This change is probably less than one order of magnitude. The nature of the floc is assumed to be sufficiently elastic, homogeneous and isotropic so that under hydrostatic stress it undergoes volume change that can be approximated by cubical compression.

Because of the nature of the settlement process, the total hydrostatic pressure is assumed to be applied in many small increments. The floc is thus compressed in small increments, while being stressed to an

extent related to the hydrostatic pressure to which it has been subjected. Assuming that no significant error is introduced by representing C_f by an average value $\bar{C}_f$, allows the substitution of u_h for Δu_h in the right-hand side of Equation (23):

$$(\Delta V/V)_s = \bar{C}_f u_h \tag{25}$$

Volume Change Resulting from Vertical Effective Stress

Consider the laterally confined cube of porous material shown in Figure 43 acted upon by an increment of vertical normal stress ($\Delta\sigma$). Because of a very slow rate of loading the stress increase is essentially effective (i.e. volume change will take place without excess pore pressure developing; an analogous situation is secondary compression). Thus

$$\Delta\sigma \cong \Delta\sigma' \tag{26}$$

Let
$$V = \Delta_x \Delta_y \Delta_z = 1 \tag{27}$$

$$\frac{\Delta V}{V} = \epsilon_z \tag{28}$$

For one-dimensional volume change

$$\epsilon_z = \Delta\sigma_z / E_z \tag{29}$$

Thus $$(\Delta V/V)_m = C\Delta\sigma' \tag{30}$$

where C is the compressibility of the material and is assumed constant only for the particular pressure increment.

Compressibility of Saturated Sediment. Consider again a deposit of sediment. On the bottom the flocs entrap water in large quantities. Because of the relatively large area over which sedimentation takes place, once burial occurs the sediment acts as though it were laterally confined. As a result, increasing *deposition* produces essentially one-dimensional volume changes.

From Equation (1) the total stress at a depth z below the sediment-water interface is:

$$\sigma_z = p_o' + u_h \tag{31}$$

or

$$p_o' = \sigma_z - u_h \tag{32}$$

According to Skempton, if ψ is negligible, then a net pressure increment ". . . will cause a volume change exactly equal to that which would result from an application of an identical pressure in the absence of pore pressure." Thus from Equation (30) the volume change caused by the effective overburden will be:

$$(\Delta V/V)_o = \bar{C}(\sigma_z - u_h) \tag{33}$$

For slow rates of deposition it is assumed that no significant error is introduced by letting $\bar{C}$ represent the average compressibility of the sediment structure over many small increments of pressure and by letting $(\sigma_z - u_h)$ represent the summation of the effective stresses resulting from these increments.

Total Volume Change Under Natural Forces

Superimposing Equations (25) and (33) gives the total volume change of the sediment caused by the *in situ* stresses to which it has been subjected:

$$(\Delta V/V)_T = \bar{C}_f u_h + \bar{C}(\sigma_z - u_h) \tag{34}$$

It must be emphasized that $\bar{C}_f$ and $\bar{C}$ are not constants. They represent average values of compressibility over a given range of hydrostatic pressure and vary with, among other things, pressure, temperature, and mineralogy.

An analogous equation to Skempton's approximate, but more correct relationship would be:

$$(\Delta V/V)_T = \bar{C}(\sigma_z - u_h)[1 - \eta u_h \tan\psi] + \bar{C}_f u_h \tag{35}$$

where η is a function depending on the relative contributions of particle arrangement and distortion to the total volume change. He also indicated that η is numerically unimportant in most cases. Consequently, the following equation relating the stresses that have acted on the

sediment particles to the total volume change is proposed:

$$(\Delta V/V)_T = \bar{C}(p_o' + \bar{C}_f/\bar{C}\ u_h) \tag{36}$$

Rewriting (36):

$$1/\bar{C}(\Delta V/V)_T = p_o' + \bar{C}_f/\bar{C}\ u_h \tag{37}$$

The left-hand side of Equation (37) represents an average bulk modulus times the unit volume change. In effect, $1/\bar{C}(\Delta V/V)_T$ is the effective stress to which the material has been subjected. Thus the equation for what has been called the apparent effective preconsolidation pressure at a depth z in a submarine sediment is:

$$p_c' = p_o' + \bar{C}_f/\bar{C}\ u_h \tag{2}$$

For fine-grained sediments, the ratio $\bar{C}_f/\bar{C}$ may be different from the same ratio if absolute values were used instead of average values; however, it is still a very, very small number. If u_h was not huge relative to p_o' and p_c', the term $(\bar{C}_f/\bar{C})u_h$ could be neglected. With reference to Equation (14) Lowe and Johnson (108) recorded that *except where neutral pressures are unusually high* the error involved in neglecting the effect of a finite contact area is negligible. For volume change Skempton's work demonstrated that a more accurate estimate of the actual effective stress was obtained by replacing the

contact area ratio in Equation (14) by a compressibility ratio similar to that shown in Equation (2).

APPENDIX D

ONE-DIMENSIONAL CONSOLIDATION

A number of theories for the consolidation of porous media are extant which are less restrictive in terms of necessary assumptions than the usually employed one-dimensional theory (Biot (12); Barden (6); Gibson, England and Hussey (51); Davis and Poulos (33); and others). In the case of the least restrictive theories which are the three-dimensional ones, Scott (170) pointed out that the mathematics involved were generally too complicated for practical use. Other theories which are less complex from a mathematical standpoint are still relatively impractical because methods for evaluating the relevant constants in real soils require complicated tests. Barden and Berry (7) indicated the best approach was to use the Terzaghi model for preliminary computations and to make qualitative modifications to account for the influence of actual conditions which violate the model's assumptions.* According to Leonards (102) the errors arising from an incorrect evaluation of soil properties generally far exceed those arising from using one-dimensional theory. For consolidation of submarine sediments, Leonard's comments are probably even more appropriate because of the relief of stresses during sampling and the nature of the sediments.

---

*Taylor (197) has presented an extensive treatment of the assumptions necessary for use of the Terzaghi theory.

Additionally, at the present time, the nature of the structures, for which settlement will be a problem, does not warrant more complex methods (see Chapter I).

Divisions of the Consolidation Process

Three divisions are commonly recognized in the *consolidation* process. They are defined here as:

1. *Initial Compression*--volume change resulting from compression and possible solution of air in a sediment sample that is not 100% saturated.

2. *Primary Consolidation*--volume change resulting from the expulsion of water from sediment voids (a hydrodynamic effect).

3. *Secondary Compression*--volume change resulting from changes in the sediment structure under essentially hydrostatic pressure.

For a sediment that is completely saturated, *initial* effects are zero; if the saturation is 95% or more, initial effects are generally assumed to be negligible in relation to primary and secondary effects. *Secondary* effects are not always significant in terrestrial deposits; however, in most fine-grained submarine sediments *secondary* appears to be important. In the initial development of the theory of one-dimensional consolidation Terzaghi did not consider *secondary* effects.

Mechanics of Primary Consolidation

Compressibility can be described as a change in mass volume caused by a change in the stress system acting on the mass. By summation of the displacement caused by small strains induced by the changed stress system, the total displacement of the mass can be determined.

According to accepted theory, primary consolidation occurs in a saturated system because the compressibility of the soil structure is much less than that of the water. As a result, before drainage begins and the instant after the load is applied, all the added pressure must be carried by the water. As drainage occurs the pressure increase is transferred from the water to the soil structure. Realization of full strain under the pressure increment requires a finite time--hydrodynamic lag.

The relationship among volumetric strain, change in sample (or layer) height, and change in void ratio for one-dimensional consolidation can be shown to be:

$$\Delta V/V = \Delta H/H = \Delta e/1+e_o \tag{38}$$

For *small strains* and after hydrodynamic lag has ended, the coefficients of volume change and compressibility can be defined respectively to be:

$$m_v = -d\epsilon/d\sigma' \tag{39}$$

$$a_v = -de/d\sigma' \tag{40}$$

The slope of the virgin part of the logarithm of effective stress vs. void ratio curve is defined as the compression index:

$$C_c = - \frac{\Delta e}{\text{one log cycle}} \tag{41}$$

Equation (41) is a more practical means of relating effective stresses and strains than either Equations (39) or (40). It can be used in conjunction with Equation (38) to provide an expression for the vertical consolidation of a laterally confined stratum of thickness H:

$$\Delta H = H(C_c/1+e_o)\log \frac{p_o' + \Delta\sigma'}{p_o'} \tag{42}$$

The validity of a simple equation such as Equation (42) depends on the extent to which the soil has been previously stressed. Various empirical methods have been used to estimate this stress. Casagrande's method (22) is widely used. Its major drawback is that where the transition between the rebound and virgin portions of the laboratory e-log $\Delta\sigma'$ curve is not distinct, considerable latitude in estimation of the preconsolidation pressure (p_c') exists. Sowers and Sowers (190) give a simpler method that is subject to less latitude in interpretation. Other more elaborate methods, such as that of Schmertmann (168) are also available.

Where p_c' is estimated approximately equal to p_o' the deposit is said to be normally consolidated. In this case the natural water content is usually less than the liquid limit and much higher than the plastic limit. If the overconsolidation ratio (p_c'/p_o') is greater than one, and the natural water content is far below the liquid limit (perhaps even below the plastic limit) the deposit is said to be

overconsolidated. If (p_c'/p_o') is much smaller than one, the deposit is underconsolidated. Generally, the water content will be far above the liquid limit in this situation. In most submarine sediments a state exists which cannot be strictly categorized by any of the above definitions. The sediment appears to be overconsolidated, but it does not seem possible that this overconsolidation could have developed in the sense it did for most terrestrial deposits. Thus p_c' for these sediments is termed the *"apparent* preconsolidation pressure." Water contents generally near or greatly in excess of the liquid limit are normal in these deposits. Leonards (102) indicated that normally consolidated clays with p_c' greater than p_o' could occur as a result of thixotropic effects, long-term secondary effects, or cementation effects.

In terrestrial deposits settlement estimates are developed somewhat differently for normally consolidated material than for overconsolidated material. Since sediments that have been deposited at a relatively slow rate in the ocean have characteristics of both normally consolidated and overconsolidated material, settlement estimates for them may require somewhat different treatment.

Rate of Primary Consolidation

Based on the Terzaghi assumptions, the decrease in excess pore water pressure in a unit time is equal to the increase in effective stress:

$$\partial u/\partial t = -\partial \sigma'/\partial t \qquad (43)$$

By use of fundamental expressions for flow in porous media and Equation (43), a nonlinear, second order, partial differential equation for the rate of consolidation at any depth can be written:

$$\partial u/\partial t = k(1+e)/a_v\gamma_w \ (\partial^2 u/\partial z^2) \qquad (44)$$

The coefficient of consolidation (c_v) is defined as:

$$c_v = k(1+e)/a_v\gamma_w \qquad (45)$$

For certain boundary conditions, Terzaghi obtained solutions for Equation (45) by using Fourier series. Because rate of consolidation is not of primary importance in this testing program, no further additional details of this solution are provided here.

Effect of Secondary

Taylor (197) showed that the main effect of not "filtering" secondary effects out of consolidations recorded for each pressure increment was to shift the curve on the void-ratio vs. logarithm of effective stress plot down and to the left--thus reducing the value of p_c' obtained, but leaving the value of C_c relatively unchanged. Similar results were found by Newland and Alley (126) for various load increment ratios up to ten.

Leonards and Altschaeffl (103) indicated that the longer it takes for the consolidation process to end, the smaller will be the ratio of subsequent secondary effects to the amount of consolidation. For this

reason the relative amount of secondary compression that occurs in the field may be much less than predicted by laboratory tests.

In general, for most normally consolidated terrestrial clays secondary will not exceed about 20% of the total settlement.

Errors Resulting from Failure to Consider Secondary Effects. While the Terzaghi development can provide a useable estimate of primary consolidation where secondary effects are relatively small, the estimate can be significantly in error where secondary effects are very large.

Taylor (197) attributed secondary to plastic action in the adsorbed water near grain-to-grain contacts and at points of nearest approach. Various other explanations of secondary agree only in that secondary is visualized as resulting from causes *not related* to hydrodynamic expulsion of pore water. Whatever its cause, where significant it generally begins before primary is complete and thus means the assumption that

$$a_v = -de/d\sigma' \tag{40}$$

is in error. Barden and Berry (7) indicated that for thin samples and small pressure increments, secondary effects can dominate the entire consolidation process.

Secondary effects seem to *predominate* where the sediment has a high organic content, or where the structural framework has not been well developed (initial stage of deposition). In both these instances

permeability is relatively low and completion of primary is retarded. Thus there is no demarcation between primary and secondary. Where structure has developed, and permeability is high enough to allow relatively rapid completion of primary, the distinction between primary and secondary will be fairly well defined, if the effect of secondary is not allowed to mask completion of primary.

Methods of Separating Primary and Secondary. Several workers (Northey (134), Burmister (22), Herrmann, Rocker and Babineau (68)) have noted that the Casagrande dial reading vs. logarithm of time procedure of separating primary consolidation from secondary compression does not give very consistent distinctions for submarine sediments. Apparently this results from the fact that secondary begins relatively soon after the increment of load is applied. Consequently if secondary is allowed to take place at all, it tends to mask distinct changes in curvature in a plot of dial reading vs. logarithm of time. The Taylor method allows prediction of the end of primary before secondary effects become significant. As a consequence, the end of primary is more distinct. Figure 44 shows three plots of strain vs. the logarithm of time indicating that for an increment of stress of 320 gm/cm^2 (i.e. $\Delta\sigma'$ = 320 gm/cm^2), the percentage strain at the completion of primary consolidation was still not indistinct after 24 hours. Figure 45 displays the same three curves, plotted with time on a square root scale. By using Taylor's method (197), the strain at the completion of primary consolidation is distinct and is considerably less than the Casagrande method would have indicated.

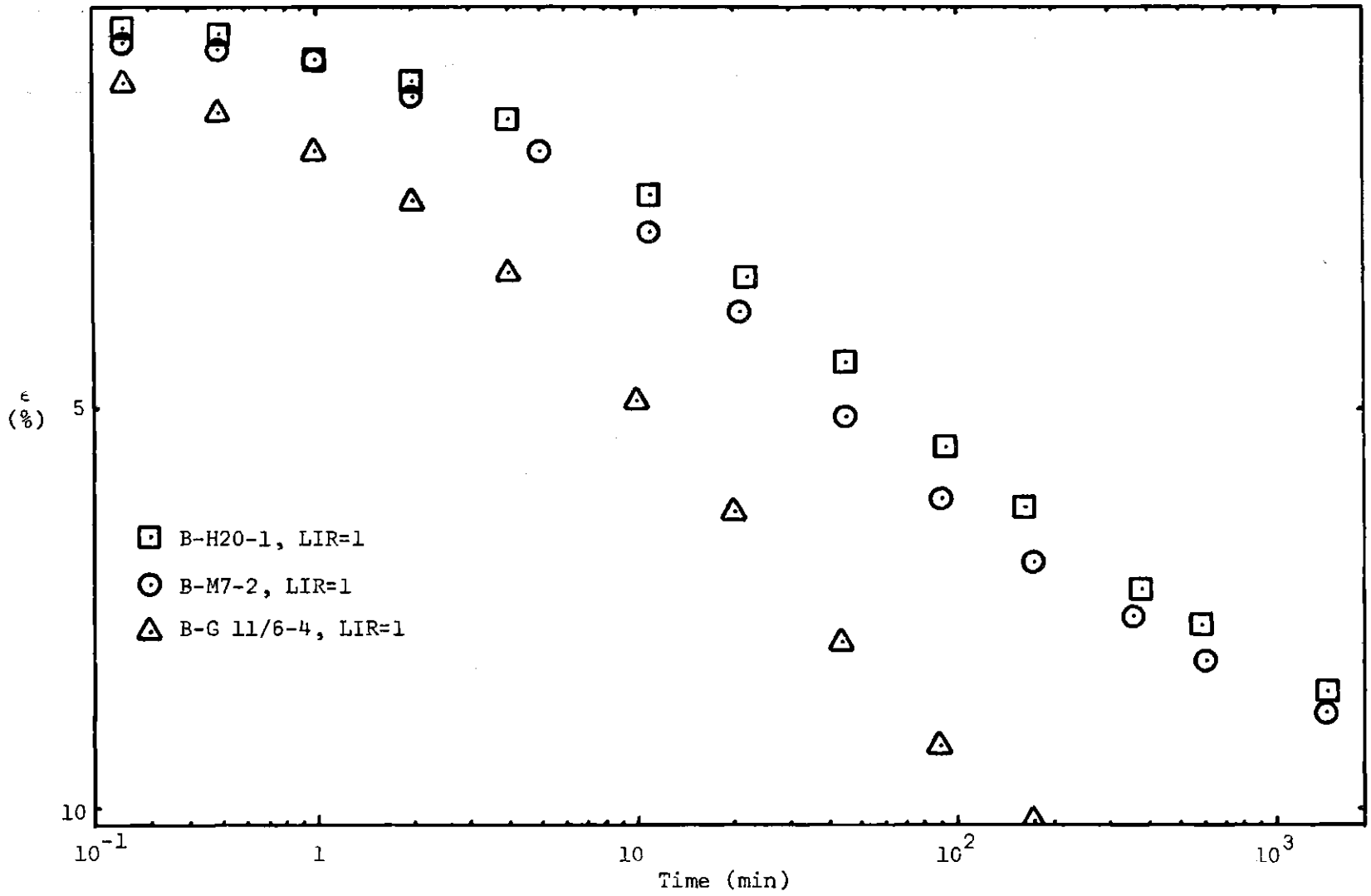

Figure 44. Strain vs. Logarithm of Time. Total Stress 640 gm/cm^2

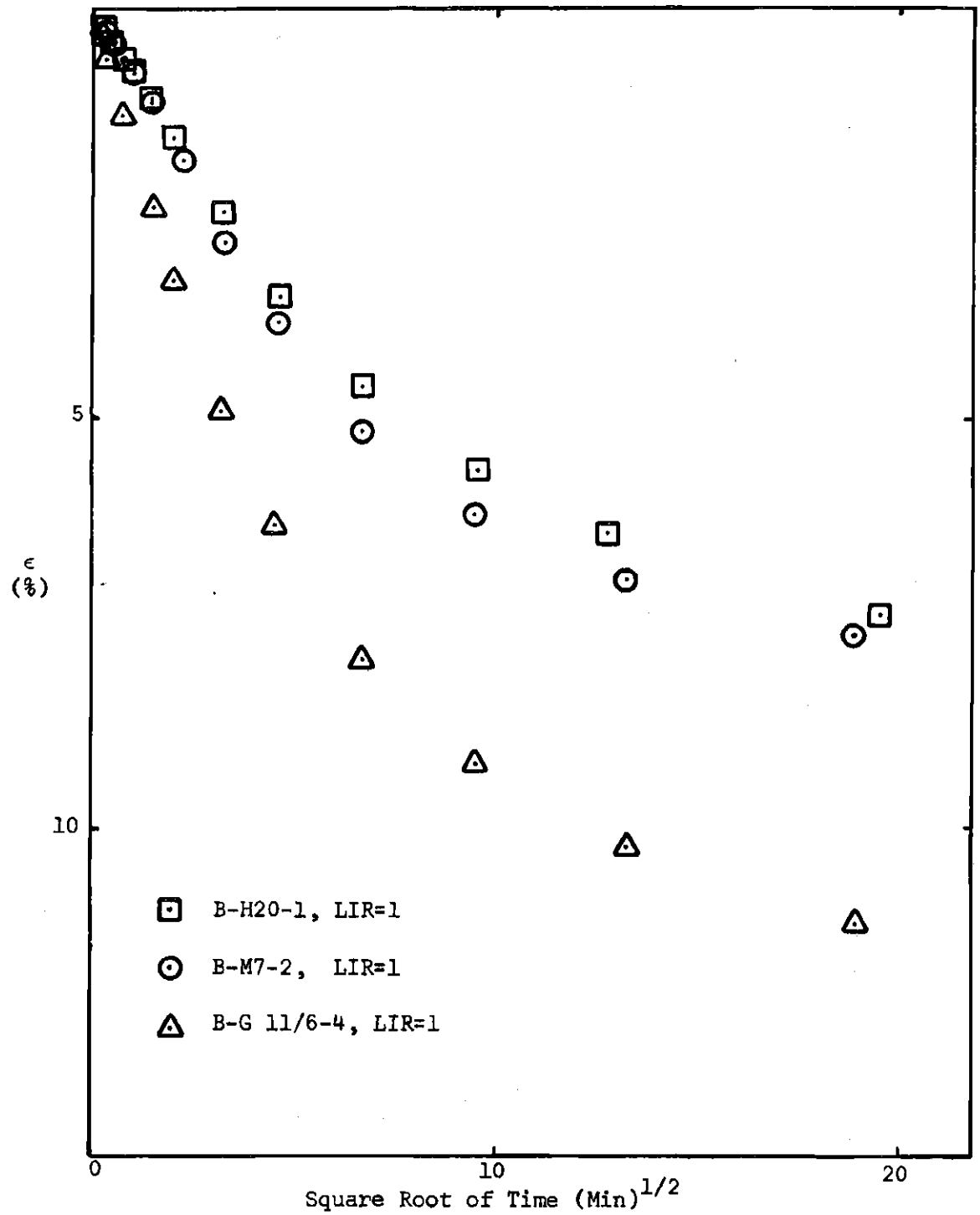

Figure 45. Strain vs. Square Root of Time
Total Stress 640 gm/cm^2

Drawbacks in Using One-Dimensional Theory for Submarine Sediments

Generally, submarine sediments occur in surficial deposits that will be relatively thick compared to the foundation width. If they were truly normally consolidated, the problem of lateral effects would probably not be significant. Since they act as though they are slightly overconsolidated, a correction for lateral effects should be made and settlement estimates reported for both corrected and uncorrected conditions (Sowers (189)).

For extremely soft sediments that have not developed a structure, elastic theory is not valid. If a structure has developed such that small increments of pressure produce *small strains*, assumptions based on elastic theory should be no worse than for terrestrial work.

Presentation of Data. All e-log $\Delta\sigma'$ plots have been presented as strain vs. the logarithm of effective stress (ϵ-log $\Delta\sigma'$). The main reason for this is that the use of strain instead of the sample void ratio provides a better comparison of the curves from a common origin--zero strain. Although within any one group of tests there was little difference in initial sample void ratio, the use of strain effectively eliminated *any* difference. Additionally, the use of ϵ requires considerably less computation than the use of void ratio.

The question of how to compute strain depends on the purpose of the test. Using the Taylor square root of time method allows considerable leeway in selection of a value to represent strain. Because initial effects were included in the CRS results, initial effects were also included in the standard test by using the R_{100} value for determining

the strain for each load increment.

Determination of C_c—

It can be shown that any slope normally determined from an e-log $\Delta\sigma'$ plot can be determined from the ϵ-log $\Delta\sigma'$ plot by employing the relationship:

$$C_j = \frac{(1+e_o)(\epsilon_2-\epsilon_1)_j}{\text{one log cycle}} \qquad j=c,s,r, \text{ etc.} \tag{46}$$

The actual slope of the virgin curve on an ϵ-log $\Delta\sigma'$ plot is defined as the strain index:

$$C_\epsilon = - \frac{\Delta\epsilon}{\text{one log cycle}} \tag{47}$$

Determination of p'_c—

The method given by Sowers and Sowers (190) is recommended for use in determining p'_c from the ϵ-log $\Delta\sigma'$ plot. On moderately disturbed submarine sediments, Richards (151) found a similar method to give more consistent results than the Casagrande method.*

Both the Sowers method and the Casagrande method were used in this testing program. Either method can be used directly with the ϵ-log $\Delta\sigma'$ plot in the same manner as from the e-log $\Delta\sigma'$ plot.

---

*Richards proposed using the intersection of a horizontal line representing e_o and the extension of the virgin curve to define p'_c.

Theoretical Relationships for Constant Rate of Strain Consolidation Tests

Assumptions

Most of the initial assumptions used in the normal one-dimensional consolidation test are made in developing CRS relationships. The assumption of a constant coefficient of permeability is erroneous; however, errors induced by assuming it to be a constant are of *major importance* to estimation of the *time rate* of primary consolidation, not to the *amount* of primary. Since this testing program was concerned with amount, the use of a coefficient of permeability that is a function of time only (see below) is an improvement over the normal assumption of a constant coefficient of permeability.

Average Effective Stress

The following development is patterned after that of Smith and Wahls (186).

Writing Equation (44) so that k is a function of depth and time gives:

$$\partial u/\partial t = 1+e/a_v\gamma_w \; \partial/\partial z(u \; \partial u/\partial z) \qquad (48)$$

Substituting Equations (40) and (43) into Equation (48) and rearranging gives:

$$\frac{1}{\gamma_w} \partial/\partial z(k \; \partial u/\partial z) = \frac{1}{1+e} \partial e/\partial t \qquad (49)$$

Assume that k is only a function of the average void ratio of

the sample. It is thus a function of time only. For thin samples and slow rates of strain, the assumption is considered reasonably valid. Thus for $k = f(\bar{e}) \neq g(z)$:

$$k/\gamma_w \, \partial^2 u/\partial z^2 = 1/1+e \, \partial e/\partial t \tag{50}$$

The testing procedure requires a constant rate of strain; therefore the rate of volume change must also be constant:

$$dV/dt = -RA \tag{51}$$

where R equals the constant rate of deformation of the upper surface of the sample.

Consider the average void ratio at any level z in the sample to be the sum of the void ratios at any time over the whole sample divided by the sample height:

$$\bar{e} = 1/H \int_o^H e dz \tag{52}$$

The total volume of the sample is equal to the volume of voids plus the volume of solids. During a consolidation test the volume of solids is a constant. Differentiating $V = V_s + V_v$ with respect to time gives:

$$dV/dt = dV_v/dt = d(eV_s)/dt \tag{53}$$

Substituting Equation (53) into Equation (51) gives:

$$de/dt = -RA/V_s = -r = \text{constant} \tag{54}$$

Thus the void ratio at any position and time is a linear function of time:

$$e(z,t) = g(z)_t + e_o \tag{55}$$

A solution of Equation (54) is obtained by assuming g(z) is a linear function such that Equation (55) becomes:

$$e = e_o - rt[1 - b/r(z-0.5H/H)] \tag{56}$$

where b is a constant that depends on the variation of void ratio with depth and time, and b/r is a dimensionless depth ratio. At the base of the sample z = H and Equation (56) becomes:

$$e_b = e_o - rt[1 - 1/2(b/r)] \tag{57}$$

For values of b/r greater than 2, Equation (57) indicates that e_b will *increase* during the test. This is very unlikely. For b/r = 0, Equation (56) gives:

$$e = e_o - rt \tag{58}$$

indicating the void ratio is uniform with depth. This is also very unlikely. Thus for practical reasons, the depth ratio must be limited to values between zero and two.

Equation (50) can be solved with appropriate boundary values. A practical solution can be obtained by assuming (1 + e) can be replaced by $(1+\bar{e})$ where $\bar{e}$ is *not* a function of z. Although this is not strictly true, Smith and Wahls compared the results obtained using this assumption to those obtained using a more rigorous solution. For $0 \leq b/r \leq 2$ the *maximum* difference was less than 2%, with the values of u obtained from the approximate solution always being the higher (except for b/r = 2).

Differentiating Equation (56) with respect to time gives:

$$de/dt = -r + b(z-0.5H/H) \tag{59}$$

Substituting $(1+\bar{e})$ for (1+e), replacing de/dt in Equation (50) by Equation (59), and rearranging:

$$\partial^2 u/\partial z^2 = r\gamma_w/k(1+\bar{e})[-1 + b/r(z/H-1/2)] \tag{60}$$

Integrating Equation (60) twice with respect to z and applying the boundary conditions--u(0,5) = 0; $\partial u/\partial z(H,t) = 0$--gives:*

*The physical significance of these two conditions is that the former results from drainage at the top of the sample and the latter results from the assumption that the slope of the curve representing the variation in excess pore pressure with depth in the sample approaches a vertical tangent at the sample base.

$$\Delta u = - \gamma_w r/k(1+\bar{e})[(2H-z^2/2) - b/r(z^2/4-z^3/6H)] \qquad (61)$$

where Δu represents the excess pore pressure above hydrostatic conditions (atmospheric pressure or the level of applied back pressure).

At the base of the sample $z = H$ and thus the excess pore pressure measured there will be:

$$\Delta u_b = -\gamma_w rH^2/k(1+\bar{e})[1/2 - b/r(1/12)] \qquad (62)$$

The average vertical effective stress over the sample in terms of total increase in applied stress and excess base pore pressure will be:

$$\Delta\sigma' = \Delta\sigma - \alpha\Delta u_b \qquad (63)$$

Where α is the ratio of the average excess pore pressure ($\Delta\bar{u}$) to the excess base pore pressure (Δu_b).

The average neutral stress over the sample at any time (t) is thus:

$$\Delta\bar{u} = 1/H \int_0^H \Delta u dz \qquad (64)$$

Substituting Equation (61) into Equation (64) and integrating gives:

$$\Delta\bar{u} = \gamma_w rH^2/k(1+\bar{e})[1/3 - b/r(1/24)] \qquad (65)$$

Thus α can be evaluated:

$$\alpha = \Delta\bar{u}/\Delta u_b = [1/3 - b/r(1/24)]/[1/2 - b/r(1/12)] \qquad (66)$$

For $0 \leq b/r \leq 2$, $0.667 \leq \alpha \leq 0.750$.

For practical values of b/r, α appears to have little effect on the average vertical effective stress.

Using a more theoretical approach Wissa, *et al.* (215) developed a relation for average vertical effective stress in nonlinear soil:

$$\Delta\sigma' = (\Delta\sigma^3 - 2\Delta\sigma^2\Delta u_b + \Delta\sigma\Delta u_b^2)^{1/3} \qquad (67)$$

For this testing program the difference, in terms of effective stress, found by using Equation (63) instead of Equation (67), which would presumably be more correct, was about 5% during the early part of the tests, and about 1% during the latter part of the tests. In terms of the ϵ-log $\Delta\sigma'$ curve as a whole, the differences did not significantly change values of C_c, p_c' or curve shape.

The preceding development is based on a linear relationship between void ratio and depth within the sample. The validity of using Equation (60) depends mainly on the variation in void ratio and thus in effective stress. The variation in the ratio $\Delta u_b/\Delta\sigma$ is an indicator of the variation in effective stress. As deviations from linearity become large, this ratio becomes large, and the assumptions used in the theory are less appropriate.

All values of average vertical effective stress computed in this testing program are based on a linear soil:

$$\Delta\sigma' = \Delta\sigma - 0.667\ \Delta u_b \tag{68}$$

Coefficient of Consolidation from the CRS Test

Although not of direct interest in the testing program, a means of evaluating c_v is desirable in normal soils work.

Measuring Δu_b during a CRS test allows k to be computed from Equation (62):

$$k = \gamma_w r H^2 / \Delta u_b (1+\bar{e})[1/2 - b/r(1/12)] \tag{69}$$

Here $\bar{e} \neq f(z)$ and thus Equation (52) can be integrated to give:

$$\bar{e} = e \tag{70}$$

Substituting Equation (69) and Equation (70) into Equation (45) gives:

$$c_v = r H^2 / a_v \Delta u_b [1/2 - b/r(1/12)] \tag{71}$$

This is in effect the same expression that Wissa, *et al.* use for their linear method. For their nonlinear method, they present a different relationship:

$$c_v = -0.434RH^2/[2\Delta\sigma m_v \log(1-\Delta u_b/\Delta\sigma)] \qquad (72)$$

They show that as $\Delta u_b/\Delta\sigma$ increases, the linear and nonlinear solutions diverge. For $\Delta u_b/\Delta\sigma$ from 0 to about 35% values of c_v obtained from linear theory vary from 1.0 to about 1.2 times those of nonlinear theory (in a relatively linear manner). Above 35%, c_v values from linear theory appear to begin to increase at an exponential rate in relation to c_v values obtained from nonlinear theory.

APPENDIX E

SOME FACTORS AFFECTING CONSOLIDATION TESTING

Friction

Side friction between the test sample and the test ring tends to reduce the effective stress the sample consolidates under at any given load. The amount of this reduction can be significant to the results of the test.

In comparing observed and laboratory results (from standard consolidation tests), Skempton (181) indicated friction could be the cause of the disagreement in values in the stress range 1 to 500 gm/cm^2. At higher stresses (500 to 10,000 gm/cm^2), he felt friction effects to be negligible. He employed metal test rings. Leonards and Girault (104) studied the friction problem. They found that at stresses around 500 gm/cm^2 the amount of friction per centimeter of sample height was about the same for samples in teflon-lined consolidation rings greased with molybdenum disulfide and ungreased steel rings (about 10%/cm). However, for stresses above 1000 gm/cm^2, the percentage friction in the steel ring dropped very rapidly leveling off at about 7%/cm as the applied stress approached 5000 gm/cm^2. The percentage friction in the teflon ring dropped less rapidly, but levelled off at about 2%/cm near 6000 gm/cm^2. Their work also indicated that side friction was less at lower rates of strain (i.e., they appear to have shown it was less at lower load increment ratios). Lo (107), in his work on secondary effects,

stated that the brass rings (lubricated with molybdenum disulfide) he used did not develop more than 10% of the applied stress in side friction. Both Rowe (165) and Bozozuk (19) indicated that use of greased metal rings is extremely effective in reducing side friction.

In this testing program the stainless steel rings used in both the CRS and standard tests were greased with molybdenum disulfide. In the CRS tests the ring was also teflon lined. The surface area of the inside of the standard ring is about 4% greater than the CRS ring.

Based on the above considerations, it is assumed that the effect of friction in this testing program might be as high as 10% of the applied stress per centimeter of sample height, or as low as 2%. Furthermore, between any two CRS tests run at the same rate, or any two standard tests, the effect of friction is the same. It is possible that relative to the CRS tests the values of effective stress recorded in the standard tests are slightly high as a result of friction. This is because the standard test ring was not teflon lined; and it had a little greater surface area.

It was noted that before and after both types of tests the test ring could be rotated or lifted without the sample moving. This indicates friction was probably not too important a factor.

Temperature

Because of the effect of temperature on the viscosity of pore water, large temperature changes during consolidation testing are undesirable. It can be shown theoretically that the coefficient of consolidation (c_v) is dependent on permeability (thus viscosity). Therefore,

this coefficient should be affected by temperature. Likewise it can be shown that the compression index (C_c) should be independent of temperature. Finn (49) showed that as temperatures were decreased from about 24 to 7°C, c_v decreased, while C_c remained relatively unchanged. According to Lo (107), temperature is the most important variable affecting secondary compression. Lo reported that an increase in temperature from about 13 to 19°C altered the shape of the curve of change in sample height vs. the logarithm of time; however, examination of the plots presented shows that for a given increment of load the increased change in height was not overly significant. As an example, over a period of 116 hours, and for a temperature increase of 6°C, the change was only 0.0178 cm. Campanella and Mitchell (26) also showed that the temperature of the test affected the location of the e-log $\Delta\sigma'$ curve, but not its shape. Successive increases in test temperature between 21° and 60°C shifted the curve down and to the left, reducing the estimated value of the effective preconsolidation pressure, but leaving C_c relatively unchanged. Studies of the rate of temperature change conducted by Paaswell (136) indicated that sudden increases in heat supplied may produce different results than if the same temperature change was applied over a longer period of time. The *changes* in temperature used in his work were relatively large, varying from minimum changes of 20 to 30°C over periods from 2 to 5 hours to maximum changes of 55°C over a period of 15 minutes. Working with samples of illite, kaolinite and montmorillonite, Kaul (84) concluded that the increase in the rate of secondary compression with increased temperatures in the range from

10° to 70°C was considerable for montmorillonite, moderate for illite, and negligible for kaolinite. For primary consolidation he considered that temperature effects could be ignored for illite and kaolinite, but where large amounts of montmorillonite were present, the effect could be significant (apparently because of changes in the thickness and structure of the diffuse double layer).

Table 3 indicates for each group of consolidation tests the maximum temperature variation in any test and the range of average test temperatures within the group. Within any one test the maximum variation was 8°C; the maximum variation between average test temperatures in any one group was 7°C. These values were extremes, and more frequent variations were respectively 0.5 to 1.5°C and 0.5 to 2.0°C. Variations in test temperature had no consistent pattern in relationship to the beginning and end of each test. Sometimes the temperature was higher at the beginning than the end, sometimes vice versa; sometimes the temperature rose toward the middle of the test, then fell toward the end; sometimes it fell toward the middle of the test, then rose toward the end.

Cores from the Georgia Coast contained relatively large amounts of montmorillonite and kaolinite. Based on the work of Kaul, it would appear that the effects of these clay minerals would be offsetting in terms of the influence of temperature on compressibility. Because of the small temperature variations recorded during the test program, and because of the relatively low temperatures at which the tests were conducted, it is assumed that the influence of temperature within any one

test, or within any group of tests, had an insignificant effect on the test results.

Sample Disturbance

As indicated in Appendix C, natural processes of consolidation produce a sediment structure which has a certain resistance to further compression. When the sediment is removed from its *in situ* environment this structure is altered and the *in situ* resistance to compression reduced. Between the time of sampling, and the time of testing, further disturbances to the structure can cause its laboratory compressibility to be changed even more. The consequence of these changes in structure is that engineering parameters determined from consolidation tests will be other than those of the *in situ* deposit. In general, as the degree of disturbance increases, the value of the effective preconsolidation pressure estimated from the e-log $\Delta\sigma'$ curve decreases and its determination becomes more difficult because of relatively indistinct changes in curvature. Examination of Figures 12 through 21 shows relatively well-defined changes in curvature for most curves. The samples are disturbed, but it is felt that the degree of disturbance is not enough to affect the use of values of p_c' and C_c computed from these figures. For any particular group of tests, there is no reason to think any one sample was any more disturbed than any of the others.

APPENDIX F

DATA FROM THE CONSOLIDATION TESTING PROGRAM

Sample Selection

All samples were selected so that no material from either the upper 25 cm or the lower 10 cm of the cores was used. In the case of the Georgia Coast cores the material utilized was taken from the top half of each core to avoid using material known to be physically over-consolidated (i.e. occurring below the Pleistocene boundary). Material from the Gulf of Maine cores generally came from the bottom halves of the cores, because the upper material had been used for preliminary tests to perfect testing technique. Samples obtained from cores from the Hudson Submarine Canyon came from the top half of one core (H20) and the bottom halves of two others (H4, H6). The reason for this was that in addition to material for the consolidation testing program, material had to be available for a number of vane shear tests at specific locations in these cores.

Consolidation Data

Tables 1, 2 and 3 (see Chapter VI) list data from the consolidation testing program. Table 13 provides information taken from strip charts for each CRS test.

Table 13. Data from CRS Test Strip Charts

$\Delta u_b/\Delta\sigma$ (%)	0.667 Δu_b gm/cm^2	$\Delta\sigma'$ gm/cm^2	ϵ (%)
RC-M3-1			
88	10.5	7.5	3.93
88	15.5	11.0	5.15
81	21.5	18.5	7.36
72	23.5	25.5	8.56
60	23.0	34.5	9.76
65	29.0	37.5	10.96
64	32.0	42.5	12.16
60	33.5	50.5	13.36
39	24.0	69.0	14.81
40	41.0	114.0	17.21
28	44.5	190.0	20.21
29	63.5	268.5	23.21
RC-G6-1			
0	0	5.0	1.45
46	5.5	12.5	2.59
62	15.0	21.5	3.56
57	20.0	32.0	4.41
48	24.5	53.0	6.32
40	29.5	81.0	8.41
31	32.5	122.5	9.91
22	30.0	182.0	11.23
18	34.5	256.5	12.57
16	36.0	304.0	14.06
10	36.5	643.5	15.79

$\Delta u_b/\Delta\sigma$ (%)	0.667 Δu_b gm/cm^2	$\Delta\sigma'$ gm/cm^2	ϵ (%)
RC-H4-1			
0	0	5.0	0.30
0	0	9.0	0.49
0	0	11.0	0.69
52	11.5	21.5	1.71
58	19.0	30.0	3.44
61	29.0	42.0	5.50
56	34.0	57.0	7.95
51	37.5	73.5	10.30
43	41.0	102.0	12.75
45	48.5	114.5	15.10
36	51.0	161.0	17.50
32	64.0	201.0	19.90
33	75.0	316.0	22.30
RP-M3-1			
0	0	5.0	0.97
72	6.5	7.0	2.24
83	12.5	10.0	3.37
53	7.0	13.0	4.57
36	6.5	23.5	5.77
46	11.0	25.0	7.02
36	14.0	43.5	9.42
22	12.5	71.5	11.82
23	22.0	124.0	15.79
19	30.5	208.5	19.96
17	37.5	289.5	22.36

$\Delta u_b/\Delta\sigma$ (%)	0.667 Δu_b gm/cm^2	$\Delta\sigma'$ gm/cm^2	ϵ (%)
RC-H20-1			
0	0	5	0.71
45	3.5	7.5	1.57
87	11.5	8.5	2.06
100	23.5	12.0	3.27
100	33.0	16.5	4.41
100	41.0	21.0	6.06
100	46.5	24.0	7.26
100	69.5	36.0	9.66
100	99.5	51.0	12.06
100	139.0	69.0	14.46
RP-H4-1			
0	0	5.0	0.30
0	2.5	13.0	0.83
80	19.0	16.5	1.62
87	29.5	21.5	2.48
66	38.5	41.5	3.86
66	44.5	57.5	5.24
62	53.0	75.5	6.62
51	64.5	126.0	9.39
52	78.5	147.0	10.65
51	91.5	178.0	12.12
51	108.5	210.5	13.50
47	135.5	293.5	16.29

Table 13. Continued

RP-H20-1			
0	0	5.0	0.40
0	0	9.0	1.28
77	11.5	11.0	1.84
92	19.0	12.0	2.66
96	25.5	14.5	3.41
96	38.5	21.5	5.09
95	48.0	27.5	6.29
92	51.5	32.5	7.49
85	55.0	42.5	8.69
78	57.5	53.5	9.89
65	65.5	85.0	12.29
53	73.5	134.5	14.69

C-G6-1			
0	0	5.0	0
4	1.0	39.0	0.56
5	2.5	73.0	1.31
4	3.5	125.0	2.06
5	6.0	188.5	2.81
5	10.0	312.5	3.90
4	12.0	398.5	4.65
4	14.5	507.0	5.40
4	16.5	621.5	6.15
3	18.0	775.5	6.90
4	36.0	1178.0	9.00
5	75.5	2278.5	13.50

RP-G6-1			
0	0	5.0	1.45
0	0	9.0	2.00
0	0	19.5	2.45
0	0	28.0	3.05
8.5	5.0	38.5	3.72
10.0	7.0	45.5	4.32
12.5	10.5	52.5	5.16
11.5	13.0	70.5	6.37
8.0	15.5	127.5	8.50
6.0	17.0	192.5	9.70
6.0	21.5	252.5	10.76
3.5	20.0	389.0	12.22
2.5	22.0	669.0	14.14

P-G6-1			
0	0	5.0	0
0	0	9.5	0.69
0	0	22.5	1.49
0	0	45.0	2.29
0	0	76.0	3.09
0	0	129.0	3.89
0	0	177.5	4.69
0.3	0.5	238.0	5.10
0.2	0.5	309.5	5.90
0.2	0.5	380.0	6.70
0.3	1.0	463.0	7.50
0.2	1.0	661.0	9.50

C-G 11/6-2			
0	0	5.0	0
0	0	9.0	0.05
7	2.0	42.5	0.48
4	2.5	86.0	1.23
5	6.5	170.5	3.10
6	8.5	192.5	4.90
7	12.0	228.5	6.70
11	21.0	266.0	10.30
10	21.5	310.5	13.90
12	31.0	345.5	16.30
13	38.5	418.0	19.90
12	46.0	513.5	23.50

P-G 11/8-2			
0	0	5.0	0.05
11	2.0	25.0	1.14
7	2.0	43.0	2.14
3	1.0	57.0	3.14
1	0.5	71.0	4.14
0	0	84.5	5.14
1	1.0	110.0	7.15
6	5.5	129.0	9.15
10	10.5	153.5	11.15
14	21.0	205.0	14.82
16	32.0	260.5	18.82
15	36.5	326.5	22.11

Table 13. Continued

P-G 11/7-4

0	0	5.0	0.15
0	0	14.0	0.37
0	0	23.0	0.70
5	1.5	52.0	1.90
7	3.5	72.5	3.10
6	4.5	102.5	4.30
8	6.5	127.0	5.50
11	12.5	165.0	7.90
13	16.5	174.0	9.10
16	22.5	199.5	10.64
18	29.5	221.5	12.44
21	39.5	248.5	14.84
24	51.0	276.5	17.24
25	65.0	325.0	20.30

C-G 11/7-4

0	0	5.0	0.15
0	0	16.0	0.68
3	0.5	24.0	1.08
8	2.5	49.0	2.28
13	7.0	88.5	3.56
16	12.5	115.5	4.76
18	18.0	144.0	5.96
18	21.5	162.5	7.16
19	24.0	191.0	8.36
23	38.5	231.0	12.10
25	53.0	277.0	16.10
25	69.0	341.0	20.86

C-H4-8

0	0	5	0.04
0	0	9	0.30
0	0	18	0.76
13	2.5	26.5	1.85
8	2.0	38	3.54
8	2.5	46.5	4.44
8	3.5	63	5.76
13	6.5	71	7.23
11	8.0	80.5	8.41
18	12.5	89.5	9.61
30	28.0	111.5	12.59
35	42.5	141	15.44
33	50.0	176	17.84
30	55.5	223.5	21.44

C-G 11/8-4

0	0	5.0	0.05
5	0.5	18.0	0.46
6	1.5	30.0	1.46
6	2.0	47.0	2.46
2	1.0	79.0	4.46
5	3.0	86.0	5.46
4	3.0	117.0	7.26
6	5.5	136.5	9.26
6	7.5	170.0	11.40
8	10.5	180.5	13.40
9	14.5	216.0	15.85
8	16.5	293.5	20.24
10	25.0	356.0	23.76

C-H4-4

0	0	5.0	0
0	0	15.5	0.38
10	1.5	21.0	0.86
8	1.5	25.0	1.34
11	2.5	33.0	2.06
14	4.0	38.5	2.84
15	5.0	44.0	4.04
17	7.0	55.0	5.56
22	11.0	64.5	6.76
19	11.0	75.5	7.96
23	17.0	96.0	10.49
22	21.5	122.5	13.24
22	26.0	151.0	15.64
23	33.5	186.0	17.88
23	49.5	274.0	22.22

C-M7-6

0	0	5.0	0.05
0	0	9.0	0.30
0	0	15.5	0.89
3	0.5	26.5	1.64
2	0.5	44.0	2.84
1	0.5	75.0	5.24
2	1.0	92.0	7.64
4	3.0	125.5	10.04
3	2.5	143.5	11.84
3	3.5	171.5	14.36
3	5.0	221.0	17.75
3	6.0	273.0	20.01
16	37.5	303.5	20.61
19	59.0	397.0	24.18

Table 13. Continued

C-H6-1

0	0	5.0	0
0	0	14.0	0.64
0	0	22.5	0.98
0	0	36.0	1.70
0	0	42.5	2.06
0	0	67.0	3.50
0	0	93.5	4.94
0	0	115.5	6.38
0	0	138.0	7.82
4	4.0	151.5	9.26
4	5.0	172.5	10.70
3	5.0	221.0	13.58
0	0	292.5	16.46
1	2.0	358.5	19.34
2	10.0	429.5	22.22
2	9.0	601.5	27.05

C-H20-3

0	0	5.0	0
0	0	9.0	0.08
30	4.5	18.0	0.76
31	11.5	44.0	2.08
29	14.5	61.0	3.28
32	18.5	92.5	4.48
27	23.0	105.5	5.68
24	25.0	130.0	6.88
23	31.0	168.0	9.28
22	37.0	215.5	11.68
20	42.5	280.5	14.08
20	50.5	331.0	16.48
16	66.5	545.0	22.00

C-H20-2

0	0	5.0	0
0	0	13.5	0.36
7	1.5	29.5	1.17
12	3.5	41.0	1.96
10	4.0	58.0	3.16
12	9.0	104.0	5.56
14	15.0	151.0	7.36
6	11.5	190.0	9.49
9	27.5	227.0	11.89
12	35.0	286.5	14.29
16	43.5	357.5	16.69
13	50.5	438.5	19.09
14	54.0	527.5	21.49

C-M3-7

0	0	5.0	0.05
0	0	22.5	0.96
0	0	40.5	2.46
0	0	51.5	3.66
0	0	67.0	4.86
7	4.0	78.5	6.06
9	5.5	90.0	7.26
15	12.5	109.5	9.66
18	18.5	134.5	11.32
19	24.0	169.0	13.72
20	32.5	213.5	16.12
19	39.5	277.5	18.52
17	54.0	431.0	23.32

C-M3-5

0	0	5	0.05
0	0	18.5	0.90
0	0	38.0	2.78
0	0	49.0	4.19
0	0	71.5	5.60
4	2.0	77.0	6.32
6	3.5	90.0	7.01
3	2.5	126.5	9.14
6	6.0	154.0	11.24
10	15.0	202.0	14.06
9	16.0	263.0	16.88
9	20.0	325.5	19.70
6	17.5	443.5	22.52

C-M3-6

0	0	5.0	0.05
0	0	28.0	1.22
0	0	36.0	2.18
2	1.0	61.5	4.46
12	5.5	66.0	5.90
0	0	98.0	7.34
8	6.5	122.0	9.98
4	4.0	164.5	11.18
6	8.5	209.0	13.22
5	9.0	288.0	16.16
3	9.0	416.0	20.21
2	7.5	529.5	23.33

Table 13. Continued

C-H4-5			
0	0	9.0	0.12
0	0	15.5	0.39
3	0.5	22.0	0.85
8	1.5	25.0	1.15
16	4.0	34.0	2.35
21	6.5	39.5	3.55
18	7.5	54.5	4.75
22	11.5	66.0	5.95
15	14.0	72.5	7.15
24	15.5	80.0	8.10
24	18.0	97.0	11.65
28	24.0	106.5	13.15
24	26.5	139.5	15.55
20	26.5	174.0	17.95
19	32.0	222.5	20.35
18	37.5	272.5	22.75

C-H4-2			
0	0	16.0	0.25
0	0	20.5	0.61
0	0	22.5	0.79
0	0	29.5	1.15
0	0	47.0	2.23
3	1.5	78.5	4.39
0	0	93.5	4.75
0	0	107.0	5.47
0	0	113.5	5.83
6	5.0	126.0	7.27
7	7.0	148.5	9.43
3	4.0	191.5	11.59
4	7.5	272.0	15.81
3	7.5	316.0	19.77

C-H4-3			
14	1.0	10.0	0.27
20	2.5	16.0	0.51
7	1.0	19.5	1.11
7	1.5	30.0	1.71
11	3.0	39.5	2.91
13	5.5	57.0	4.11
11	5.0	62.5	5.31
9	6.0	92.0	6.51
8	6.0	109.5	7.71
7	7.5	146.0	10.11
7	9.0	186.5	12.51
4	6.5	231.5	14.91
8	16.5	303.5	18.51
7	21.0	418.5	22.25
8	33.0	601.5	28.25

C-H4-1			
0	0	14.0	0.29
0	0	20.5	0.65
0	0	25.0	0.83
0	0	29.5	1.19
0	0	38.0	1.55
5	2.0	56.0	2.99
6	3.0	70.5	4.43
1	0.5	97.5	5.87
0	0	129.0	7.31
0	0	167.0	9.47
0	0	208.5	11.63
0	0	255.0	13.79
2	3.0	301.0	15.95
2	6.0	386.5	19.86

C-H4-7			
0	0	5.0	0.04
0	0	13.5	0.31
0	0	22.5	1.12
0	0	26.5	2.28
0	0	31.0	3.48
0	0	40.0	4.68
0	0	51.0	5.88
0	0	68.0	7.08
0	0	75.5	8.28
0	0	86.5	9.48
0	0	115.5	11.88
2	1.5	142.5	14.28
9	11.0	170.5	17.24
9	14.5	235.5	20.84
9	18.0	287.5	24.44
9	27.0	437.5	30.11

C-H4-6			
0	0	5.0	0
0	0	9.0	0.12
0	0	18.0	0.42
0	0	22.5	0.78
0	0	37.5	1.98
0	0	53.0	3.18
0	0	64.0	4.38
0	0	73.0	5.58
0	0	80.0	6.78
0	0	88.5	7.98
0	0	108.5	10.38
0	0	133.0	12.78
0	0	142.0	15.18
0	0	208.0	19.12

Table 13. Continued

C-H4-2 Continued

4	11.5	427.0	23.37
4	18.0	589.5	27.68

C-M7-1

0	0	5.0	0.05
0	0	9.0	0.30
0	0	24.5	1.45
0	0	31.0	2.05
0	0	44.5	3.25
0	0	57.5	4.45
0	0	71.0	5.65
0	0	82.5	6.85
2	2.0	118.5	9.25
5	5.0	145.5	11.05
5	5.0	163.0	12.25
8	11.0	138.5	13.08
8	12.0	201.5	14.45
18	41.0	303.5	19.52
19	58.0	402.0	22.52

P-H4-2

0	0	9.5	0.28
0	0	21.0	0.95
0	0	25.5	1.25
0	0	29.5	1.85
5	1.5	50.5	3.38
2	1.0	62.0	4.58
5	2.0	63.5	5.78
7	4.0	83.5	6.98
3	2.0	87.0	8.20
5	4.0	116.0	10.60

C-H4-1 Continued

3	9.5	490.0	22.74
2	9.0	626.0	25.62

P-M3-4

0	0	5.0	0.05
28	4.5	22.0	1.18
16	6.5	54.5	4.06
13	6.5	71.0	5.50
7	5.5	110.0	7.66
8	7.5	134.5	9.82
8	9.5	159.5	11.44
7	9.5	193.0	12.88
3	6.0	257.0	15.76
5	9.5	283.0	17.37
6	12.5	304.5	18.46

P-H6-3

0	0	5.0	0
0	0	18.5	0.59
7	1.0	21.5	0.85
6	1.0	23.0	1.03
3	1.0	45.5	2.27
4	2.0	75.0	3.87
3	2.0	93.0	4.95
3	3.0	136.0	7.83
4	5.0	172.5	10.44
6	9.5	203.5	12.84

C-H4-6 Continued

0	0	265.5	23.75
0	0	323.5	26.14

P-H4-1

31	2.0	7.5	0.28
7	1.0	20.0	0.99
11	2.5	32.0	2.46
0	0	54.5	6.08
5	4.0	117.0	9.78
7	7.5	159.5	12.18
8	11.0	202.5	14.58
9	15.5	242.5	16.98
10	23.0	310.0	19.38
10	24.5	357.5	21.78
11	37.0	457.0	25.22

P-H6-1

0	0	5.0	0
0	0	14.5	0.66
0	0	24.0	0.93
0	0	28.5	1.29
0	0	37.5	1.83
0	0	63.0	3.65
0	0	102.0	5.76
0	0	160.0	8.67
3	4.0	177.5	10.47
4	6.0	196.0	12.27

Table 13. Continued

P-H4-2 Continued			
3	3.0	174.5	13.00
4	5.5	195.5	15.40
7	14.5	283.5	19.60
9	21.0	317.0	21.40
11	34.5	427.5	26.24

P-H20-2			
0	0	5.0	0
26	2.5	12.0	0.29
27	4.0	18.5	0.76
50	13.5	27.0	1.24
36	15.5	47.0	1.84
36	17.0	54.5	2.44
26	22.0	107.0	4.84
23	26.5	150.5	7.24
19	30.0	205.5	9.64
19	37.0	252.0	12.04
16	41.5	338.0	14.44
16	50.5	412.0	16.84
16	65.0	536.5	21.41

P-H6-3 Continued			
7	12.0	249.0	15.24
9	20.0	309.5	19.92
10	32.5	440.5	25.82

P-M7-1			
0	0	5.0	0.05
0	0	14.5	0.48
0	0	17.0	0.79
0	0	30.0	2.07
0	0	46.0	3.83
3	3	74.5	6.23
7	5.5	105.5	8.63
11	11.5	144.5	11.03
17	24.0	190.5	13.43
21	42.5	260.5	16.24
22	56.5	324.5	18.64
22	70.5	402.0	21.04

P-H6-1 Continued			
4	7.0	249.5	15.01
4	8.5	307.5	18.48
5	11.0	335.5	20.28
4	13.5	532.5	26.94

NOTE: All values of Δu_b > 72 gm/cm^2 are extrapolated.

[1]Equipment off for 24 hours.

APPENDIX G

SETTLEMENT ANALYSIS

Introduction

Several studies have been made to see how well terrestrial soil mechanics techniques apply to the prediction of the settlement of structures on ocean-type sediments (Keller (87); Hironaka and Smith (71); Inderbitzen and Simpson (79); Herrmann, Rocker and Babineau (68); and others). Keller's work was in relatively shallow water. Hironaka and Smith compared the settlement of a special structure for testing degradation of various materials, to estimates made from values of C_c determined from the relationship $C_c = 0.009\ (w_1-10)$. Actual settlement was estimated from apparent mud line markings on the recovered structure. Only the work of Inderbitzen and Simpson and that of Herrman, Rocker and Babineau is germaine to the methods of settlement estimation developed from this testing program. In the former case, visual determinations of *total* settlement at two different times were made from the research submarine DEEP QUEST. The site was the San Diego Trough where the water depth was 1240 m. Three different test shapes were employed. The pressure exerted on the clayey-silt was either 40 or 75 gm/cm^2. Insufficient data were available from the testing program to allow primary and secondary effects to be separated. Of the actual field tests made to date which were found in the literature only that of Herrmann, Rocker and Babineau was conducted in sufficient detail to

allow separate estimates of immediate, primary and secondary effects.

The Problem of Settlement in Soft Submarine Sediments

As indicated in Appendix D, volume change can be somewhat arbitrarily divided into initial, primary and secondary effects. In addition to volume change, when loads are placed on terrestrial soils that act in a relatively elastic manner, deformation can take place under the imposed shear stresses at constant volume without significant dissipation of excess pore pressure. This type of deformation is distinguished here from initial effects and is called *immediate settlement or elastic distortion.* If ocean sediments can be assumed to act elastically, then immediate settlement will occur when loads are placed on them. In many cases the upper centimeters of these sediments lack sufficient structural rigidity to support the load elastically and *fail* as plastic materials (Richards (151)). The result is that the load will sink a certain depth into the sediment, causing what can be termed a mud wave or displacement effect. This process may obliterate any elastic distortion that might have occurred. In effect, it can also act as an excavation, in that it causes minor relief of overburden stresses; however, the process is so rapid, and probably involves such a relatively small stress relief, that the effects on the following consolidation process are assumed to be minimal. Richards (149) and Inderbitzen and Simpson (79) have proposed that this displacement effect can be approximated by extrapolating a vane shear strength vs. depth profile from a relatively undisturbed gravity core so that an estimate of the vane shear strength near the sediment-water interface can be obtained.

Assuming that this profile approximates the undrained strength, they proposed using the known submerged weight of the structure and a bearing capacity equation which reflects the foundation shape and an assumed frictionless soil, to predict, based on bearing capacity failure, where the structure will cease sinking into the sediment.

Where the upper centimeters of the sediment have sufficient structural rigidity to act relatively elastically, the mud wave effect will be minimal and elastic distortion will not be obscured. For this situation, Kretschmer and Lee (93) proposed a procedure developed from studies of plate bearing tests and sediment shear strength. This method appears to include any small displacement effect and the elastic distortion caused by the structure.

Some Factors that Introduce Error into Estimates of Immediate Settlement

As indicated in Chapter I, it was only within the last few years that large loads have successfully been incrementally placed on shallow foundations well beyond normal diver construction capability. Consequently, in the past, structures with shallow foundations have been positioned as a unit. Since the dynamic effect of placing the foundation can change how deeply it will sink into the sediment, estimates of displacement effect/elastic distortion can be significantly in error because of the rate at which the foundation is placed. Additionally, it must be emphasized that any method of estimating elastic distortion where the modulus of elasticity is used, is very sensitive to sampling disturbance.

Whether or not values of elastic distortion should be added to

estimates of consolidation settlement appears to depend on how consolidation estimates are made. According to Leonards (102), it is common practice when conducting standard laboratory consolidation tests to include immediate and secondary effects of all previous increments in the calculation of the consolidated void ratio under subsequent increments. In a general way this practice tends to compensate for the *amount* of immediate settlement that occurs in the field. For normally consolidated clay, Leonards was of the opinion that the addition of immediate settlements were probably not warranted if consolidation tests were interpreted in the conventional manner.

Summary of the Problem

Settlement of a structure placed on a submarine sediment that undergoes some plastic deformation in the upper centimeters is viewed as having four components which may have arbitrarily defined starting and ending points. Initial compression would be a fifth component if undissolved gas were present.

1. Displacement Effect (mud waving).
2. Elastic Distortion (deformation at no volume change).
3. Primary Consolidation (deformation under hydrodynamic conditions).
4. Secondary Compression (deformation under hydrostatic conditions).

Only category three is examined in this testing program.

Ocean Foundation Tests

Foundation and Equipment

The following information is based on the work of Herrmann, Rocker, and Babineau (68), and data supplied by Rocker (159), and Herrmann (66).

"LOBSTER" (Long-Term Ocean Bottom Settlement Test for Engineering Research) is an instrumented foundation used as a test device, whereas the FMS (Foundation Monitor System) is an instrument that can be attached to any sea-floor foundation to be monitored.

The LOBSTER system--L-series tests--is a foundation that monitors its own settlement. Footing size and applied pressure can be varied with a range limited by the emplacement apparatus. Up to 50 gm/cm^2 can be applied with a 1.3 m diameter circular foundation. Larger stresses can be developed with smaller footings. Analytical and experimental studies showed that for LOBSTER loading conditions no measurable sediment compression would occur below a depth of about 2.3 m. An isolation tube with a reference probe was driven through the foundation bottom to a depth of about 3.0 m. Sensors recorded the downward movement of the foundation relative to the reference probe.

The 50 gm/cm^2 loading was established because it would insure no bearing capacity failures in many soft seafloor deposits.

The FMS--FM-series tests--is a subsequent development for use on any type foundation. This system monitors total settlement and tilting. A remote reference module is connected to the instrument housing by an umbilical cord. According to Herrmann, Rocker and Babineau the

reference module ". . . is designed and implanted in a way to assure negligible vertical movement. . . ," thus allowing actual total settlement of the foundation to be measured. The submerged weight of both the foundation monitor and the reference module can be varied. Stresses are generally computed to a depth equal to twice the characteristic dimension of the foundation. For tests FM2 and FM3, the foundation and FMS combined to produce a pressure increase of 75 gm/cm^2. In the first test the FMS was placed by a remotely controlled vehicle after the foundation had been positioned. In the second test the FMS and the foundation were lowered as a unit.

Site Data

Coring. Cores used for consolidation tests were either taken by a hydro plastic-corer (400 m site--TH-1, TH-2) or by a fixed piston corer operating from a bottom-sitting platform (400 m site--TH-7, 200 m site SNCI-56). The results of certain tests performed on the cores are listed in Table 14.

200 Meter Site. Two cores were taken at this site. These two cores and the actual emplacement locations were within 150 m of each other. Between the two cores the uniformity was only fair, but 13 cores from a site 2300 m away displaced good areal uniformity. The grain size profile showed some variation over about the first 30 to 50 cm; below that range the sediment was relatively uniform. Consolidation tests were conducted on core SCNI-56.

400 Meter Site. Eight cores were taken within 450 m of the center of the actual emplacement location. Areal and vertical

Table 14. Data from Ocean Test Sites

Core (Depth in Meters)	Latitude N.	Longitude W.	w %	e_o	S_T	w_l	I_p	I_l	γ_m gm/cm^3	$CaCO_3$ %	Organic Carbon %
SCNI56 (200)	34°17.2'	119°42.7'	50	1.07-1.73	1.4-6.5	45	20	1.0	1.80	0.3-0.6[2]	0.7-1.1[2]
TH1[1] (400)	34° 9.5'	119°45.5'	105-133	2.61-3.28	3.0	85	45	1.6	1.48	0.9	2.2
TH2[1] (390)	34° 9.5'	119°44.8'	120-135	2.66-2.82	2.7	100	50	1.4	1.48	1.2	2.4
TH7[1] (400)	34° 9.4'	119°45.4'	82-109	2.00-2.26	1.1-4.2	85	45	1.0-1.5	1.48	-	-

NOTE: All values are averages. Significant variation from the average are indicated by a range of values.

[1]Values pertain to that section of the core used in consolidation testing program.

[2]Values are from core SCNI55.

uniformity was good. Four consolidation tests were conducted on core TH-7 which had similar plasticity, but less clay content, than the other two cores used in the consolidation testing program (TH-1 two tests, TH-2 one test).

Consolidation Tests. Core sections were stored upright in a 100% humidity environment. Standard consolidation tests were run in a modified Karol-Warner consolidometer with applied pressures varying from 2 to 16,000 gm/cm^2. Loads were applied at intervals of approximately 24 hours. Some smaller loads were applied sooner, if consolidation had ceased. In all cases, LIR equaled 1.0. The sample was surrounded with salt water. Test temperature was 20°C. Some tests were run with a back pressure of about 2 kg/cm^2 in an Anteus consolidometer. Results from tests with and without back pressure showed no significant variation. Samples in both types of tests were 6.35 cm in diameter by 1.91 cm high.

Stress Distribution

All settlement computations *reported here* were made using charts showing stress distributions for a circular foundation resting on a Boussinesq elastic half-space. Use of this method is based on the assumption that the deposit acts as though it was a semi-infinite, homogeneous, isotropic elastic material. The foundation is assumed to be sufficiently rigid in terms of applied loads so that the stress distribution under it is *relatively* uniform. Settlement was computed for each layer based on p_c' values from ϵ-log $\Delta\sigma'$ curves replotted as described later in this appendix from data furnished by Herrmann (65).

Because of the unique nature of submarine sediments, the following equation is proposed for use in computing primary consolidation on these materials:

$$\Delta H = \sum_{i=1}^{n} H_i \left(C_\epsilon \log \frac{p_c' + \Delta\sigma'}{p_c'} \right)_i \qquad (4)$$

where $\Delta\sigma'$ represents the stress increase at the midpoint of each layer, and p_c' is the apparent mid-layer preconsolidation pressure, *not* the computed effective overburden pressure.

Corrections to Standard Laboratory Tests

Correction for Lateral Deformation. As indicated in Appendix D, one-dimensional consolidation theory assumes that the sediment is laterally confined. For relatively small loads over large areas--such as the accumulation of sediment--this assumption is relatively valid. However, when a structural load is placed on a deep deposit of soft submarine clay, the dimensions of the foundation are likely to be relatively small compared to the depth of the deposit. Skempton and Bjerrum (182) indicated that the lateral effects are generally small if the material is normally consolidated, but can be significant if it is overconsolidated. As previously indicated, most submarine sediments display characteristics of both types of soils and thus form an anomalous category called "apparently preconsolidated."

Based on the semi-empirical method of Skempton and Bjerrum corrections can be applied to estimates of primary consolidation made from laboratory tests. Scott (170) indicated that corrections for lateral

effects rarely exceeded 20%, and in view of the uncertainty regarding actual *in situ* processes, they would probably be of little significance. For submarine sediments corrections for lateral effects are felt to be worth considering in view of the unusual nature of these materials.

Correction for Secondary Effects. Figures 19, 20 and 21 provide a comparison of ϵ-log $\Delta\sigma'$ curves from three cores, representing three different sites. The less-than-two-micron fraction from two sites was mainly chlorite and illite; from the third site it was mainly montmorillonite and kaolinite. It is apparent from the figures and from Table 3 that values of C_c determined within each group of curves have little variation. However, the method by which ϵ was computed (i.e. using R_{100} or R_f) is noted to have a significant effect on the value of p_c' obtained from each curve. Grain size analysis made on material from various levels in core SCNI-56 indicated that at the 200 m foundation test site the sand-silt-clay ratio (average values) was 4%-80%-16%. Determinations in the upper part of the core were considered more important. For the 400 m test site the ratio was: 5%-68%-27% for core TH-7, 5%-49%-46% for TH-1, and 4%-50%-46% for TH-2. No X-ray diffraction data were available, but, based on the work of Griffin, Windom, and Goldberg (55), the less-than-two-micron fraction would probably have a clay mineral distribution something like:

Chlorite	10%
Kaolinite	10%
Illite	20% to 30%
Montmorillonite	30% to 50%

This distribution is in accord with Weaver, 1973, who estimated that cores from these sites would have clay mineral contents which in

general would be bounded by the two extremes of clay mineral contents found in cores used in this testing program.

As indicated in the discussion of results CRS tests conducted at rates so that hydrodynamic effects were significant, but not excessive, appear to provide the most accurate picture of primary consolidation in the region of p_c' and C_c. It was also indicated that values of p_c' determined by computing ϵ from values of R_{100} for tests where each increment was allowed to remain on the sample 24 hours, were apparently not significantly different from values of p_c' determined from curves where ϵ had been computed using values of R_{100} and each increment had been put on as soon as R_{100} was reached. It would appear that the best estimate of p_c' that could be made from a standard consolidation test with load increments of 24 hours duration can be made by using ϵ determined from values of R_{100}.* As previously indicated, data from the 200 m and 400 m test sites provided by Herrmann (65) was used to develop plots of ϵ-log $\Delta\sigma'$ using values of R_{100}. Values of p_c' determined from these plots were used in preparing Figure 46.

Settlement Computations

Table 15 lists the computations for one foundation test at the 200 m site (FM-2) and two at the 400 m site (L-3, FM-3). For each test two plots similar to Figure 46 were prepared--one for the foundation centerline and one for the foundation edge. The apparent preconsolidation pressure for each consolidation test (as determined using the Sowers' method) was plotted vs. depth. For the 400 m site the plot was

*As long as initial effects are not significant.

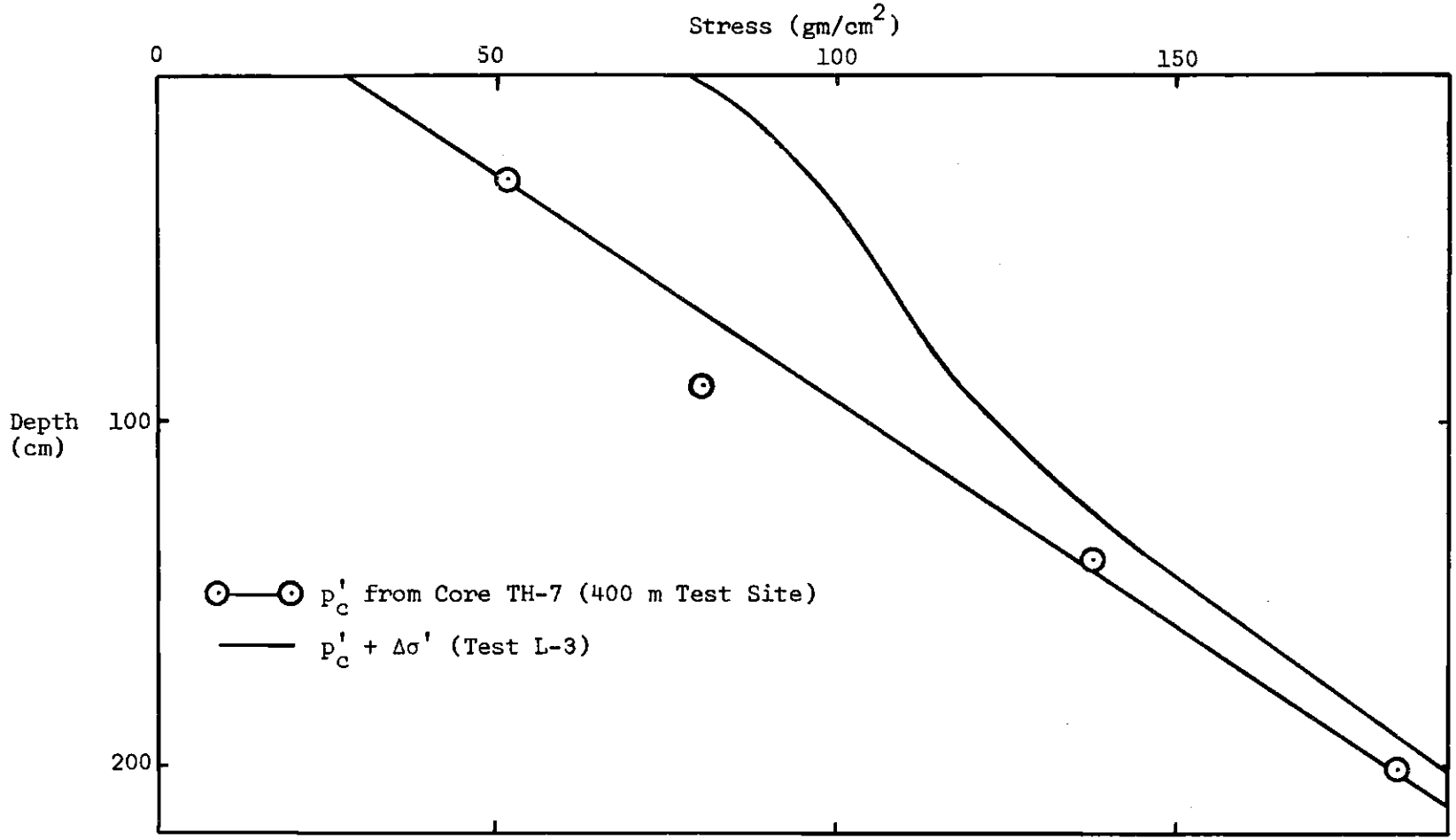

Figure 46. Apparent Preconsolidation Pressure and Stress Increase Caused by Foundation vs. Depth

Table 15. Settlement Calculations (Centerline)

Test	Layer Thickness	(1) p_c' gm/cm^2	(2) $\Delta\sigma'$ gm/cm^2	(3) $p_c'+\Delta\sigma'$ gm/cm^2	(4) (3)÷(1)	(5) log (4)	(6) H cm	(7) C_ϵ	(8) (5)(6)(7) cm	(9) ΔH cm
FM-2 (200 m Site)	0-20	79.0	75.0	154.0	1.98	0.297	20	0.136	0.81	
	20-45	96.0	72.5	168.5	1.76	0.244	25	0.127	0.78	
	45-135	145.0	48.5	193.5	1.33	0.125	90	0.130	1.46	
	135-230	217.0	23.0	240.0	1.11	0.044	95	0.167	0.70	
	230-370	287.0	11.5	298.5	1.04	0.018	140	0.167	0.42	
										4.17
L-3 (400 m Site)	0-20	36.0	50.0	86.0	2.39	0.378	20	0.185	1.40	
	20-50	55.0	43.5	98.5	1.79	0.253	30	0.202	1.53	
	50-90	81.5	29.0	110.5	1.36	0.132	40	0.224	1.18	
	90-160	120.0	14.0	134.0	1.12	0.048	70	0.238	0.80	
	160-305	206.0	6.5	212.5	1.03	0.013	145	0.222	0.42	
										5.33
FM-3 (400 m Site)	0-20	36.0	75.0	111.0	3.08	0.488	20	0.185	1.81	
	20-50	55.0	71.5	126.5	2.30	0.362	30	0.202	2.19	
	50-90	81.5	58.0	139.5	1.71	0.233	40	0.224	2.09	
	90-140	117.5	39.5	156.0	1.33	0.122	50	0.234	1.43	
	140-190	155.5	28.0	183.5	1.18	0.072	50	0.203	0.73	
	190-370	240.0	12.0	252.0	1.05	0.022	180	0.226	0.90	
										9.15

essentially linear (Figure 46). At the 200 m site, except for the two shallowest tests, the plot was also linear. These two tests appear to be of questionable value: The one nearest the sediment surface appears quite disturbed, while the dial reading vs. time values from the second test are erratic. Superimposed on the plot of p_c' vs. depth, is a plot of the stress increase vs. depth caused by the foundation. Depending on the rate of change of this second curve, the sediment profile was divided into layers so that within any layer the curve was linear. Thus for each layer the mid-layer values of p_c' and $p_c' + \Delta\sigma'$ are approximately equal to the average stress in the layers. Values of C_ϵ, corresponding to the depth of the middle of each layer were determined from the curves of C_c and e_o vs. depth (Figures A-2 and A-3 in Herrmann, Rocker, and Babineau (68)). Values of C_ϵ, p_c', and $p_c' + \Delta\sigma'$, and stratum thickness were used in Equation (4) to compute primary consolidation.

The maximum value of consolidation was computed under the foundation centerline. Average values were computed based on the assumption of a relatively uniform stress distribution--a parabolic curve through the maximum centerline value and the edge values was used.

Correction for Lateral Effects at the Foundation Sites. Based on the work of Moore (see Appendix B) a *rough* estimate of the A pore pressure parameter was made. Skempton and Bjerrum (182) recommended the use of A values between 0.5 and 1.0 for computing the settlement of structures founded on normally consolidated deposits where lateral effects could be significant. Moore's work showed that the *upper few meters* of some ocean sediments have A_f values which range from about

0.6 to 1.0. Although A is not a constant, it is assumed that this range of values could be representative of the sediment at the foundation test sites. Therefore correction factors based on 0.6 less than A less than 1.0 have been used. The values selected are those proposed by Skempton and Bjerrum (182) as reevaluated by Scott (170). Thus the total estimated settlement caused by primary consolidation is:

$$\Delta H_c = C_F \Delta H \tag{73}$$

where C_F is the correction factor corresponding to the A value used.* Table 8 lists the average and maximum computed settlements corrected for lateral spreading. For both test sites the *maximum* value has been corrected using the *range of A values* previously indicated--the corresponding C_F values were 0.7 and 1.0. For the 200 m site, the *average* value has been corrected using a C_F = 0.85 (the middle of the range). For the 400 m site, the *average* values have been corrected using C_F = 1.0. The reason for the difference is that although the sediments at the 200 m site seemed slightly more sensitive, they were less compressible, less plastic, and displayed relatively greater apparent preconsolidation with depth. For these reasons it is felt the effect of lateral conditions other than those assumed would cause a decrease in the amount of vertical consolidation at this site.

---

*In terrestrial work it would probably be more appropriate to use a separate C_F for each layer if values of A were known. Since *this* estimate involves little more than an educated guess for the A values, the use of one C_F for the whole analysis seems justified.

Actual Foundation Settlement as a Result of Primary Consolidation

Figure 47 has been developed based on the data provided by Figures 6, 14, 15 and C-2a in Herrmann, Rocker and Babineau (68). In essence this figure is a Taylor square root of time plot where the characteristic straight line portion of the curve can be used to estimate the completion of settlement of the actual foundation due to primary consolidation. Estimation of the actual amount of settlement from the curves in Figure 47 varies. This is because of differing foundation emplacement conditions.

Test FM-2. At the 200 m site it was possible to make visual observations to correlate the recorded settlement with the sediment-water interface. Thus the data from Figures 14 and C-2a in Herrmann, Rocker and Babineau, replotted in Figure 47 represents all of primary and some of secondary. Primary can be considered to include all the settlement from the zero value to the R_{100} value.

Test L-3. No visual observations were possible at the 400 m site. For this reason the data from Figures 6 and C-2a in Herrmann, Rocker and Babineau, replotted in Figure 47 apparently represent the major portion (perhaps all) of primary and some secondary. The reason for this is that scale zero represents the first data point recorded by LOBSTER and not necessarily the beginning of primary. Thus primary settlement is assumed to be approximately the settlement indicated between the zero value and R_{100}.

Test FM-3. In addition to not having visual data, test accuracy was further clouded by an apparent bearing capacity failure recorded by

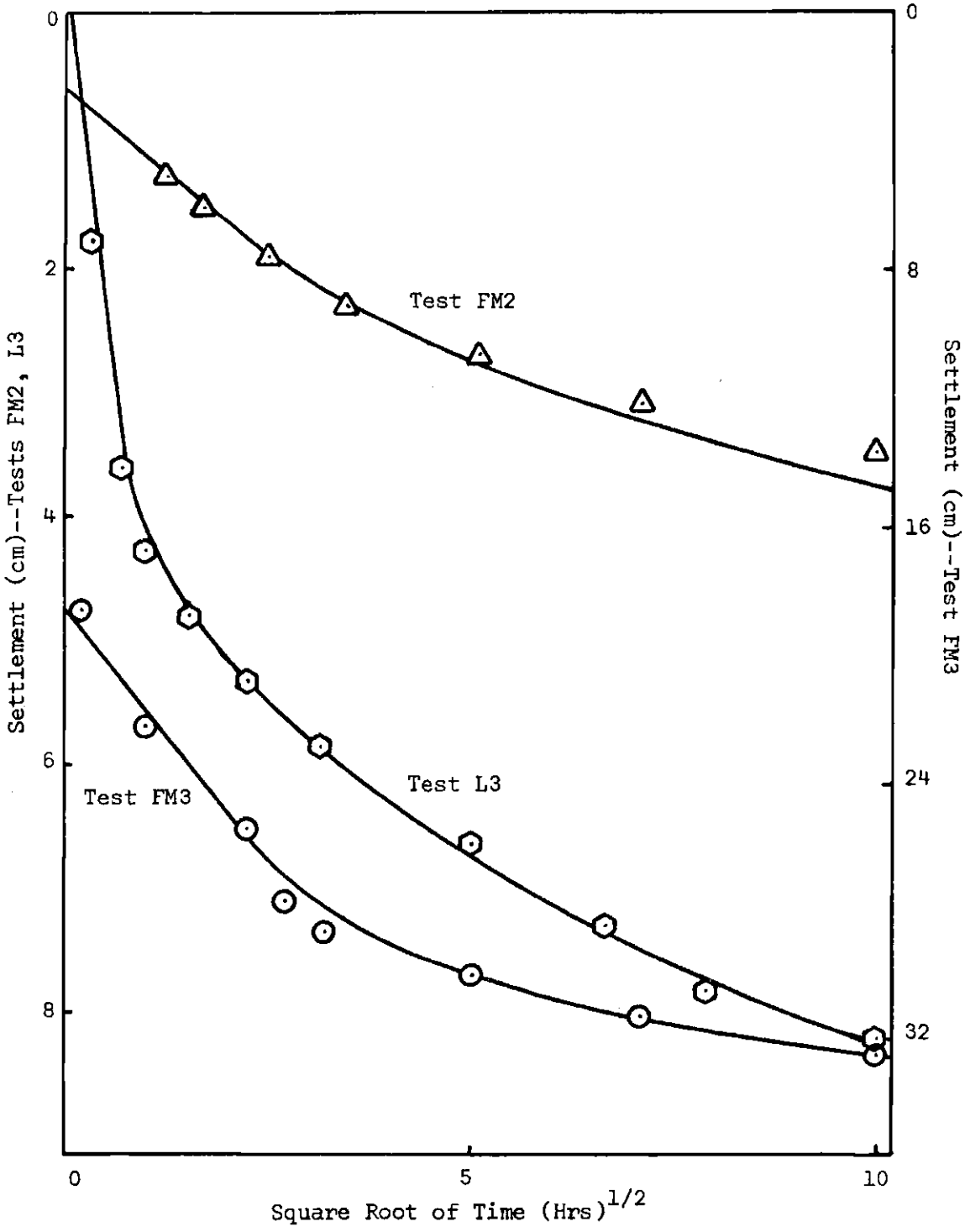

Figure 47. Settlement of Test Foundations

the sensing system. Herrmann, Rocker and Babineau present data corrected to the best of their ability in their Figures 15 and C-2a. The data are replotted in Figure 47. Because of the bearing capacity failure, it is felt that the best estimate of settlement caused by primary consolidation results from using the $R_{100}-R_0$ value from Figure 47.

Actual Settlements. Values of actual settlement caused by primary consolidation estimated for each test are listed in Table 8.

BIBLIOGRAPHY

1. Almagor, G., "Interpretation of Strength and Consolidation Data From Some Bottom Cores Off Tel-Aviv--Palmakhim Coast Israel," *Marine Geotechnique*, Adrian F. Richards, ed., Urbana, Ill.: U. of Illinois Press, 1967, pp. 131-153.

2. Altschaeffl, A. G., and Valent, P. J., discussion of "Engineering Properties of Submarine Soils: State-of-the Art Review," *Journal of the Soil Mechanics and Foundations Division, ASCE*, Vol. 97, No. SM5, May, 1971, pp. 820, 821.

3. Anderson, D. G., and Herrman, H. G., "Seafloor Foundations: Analysis of Case Histories," *Technical Report R-731*, U. S. Naval Civil Engineering Laboratory, Port Hueneme, Calif., June, 1971.

4. Arman, Ara, "Engineering Classification of Organic Soils," *Highway Research Record*, No. 310, 1970, pp. 75-89.

5. "Atlantis Program Proposal," *Mission and Experiment Plan*, Vol. II, IV, Prepared for the University of Miami by Chrysler Space Division, New Orleans, La., May, 1969.

6. Barden, Laing, "Consolidation of Clay with Non-Linear Viscosity," *Geotechnique*, Vol. XV, No. 4, December, 1965, pp. 345-362.

7. Barden, Laing, and Berry, Peter L., closure to "Consolidation of Normally Consolidated Clay," *Journal of the Soil Mechanics and Foundation Division*, ASCE, Vol. 93, No. SM 1, January, 1967, pp. 121.

8. Barden, Laing, and Berry, Peter L., "Consolidation of Normally Consolidated Clay," *Journal of the Soil Mechanics and Foundations Division*, ASCE, Vol. 91, No. SM 5, September, 1965, pp. 15-35.

9. Bartlett, John, *Familiar Quotations*, 13th ed., Boston: Little Brown and Co., 1955.

10. Bennett, R. H., Keller, G. H., and Busby, R. F., "Mass Property Variability in Three Closely Spaced Deep-Sea Sediment Cores," *Journal of Sedimentary Petrology*, Vol. 40, No. 3, September, 1970, pp. 1038-1043.

11. Bigham, Gary N., "Clay Mineral Transport on the Inner Continental Shelf of Georgia," *Abstracts with Programs*, Geological Society of America, Vol. 4, No. 2, February, 1972, pp. 61-62.

12. Biot, M. A., "General Theory of Three-Dimensional Consolidation," *Journal of Applied Physics*, Vol. 12, No. 75, February, 1941, pp. 155-164.

13. Bjerrum, L., "The Effective Shear Strength Parameters of Sensitive Clays," *Proceedings*, Fifth International Conference on Soil Mechanics and Foundation Engineering, Vol. 1, Paris, 1961, pp. 23-28.

14. Bjerrum, L., "Engineering Geology of Norweigan Normally-Consolidated Marine Clays as Related to Settlement of Buildings," *Geotechnique*, Vol. XVII, No. 2, June, 1967, pp. 81-118.

15. Bjerrum, L., "Fundamental Considerations on the Shear Strength of Soil," *Geotechnique*, Vol. II, No. 3, September, 1951, pp. 209-218.

16. Black, C. A., Evens, D. D., White, J. L., Ensminger, L. E., and Clark, F. E., eds., *Methods of Soil Analysis*, Vol. 2, American Society of Agronomy, Inc., Madison, Wis., 1965.

17. Bouma, Arnold H., Sweet, William E., Jr., Dunlap, Wayne A., and Bryant, William R., "Comparison of Geological and Engineering Parameters of Marine Sediments," *Preprints Paper No. 1514, Offshore Technology Conference*, Houston, Texas, May 1-3, 1972, pp. 21-34.

18. Bowles, F. A., "Microstructure of Sediments: Investigations with Ultrathin Sections," *Science*, Vol. 159, No. 3820, Mar. 15, 1968, pp. 1236, 1237.

19. Bozozuk, M., "Effect of Sampling, Size and Storage on Test Results for Marine Clay," *Symposium on Sampling of Soil and Rock, Special Technical Publication No. 493*, American Society for Testing Materials, 1971, pp. 121-131.

20. Brumund, W. F., Personal communication, June, 1972.

21. Bryant, William R., Cernock, Paul, Morelock, Jack, "Shear Strength and Consolidation Characteristics of Marine Sediments From the Western Gulf of Mexico," *Marine Geotechnique*, Adrian F. Richards, ed., Urbana, Ill: U. of Illinois Press, 1967, pp. 41-62.

22. Burmister, D. M., "Strain-rate Behavior of Clay and Organic Soils," *Symposium on Time Rates of Loading in Soil Testing (Papers on Soils), Special Technical Publication No. 254,* American Society for Testing Materials, 1960, pp. 88-105.

23. Burns, R. E., "Free-Fall Behavior of Small, Light-Weight Gravity Cores," *Marine Geology,* Vol. 4, Nos. 1, March, 1966, pp. 1-9.

24. Byrne, Peter M., discussion of "Consolidation Under Constant Rates of Strain," *Journal of the Soil Mechanics and Foundations Division, ASCE,* Vol. 96, No. SM 1, January, 1970, pp. 346-349.

25. Callender, Gordon W., Jr., "An Examination of Available Sedimentary Data from the Continental Slope off Certain Major Rivers of the World," Special Problem Submitted to Dr. C. E. Weaver (unpublished), Summer, 1970.

26. Campanella, Richard G., and Mitchell, James K., "Influence of Temperature Variations on Soil Behavior," *Journal of the Soil Mechanics and Foundations Division,* ASCE, Vol. 94, No. SM 3, May, 1968, pp. 709-734.

27. Carpenter, S. H., Thompson, L., and Bryant, W. R., "Viscoelastic Properties of Marine Sediments," *Report No. Alm-REF-72-8-T,* Dept. of Oceanography, Texas A. and M. University, September, 1972.

28. Casagrande, A., "The Determination of the Preconsolidation Load and Its Practical Significance," *Proceedings,* First International Conference on Soil Mechanics and Foundation Engineering, Vol. 3, Cambridge, Mass., 1936, pp. 60-64.

29. Chilinger, G. V., and Knight, L., "Relationship Between Pressure and Moisture Content of Kaolinite, Illite, and Montmorillonite Clays," *Bulletin,* American Association of Petroleum Geologists, Vol. 44, No. 1, January, 1960, pp. 101-106.

30. Chmelik, Frank Bernard, "An Investigation of Changes Induced in Macrostructure in Pelitic Sediments During Primary Consolidation," *Reports No. A/M-REF-70-8-T,* Institute of Statistics, Texas A. and M. University, January, 1970.

31. Crawford, Carl B., "Interpretation of the Consolidation Tests," *Journal of the Soil Mechanics and Foundations Division,* ASCE, Vol. 90, No. SM 5, September, 1964, pp. 87-102.

32. Crawford, Carl B., "The Resistance of Soil Structure to Consolidation," *Canadian Geotechnical Journal,* Vol. 2, No. 2, May, 1965, pp. 90-115.

33. Davis, E. H., and Poulos, H. G., "The Use of Elastic Theory for Settlement Prediction Under Three-Dimensional Conditions," *Geotechnique*, Vol. XVIII, No. 1, March, 1968, pp. 67-91.

34. Delflache, A. P., Bryant, W. R., and Cernock, P. J., "Determination of Compressibility of Marine Sediments from Compressional-Wave Velocity Measurements," *Preprints Paper No. 1328*, Offshore Technology Conference, Houston, Texas, April 19-21, 1971, pp. 33-42.

35. Demars, K. R., and Taylor, R. J., "Naval Seafloor Soil Sampling and In-Place Test Equipment: A Performance Evaluation," *Technical Report R-730*, U. S. Naval Civil Engineering Laboratory, Port Hueneme, Calif., June, 1971.

36. Dott, R. H., "Dynamics of Subaqueous Gravity Depositional Process," *Bulletin*, American Association of Petroleum Geologists, Vol. 47, No. 1, January, 1963, pp. 104-128.

37. Drake, C. L., Ewing, J. F., and Stockhard, H., "Continental Margin of Eastern United States," *Canadian Journal of Earth Sciences*, Vol. 5, No. 4, Part 2, August, 1968, pp. 993-1010.

38. Einsele, Gerhard, "Sedimentary Processes and Physical Properties of Cores from the Red Sea, Gulf of Aden, and Off the Nile Delta," *Marine Geotechnique*, Adrian F. Richards, ed., Urbana, Ill.: U. of Illinois Press, 1967, pp. 154-169.

39. Emery, K. O., and Hulsemann, J., "Shortening of Sediment Cores Collected in Open Barrel Gravity Corers," *Sedimentology*, Vol. 3, No. 8, August, 1964, pp. 144-154.

40. Emrich, W. J., "Performance Study of Soil Sampler for Deep-Penetration Marine Borings," *Symposium on Sampling of Soil and Rock, Special Technical Publication No. 493*, American Society for Testing Materials, 1971, pp. 30-50.

41. Ericson, D. B., Ewing, M., Wollin, G., and Heezen, B., "Atlantic Deep-Sea Sediment Cores," *Geological Society of America*, Vol. 72, No. 2, February, 1961, pp. 193-289.

42. Esrig, M. E., Davison, M. T., and Peck, R. B., "Report on Consolidation of Soils Under High Pressures," Engineering Experiment Station, University of Illinois, Unpublished report.

43. "Estimating Consolidation Settlements of Shallow Foundations on Overconsolidated Clay," *An Application Bulletin*, Highway Research Board, August, 1971.

44. "Estimation of *In Situ* Maximum Past (Preconsolidation) Pressure of Saturated Clays From Results of Laboratory Oedometer Tests," *An Application Bulletin* (Draft), Highway Research Board, December, 1971.

45. Faas, Richard, "Preliminary Report on Foraminiferal Distribution in the Deep Basins in the Gulf of Maine," *Maritime Sediments*, Vol. 7, No. 1, April, 1971, pp. 19-22.

46. Faas, Richard, and Toth, David J., "Organo-Sediment Relationships in the Wilkinson Basin, Gulf of Maine" (Draft), 1972.

47. Fanning, Kent A., and Pilson, Michael, E. Q., "Interstitial Silica and pH in Marine Sediments: Some Effects of Sampling Procedures," *Science*, Vol. 173, No. 4003, Sept. 24, 1971, pp. 1228-1231.

48. Fenske, C. W., "Deep Vane Tests in Gulf of Mexico," *Symposium on Vane Shear Testing of Soils, Special Technical Publication No. 193*, American Society for Testing Materials, 1957, pp. 16-25.

49. Finn, F. N., "Effect of Temperature on the Consolidation-Characteristics of Remolded Clay," *Symposium on Consolidation Testing of Soils, Special Technical Publication No. 126*, American Society for Testing Materials, 1951, pp. 65-71.

50. Friedman, G. M., Fabricand, B. P., Imbimbo, E. S., Brey, M. E., and Sanders, J. E., "Chemical Changes in Interstitial Waters from Continental Shelf Sediments," *Journal of Sedimentary Petrology*, Vol. 38, No. 4, Dec., 1968, pp. 1313-1319.

51. Gibson, R. E., England, G. L., and Hussey, M. J. L., "The Theory of One-Dimensional Consolidation of Saturated Clays," *Geotechnique*, London, Vol. XVII, No. 3, Sept., 1967, pp. 261-273.

52. Ginsburg, R. N., "Early Diagenesis and Lithification of Shallow-Water Carbonate Sediments in South Florida," *Regional Aspects of Carbonate Deposition, Special Publication No. 5*, Society of Economic Paleontologists and Mineralogists, 1957, pp. 80-100.

53. Gorsline, D. S., "Bottom Sediments of the Atlantic Shelf and Slope Off the Southern United States," *Journal of Geology*, Vol. 71, No. 4, July, 1963, pp. 422-440.

54. Greenland, D. J., "Interaction Between Clay Minerals and Organic Compounds in Soils; Part II. Adsorption of Soil Organic Compounds and Its Effects on Soil Properties," *Soils and*

Fertilizers, Vol. 28, No. 6, 1965, pp. 521-528.

55. Griffin, J. J., Windom, H., and Goldberg, E. D., "The Distribution of Clay Minerals in the World Ocean," *Deep-Sea Research*, Vol. 15, No. 4, Aug., 1968, pp. 433-459.

56. Grim, R. E., *Applied Clay Mineralogy*, New York: McGraw-Hill Book Co., 1962.

57. Grim, R. E., *Clay Mineralogy*, 2nd ed., New York: McGraw-Hill Book Co., New York, 1968.

58. Halwachs, J. E., and Monney, N. T., "Analysis of Sediment Shear Strength at Varying Rates at Strain," *The Journal of Environmental Sciences*, Vol. 15, No. 4, July/August, 1972, pp. 27-31.

59. Hamilton, E. L., "Consolidation Characteristics and Related Properties of Sediments from Experimental Mohole (Guadalupe Site)," *Journal of Geophysical Research*, Vol. 69, No. 20, Oct. 15, 1964, pp. 4257-4269.

60. Hamilton, E. L., "Elastic Properties of Marine Sediments," *Journal of Geophysical Research*, Vol. 76, No. 2, Jan. 10, 1971, pp. 579-604.

61. Hamilton, E. L., "Low Sound Velocities in High-Porosity Sediments," *Journal of the Acoustical Society of America*, Vol. 28, No. 1, January, 1956, pp. 16-19.

62. Hamilton, E. L., Shumway, G., Menard, H. W., and Shipek, C. J., "Acoustic and Other Physical Properties of Shallow-Water Sediments Off San Diego," *Journal of the Acoustical Society of America*, Vol. 28, No. 1, January, 1956, pp. 1-15.

63. Harrison, W., Lynch, M. P., and Altschaeffl, A. G., "Sediments of Lower Chesapeake Bay, With Emphasis on Mass Properties," *Journal of Sedimentary Petrology*, Vol. 34, No. 4, December, 1964, pp. 727-755.

64. Heezen, B. C., Tharp, M., and Ewing, M., "The Floors of the Oceans: I. The North Atlantic," *Special Paper No. 65*, Geological Society of America, 1959.

65. Herrmann, H. G., "Foundations for Small Seafloor Installations," *Technical Note N-1246*, U. S. Naval Civil Engineering Laboratory, Port Hueneme, Calif., September, 1972.

66. Herrmann, H. G., Personal communication, October, 1972.

67. Herrmann, H. G., Raecke, D. A., and Albertsen, N. D., "Selection of Practical Seafloor Foundation Systems," *Technical Report R-761*, U. S. Naval Civil Engineering Laboratory, Port Hueneme, Calif., March, 1972.

68. Herrmann, H. G., Rocker, K., Jr., and Babineau, P. H., "LOBSTER and FMS: Devices for Monitoring Long-Term Seafloor Foundation Behavior," *Technical Report R-775*, U. S. Naval Civil Engineering Laboratory, Port Hueneme, Calif., 1972.

69. Hironaka, M. C., "Engineering Properties of Marine Sediments Near San Miguel Island, California," *Technical Report R-503*, U. S. Naval Civil Engineering Laboratory, Port Hueneme, Calif., Dec., 1966.

70. Hironaka, M. C., and Hoffman, W. E., "Site Surveying for Ocean Floor Construction," *Technical Report R 691*, U. S. Naval Civil Engineering Laboratory, Port Hueneme, Calif., August, 1970.

71. Hironaka, M. C., and Smith, Raymond J., "Foundation Study for Materials Test Structure," *Journal of the Soil Mechanics and Foundations Division*, ASCE, Vol. 95, No. SM 6, November, 1969, pp. 1431-1451.

72. Hirst, Terence J., "Geotechnical Evaluation of Sea-Floor Development and Demonstration Areas" (abstract), *Transactions*, American Geophysical Union, Vol. 53, No. 4, April, 1972, pp. 411.

73. Howard, James D., Personal communication to George F. Sowers, June, 1971.

74. "Hudson Canyon Carries Pollutants to Deep Sea," *Marine Resources Digest--Marine Biology Digest*, Vol. 5, No. 3, December, 1972, pp. 3-4.

75. Hvorslev, M. Juul, *Subsurface Exploration and Sampling of Soils for Civil Engineering Purposes*, Corps of Engineers, U. S. Army, Waterways Experiment Station, Vicksburg, Miss., 1949.

76. "Hydro Plastic-Corer, Class 84," *Drawing No. 84-1-C through 84-34-A* and *84-45-D through 84-57-A*, U. S. Department of Commerce, Coast and Geodetic Survey, 1967.

77. Inderbitzen, A. L., "A Study of the Effects of Various Core Samples on Mass Physical Properties in Marine Sediments," *Journal of Sedimentary Petrology*, Vol. 38, No. 2, June, 1968, pp. 473-489.

78. Inderbitzen, A. L. and Simpson, F., "A Comparison of the Test Results of Vane and Direct Shear Tests Made on Recent Marine Sediments," *Report No. LMSC-694965,* Lockheed Missiles and Space Co., Sunnyvale, Calif., November, 1969.

79. Inderbitzen, A. L., and Simpson, F., "Predicted Versus Actual Settlement of Cement Blocks Into the Sea Floor," *Report No. LMSC-698661,* Lockheed Missiles and Space Co., Sunnyvale, Calif., February, 1971.

80. *Instruction Manual for Obtaining Oceanographic Data,* Publication No. 607, 3rd ed., U. S. Naval Oceanographic Office, 1968.

81. Jones, R. A., "Design, Placement, and Retrieval of Submersible Test Units at Deep-Ocean Test Sites," *Technical Report R-369,* U. S. Naval Civil Engineering Laboratory, Port Hueneme, Calif., May, 1965.

82. Kaplan, David M., "Sources of Holocene and Late Pleistocene Sediments on the Continental Shelf Off Georgia," Master of Science Thesis submitted to the University of Georgia, Athens, Ga., 1971.

83. Kaul, B. K., "Influence of Adsorbed Water on Secondary Compression of Clays," *Journal of the Institution of Engineers* (India), Vol. 50, Part CI-5, No. 9, May, 1970a, pp. 215-219.

84. Kaul, B. K., "Temperature Effects on the Compressibility of Clay Minerals," *Journal of the Institution of Engineers* (India), Vol. 51, Part CI-1, No. 1, September, 1970b, pp. 16-18.

85. Keller, George H., "Cruise Report for Phase II ALVIN Dive Series in the Outer Hudson Submarine Canyon," *Reference RF 203-15h (1)-617,* National Oceanic and Atmospheric Administration, Marine Geology and Geophysics Laboratory, Miami, Fla., Sept. 29, 1972.

86. Keller, George H., "Engineering Properties of Some Sea-Floor Deposits," *Journal of the Soil Mechanics and Foundations Division,* ASCE, Vol. 95, No. SM 6, November, 1969, pp. 1379-1392.

87. Keller, George H., "Investigations of the Application of Standard Soil Mechanics Techniques and Principles to Bay Sediments," *IMR 0-6-64* (unpublished manuscript), U. S. Naval Oceanographic Office, Washington, D.C., 1964.

88. Keller, George H., "Mass Properties of the Sea Floor in a Selected Depositional Environment," *Civil Engineering in the Oceans II,*

Proceedings ASCE Conference, Miami Beach, Fla., December, 1969, pp. 857-877.

89. Keller, George H., Personal communication, September, 1971.

90. Keller, George H., Personal communication, February, 1973.

91. Keller, George H., Richards, A. F., and Recknagel, J. H., "Prevention of Water Loss Through CAB Plastic Sediment Core Liners," *Deep-Sea Research*, Vol. 8, No. 2, April, 1961, pp. 148-151.

92. Kögler, F. C., "Geotechnical Properties of Recent Marine Sediments from the Arabian Sea and the Baltic Sea," *Marine Geotechnique*, Adrian F. Richards, ed., Urbana, Ill.: U. of Illinois Press, 1967, pp. 170-176.

93. Kretschmer, T. R., and Lee, H. J., "Plate Bearing Tests on Seafloor Sediments," *Technical Report R-694*, U. S. Naval Civil Engineering Laboratory, Port Hueneme, Cal., September, 1970.

94. Krumbein, W. C., and Sloss, L. L., *Stratigraphy and Sedimentation*, 2nd ed., San Francisco: W. H. Freeman and Co., 1963.

95. LaFond, Eugene C., and LaFond, Katherine G., "Oceanic Factors Pertinent to Shelf Installations," *Civil Engineering in the Oceans II*, Proceedings ASCE Conference, Miami Beach, Fla., December, 1969, pp. 783-803.

96. Lambe, T. W., "Physico-chemical Properties of Soils: Role of Soil Technology," *Journal of the Soil Mechanics and Foundations Division*, ASCE, Vol. 85, No. SM 2, April, 1959, pp. 55-70.

97. Lambe, T. W., *Soil Testing for Engineers*, New York: John Wiley and Sons, 1951.

98. Lambe, T. W., "The Structure of Inorganic Soil," *Proceedings*, American Society of Civil Engineers, Vol. 79, Separate Paper No. 315, October, 1953, pp. 1-49.

99. Langer, K., "Influence of Speed of Loading Increment on the Pressure Void Ratio Diagram of Undisturbed Soil Samples," *Proceedings*, First International Conference on Soil Mechanics and Foundation Engineering, Vol. 2, Cambridge, Mass., 1936, pp. 116-118.

100. Laughton, A. S., "Sound Propagation in Compacted Ocean Sediments," *Geophysics*, Vol. 22, No. 2, April, 1957, pp. 233-260.

101. Lee, Kenneth L., and Black, David K., "Time to Dissolve Air Bubbles in Drain Line," *Journal of the Soil Mechanics and*

Foundations Divisions, ASCE, Vol. 98, No. SM 2, February, 1972, pp. 181-194.

102. Leonards, G. A., "Engineering Properties of Soils," *Foundation Engineering,* G. A. Leonards, ed., New York: McGraw-Hill Book Co., Inc., 1962, pp. 66-240.

103. Leonards, G. A., and Altschaeffl, A. G., "Compressibility of Clay," *Journal of the Soil Mechanics and Foundation Division,* ASCE, Vol. 90, No. SM 5, September, 1964, pp. 133-155.

104. Leonards, G. A., and Girault, P., "A Study of the One-dimensional Consolidation Test," *Proceedings,* Fifth International Conference on Soil Mechanics and Foundation Engineering, Vol. 1, London, 1961, pp. 213-218.

105. Leonards, G. A., and Ramiah, B. K., "Time Effects in the Consolidation of Soils," *Symposium on Time Rates of Loading in Soil Testing, Special Technical Publication No. 254,* American Society for Testing Materials, 1959, pp. 116-130.

106. Ling, Shun C., "State-of-the-Art of Marine Soil Mechanics and Foundation Engineering," *Report No. TR-S-72-11,* U. S. Corps of Engineers, Waterways Experiment Station, August, 1972.

107. Lo, K. Y., "Secondary Compression of Clays," *Journal of the Soil Mechanics and Foundations Division,* ASCE, Vol. 87, No. SM 4, August, 1961, pp. 61-87.

108. Lowe, John, III, and Johnson, Thaddeus C., "Use of Back Pressure to Increase Degree of Saturation of Triaxial Test Specimens," *Research Conference on Shear Strength of Cohesive Soils,* ASCE Conference Papers, Boulder, Colo., June, 1960, pp. 819-836.

109. Lowe, J., III, Zaccheo, P. F., and Feldman, H. S., "Consolidation Testing with Back Pressure," *Design of Foundations for Control of Settlement,* ASCE Conference Papers, Evanston, Ill., June, 1964, pp. 73-90.

110. Macintyre, I. G., and Milliman, J. D., "Physiographic Features on the Outer Shelf and Upper Slope, Atlantic Continental Margin, Southeastern United States," *Bulletin,* Geological Society of America, Vol. 81, No. 9, Sept. 1970, pp. 2577-2598.

111. Matthews, Clarence S., "Consolidation at a Constant Rate of Strain," Special Problem presented to the School of Civil Engineering, Georgia Institute of Technology in partial fulfillment of the requirements for the degree of Master of

Science in Civil Engineering, September, 1972.

112. McClelland, Bramlette, "Land Experience as a Background for Offshore Sampling Review," Paper given at the Coastal and Ocean Engineering Short Course, Texas A. and M. University, College Station, Texas, August 2-13, 1971, pp. 1-5.

113. McClelland, Bramlette, "Progress of Consolidation in Delta Front and Prodelta Clays of the Mississippi River," *Marine Geotechnique*, Adrian F. Richards, ed., Urbana, Ill.: U. of Illinois Press, 1967, pp. 22-40.

114. McCoy, F. W., Jr., Von Herzen, R. P., Owen, D. M., and Boutin, P. R., "Deep-sea Corehead Camera Photography and Piston Coring," *Deep-Sea Research*, Vol. 8, No. 3, March, 1971, pp. 361-373.

115. Meade, R. H., "Factors Influencing the Early Stages of the Compaction of Clays and Sands--Review," *Journal of Sedimentary Petrology*, Vol. 36, No. 4, December, 1966, pp. 1085-1101.

116. Miller, Donald G., Jr., and Richards, Adrian, F., "Consolidation and Sedimentation Compression Studies of a Calcareous Core, Exuma Sound, Bahamas," *Revision of Report Dated 16 January, 1969*, Dept. of Geology, University of Illinois, July, 1969.

117. Milliman, John D., Pilkey, Orrin H., and Ross, David A., "Sediments of the Continental Margin off the Eastern United States," *Bulletin*, Geological Society of America, Vol. 83, No. 5, May, 1972, pp. 1315-1334.

118. Mitchell, James K., Singh, Awtar, and Campanella, Richard G., "Bonding, Effective Stresses, and Strengths of Soils," *Journal of the Soil Mechanics and Foundations Division*, ASCE, Vol. 95, No. SM 5, September, 1969, pp. 1219-1246.

119. Monney, N. T., "An Engineering Evaluation of Marine Sediments," *Proceedings*, Offshore Exploration Conference, New Orleans, 1968, 24 pages.

120. Moore, D. G., "Shear Strength and Related Properties of Sediments from Experimental Mohole (Guadalupe site)," *Journal of Geophysical Research*, Vol. 69, No. 20, Oct. 15, 1964, pp. 4271-4291.

121. Murray, H. W., "Topography of the Gulf of Maine, Field Season of 1940," *Bulletin*, Geological Society of America, Vol. 58, No. 2, February, 1947, pp. 153-196.

122. Myers, John J., Holm, Carl H., and McAllister, R. F., eds.,

Handbook of Ocean and Underwater Engineering, New York: McGraw-Hill Book Company, 1969.

123. Nacci, Vito A., and Huston, Milton T., "Structure of Deep Sea Clays," *Civil Engineering in the Oceans II*, Proceedings ASCE Conference, Miami Beach, Fla., December, 1969, pp. 599-619.

124. Nafe, John E., and Drake, Charles L., "Variation with Depth in Shallow and Deep Water Marine Sediments of Porosity, Density and The Velocities of Compressional and Shear Waves," *Geophysics*, Vol. 22, No. 3, July, 1957, pp. 523-552.

125. Neiheisel, J., and Weaver, C. E., "Transport and Deposition of Clay Minerals Southeastern United States," *Journal of Sedimentary Petrology*, Vol. 37, No. 4, December, 1967, pp. 1084-1116.

126. Newland, P. L., and Alley, B. H., "A Study of the Consolidation Characteristics of a Clay," *Geotechnique*, Vol. X, No. 2, June, 1960, pp. 62-74.

127. Nielsen, John P., "Consolidation Characteristics of Pure Clays and Pelagic Sediments," *Technical Report R-477*, U. S. Naval Civil Engineering Laboratory, Port Hueneme, Calif., 1966.

128. Nishida, Y., "A Brief Note on Compression Index of Soil," *Journal of the Soil Mechanics and Foundations Division*, ASCE, Vol. 82, No. SM 3, July, 1965, pp. 1027-1 to 1027-14.

129. Noorany, I., "Engineering Properties of Submarine Calcareous Soils from the Pacific," *Report No. NOAA-71 10284*, Dept. of Civil Eng., San Diego State College, San Diego, Calif., July, 1971a.

130. Noorany, I., "Engineering Properties of Submarine Clays from the Pacific," *Report No. NOAA-71 10283*, Dept. of Civil Eng., San Diego State College, San Diego, Calif., August, 1971b.

131. Noorany, I., "Underwater Soil Sampling and Testing--State-of-the-Art Review," Paper presented at the Seventy-fourth Annual Meeting of the American Society for Testing Materials, Atlantic City, N. J., June, 1971.

132. Noorany, I., and Gizienski, Stanley F., "Engineering Properties of Submarine Soils: State-of-the-Art Review," *Journal of the Soil Mechanics and Foundations Division*, ASCE, Vol. 96, No. SM 5, September, 1970, pp. 1735-1762.

133. Noorany, I., and Poormand, I., "Effect of Sampling on the Consolidation of Soft Clay," *Soil Mechanics Research Report,* Dept. of Civil Eng., San Diego State College, San Diego, Calif., November, 1970.

134. Northey, R. D., "Rapid Consolidation Tests for Routine Investigations," *Proceedings,* Second Australia-New Zealand Conference on Soil Mechanics and Foundation Engineering, Christchurch, N. Z., 1956, pp. 20-24.

135. Olson, Roy E., and Gholamreza, M., "Mechanisms Controlling Compressibility of Clays," *Journal of the Soil Mechanics and Foundations Division,* ASCE, Vol. 96, No. SM 6, November, 1970, pp. 1863-1878.

136. Paaswell, Robert E., "Temperature Effects on Clay Soil Consolidation," *Journal of the Soil Mechanics and Foundations Division,* ASCE, Vol. 93, No. SM 3, May, 1967, pp. 9-22.

137. Parker, A., "Mineralogy and Geotechnical Properties of a Deep Sea Carbonate Sediment," *Geotechnique,* Vol. 22, No. 1, March, 1972, pp. 155-159.

138. Pawlowicz, E. F., "Ocean Engineering Significance of Marine Seismic Reflection Profiling Technology," *Technical Note N-1157,* U. S. Naval Civil Engineering Laboratory, Port Hueneme, Calif., May, 1971.

139. Peck, Ralph B., Hanson, Walter E., and Thornburn, Thomas H., *Foundation Engineering,* Modern Asia Edition, Tokyo: Charles E. Tuttle Company, 1959.

140. Perlow, Michael, Jr., and Richards, Adrian F., "In-Place Geotechnical Measurements from Submersible Alvin in Gulf of Maine Soils," *Preprints Paper No. 1543,* Offshore Technology Conference, Houston, Texas, May 1-3, 1972, pp. 333-340.

141. Pilkey, Orrin H., "Heavy Minerals of the U. S. South Atlantic Continental Shelf and Slope," *Bulletin,* Geological Society of America, Vol. 74, No. 5, May, 1963, pp. 641-648.

142. Pilkey, O. H., "Size Distribution and Mineralogy of the Carbonate Fraction of United States South Atlantic Shelf and Upper Slope Sediments," *Marine Geology,* Vol. 2, December, 1964, pp. 121-136.

143. Pilkey, O. H., Schnitker, D., and PeVear, D. R., "Oolites on the Georgia Continental Shelf Edge," *Journal of Sedimentary Petrology,* Vol. 36, No. 2, June, 1966, pp. 462-467.

144. Raecke, D. A., "Supplement to 'Seafloor Foundations: Analysis of Case Histories,'" *Technical Report R-731S*, U. S. Naval Civil Engineering Laboratory, Port Hueneme, Calif., January, 1973.

145. Raecke, D. A., and Migliore, H. J., "Seafloor Pile Foundatins: State-of-the-Art, and Deep-Ocean Emplacement Concepts," *Technical Note N-1182*, U. S. Naval Civil Engineering Laboratory, Port Hueneme, Calif., October, 1971.

146. Resendiz, D., "Considerations of the Solid-Liquid Interaction in Clay-Water Systems," *Proceedings*, Sixth International Conference on Soil Mechanics and Foundation Engineering, Vol. I, Toronto, 1965, pp. 97-100.

147. "Retrieval of Deep Sea Structures," *The Military Engineer*, Vol. 64, No. 421, September-October, 1972, pp. 354, 355.

148. Reuter, J. H., Personal communication, December, 1972.

149. Richards, A. F., "Investigations of Deep-Sea Sediment Cores--I. Shear Strength, Bearing Capacity, and Consolidation," *Technical Report TR-63*, U. S. Navy Hydrographic Office, Washington, D. C., August, 1961.

150. Richards, A. F., "Investigations of Deep-Sea Sediment Cores--II. Mass Physical Properties," *Technical Report TR-106*, U. S. Navy Hydrographic Office, Washington, D. C., October, 1962.

151. Richards, A. F., "Local Sediment Shear Strength and Water Content Variability on the Continental Slope off New England," *Papers in Marine Geology*, Shepard Commemorative Volume, R. L. Miller, ed., New York: The MacMillan Co., 1964, pp. 474-484.

152. Richards, Adrian F., and Hamilton, Edwin L., "Investigation of Deep-sea Sediment Cores, III, Consolidation," *Marine Geotechnique*, Adrian F. Richards, ed., Urbana, Ill.: U. of Illinois Press, 1967, pp. 93-117.

153. Richards, A. F., and Keller, G. H., "In Place Measurement of Shear Strength and Bulk Density in Gulf of Maine Clays" (abstract), *Transactions*, American Geophysical Union, Vol. 49, No. 1, 1968, pp. 221, 222.

154. Richards, Adrian F., and Keller, George H., "A Plastic-barrel Sediment Corer," *Deep-Sea Research*, Vol. 8, No. 3/4, December, 1961, pp. 306-312.

155. Richards, Adrian F., and Parker, Harvey W., "Surface Coring for Shear Strength Measurements," *Civil Engineering in the*

Oceans I, ASCE Conference, San Francisco, September, 1967, pp. 445-489.

156. Richards, A. F., and Perlow, M., Jr., "Variability of Geotechnical Properties of Lutite in Wilkinson Basin, Gulf of Maine, As Measured in Place From Submersible *Alvin*," *Bulletin,* American Association of Petroleum Geologists, Vol. 56, No. 3, March, 1972, pp. 647-648.

157. Robertson, E. C., "Laboratory Consolidation of Carbonate Sediment," *Marine Geotechnique,* Adrian F. Richards, ed., Urbana, Ill.: U. of Illinois Press, 1967, pp. 118-127.

158. *Rock Color Chart,* prepared by the Rock-Color Chart Committee, The Geological Society of America, reprinted 1963.

159. Rocker, K., Jr., Personal communication, September, 1972.

160. Rosenqvist, I. Th., "Investigations on the Clay-Electrolyte-Water System," *Publication No. 9,* Norwegian Geotechnical Institute, 1955.

161. Rosenqvist, I. Th., "Physico-chemical Properties of Soils: Soil-Water Systems," *Journal Soil Mechanics and Foundations Division,* ASCE, Vol. 85, No. SM 2, April, 1959, pp. 31-53.

162. Rosfelder, Andre M., and Marshall, Neil F., "Obtaining Large, Undisturbed and Orientated Samples in Deep Water," *Marine Geotechnique,* Adrian F. Richards, ed., Urbana, Ill.: U. of Illinois Press, 1967, pp. 243-263.

163. Ross, David A., "Source and Dispersion of Surface Sediments in the Gulf of Maine-Georges Bank Area," *Journal of Sedimentary Petrology,* Vol. 40, No. 3, September, 1970, pp. 906-920.

164. Ross, D. A., and Riedel, W. R., "Comparison of Upper Parts of Some Piston Cores with Simultaneously Collected Open-barrel Cores," *Deep-Sea Research,* Vol. 14, No. 3, June, 1967, pp. 285-294.

165. Rouse, Hunter, *Elementary Mechanics of Fluids,* New York: John Wiley and Sons, Inc., 1946.

166. Rowe, Peter W., discussion to "Consolidation Testing With Back Pressure," *Design of Foundations for Control of Settlement,* ASCE Conference Papers, Evanston, Ill., June, 1964, pp. 91.

167. Schiffman, Robert L., Chen, Albert T-F, and Jordan, Jane C., "An Analysis of Consolidation Theories," *Journal of the*

Soil Mechanics and Foundations Division, ASCE, Vol. 95, No. SM 1, January, 1969, pp. 285-312.

168. Schmertmann, J. M., "The Undisturbed Consolidation Behavior of Clays," *Transactions*, ASCE, Vol. 120, 1955, pp. 1201-1233.

169. Scott, R. F., "In-Place Soil Mechanics Measurements," *Marine Geotechnique*, Adrian F. Richards, ed., Urbana, Ill.: U. of Illinois Press, 1967, pp. 264-273.

170. Scott, Ronald F., *Principles of Soil Mechanics*, Palo Alto, Cal.: Addison-Wesley Publishing Inc., 1963.

171. Seed, H. B., "Settlement Analysis, A Review of Theory and Testing Procedures," *Journal of the Soil Mechanics and Foundations Divisions*, ASCE, Vol. 91, No. SM 2, March, 1965, pp. 39-48.

172. Shepard, F. P., "Nomenclature Based on Sand-Silt-Clay Ratios," *Journal of Sedimentary Petrology*, Vol. 24, No. 3, September, 1954, pp. 151-158.

173. Shepard, F. P., *Submarine Geology*, 2nd ed., New York: Harper and Row, 1963.

174. Shepard, Francis P., and Dill, Robert F., *Submarine Canyons and Other Sea Valleys*, Chicago: Rand McNally Co., 1966.

175. Shepard, F. P., and Moore, D. G., "Central Texas Coast Sedimentation: Characteristics of Sedimentary Environment, Recent History and Diagenesis," *Bulletin*, American Association of Petroleum Geologists, Vol. 39, No. 8, August, 1955, pp. 1463-1593.

176. Shibata, Toru, "On the Shear Strength of Normally Consolidated Clay Measured in Vane Tests" (from English abstract), *Transactions*, Japan Society of Civil Engineers, No. 138, February, 1967, pp. 39-48.

177. Siever, R., Beck, K., and Berner, R. A., "Composition of Interstitial Waters of Modern Sediments," *Journal of Geology*, Vol. 73, No. 1, January, 1965, pp. 39-73.

178. Sillen, L. G., "The Ocean as a Chemical System," *Science*, Vol. 156, No. 3779, June 2, 1967, pp. 1189-1197.

179. Skempton, A. W., "The Colloidal 'Activity' of Clays," *Proceedings*, Third International Conference on Soil Mechanics and Foundation Engineering, Vol. 1, Zurich, 1953, pp. 57-61.

180. Skempton, A. W., "Effective Stress in Soils, Concrete and Rocks," *Pore Pressure and Suction in Soils*, London: Butterworths, 1961, pp. 4-16.

181. Skempton, A. W., "Notes on the Compressibility of Clays," *Quarterly Journal of the Geological Society of London*, Vol. 100, part 1, 1944, pp. 119-135.

182. Skempton, A. W., and Bjerrum, L., "A Contribution to the Settlement Analysis of Foundations on Saturated Clay," *Geotechnique*, Vol. VII, No. 4, December, 1957, pp. 168-178.

183. Skempton, A. W., and Northey, R. D., "The Sensitivity of Clays," *Geotechnique*, Vol. III, No. 1, June, 1952, pp. 30-53.

184. Smith, R. J., and Nunes, L., "Undeformed Sectioning of Plastic Core Tubing," *Deep-Sea Research*, Vol. 11, No. 2, April, 1964, pp. 261-262.

185. Smith, Ronald E., and Wahls, Harvey E., closure to "Consolidation Under Constant Rates of Strain," *Journal of the Soil Mechanics and Foundations Division*, ASCE, Vol. 97, No. Sm 1, January, 1971, pp. 238.

186. Smith, Ronald E., and Wahls, Harvey E., "Consolidation Under Constant Rates of Strain," *Journal of the Soil Mechanics and Foundations Division*, ASCE, Vol. 95, No. SM 2, March, 1969, pp. 519-539.

187. *Soil Mechanics, Foundations and Earth Structures*, NAVFAC DM 7, Naval Facilities Engineering Command, 1971.

188. Sowers, George F., personal communication, February, 1973.

189. Sowers, G. F., "Shallow Foundations," *Foundation Engineering*, G. A. Leonards, ed., New York: McGraw-Hill Book Co., Inc., 1962, pp. 525-632.

190. Sowers, George B., and Sowers, George F., *Introductory Soil Mechanics and Foundations*, 3rd ed., New York: The Macmillan Co., 1970.

191. Stanley, Daniel J., and Blanchard, Laurie R., "Scanning of Long Unsplit Cores by X-radiography," *Deep-sea Research*, Vol. 14, No. 3, June, 1967, pp. 379-380.

192. Stetson, H. C., "Summary of Sedimentary Conditions of the Continental Shelf Off the East Coast of the United States," *Recent Marine Sediments*, P. D. Trask, ed., Tulsa, Okla.: American Association of Petroleum Geologists, 1939, pp. 230-244.

193. Stiles, Newell T., and Kessler, Richard S., "Submarine Sediment Investigation in the Vicinity of the Planned Sealab III Habitat," *Report No. NOO-IR-69-2B*, Naval Oceanographic Office, Washington, D. C., July, 1969.

194. Sverdrup, H. V., Johnson, M. W., and Fleming, R. H., eds., *The Oceans: Their Physics, Chemistry and General Biology*, New York: Prentice-Hall, 1946.

195. Swift, D. J. P., "Outer Shelf Sedimentation: Processes and Products," *The New Concepts of Continental Margin Sedimentation*, Short Course Lecture Notes, American Geological Institute, Philadelphia, Pa., Nov. 7-9, 1969, pp. DS-5-1 to DS-5-26.

196. Tan, T-K, discussion in "Soil Properties and Their Measurements," *Proceedings*, Fourth International Conference on Soil Mechanics and Foundation Engineering, Vol. 3, London, 1958, pp. 87-89.

197. Taylor, Donald W., *Fundamentals of Soil Mechanics*, New York: John Wiley and Sons, Inc., 1948.

198. Terzaghi, Karl, *Erdbaumchanik auf Bodenphysikalischer Grundlage*, Leipzig: F. Deuticke, 1925.

199. Terzaghi, K., "Influence of Geological Factors on the Engineering Properties of Sediments," *Economic Geology*(50th Anniversary Volume), 1955, pp. 557-618.

200. Terzaghi, Karl, *Theoretical Soil Mechanics*, New York: John Wiley and Sons, Inc., 1943.

201. Torphy, S. R., and Zeigler, J. M., "Submarine Topography of Eastern Channel, Gulf of Maine," *Journal of Geology*, Vol. 65, No. 4, July, 1957, pp. 433-441.

202. Tucholke, Brian E., and Hollister, Charles D., "Late Pleistocene and Holocene Sedimentation in the Western Gulf of Maine" (abstract), *Transactions*, American Geophysical Union, Vol. 53, No. 4, April, 1972, p. 442.

203. Uchupi, E., and Tagg, A. R., "Microrelief of the Continental Margin South of Cape Lookout, North Carolina," *Bulletin*, Geological Society of America, Vol. 77, No. 4, April, 1966, pp. 427-430.

204. Ural, M. V., "An Experimental Study of the Compressibility of Remodeled Clay at High Pressures," A thesis presented to the University of Illinois in partial fulfillment of the degree of Master of Science, 1945.

205. Van Zelst, T. W., "An Investigation of the Factors Affecting Laboratory Consolidation of Clays," *Proceedings*, Second International Conference on Soil Mechanics and Foundation Engineering, Vol. VII, Rotterdam, 1948, pp. 52-61.

206. Vey, E., and Nelson, R. D., "Environmental Effects on Engineering Properties of Deep Ocean Sediments," *Report No. CR 67.020*, U. S. Naval Civil Engineering Laboratory, Port Hueneme, Calif., December, 1966.

207. Vey, E., and Nelson, R. D., "Environmental Effects on Engineering Properties of Deep Ocean Sediments Phase II," *Report No. CR 68.014*, U. S. Naval Civil Engineering Laboratory, Port Hueneme, Calif., June, 1968.

208. Wahls, H. E., "Analysis of Primary and Secondary Consolidation," *Journal of the Soil Mechanics and Foundations Division*, ASCE, Vol. 88, No. SM 6, December, 1962, pp. 207-231.

209. Wahls, H. E., and DeGodoy, N. S., discussion of "Interpretation of the Consolidation Test," *Journal of the Soil Mechanics and Foundation Division*, ASCE, Vol. 91, No. SM 3, May, 1965, pp. 147-152.

210. Wang, J. H., "The Effect of Ions on the Self-diffusion and Structure of Water in Aqueous Electrolytic Solutions," *Journal of Physical Chemistry*, Vol. 58, No. 9, September, 1954, pp. 686-692.

211. Weaver, C. E., Personal communication, January, 1973.

212. Whitman, R. V., Richardson, A. M., Jr., and Healy, K. A., "Time-lags in Pore Pressure Measurements," *Proceedings*, Fifth International Conference on Soil Mechanics and Foundation Engineering, Vol. 1, Paris, 1961, pp. 407-411.

213. Wilson, J. V., Hitchcock, R. D., and Mittleman, J. R., "Emplacement of a Heavy Load onto a Seafloor Foundation: Concept Development and Analysis," *Technical Report No. R-769*, U. S. Naval Civil Engineering Laboratory, Port Hueneme, Calif., July, 1972.

214. Wissa, Anwar E. Z., "Pore Pressure Measurement in Saturated Stiff Soils," *Journal of the Soil Mechanics and Foundations Division*, ASCE, Vol. 95, No. SM 4, July, 1969, pp. 1063-1073.

215. Wissa, Anwar E. Z., Christian, John T., Davis, Edward H., and Heiberg, Sigurd, "Consolidation at Constant Rate of Strain," *Journal of the Soil Mechanics and Foundations Division*, ASCE, Vol. 97, No. SM 10, October, 1971, pp. 1393-1413.

216. Yousse, F., Sabey, A., and Ramli, A., "Temperature Changes and Their Effects on Some Physical Properties of Soils," *Proceedings*, Fifth International Conference on Soil Mechanics and Foundation Engineering, Vol. 1, Paris, 1961, pp. 419-421.

217. Zarudzki, Efk, "Organic Reef Alignments on Continental Margin South of Cape Hatteras," *Bulletin*, Geological Society of America, Vol. 79, No. 12, December, 1968, pp. 1867-1870.

218. ZoBell, C. E., "Studies on Redox Potential of Marine Sediments," *Bulletin*, American Association of Petroleum Geologists, Vol. 30, No. 4, April, 1946, pp. 477-513.

VITA

After graduation from Metairie Park Country Day School in Metairie, Louisiana, Gordon Warren Callender, Jr., attended the United States Naval Academy. Graduating with distinction, he was commissioned an Ensign in the Navy's Civil Engineer Corps on 7 June 1961. During Operation DEEP FREEZE 1966 LT Callender was the Officer in Charge of Byrd Station, Antarctica. For his part in the first night landing in the interior of the continent (to evacuate a critically ill man) he was awarded the Navy Commendation Medal. During the Vietnam conflict he served on two deployments with U. S. Naval Mobile Construction Battalion 133 in the Hue area. While with the SEABEES he was awarded a Bronze Star for his effort in widening and repaving National Route One; a second Navy Commendation Medal for service in support of combat operations; an Army Commendation Medal for assistance provided to the 101st Airborn Division and the XXIVth Corps; a Vietnamese Cross of Gallantry for efforts in providing a water well to a South Vietnamese Army outpost interdicting the coastal infiltration route just below the DMZ; and two Vietnamese Technical Medals for repairs to the main highway bridges at Hue and between Hue and Quang Tri.

His professional activity includes several articles published in Military Engineering journals, and membership in the Society of American Military Engineers, the American Society of Civil Engineers, and the American Military Institute. He is a registered civil engineer and

land surveyor in Louisiana.

Gordon and Ann Callender are the proud parents of two little girls--Winter and Catherine.